Université de Strasbourg

Habilitation à Diriger des Recherches

Caractérisation des interactions hôte-virus et nouvelles stratégies antivirales dans le cadre des hépatites B et D

Dr Eloi R. VERRIER
Chargé de recherche Inserm
Institut de Recherche sur les Maladies Virales et Hépatiques
Inserm / Unistra UMR_S1110 – LabEx HEPSYS

Garant
Pr Thomas F. BAUMERT, MD

Jury

Dr Ali AMARA, HDR	Rapporteur
Dr Nicole PAVIO, HDR	Rapportrice
Pr Philippe ROINGEARD, HDR	Rapporteur
Pr Carine MEIGNIN, HDR	Examinatrice
Dr Johan NEYTS, PhD	Examinateur
Dr Sabine RIFFAULT, HDR	Examinatrice

Inserm
La science pour la santé
From science to health

HepSYS

Université de Strasbourg

REMERCIEMENTS

Je tiens en premier lieu à remercier le professeur Thomas Baumert, directeur de l'Institut de Recherche sur les maladies Virales et Hépatiques, de s'être porté garant de ma candidature et pour son soutien au sein de son unité depuis plus de sept ans. Je remercie également le docteur Catherine Schuster pour son soutien indéfectible et ses conseils toujours précieux et avisés.

J'ai une pensée particulière pour les collègues et étudiants qui ont partagé mon quotidien pour leur esprit d'équipe irréprochable et leur abnégation dans des situations parfois désespérées. Charlotte et Laura, bien sûr, sans qui rien n'aurait été possible, mais aussi Carla, Emilie, Hussein, Che, Frank, Antonio, Laetitia, Yim, Sarah, Gaëtan, Vincent, Solène, Margaux, ainsi qu'à tout le personnel de l'unité U1110. Une pensée particulière à Anne et son bureau (presque) toujours ouvert.

Je remercie également l'Université de Strasbourg, l'Inserm et l'ANRS pour leur soutien.

Ce travail est le fruit de collaborations multiples, diverses et toujours fécondes. Je remercie en ce sens très chaleureusement Julie Lucifora et David Durantel du CRCL de Lyon, ainsi que Camille Sureau de l'INTS, pour leur soutien de la première heure et les perspectives réjouissantes des projets à venir. Je remercie également l'équipe de la plateforme de criblage de l'IGBMC, notamment Amélie Weiss et Laurent Brino pour leur très fructueuse collaboration. J'ai également une pensée particulière pour Michael Nassal de l'Université de Fribourg pour nos échanges toujours riches et intenses.

Enfin, ce manuscrit étant l'aboutissement de plus de dix de recherche, je tiens dans ces quelques lignes à remercier mes collègues et superviseurs passés, en tout premier lieu Thomas Heams d'AgroParisTech qui a suivi mes premiers pas, mais également Christophe Marcireau (Sanofi), Christelle Langevin, Nicolas Dechamp, Pierre Boudinot et Edwige Quillet de l'Inra(e).

Table des matières

1. CURRICULUM VITAE

Eloi, Rémi, Dominique VERRIER, né le 20 juin 1984 à Villeneuve-la-Garenne (92)
Marié, deux enfants
Langues parlées : Français (langue maternelle), Anglais (courant), Allemand (scolaire)

1.1 Diplômes

10/2009 – 01/2013 **Doctorat ParisTech**
Etablissement : AgroParisTech (Paris, FRA)
Spécialité : Sciences de la Vie et de la Santé
Date de soutenance : 09 janvier 2013
Directeurs : E. Quillet (DR1 INRA), P. Boudinot (DR1 INRA)
Mention : Très honorable

09/2008 – 09/2009 **Master Sciences, Santé et Applications**
Etablissement : Université Paris Diderot – Paris 7 (FRA)
Spécialité : Génétique
Mention : Bien

09/2005 – 09/2009 **Ingénieur AgroParisTech**
Etablissement : AgroParisTech (Paris, FRA)
Spécialité : Agronomie à vocation générale

1.2 Situation professionnelle actuelle

Depuis 11/2018 **Chargé de Recherche Classe Normale Inserm (CRCN)**
Laboratoire : UMR_S1110 Inserm / Unistra (Strasbourg, FRA)
Direction : Pr T.F. Baumert
Thématiques : Interactions hôte-virus, VHB, VHD, maladie hépatite.

1.3 Expériences précédentes

02/2013 – 10/2018 **Chercheur postdoctoral**
Laboratoire : UMR_S1110 Inserm / Unistra (Strasbourg, FRA)
Direction : Pr T.F. Baumert
Thématiques : Interactions hôte-virus, VHB, VHD, maladie hépatite.
Financement : Allocation de recherche ANRS (2015-2018)

10/2009 – 11/2012 **Doctorant**
Laboratoire : INRA UMR1313 & UR892 (Jouy-en-Josas, FRA)
Direction : Dr E. Quillet & Dr P. Boudinot
Thématiques : Interactions hôte-virus, Résistance antivirale, VSHV, Truite-arc-en-ciel, Génétique animale.

01/2009 – 07/2009 **Stage M2**
Laboratoire : CNRS UMR7592 (Paris, FRA)
Direction : Dr S. Lefebvre
Thématique : Amyotrophie spinale, SMN.

09/2007 – 08/2008 **Stage de césure**
Laboratoire de Génétique de la levure, Sanofi-Aventis (Vitry, FRA)
Direction : Dr C. Marcireau
Thématique : Complexe APC/C, criblage cellulaire

1.4 Activités d'enseignement universitaire

Depuis 2017	**Conférences pour étudiants M1/M2 – 3h (bisannuel)** Lieu : Université de Strasbourg (FRA) Master Biologie des Micro-Organismes (Pr D. Gilmer) Thème : Virologie, Interaction hepatocytes/VHB-VHD
17/11/2015	**TD – étudiants DFSAM1 (ex DCEM2) – 1h** Lieu : Faculté de Médecine de Strasbourg (FRA) Thème : Pathologie digestive médico-chirurgicale
10/10/2011 -19/10/2011	**Organisation d'un module d'enseignement doctoral - 64h** Lieu : Tallinn University of Technology (TTÜ, Tallinn, EST) Thème : « Immunoregulation. Cytokines and Interferons ». Co-organisation des cours et de l'emploi du temps. Dispense de cours magistraux (4h30) et de travaux pratiques (15h). Coordinateur : Dr S. Rüütel

1.5 Prix et distinctions

2015, 2017, 2018	« Full Travel Grant » - EASL International Liver Congress
2015, 2016, 2018	« Travel Grant » - The International HBV Meeting
2014	Médaille d'Argent 2013 - Académie d'Agriculture de France
2014	Prix de thèse 2013 - Association Française de Zootechnie

1.6 Encadrement

a. Encadrement d'étudiants

2018-2020	**Encadrant non HDR** : Etudiant en thèse – V. Turon-Lagot Financement : ATER Unistra (4e année) Thème : Interactions hépatocytes-VHD Publication : **Turon Lagot V,** Saviano A, Schuster C, Baumert TF, **Verrier ER**. Targeting the host for new therapeutic perspectives in hepatitis D. J Clin Med 20209(1):222.
2017-2020	**Encadrant non HDR** : Etudiante en thèse – L. Heydmann Financement : interne (assistance ingénieure en poste) Thème : facteurs hépatiques et infection par le VHB Publication : **Verrier ER, Heydmann L**, Baumert TF, Schuster C. Le transporteur d'acides biliaires NTCP, un acteur majeur dans l'infection par les virus humains des hépatites offrant de nouvelles perspectives thérapeutiques. Virologie 2018;22:55-66.
2016-2019	**Encadrant non HDR** : Etudiante en thèse – C. Eller Financement : Inserm Thème : Rôle de CDKN2C dans l'infection par le VHB Publication : ***Eller C*, Heydmann L*,*** *[…],* ***Verrier ER$****, Baumert TF$. A genome-wide gain-of-function screen identifies CDKN2C as a HBV host factor (En révision à Nat Commun ; *co-premier auteur ; $co-dernier auteur, co-auteur correspondant)*

2014-2017	**Encadrant non HDR** : Etudiante en thèse – Dr S.A. Yim. Financement : Région Alsace Thème : VHB et senseurs de l'immunité innée Publication : **Verrier ER*, Yim SA***, *et al.*, Hepatitis B virus evasion from cGAS sensing in human hepatocytes. Hepatology 2018;68(5):1695-1709. (**co-premier auteur*)
2016	**Encadrant** : Etudiante M2 – L. Heydmann (6 mois) Thème : VHB et senseurs de l'immunité innée
2012	**Encadrant** : Etudiante M1 – A. Ehanno (3 mois) Thème : Résistance SHV chez la truite arc-en-ciel : analyse de survie Publication : **Verrier ER**, **Ehanno A**, *et al.*, Lack of correlation between the resistances to two rhabdovirus infections in rainbow trout. Fish Shellfish Immunol 2013;35:9-17.
Depuis 2011	Encadrant régulier de stagiaires BTS/DUT

b. Encadrement de techniciens/ingénieurs

2019-2020	**Maitre d'apprentissage** : Apprentie / Etudiante L3 – S. Jachez (1 an) Thème : interaction hépatocytes-VHD. Financement : Inserm
Depuis 2013	**Encadrement** : 1 technicienne de recherche (C. Bach) et une assistante ingénieure (L. Heydmann) Au sein de l'U1110. Mission : En tant que coordinateur des projets VHB/VHD de l'unité : Orientation des projets, répartition des tâches, organisation du travail, suivi régulier (réunions hebdomadaires), coordination avec le directeur.

1.7 Evaluation et expertise

Depuis 2019	Review Editor pour la revue Frontiers in Microbiology
Depuis 2020	Membre du Conseil Scientifique des Journées Francophones de Virologie
2019	Expert pour l'évaluation des dossiers AAP IDEX Lyon 2019
2019	Expert pour l'évaluation des dossiers AAP DIM1HEALTH 2019

1.8 Liste de publications

(Les noms des étudiantes et étudiants encadrés sont soulignés)

a. Articles originaux

1. **Verrier ER***, Weiss A, Bach C, Heydmann L, Kopp A, El Saghire H, Crouchet E, Pessaux P, Garcia T, Pale P, Zeisel MB, Sureau C, Schuster C, Brino L, Baumert TF*. A combined small molecule and loss-of-function screen uncovers estrogen receptor alpha and CAD as host factors for HDV infection and antiviral targets. **Gut** 2020;69(1):158-167 (IF : 17,94). *auteurs correspondant

2. Lupberger J, Croonenborghs T, Van Renne N, Roca Suarez AA, Jühling F, Virzi A, Bandiera S, Mezaros G, Mukherji A, Heymann L, **Verrier ER**, Oudot MA, El Saghire H, Bartenschlager R, Mertins P, Ramberger E, Fereshetian S, Carr AS, Jovanocic N, Zeisel MB, Chayama K, Ricci R, Bardeesy NM, Fujiwara N, Hoshida Y, Pochet N, Baumert TF. A temporal proteogenomic atlas of HCV-host interactions unravels cell circuits driving viral and metabolic liver disease. **Gastroenterology** 2019;157(2):537-551. (IF : 19,23)

3. **Verrier ER***, Yim SA, Heydmann L, El Saghire H, Mailly L, Bach C, Durand S, Lucifora J, Durantel D, Pessaux P, Manel N, Zeisel MB, Pochet N, Schuster C, Baumert TF*. Hepatitis B virus evasion from cGAS sensing in human hepatocytes. **Hepatology** 2018;68(5):1695-1709. (IF : 14,97). *auteurs correspondant

4. **Verrier ER**, Genet C, Laloë D, Jaffrezic F, Rau A, Esquerre D, Dechamp N, Ciobotaru C, Hervet C, Krieg F, Jouneau L, Klopp C, Quillet E, Boudinot P. Genetic and transcriptomic analyses provide new insights on the early antiviral response to VHSV in resistant and susceptible rainbow trout. **BMC Genomics** 2018;19:482 (IF : 3,50).

5. Crouchet E, Lefevre M, **Verrier ER**, Baumert TF, Schuster C. Extracellular lipid-free apolipoprotein E inhibits HCV replication and induces ABCG1-dependent cholesterol efflux. **Gut** 2017:66:896-907 (IF 17,94).

6. **Verrier ER***, Colpitts CC*, Bach C, Heydmann L, Zona L, Xiao F, Thumann C, Crouchet E, Gaudin R, Sureau C, Cosset FL, McKeating JA, Pessaux P, Hoshida Y, Schuster C, Zeisel MB, Baumert TF. Solute Carrier NTCP Regulates Innate Antiviral Immune Responses Targeting Hepatitis C Virus Infection of Hepatocytes. **Cell Rep** 2016;17(5):1357-1368 (IF : 7,82). *co-premiers auteurs

7. **Verrier ER**, Colpitts CC, Bach C, Heydmann L, Weiss A, Renaud M, Durand SC, Habersetzer F, Durantel D, Abou-Jaoude G, Lopez Ledesma MM, Felmlee DJ, Soumillon M, Croonenborghs T, Pochet N, Nassal M, Schuster C, Brino L, Sureau C, Zeisel MB, Baumert TF. A targeted functional RNAi screen uncovers Glypican 5 as an entry factor for hepatitis B and D viruses. **Hepatology** 2016;63:35–48. (IF 14,97).

8. **Verrier ER**, Ehanno A, Biacchesi S, Le Guillou S, Dechamp N, Boudinot P, Bremont M, Quillet E. Lack of correlation between the resistances to two rhabdovirus infections in rainbow trout. **Fish Shellfish Immunol** 2013;35:9-17. (IF 3,30).

9. **Verrier ER**, Dorson M, Mauger S, Torhy C, Ciobotaru C, Hervet C, Dechamp N, Genet C, Boudinot P, Quillet E. Resistance to a rhabdovirus (VHSV) in rainbow trout: identification of a major QTL related to innate mechanisms. **PLoS One** 2013;8:e55302 (IF 2,78).

10. **Verrier ER**, Langevin C, Tohry C, Houel A, Ducrocq V, Benmansour A, Quillet E, Boudinot P. Genetic resistance to rhabdovirus infection in teleost fish is paralleled to the derived cell resistance status. **PLoS One** 2012;7:e33935. (IF 2,78).

11. Renvoisé B, Quérol G, **Verrier ER**, Burlet P, Lefebvre S. A role for protein phosphatase PP1γ in SMN complex formation and subnuclear localization to Cajal bodies. **J Cell Sci** 2012;125(Pt 12):2862-74 (IF 4,52).

Publications originales en révision

1. Eller C, Heydmann L*, Colpitts C, El Saghire H, Piccioni F, Majzoub K, Lupberger J, Nassal M, Cowley GS, Pessaux P, Sureau C, Schuster C, Root DE, **Verrier ER**$, Baumert TF$. A genome-wide gain-of-function screen identifies CDKN2C as a HBV host factor. (**Nat Commun** IF 11,88). *co-premiers auteurs. $co-derniers auteurs, co-auteurs correspondant.*

*2. **Verrier ER***, Jülhing F*, Saviano A*, El Saghire H, Heydmann, L, Pessaux P, Pochet N, Schuster C, Baumert TF. Single-cell RNA-Seq of HBV-induced hepatocellular carcinoma reveals viral compartmentalization and cancer heterogeneity. (**J Clin Invest** IF 12,28). *co-premiers auteurs.*

*3. Crouchet E, […], **Verrier ER**, […], Baumert TF. Fast-track liver disease chemoprevention discovery using a clinical gene signature-inducible human cell culture model. (**Cancer Cell** IF 23,92)*

b. Revues

1. Turon-Lagot V, Saviano A, Schuster C, Baumert TF, **Verrier ER***. Targeting the host for new therapeutic perspectives in hepatitis D. **J Clin Med** 2020;9(1):222 (IF : 5,69). * auteur correspondant.

2. Turon-Lagot V, Saviano A, Schuster C, **Verrier ER***. Virus de l'hépatite D : cycle viral et nouvelles stratégies thérapeutiques. **Virologie** 2019;23(3):149-159 (IF : 0,16). * auteur correspondant.

3. Eller C, Heydmann L, Colpitts CC, **Verrier ER**, Schuster C, Baumert TF. The functional role of sodium taurocholate cotransporting polypeptide NTCP in the life cycle of hepatitis B, C and D viruses. **Cell Mol Life Sci** 2018;75:3895-3905. (IF : 7,01)

4. **Verrier ER***, Heydmann L, Baumert TF, Schuster C. Le transporteur d'acides biliaires NTCP, un acteur majeur dans l'infection par les virus humains des hépatites offrant de nouvelles perspectives thérapeutiques. **Virologie** 2018 ;22 :55-66 (IF : 0,16). * auteur correspondant

5. **Verrier ER**, Colpitts CC, Schuster C, Zeisel MB, Baumert TF. Cell Culture Models for the Investigation of Hepatitis B and D Virus Infection. **Viruses** 2016;8(9): E261. (IF : 3,8).

6. **Verrier ER**, Colpitts CC, Sureau C, Baumert TF. Hepatitis B virus receptors and molecular drug targets. **Hepatol Int** 2016;10(4):567-73. (IF : 5,49).

7. Baumert TF, **Verrier ER**, Nassal M, Chung RT, Zeisel MB. Host-targeting agents for treatment of hepatitis B virus infection**. Curr Opin Virol** 2015;14:41-46. (IF 5,4).

8. Colpitts CC, **Verrier ER**, Baumert TF. Targeting viral entry for treatment of hepatitis B and C virus infections. **ACS Infect Dis** 2015;1:420–427. (IF 4,9).

9. **Verrier ER***, Langevin C, Quillet E, Boudinot P. Analyse génétique de la résistance aux rhabdovirus chez la truite arc-en-ciel (Oncorhynchus mykiss). **Virologie** 2013;17:426-441. (IF 0.16).* auteur correspondant

10. **Verrier ER**, Langevin C, Benmansour A, Boudinot P. Early antiviral response and virus-induced genes in fish. **Dev Comp Immunol** 2011;35:1204-1214. (IF 3,12).

c. Editoriaux

1. **Verrier ER**, Majzoub K, Baumert TF. Hepatitis D Virus Infection Revisited. Gastroenterology. 2019;157:1431-1432. (IF 19,23)

2. **Verrier ER**, Schuster C, Baumert TF. Advancing hepatitis B virus entry inhibitors. **J Hepatol** 2017; 66(4):677-679. (IF 18,95)

3. **Verrier ER**, Wieland S, Baumert TF. Retinoic acid-inducible gene 1 and sensing of hepatitis B virus revisited. **Hepatology** 2015;62:970-972. (IF 14,94)

4. **Verrier ER**, Gack MU, Baumert TF. cGAS, innate immune responses and viral hepatitis. **Hepatology** 2014;60:1098-1100. (IF 14,94)

d. Conférences invitées

1. **Verrier ER**. Cellular factors involved in viral entry. 6th ANRS HBV Cure Workshop. **05/2019** (Paris, FRA)

2. **Verrier ER**. Tackling the Hepatitis D virus / HBV superinfection. LabEx Hepsys Winter School. **11/2018** (Strasbourg, FRA)

3. **Verrier ER**. Identification of host-factors involved in Hepatitis B and Delta virus infections. 7e édition du colloque de Génomique Fonctionnelle du Foie. **03/2018** (Lyon, FRA)

4. **Verrier ER.** High-throughput HDV and HBV infection models for screening of antivirals and host-targeting compounds. *Invitation au séminaire hebdomadaire de la VIM – INRA domaine de Vilvert.* 11/**2015** (Jouy-en-Josas, FRA)

e. Présentations orales - congrès internationaux

1. **Verrier ER**, Croonenborghs T, Heydmann L, Bach C, Schuster C, Zeisel MB, Pochet N, Baumert TF. Single-cell transcriptomic profiling to unravel the host cell responses to hepatitis B virus infection. *EASL International Liver Congress™ 2017.* **04/2017** (Amsterdam, PB) (**Bourse de voyage [BV]**)

2. **Verrier ER**, Colpitts CC, Bach C, Heydmann L, Zona L, Xiao F, Thumann C, Crouchet E, Gaudin R, Sureau C, Cosset FL, McKeating JA, Pessaux P, Hoshida Y, Schuster C, Zeisel MB, Baumert TF. Solute Carrier NTCP Regulates Innate Antiviral Immune Responses Targeting Hepatitis C Virus Infection of Hepatocytes. *2016 International HBV Meeting*. **10/2016** (Seoul, KOR) (**BV**)

3. **Verrier ER**, Colpitts CC, Bach C, Heydmann L, Weiss A, Renaud M, Durand SC, Habersetzer F, Durantel D, Abou-Jaoude G, Lopez Ledesma MM, Felmlee DJ, Soumillon M, Croonenborghs T, Pochet N, Nassal M, Schuster C, Brino L, Sureau C, Zeisel MB, Baumert TF. A targeted RNAi screen using a high-throughput infectious model system uncovers Glypican GPC5 as a host factor for hepatitis B and D virus entry. *2015 International Meeting on Molecular Biology of Hepatitis B Viruses*. **10/2015** (Bad Nauheim, ALL) (**BV**)

4. **Verrier ER**, Bach C, Heydmann H, Weiss A, Renaud M, Fritsch P, Habersetzer F, Abou-Jaoudé G, Durantel D, Schuster C, Brino L, Sureau C, Zeisel MB, Baumert TF. A targeted RNAi screen using a high-throughput infectious model system uncovers Glypican GPC5 as a host factor for hepatitis B and D virus entry. *50th EASL International Liver Congress™ 2015*. **04/2015** (Vienne, AUT) (**BV**) **Session plénière.**

5. **Verrier ER**, Dorson M, Dechamp N, Torhy C, Le Guillou S Ciobotaru C, Genet C, Boudinot P, Quillet E. Uncovering the genetic architecture of response to VHSV in rainbow trout. *The International Symposium on Genetics in Aquaculture XI*. **06/2012** (Auburn, USA)

6. **Verrier ER**, Dorson M, Dechamp N, Torhy C, Le Guillou S, Ciobotaru C, Genet C, Boudinot P, Quillet E. Using clonal lines of rainbow trout as model for studying antiviral response in rainbow trout. *11th. annual meeting of the Complex Trait Community*, **06/2012** (Paris, FRA).

f. Présentations orales – congrès/séminaires nationaux

1. **Verrier ER**. L'entrée cellulaire du VHB et du VHD. *Jeunes Hépatologues Conférence*. **06/2017**. (Saint-Maximin-la-Sainte-Beaume, FRA)

2. **Verrier ER**, Colpitts CC, Bach C, Heydmann L, Zona L, Xiao F, Thumann C, Crouchet E, Gaudin R, Sureau C, Cosset FL, McKeating JA, Pessaux P, Hoshida Y, Schuster C, Zeisel MB, Baumert TF. Solute carrier NTCP regulates expression of innate antiviral immune responses targeting hepatitis C virus infection of hepatocytes. *XIXe Journées Francophones de Virologie*. **03/2017** (Paris, FRA)

3. **Verrier ER**, Colpitts CC, Bach C, Heydmann L, Zona L, Xiao F, Thumann C, Crouchet E, Gaudin R, Sureau C, Cosset FL, McKeating JA, Pessaux P, Hoshida Y, Schuster C, Zeisel MB, Baumert TF. Solute carrier NTCP regulates expression of innate antiviral immune responses targeting hepatitis C virus infection of hepatocytes. *17e Réunion du Réseau National Hépatites – ANRS* **03/2017** (Paris, FRA)

4. **Verrier ER**, Bach C, Heydmann H, Weiss A, Renaud M, Fritsch P, Habersetzer F, Abou-Jaoudé G, Durantel D, Schuster C, Brino L, Sureau C, Zeisel MB, Baumert TF. A targeted RNAi screen using a high-throughput infectious model system uncovers Glypican GPC5 as a host factor for hepatitis B and D virus entry. *15ème Réunion du Réseau National Hépatites*. **01/2015** (Paris, FRA)

g. Présentations orales – colloques locaux/internes

1. **Verrier ER**. Functional genomics to uncover novel targets for HBV and HDV cure. *LabEx HepSYS Scientific Advisory Board* - **11/2017** (Strasbourg, FRA).

2. **Verrier ER**. Functional genomics of hepatitis B/D virus-host interactions to discover novel targets for viral cure. *Evaluation HCERES 2017.* **01/2017** (Strasbourg, FRA)

3. **Verrier ER**, Colpitts CC, Bach C, Heydmann L, Zona L, Xiao F, Thumann C, Crouchet E, Gaudin R, Sureau C, Cosset FL, McKeating JA, Pessaux P, Hoshida Y, Schuster C, Zeisel MB, Baumert TF. Solute Carrier NTCP Regulates Innate Antiviral Immune Responses Targeting Hepatitis C Virus Infection of Hepatocytes. *2016 Gastro-Regio Meeting*. **12/2016** (Bâle, CH)

4. **Verrier ER**, Bach C, Heydmann H, Weiss A, Renaud M, Fritsch P, Habersetzer F, Abou-Jaoudé G, Durantel D, Schuster C, Brino L, Sureau C, Zeisel MB, Baumert TF. A targeted RNAi screen using a high-throughput infectious model system uncovers Glypican GPC5 as a host factor for hepatitis B and D virus entry. *Gastro-Regio meeting 2014*. **12/2014** (Strasbourg, FRA)

5. **Verrier ER.** Bach C, Heydmann H, Weiss A, Renaud M, Fritsch P, Habersetzer F, Abou-Jaoudé G, Durantel D, Schuster C, Brino L, Sureau C, Zeisel MB, Baumert TF. Striving toward a HBV cure. *LabEx HepSYS Scientific Advisory Board* - **07/2014** (Strasbourg, FRA)

6. **Verrier ER**., Torhy C., Quillet E., Boudinot P. Validation d'un modèle cellulaire de résistance à la SHV chez la truite arc-en-ciel. *Colloque annuel de l'association des doctorants de l'INRA de Jouy-en-Josas*, mai **2011** (Jouy-en-Josas, FRA). **Prix de la meilleure présentation.**

1.9 Financement des projets de recherche

PI: principal investigator

2020-2022 Agence Nationale de la Recherce sur le Sida et les Hépatites Virales (ANRS) – 126k€.
PI (projet ECTZ104527)

2020-2022 ANRS – 18,5k€.
Partenaire (projet ECTZ102776 ; PI : J. Lucifora, CRCL, Lyon)

2019-2021 ANRS – 132k€
Co-PI (projet ECTZ87384 ; co-PI : T. Baumert)

2018-2020 National Institute of Health (NIH) : R03 grant – 50k€
Partenaire et rédacteur du projet (projet NIAID 1R03AI131066-01A1 ; PI : T. Baumert et N. Pochet, Broad Institute of MIT and Harvard, Cambridge, USA).

2015-2018 ANRS
Allocation nominative de recherche (ECTZ50121)

2015-2017 ANRS - 70k€
Partenaire et rédacteur du projet (projet 15/99 ; PI : T. Baumert)

2014-2018 Agence Nationale de la Recherche (ANR) : Consortium européen Infect-ERA – 349k€
Co-rédacteur du projet (projet Infect-ERA hepBccc ; PI : T. Baumert et M. Nassal, University of Freiburg, ALL)

2. INTRODUCTION GENERALE

Les infections virales représentent un problème de santé publique mondiale. Les stratégies antivirales se heurtent à des difficultés liées aux propriétés intrinsèques des virus, parasites intracellulaires stricts, à leur potentiel de transmission et leur très grande diversité. Une lutte efficace contre les virus suppose une connaissance fine des interactions entre le virus et son hôte. Le fil conducteur de mon parcours repose sur la caractérisation de ces interactions dans deux modèles hôte-virus, afin de mieux comprendre les mécanismes d'infection et de résistance à ces infections, et de développer de nouvelles stratégies de lutte antivirale : (i) comprendre les mécanismes mis en jeu dans la résistance aux infections à rhabdovirus chez la truite arc-en-ciel (ii) identifier et caractériser des facteurs hépatiques impliqués dans les infections par les virus des hépatites B et D dans le but de développer de nouvelles stratégies thérapeutiques. Ces deux thématiques sont caractérisées par un accès aux outils et aux modèles limité : (i) le manque d'accès aux outils de la génomique chez la truite arc-en-ciel en comparaison des autres modèles animaux limite l'étude des facteurs cellulaires impliqués dans les infections virales ; (ii) l'absence historique de modèles d'infection *in vitro* simples pour les hépatites B et D a considérablement freiné la caractérisation moléculaire des interactions entre ces virus et leurs cellules cibles, les hépatocytes. Dans ce contexte, les stratégies intégratives que j'ai menées combinant plusieurs approches complémentaires à différents niveaux d'étude (moléculaire, cellulaire, organisme) ont permis des avancées significatives dans les processus mis en jeu au cours de l'infection et dans le développement de nouvelles solutions de lutte contre ces infections. Ces stratégies reposent sur des collaborations efficaces avec des acteurs reconnus issus de disciplines variées (virologistes, généticiens, bio-informaticiens, chimistes…) et le développement de projets innovants impliquant des technologies à haut débit. Le programme de recherche du groupe que je coordonne au sein de l'UMR_S1110 et que je présente dans ce manuscrit s'inscrit dans cette lignée, en proposant une approche multimodale pour le développement de nouvelles solutions thérapeutiques dans le cadre des infections par les virus des hépatites B et D, basées sur l'utilisation de molécules ciblant l'hôte. Nous ambitionnons de produire une liste de facteurs hépatocytaires impliqués dans les cycles viraux, pour une meilleure compréhension des mécanismes d'infections et la caractérisation de nouvelles cibles pour l'éradication de ces menaces majeures de santé publique.

PRINCIPAUX RESULTATS

3. RESISTANCE AU VSHV CHEZ LA TRUITE ARC-EN-CIEL

Ce chapitre résume les travaux réalisés au cours de ma thèse, entre octobre 2009 et novembre 2012, dans les équipes Génétique en Aquaculture (UMR1313 Génétique Animale et Biologie Intégrative de l'INRAE [anciennement INRA]) et Infection et Immunité des Poissons (UR892 Virologie et Immunologie Moléculaire de l'INRAE [anciennement INRA]), sur la compréhension des interactions hôte-virus chez la truite arc-en-ciel (*Onchorynchus mykiss*). Ces travaux s'intègrent dans un projet pluridisciplinaire visant à mieux comprendre les bases génétiques de la résistance aux maladies, et notamment aux viroses, chez la truite arc-en-ciel, espèce d'élevage majeure en Europe et notamment en France. Ces travaux sont résumés dans une revue intégrée en annexe 1 du présent manuscrit (Verrier et al., Virologie 2013 (1)).

3.1 Introduction

La truite arc-en-ciel (*Oncorhynchus mykiss*) est l'une des espèces de poisson les mieux connues dans un grand nombre de domaines, y compris l'immunologie (2, 3). Deux Novirhabdovirus, le virus de la septicémie hémorragique virale (VSHV) et le virus de la nécrose hématopoïétique infectieuse (VNHI), sont connus pour provoquer des pertes importantes dans les élevages aquacoles (impact économique élevé) (4). Cette étude combine une approche génétique et une approche de réponse cellulaire à l'infection pour tenter de mieux comprendre les mécanismes de résistance contre ces virus majeurs. L'objectif est double : améliorer la santé des cheptels aquacoles et mieux comprendre les mécanismes d'interactions hôte-virus chez les vertébrés.

3.2 Cartographie d'un QTL majeur de résistance au VSHV

Méthode : L'objectif était d'identifier les régions du génome de la truite arc-en-ciel impliquées dans la résistance au VSHV *via* deux familles de deuxième génération issues de poissons sensibles et résistants. A l'aide de marqueurs génétiques (microsatellites), un criblage a été réalisé sur l'ensemble du génome et le génotype aux marqueurs a été corrélé à la survie des poissons.

Résultats : Mes travaux ont permis d'identifier un QTL (pour *Quantitative Trait Locus*, région chromosomique associée à la variation d'un caractère quantitatif, voir Verrier et al., Virologie 2013 (1) en annexe) majeur de résistance à la SHV expliquant jusqu'à 65% de la variance phénotypique (caractère mesuré : durée de survie après infection) (5). De plus, ce QTL contrôle à la fois la survie et la croissance virale in vitro sur explant de nageoire, confirmant au niveau du génome les observations

préliminaires indiquant une corrélation entre ce phénotype et la survie des poissons (6). Ce résultat suggère que les mécanismes majeurs de résistance au VSHV sont de nature non spécifique.

Publication associée : Verrier ER et al., PLoS One 2013;8,e55302

3.3 Approche cellulaire et importance des mécanismes innés dans la résistance au VHSV

Méthode : En parallèle de ces résultats, j'ai développé un modèle fonctionnel *in vitro* de lignées cellulaires à partir de lignées isogéniques de truites arc-en-ciel. Les lignées isogéniques avaient été précédemment obtenues au laboratoire après deux générations successives reproduites par gynogenèse (forme particulière de parthénogenèse, voir (1) en annexe) (7). Ces familles sont composées de poissons homozygotes à tous les locus et tous identiques entre eux. Les premières expériences d'infection de ces lignées par le VSHV avaient montré une grande diversité de résistance entre les différentes lignées isogéniques (7). À partir d'ovaires de poissons issus de ces lignées, j'ai dérivé des lignées cellulaires fibroblastiques immortalisées sensibles à l'infection par le virus.

Résultats : Une corrélation remarquable est observée entre la résistance à l'infection des lignées cellulaires et la survie des poissons dont elles sont issues, confirmant définitivement le rôle déterminant de mécanismes innés dans la résistance (8). Par ailleurs, l'expression précoce d'IFNΦ1 semble jouer un rôle important dans la résistance d'une des lignées. Comme chez les mammifères, les interférons (IFNs) sont des cytokines médiatrices d'une réponse antivirale précoce et non spécifique dans les cellules (9, 10). La présence dans la région du QTL d'un gène codant pour un senseur cellulaire antiviral capable d'induire les IFNs (*tlr7/8*) renforce cette hypothèse (11).

Publication associée : Verrier ER et al. PLoS One 2012;7, e33935

3.4 Combinaison des deux approches et caractérisation du QTL majeur

Méthode : L'objectif était de combiner les deux approches en validant la présence du QTL à l'aide d'un croisement entre une lignée isogénique sensible et une résistante au VHSV. En parallèle, j'ai continué de caractériser le modèle cellulaire à l'aide d'une étude transcriptomique à haut débit (RNAseq) dans les lignées cellulaires dérivées de ces deux lignées isogéniques en présence du virus.

Résultats : Cette étude confirme la présence du QTL majeur dans le backcross impliquant les deux lignées isogéniques (12). Par ailleurs, ce croisement permet de définir un intervalle de confiance du QTL et de préciser finement sa localisation. L'importance de l'expression précoces des gènes de

l'immunité innée (IFN et IFN-stimulated genes ou ISGs) dans la lignée résistante en présence de virus est également confirmée par RNAseq. Ces travaux confirment l'importance des mécanismes innés dans la résistance au VSHV et définissent un ensemble de marqueurs potentiels de résistance.

Publication associée : Verrier ER et al., BMC Genomics 2018;19:482 (en annexe 2 du manuscrit)

3.5 Absence de Corrélation entre résistance à deux rhabdovirus chez la truite arc-en-ciel

Méthode : L'objectif était d'aborder la résistance aux virus par une troisième approche, en jouant sur les variations de mécanismes de virulence entre espèces de rhabdovirus étroitement apparentées comme le VSHV et le VNHI, un autre rhabdovirus, en utilisant des méthodes statistiques d'analyse de survie *via* un logiciel dédié.

Résultats : L'infection des lignées isogéniques avec le VNHI, un virus de la même famille que le VSHV, indique qu'il n'y a pas de corrélation entre les résistances à ces infections (13). Ceci suggère l'existence de modalités distinctes d'élaboration de la résistance. Cependant les premiers résultats sur cellules semblent montrer que la résistance à ce virus dépend également de facteurs innés (Verrier 2013, https://hal.archives-ouvertes.fr/pastel-00914894). De plus de précédentes études ont indiqué les rôles primordiaux des stades précoces dans les conséquences d'une infection au VNHI chez la truite arc-en-ciel (14), suggérant des mécanismes similaires au VSHV mais à des niveaux différents.

Etudiante encadrée : Aude Ehanno (M1)

Publication associée : Verrier ER, Ehanno A et al. Fish Shellfish Immunol 2013;35(1):9-17

3.6 Conclusion et perspectives

Cette étude a démontré l'influence d'une région majeure impliquée dans la résistance au VSHV. La présence d'un QTL majeur favorise la mise en place de schémas de sélection pour la résistance à ce virus ouvrant ainsi la perspective d'une amélioration de la santé des élevages aquacoles. Le séquençage du génome de la truite représente par ailleurs une opportunité pour la caractérisation fine de la région du QTL à la recherche du ou des facteurs de résistance (15). Par ailleurs, les résultats démontrent sans équivoque le rôle clé des mécanismes innés dans la résistance de la truite à l'un de ses principaux virus. En proposant des bases nouvelles pour aborder l'analyse des interactions hôte-virus chez la truite, ils ouvrent la voie à la découverte de mécanismes potentiellement nouveaux dans la réponse des poissons à ces infections et à une meilleure compréhension de ces mécanismes chez les vertébrés.

4. INTERACTIONS HOTE-VIRUS DES HEPATITES B ET D

Ce chapitre synthétise l'ensemble des mes travaux réalisés à l'Institut de recherche sur les maladies virales et hépatiques (Université de Strasbourg, Inserm, UMR_S1110) à Strasbourg sous la direction du Pr Thomas Baumert depuis février 2013. Cette unité est internationalement reconnue pour ses contributions sur l'étude des interactions hôte-virus dans le cadre des hépatites virales humaines B, C, D. Mes travaux s'intègrent dans le programme de recherche du laboratoire visant à mieux caractériser les facteurs de l'hôte impliqués dans le cycle infectieux des virus hépatiques et leur impact sur la physiopathologie du foie.

4.1 Introduction

L'infection chronique par le virus de l'hépatite B (VHB) est une des principales causes de maladies hépatiques dans le monde et la première cause mondiale de cancer du foie (16, 17). Les patients chroniquement infectés ont 100 fois plus de chances de développer un carcinome hépatocellulaire (CHC) que les patients sains (18). Malgré l'existence d'un vaccin préventif très efficace, on estime à 2 milliards le nombre de personnes ayant été exposées au VHB et au moins 250 millions de patients sont chroniquement infectés dans le monde (16, 17). Le VHB est un petit virus enveloppé hépatotrope de la famille des *Hepadnaviridae* infectant exclusivement les hépatocytes. Il est caractérisé par un génome de petite taille présent dans les particules infectieuses sous la forme d'un ADN circulaire relâché (ADNrc) partiellement double brin de 3,2kb (19). Les virions – ou particules de Dane – de 42nm de diamètre se lient initialement à la surface les hépatocytes via l'interaction des protéines d'enveloppe (HBsAg pour *Hepatitis B surface antigen*) avec les protéoglycanes à sulfate d'héparane (HSPG) cellulaires (20, 21). Cette liaison entraine un changement de conformation d'HBsAg induisant la liaison spécifique du domaine preS1 de la grande protéine d'enveloppe au récepteur du virus, le transporteur d'acide biliaire NTCP (Pour *Na/taurocholate co-transporting polypeptide*), presqu'exclusivement exprimé à la surface basolatérale des hépatocytes et probablement responsable de l'hépatotropisme du virus (22-25). Cette interaction induit l'entrée du virus dans la cellule par endocytose selon un mécanisme encore discuté (pour une revue détaillée sur l'entrée du virus dans les hépatocytes, voir (26)). Au sein du noyau, l'ADN génomique est converti en un ADN circulaire clos de façon covalente (ADNccc) servant de matrice à la transcription de tous les ARNs viraux par l'intermédiaire de la machinerie de transcription cellulaire (27). Cet ADNccc, « minichromosome » viral associé aux histones, est le réservoir du virus responsable de la persistance virale dans les hépatocytes. Il n'est notamment pas ciblé par les traitements actuels, qui ciblent la rétrotranscription de l'ARN pré-génomique (ARNpg) en ADNrc lors de la production de nouvelles particules virales.

Ces traitements, basés sur l'utilisation de l'interféron alpha pegylé et d'analogues de nucléos(t)ides permettent le contrôle de la réplication virale mais pas l'élimination complète du virus chez un patient infecté (17). Ainsi, de nouvelles stratégies thérapeutiques permettant la clairance virale sont attendues par le monde médical.

Parmi les patients infectés par le VHB, environ 10% sont co-infectés par le virus de l'hépatite D (VHD) (28, 29). Le VHD est un petit virus à ARN, satellite du VHB, utilisant les protéines d'enveloppe du VHB pour l'assemblage de ses virions (30). Seul membre du genre des *Deltavirus*, c'est le plus petit virus connu capable d'infecter des animaux, caractérisé par un génome à ARN circulaire de polarité négative de 1,7 kb comparable à ceux de certains viroïdes de plantes (31). Partageant les protéines d'enveloppe du VHB, le VHD utilise le même récepteur NTCP à la surface des hépatocytes (25, 26). Caractérisé par un génome ne codant qu'une seule protéine, l'antigène delta (HDAg pour *hepatitis D antigen*) existant sous deux formes (« L » pour *long* et « S » pour *short*), le virus détourne les ARN polymérases cellulaires pour sa réplication, notamment l'ARN polymérase II, utilisant habituellement l'ADN comme matrice pour la transcription des ARNm (32). Pour une revue détaillée du cycle viral du VHD, voir Turon-Lagot et al., Virologie 2019 (29) en annexe du manuscrit. La co-infection par le VHD chez les patients VHB entraine une aggravation des complications hépatiques en comparaison de la mono-infection VHB, caractérisée par une plus forte probabilité d'insuffisance hépatique et une progression plus rapide de la maladie hépatique vers la cirrhose et le CHC (33). Par conséquent, l'infection chronique par VHD est considérée comme la forme d'hépatite virale la plus sévère. Comme pour le VHB, aucun traitement ne permet la clairance virale (32). Dans le contexte du développement de nouvelles stratégies antivirales, les traitements ciblant l'hôte et notamment les facteurs cellulaires impliqués dans les cycles viraux sont prometteurs (pour une revue sur les nouvelles stratégies thérapeutiques en développement contre le VHD, voir Turon-Lagot et al., Virologie 2019 (29) en annexe 3 du manuscrit). Cependant, l'absence de modèle cellulaire supportant l'infection par ces virus a longtemps limité les connaissances des mécanismes moléculaires clés des interactions hôte-virus, notamment au cours de l'entrée virale, de la formation de l'ADNccc du VHB, et de la reconnaissance du VHB par les senseurs de l'immunité innée, qui restent aujourd'hui largement méconnus. Par ailleurs, les mécanismes moléculaires impliqués dans la réplication du VHD sont largement méconnus (pour une revue sur les modèles d'études des deux virus, voir (34)).

En 2012, le transporteur d'acides biliaires NTCP a été le premier récepteur du VHB et du VHD identifié à la surface des hépatocytes (22, 23). La surexpression de NTCP dans les lignées hépatocytaires leur confère une sensibilité à l'infection (22, 23), faisant ainsi de ces lignées le premier modèle robuste d'infection pour l'étude des cycles viraux complets du VHB et du VHD. A mon arrivée

au laboratoire, le but de mon projet a été de développer les modèles cellulaires d'infection par les virus VHB et VHD (indisponibles dans la communauté scientifique à cette époque) afin de les exploiter à l'aide d'une approche multimodale pour (i) caractériser les mécanismes moléculaires de l'entrée de ces virus dans les cellules (ii) mieux comprendre les interactions entre ces virus et les hépatocytes et (iii) identifier de nouvelles cibles thérapeutiques. Comme illustré par l'exemple d'un autre virus majeur ciblant le foie, le virus de l'hépatite C (VHC), combiner des modèles d'infection haut-débit avec des outils de génomique fonctionnelle ou de criblage de petites molécules a fait progresser la compréhension des interactions hôte-virus, aboutissant à des traitements très efficaces contre l'infection par le VHC (clairance virale) (35). Le développement des nouveaux modèles d'infection couplés aux technologies à haut débit offre une opportunité unique de découvrir de nouvelles cibles thérapeutiques dont l'identification était précédemment impossible.

A mon arrivée à l'unité, ma première mission a été d'établir au laboratoire des modèles d'infection par le VHB et le VHD, basés sur la surexpression du récepteur NTCP dans des lignées cellulaires hépatiques dont elles sont naturellement dépourvues (Huh7, Huh7.5.1 et HepG2) (36-38). J'ai également supervisé la mise au point de plusieurs méthodes de production de virus VHB et VHD permettant un accès permanent à une source d'inoculum infectieux et l'optimisation des conditions d'utilisation de ces modèles, qui sont caractérisés par des temps d'infection très longs (7 jours pour le VHD, 10 jours pour le VHB), pour les adapter aux études à haut débit. L'exploitation de ces modèles fut à la base de nombreux projets de l'unité impliquant la mise en place de collaborations avec des unités de recherche nationales et internationales comme le Centre de recherche en cancérologie (CRCL) de Lyon, l'Institut national de transfusion sanguine (Paris), L'Université de Fribourg (Allemagne), ou encore le Broad Institute of MIT and Harvard (Cambrige, USA). M'appuyant sur l'expertise du laboratoire dans les interactions VHC-hépatocytes, j'ai également entretenu localement des liens étroits avec la plateforme de criblage à haut débit de l'Institut de Génétique et de Biologie Moléculaire de la Souris (IGBMC, Illkirch, Bas-Rhin). En parallèle, j'ai utilisé le modèle cellulaire hépatocytaire - exprimant NTCP - pour étudier le rôle de NTCP dans l'infection par un autre virus majeur ciblant le foie, le VHC. Cette étude, qui démontre pour la première fois qu'un facteur hépatocytaire est impliqué dans l'entrée de trois virus hépatotropes, est un pas en avant dans la compréhension des mécanismes moléculaires mis en jeu dans le cas de co-infection VHB/VHC qui sont fréquentes dans certaines catégories de patients - utilisateurs de drogues injectables notamment (voir Verrier et al., Cell Rep 2016 (39) en annexe 4 de ce manuscrit). Par ailleurs, pour la réalisation de ces projets depuis 2013, j'ai supervisé une technicienne de recherche et co-encadré 4 étudiants en thèse et un chercheur postdoctoral. Les trois articles issus de ce travail à mon sens les plus pertinents dans le cadre de ce manuscrit y sont intégrés. Les autres articles sont disponibles en annexe.

4.2 GPC5 est un facteur d'entrée du VHB et du VHD dans les hépatocytes

Dans un premier temps, j'ai ciblé l'étape de l'attachement du VHB et du VHD (virus partageant les mêmes enveloppes virales) à la surface des hépatocytes. Les protéoglycanes à sulfate d'héparane (HSPG) sont responsables de l'attachement à la surface cellulaire précédant l'interaction de ces virus avec le récepteur NTCP (20). Cependant, le/les membre(s) des HSPG responsable(s) de cet attachement étaient inconnus. En utilisant une petite banque de siRNA ciblant les principaux membres de la famille des HSPG, j'ai effectué un criblage ciblé pour évaluer le rôle des protéines des HSPG dans l'entrée du VHD, utilisé dans ce cas comme une « pseudoparticule » VHB, portant les mêmes protéines d'enveloppe. Ce criblage a permis d'identifier glypican 5 (GPC5) comme un facteur préférentiel d'attachement pour VHD à la surface des cellules (38). J'ai confirmé le rôle de GPC5 dans l'entrée virale du VHD par l'utilisation (i) d'un anticorps monoclonal ciblant GPC5 inhibant l'infection par le VHD de façon dose-dépendante et (ii) d'hépatocytes primaires humains (PHH) et du siRNA ciblant GPC5. Le rôle de GPC5 dans l'entrée du VHB a ensuite été confirmé par des méthodes similaires. J'ai par ailleurs montré que l'anticorps ciblant GPC5 inhibait l'attachement du VHD et du VHB à la surface des cellules, et que cette inhibition était levée lorsque l'anticorps était ajouté post-inoculation virale, confirmant le rôle de GPC5 dans les étapes précoces de l'attachement viral. Enfin, le prétraitement des virions VHB avec une protéine GPC5 recombinante neutralise les particules virales, inhibant ainsi leur attachement à la surface des cellules. Ce résultat confirme une interaction directe entre GPC5 et les protéines d'enveloppe du VHB et du VHD (38). Afin d'appliquer ses résultats chez les patients, l'implication de GPC5 dans l'infection a été confirmée par une approche génétique. En collaboration avec le Prof. P. Bielawski (Gdansk, POL), nous avons démontré une association entre le polymorphisme de GPC5 à un SNP et l'infection chronique par le VHB dans une cohorte composée de 161 patients chroniquement infectés et 100 patients sains contrôles (Rybicka, Verrier et al., manuscrit en préparation). Ce résultat soutient l'implication de GPC5 dans l'infection par le virus, s'il nécessite d'être confirmé dans des cohortes de plus grandes envergures et qu'il convient de valider l'effet fonctionnel de la mutation en question sur l'entrée du VHB dans les cellules. Les résultats de ces travaux identifient GPC5 comme facteur spécifique d'attachement à la surface cellulaire et valident notre approche pour l'identification de nouveaux facteurs cellulaires impliqués dans les infections VHB/VHD. Les modèles d'infection que j'ai mis au point constituent, de fait, des outils très puissants pour l'identification et la caractérisation de nouvelles interactions hôtes-virus hépatiques.

Collaborations majeures : N. Pochet (Broad Institute, Cambridge, USA) ; M. Nassal, (U. Freiburg, ALL) ; L. Brino (IGBMC, Illkirch) ; C. Sureau (INTS, Paris) ; P. Bielawski (Gdansk, POL)

Publication associée : Verrier ER, et al., Hepatology 2016;63:35-48 (en annexe 5 du manuscrit)

4.3 Etude de l'interaction entre le VHB et le senseur d'ADN cGAS

La reconnaissance du VHB par les senseurs de l'immunité innée est un domaine peu connu et controversé (40). Le VHB est aujourd'hui considéré comme un virus « silencieux », échappant aux senseurs cellulaires (40). La récente découverte de cGAS comme senseur majeur d'ADN étranger – et notamment de l'ADN des rétrovirus dont le VIH (41) – en fait un candidat de choix pour la détection de l'ADN du VHB dans les cellules infectées. Le but de ce projet a été d'étudier les interactions entre le VHB et le senseur cGAS à l'aide de nos modèles d'études, et d'un set de 32 gènes antiviraux dont l'expression est induite par l'activation de cGAS (42). Après avoir vérifié que les voies de signalisation de l'immunité innée – dont celles liées à la détection de l'ADN – étaient fonctionnelles dans nos modèles d'études, nous avons confirmé que l'infection par le VHB n'induisait pas de réponse IFN de type I ou III, ni l'expression des gènes antiviraux (ISGs) régulés par cGAS. Cependant, la transfection d'ADN génomique du VHB nu (ADNrc) induit l'expression de ces gènes. De plus, cette induction n'est plus observée dans les cellules KO pour le gène *MB21D1* (qui code pour la protéine cGAS), suggérant que cGAS peut détecter l'ADN du VHB, mais que cette détection est impossible ou empêchée durant l'infection, probablement par la protection du génome dans la capside durant le transport cytoplasmique de la particule virale. Ces observations ont été confirmées dans les PHH. En utilisant des expériences de perte- et gain- de fonction de cGAS, nous avons observé que la voie cGAS est fonctionnelle et active contre l'infection VHB. En effet, lorsque cGAS est surexprimée, la réplication et le taux d'ADNccc du VHB sont réprimés dans la cellule, faisant écho à de précédentes observations que cGAS induit une réponse antivirale à large spectre efficace contre de nombreux virus y compris en l'absence d'induction par les acides nucléiques viraux (42). De plus, cette voie de signalisation est inhibée par l'infection elle-même, comme le montre la diminution d'expression de cGAS et de ses effecteurs dans les lignées cellulaires et dans les souris chimériques infectées par le virus sur un long terme. Nos résultats suggèrent un double mécanisme d'évasion de la voie cGAS par le VHB (i) en protégeant le génome des senseurs de l'immunité au sein de la capside, (ii) en réprimant l'expression de cGAS et de ses effecteurs. Ces travaux ont permis d'identifier un nouveau mécanisme d'échappement du VHB face à la réponse antivirale, et ouvre de nouvelles pistes pour des stratégies thérapeutiques, en activant la voie cGAS/STING chez les patients à l'aide d'agonistes de cGAS par exemple.

Collaborations majeures : N. Manel (Institut Curis, Paris) ; J. Lucifora & D. Durantel (CRCL, Lyon) ; N. Pochet (Broad Institute, Cambridge, USA) ; Ivan Hirsch (Charles University, Prague, CZE)

Etudiante co-encadrée : Seung-Ae YIM (doctorante) & Laura Heydmann (étudiante M2)

Publication associée : Verrier ER, Yim SA et al., Hepatology 2018;68:1695-1709

Verrier ER, Yim SA et al., Hepatology 2018;68:1695-1709

HEPATOLOGY

HEPATOLOGY, VOL. 68, NO. 5, 2018

Hepatitis B Virus Evasion From Cyclic Guanosine Monophosphate–Adenosine Monophosphate Synthase Sensing in Human Hepatocytes

Eloi R. Verrier,[1*] Seung-Ae Yim,[1*] Laura Heydmann,[1] Houssein El Saghire,[1] Charlotte Bach,[1] Vincent Turon-Lagot,[1] Laurent Mailly,[1] Sarah C. Durand,[1] Julie Lucifora,[2] David Durantel,[2] Patrick Pessaux,[1,3] Nicolas Manel,[4,5] Ivan Hirsch,[6] Mirjam B. Zeisel,[1] Nathalie Pochet,[7] Catherine Schuster,[1*] and Thomas F. Baumert[1,3*]

Chronic hepatitis B virus (HBV) infection is a major cause of chronic liver disease and cancer worldwide. The mechanisms of viral genome sensing and the evasion of innate immune responses by HBV infection are still poorly understood. Recently, the cyclic guanosine monophosphate–adenosine monophosphate synthase (cGAS) was identified as a DNA sensor. In this study, we investigated the functional role of cGAS in sensing HBV infection and elucidate the mechanisms of viral evasion. We performed functional studies including loss-of-function and gain-of-function experiments combined with cGAS effector gene expression profiling in an infectious cell culture model, primary human hepatocytes, and HBV-infected human liver chimeric mice. Here, we show that cGAS is expressed in the human liver, primary human hepatocytes, and human liver chimeric mice. While naked relaxed-circular HBV DNA is sensed in a cGAS-dependent manner in hepatoma cell lines and primary human hepatocytes, host cell recognition of viral nucleic acids is abolished during HBV infection, suggesting escape from sensing, likely during packaging of the genome into the viral capsid. While the hepatocyte cGAS pathway is functionally active, as shown by reduction of viral covalently closed circular DNA levels in gain-of-function studies, HBV infection suppressed cGAS expression and function in cell culture models and humanized mice. *Conclusion*: HBV exploits multiple strategies to evade sensing and antiviral activity of cGAS and its effector pathways. (HEPATOLOGY 2018; 68:1695-1709).

With more than 250 million chronically infected patients, hepatitis B virus (HBV) infection is a leading cause of liver disease and hepatocellular carcinoma.[1,2] Current antiviral therapies effectively control viral load but largely fail to cure.[3] HBV is a partially double-stranded DNA (dsDNA) virus infecting human hepatocytes after initial attachment to heparan sulfate proteoglycans and its receptor Na^+/taurocholate cotransporting polypeptide (NTCP; reviewed in Verrier et al.[4]). Following uncoating, the viral nucleocapsid is released into the cytoplasm. The viral genome is imported into the nucleus through mechanisms which are still poorly understood. The viral genome is converted in the nucleus into a covalently closed circular DNA (ccc DNA).[5] This minichromosome serves as a template

Abbreviations: Cas9, CRISPR-associated 9; cccDNA, covalently closed circular DNA; cDNA, complementary DNA; cGAMP, cyclic guanosine monophosphate–adenosine monophosphate; cGAS, cyclic guanosine monophosphate–adenosine monophosphate synthase; CRISPR, clustered regularly interspaced short palindromic repeats; DIG, digoxigenin; dsDNA, double-stranded DNA; FDR, false discovery rate; FISH, fluorescence in situ hybridization; GAPDH, glyceraldehyde 3-phosphate dehydrogenase; GSEA, gene set enrichment analysis; HBsAg, hepatitis B surface antigen; HBV, hepatitis B virus; HIV, human immunodeficiency virus; IAR, innate antiviral response gene set; IFI16, IFN-γ-inducible protein 16; IFN, interferon; IFNB1, IFN beta 1; IFNL1, IFN lambda 1; ISG, IFN-stimulated gene; KO, knockout; MB21D1, Mab-21 domain-containing protein 1; MOI, multiplicity of infection; NTCP, Na^+/taurocholate cotransporting polypeptide; ORF, open reading frame; PEG, polyethylene glycol; pgRNA, pregenomic RNA; PHH, primary human hepatocyte; poly(I:C), polyinosinic:polycytidylic acid; rcDNA, relaxed circular DNA; SeV, Sendai virus; sgRNA, single-guide RNA; siRNA, small interfering RNA; STING, stimulator of IFN genes; TBK1, TANK binding kinase 1; TMEM173, transmembrane protein 173; uPA/SCID-bg, urokinase-type plasminogen activator/severe combined immunodeficient beige.

Received December 14, 2017; accepted April 18, 2018.

Additional Supporting Information may be found at onlinelibrary.wiley.com/doi/10.1002/hep.30054/suppinfo.

for both pregenomic RNA (pgRNA) and viral mRNA transcription. While recent studies have suggested sensing of the pgRNA or other HBV RNAs by either MDA5[6] or RIG-I,[7] the recognition of the viral nucleic acids by the regular pattern recognition receptors remains elusive. In general, HBV does not or does only marginally activate innate immune responses in cell culture models and *in vivo*,[8-14] leading to the concept that HBV behaves like a "stealth" virus avoiding viral DNA and RNA sensing.[15] Other studies have suggested an active inhibition of the innate immune responses by HBV proteins.[16] Consequently, the interaction of HBV and the innate immune system of hepatocytes, and in particular the sensing of HBV DNA, is only poorly understood.

Foreign DNA recognition by cytosolic DNA sensors triggers an early antiviral innate immune response, including type I and type III interferon (IFN) production.[17] Recently, the cyclic guanosine monophosphate–adenosine monophosphate (cGAMP) synthase (cGAS) was identified as a DNA sensor exhibiting antiviral activity against a broad range of DNA and RNA viruses.[18-20] cGAS is encoded by the Mab-21 domain-containing protein 1 (*MB21D1*) gene and directly binds to dsDNAs, inducing the production of cGAMP, which is recognized by the stimulator of IFN genes (STING, encoded by transmembrane protein 173 [*TMEM173*]), triggering the expression of IFN-stimulated genes (ISGs) through TANK binding kinase 1 (TBK1) activation.[21-23] While two studies have investigated cGAS–HBV interactions in viral replication and assembly,[24,25] the functional role of cGAS in sensing of the viral genome during natural infection of human hepatocytes remains unknown.

The understanding of HBV–host interactions, including the innate immune response after infection, has been hampered for a long time by the absence of a robust cell culture model system for the study of viral infection.[26] The development of HBV-susceptible NTCP-overexpressing hepatoma cells, such as HepG2-NTCP cells, allows the study of the full life cycle in a robust and easy-to-use cell culture model.[26] HepG2 cells are capable of mounting an efficient innate immune response after infection by hepatitis C virus.[27] Moreover, another study took advantage of HBV-infected HepG2-NTCP for studying the interaction

*These authors contributed equally to this work, as first authors.
**These authors contributed equally to this work, as senior authors
Supported by the European Union (ERC-AdG-2014-671231-HEPCIR, EU H2020-667273-HEPCAR, EU-InfectEra HepBccc), the National Institutes of Health (National Institute of Allergy and Infectious Diseases, 1R03AI131066-01A1 and U19AI123862; National Cancer Institute, R21 CA209940), the Agence Nationale de Recherches sur le Sida et les Hepatites Virales (ANRS, 2015/1099), the Fondation ARC pour la Recherche sur le Cancer (TheraHCC IHUARC IHU201301187, GACR 17-15422S), and a PhD fellowship of the Région Alsace, France. The work has been published under the framework of the LABEX ANR-10-LABX-0028_HEPSYS and benefits from funding from the state managed by the French National Research Agency as part of the Investments for the Future program. E.R.V. was supported by a fellowship from the ANRS (ECTZ50121).

View this article online at wileyonlinelibrary.com.
DOI 10.1002/hep.30054

Potential conflict of interest: Dr. Pessaux consults for Integra and Merck. He owns stock in Virtualisure.

ARTICLE INFORMATION:

From the [1]Université de Strasbourg, Inserm, Institut de Recherche sur les Maladies Virales et Hépatiques UMRS_1110, Strasbourg, France; [2]Inserm, U1052, Cancer Research Center of Lyon (CRCL), Université de Lyon (UCBL1), CNRS UMR_5286, Centre Léon Bérard, Lyon, France; [3]Pôle Hépato-Digestif, Institut Hospitalo-Universitaire, Hôpitaux Universitaires de Strasbourg, Strasbourg, France; [4]Immunity and Cancer Department, Institut Curie, PSL Research University, Paris, France; [5]Inserm, U932, Paris, France; [6]Department of Genetics and Microbiology, Faculty of Science, Biocev, Charles University; Institute of Organic Chemistry and Biochemistry, CAS, IOCB & Gilead Research Center, Prague, Czech Republic; [7]Ann Romney Center for Neurologic Diseases, Department of Neurology, Brigham and Women's Hospital, Harvard Medical School, Boston, MA; Cell Circuits Program, Broad Institute of MIT and Harvard, Cambridge, MA.

ADDRESS CORRESPONDENCE AND REPRINT REQUESTS TO:

Thomas F. Baumert, M.D., Catherine Schuster, Ph.D.,
or Eloi R. Verrier, Ph.D.
Inserm UMRS_1110, Institut de Recherche sur les Maladies Virales et Hépatiques
3 Rue Koeberlé
67000 Strasbourg, France
E-mail: thomas.baumert@unistra.fr,
catherine.schuster@unistra.fr, or e.verrier@unistra.fr
Tel: +33-3-68-85-37-03

between RIG-I and HBV RNA,[7] suggesting that this cell line is suitable for the study of the innate immune response after HBV infection. Here, we aimed to understand the functional role of cGAS for the HBV life cycle in human hepatocytes and unravel the mechanisms of viral evasion using loss-of-function and gain-of-function experiments combined with cGAS effector gene expression profiling in human liver chimeric mice.

Patients and Methods

HUMAN SUBJECTS

Human material including liver tissue from patients undergoing surgical resection or HBV-positive serum was obtained with informed consent from all patients. Protocols were approved by the Ethics Committee of the University of Strasbourg Hospitals, France (CPP 10-17 and DC-2016-2616).

ANIMAL EXPERIMENTATION

All mice were kept in a specific pathogen-free animal housing facility at Inserm UMRS_1110. The respective protocols were approved by the Ethics Committee of the University of Strasbourg Hospitals and authorized by the French Ministry of Research (nos. 02014120416254981AL/02/19/08/12, AL/01/18/08/1202014120416254981, 0201412051105 4408). Mice were kept in individual ventilated cages, with bedding composed of irradiated sawdust and chips from spruce and pine and enriched with cotton cocoon and aspen bricks. The animal diet consisted of 25 kGy irradiated RM3(E) (SDS) and mice were not fasted. Primary human hepatocytes (PHHs) were transplanted into 3-week-old urokinase-type plasminogen activator/severe combined immunodeficient beige (uPA/SCID-bg) mice (male and female) by intrasplenic injection as described.[28] Engraftment and viability of PHHs were assessed by quantification of human serum albumin by enzyme-linked immunosorbent assay (E80-129; Bethyl Laboratories).[28] uPA/SCID-bg mice were then infected with serum-derived HBV and sacrificed 16 weeks after virus inoculation. Serum HBV load was determined by quantitative PCR (Realtime HBV viral load kit; Abbott) before sacrifice. Interventions were all performed during light cycle.

CELL LINES AND HUMAN HEPATOCYTES

HEK 293T[29] and HepG2-NTCP[30] cells as well as isolation of PHHs have been described.[29]

REAGENTS AND PLASMIDS

Dimethyl sulfoxide (DMSO), PEG 8000 (polyethylene glycol), polyinosinic:polycytidylic acid (poly [I:C]), and calf thymus DNA (control dsDNA) were obtained from Sigma-Aldrich; pReceiver-Lv151 plasmid was from GeneCopoeia; and lentiCas9-Blast and lentiGuide-Puro plasmids were gifts from Feng Zhang (Addgene 52962 and 52963).

SMALL INTERFERING RNAs FOR FUNCTIONAL STUDIES

Pools of ON-TARGET plus (Dharmacon) small interfering RNA (siRNA) targeting *MB21D1* (cGAS), *TMEM173* (STING), *TBK1*, and IFN-γ-inducible protein 16 (*IFI16*) expression were reverse-transfected into HepG2-NTCP using Lipofectamine RNAi-MAX (Invitrogen) as described.[29] RNA was purified from cells harvested 2 days after transfection, and gene expression was analyzed using quantitative RT-PCR.

HepG2-NTCP-cGAS OVEREXPRESSING AND *MB21D1* KNOCKOUT CELLS

Lentivirus particles were generated in HEK 293T cells by cotransfection of plasmids expressing the human immunodeficiency virus (HIV) gap-pol, the vesicular stomatitis virus glycoprotein, and either the human *MB21D1* full open reading frame (ORF) encoding plasmid, the *MB21D1*-targeting single-guide RNA (sgRNA) encoding plasmids, or the clustered regularly interspaced short palindromic repeats (CRISPR)–associated 9 (Cas9) expressing plasmid, in a ratio of 10:3:10. HepG2-NTCP cells were then plated and transduced with lentivirus encoding either the human *MB21D1* ORF or the ORF of the gene for enhanced green fluorescent protein in pReceiver-Lv151 vector (GeneCopoeia) as a control. After 3 days, transduced cells were selected with 200 μg/mL of neomycin (G418). The cGAS-overexpressing and control HepG2-NTCP cells were then further cultured in the presence of G418 at 200 μg/mL. For the

generation of *MB21D1* knockout (KO) cell lines, one *MB21D1*-targeting sgRNA was designed using CRISPR Design Tool (Broad Institute, http://www.genome-engineering.org/). The sgRNA sequence targeting exon 1 of *MB21D1* (sgcGAS 5′-CACCGC GGCCCCCATTCTCGTACGG-3′) was inserted into lentiGuide-Puro plasmid.[31] We first generated Cas9-expressing HepG2-NTCP cells after transduction of cells with the lentiCas9-Blast plasmid.[31] Cells were then selected with 6 μg/mL blasticidin for 10 days. HepG2-NTCP-Cas9 cells were seeded in six-well plates at 50% confluence 24 hours prior to transduction with the sgcGAS-encoding plasmid. Subpopulations of cells were selected from the whole population and cultured independently. cGAS expression was controlled by western blot. Finally, two cGAS-KO cell lines (cGAS_KO#1 and cGAS_KO#2) were selected.

ANALYSIS OF GENE EXPRESSION USING QUANTITATIVE RT-PCR

Total RNA was extracted using ReliaPrep RNA Miniprep Systems (Promega) and reverse-transcribed into complementary DNA (cDNA) using the Maxima First Strand cDNA Synthesis Kit (Thermo Scientific) according to the manufacturer's instructions. Gene expression was then quantified by quantitative PCR using a CFX96 thermocycler (Bio-Rad). Primers and TaqMan probes for *MB21D1* (cGAS), *TMEM173* (STING), *TBK1*, *IFI16*, IFN beta 1 (*IFNB1*), IFN lambda 1 (*IFNL1*), and glyceraldehyde 3-phosphate dehydrogenase (*GAPDH*) mRNA detection were obtained from ThermoFisher (TaqMan Gene Expression Assay; Applied Biosystems). All values were normalized to *GAPDH* expression.

PROTEIN EXPRESSION

The expression of cGAS, STING, and β-actin proteins was assessed by western blot as described[30] using two polyclonal rabbit anti-cGAS antibodies (HPA031700, Sigma, and NBP1-86761, Novus Biologicals; see Supporting Information), a polyclonal rabbit anti-STING antibody (19851-1-AP; Proteintech), and a monoclonal anti-β-actin antibody (mAbcam8226; Abcam). Protein expression was quantified using ImageJ software.

INFECTION OF HepG2-NTCP CELLS AND PHHs

The purification of infectious recombinant HBV particles from HepAD38 cells and infection of HepG2-NTCP cells have been described.[30] Briefly, HepG2-NTCP and derived cells were plated 1 day prior to incubation with HBV in the presence of 4% PEG at a multiplicity of infection (MOI) of ~500 GEq/cell except where otherwise stated. Sixteen hours after HBV inoculation, cells were washed with phosphate-buffered saline and then cultured in 3.5% DMSO primary hepatocyte maintenance medium for 10 days. HBV infection was assessed by quantification of HBV pgRNA using quantitative RT-PCR or HBV total DNA using quantitative PCR as described[30] or by immunofluorescence using anti–hepatitis B surface antigen (HBsAg) antibody (1044/329; Bio-Techne) and AF647-labeled goat antibody targeting mouse immunoglobulin Gs (115-605-003; Jackson Research) as described.[30] Southern blot detection of HBV cccDNA was performed using digoxigenin (DIG)-labeled (Roche) specific probes as described.[32] Total DNA from HBV-infected cells was extracted using the Hirt method as described.[33] Specific DIG-labeled probes for the detection of HBV and mitochondrial DNAs were synthetized using the PCR DIG Probe Synthesis Kit (Roche) and the primers indicated in Supporting Table S1. PHHs were plated 1 day prior to incubation with a HBV preS1 or a control peptide for 1 hour at 37°C as described.[30] PHHs were then infected with recombinant HBV particles for 10 days. HBV infection was assessed by quantification of HBV pgRNA using quantitative RT-PCR and immunofluorescence as described above.

SENDAI VIRUS INFECTION

HepG2-NTCP cells and PHHs were infected with Sendai virus (SeV) DI-H4 at an MOI of 10 as described.[13]

EXTRACTION OF HBV RELAXED CIRCULAR DNA FROM HBV INFECTIOUS PARTICLES

HBV relaxed circular DNA (rcDNA) was extracted from HBV preparations using the QiaAMP DNA MiniKit protocol (Qiagen). PEG-precipitated cell supernatants from naive HepG2-NTCP cells were used as nonvirion controls. The presence of HBV

DNA was confirmed by PCR and quantified by quantitative PCR as described[30] (see Supporting Information). One microgram of rcDNA or dsDNA (calf thymus DNA) was transfected in cells using Lipofectamine 2000 (Invitrogen) and the CalPhos Mammalian Transfection Kit (Clontech) according to the manufacturers' instructions. Cells transfected with HepG2-NTCP control supernatants were used as a control. Three days after transfection, total RNA was extracted and purified as described above.

TRANSCRIPTOMIC ANALYSIS BY DIGITAL MULTIPLEXED GENE PROFILING USING nCOUNTER NanoString

Transcriptomic analyses using nCounter NanoString were performed according to the manufacturer's instructions. Specific probes for a set of 36 innate antiviral response-related (IAR) genes (according to Schoggins et al.[20] and additional genes listed in Supporting Table S2) were obtained from the manufacturer. HepG2-NTCP cells, HepG2-NTCP-derived cell lines, and PHHs either were infected with HBV or SeV or were transfected with poly(I:C) (100 ng) for 2 days. Alternatively, HepG2-NTCP-Cas9 and HepG2-NTCP-KO_cGAS#2 cells were transfected with rcDNA (1 μg) or dsDNA (calf thymus DNA, 1 μg) for 3 days. Total RNA was then extracted and subjected to the nCounter Digital Analyzer system (NanoString). Alternatively, total liver RNA was extracted from HBV-infected mice, and gene expression was assessed by either quantitative RT-PCR (*MB21D1* expression) or the nCounter Digital Analyzer system. The 36 genes were considered to be an artificial gene set, the IAR gene set. Its perturbation by infection, transfection, or gain-of-function/loss-of-function studies was assessed through gene set enrichment analysis (GSEA).[34] GSEA determines whether an *a priori* defined set of genes shows statistically significant differences between two biological states. A false discovery rate (FDR) < 0.05 was considered statistically significant. Heatmaps illustrating the induction (red) or repression (blue) of the genes of the IAR compared to control were illustrated using Morpheus software (Broad Institute of MIT and Harvard, Cambridge, MA). Heatmaps illustrating the induction (red) or repression (blue) of individual genes in chimeric mouse livers were designed using GenePattern (Broad Institute of MIT and Harvard).

FLUORESCENCE *IN SITU* HYBRIDIZATION ANALYSES

Fluorescence *in situ* hybridization (FISH) analyses were performed as described.[28,35] Briefly, liver samples were collected from mice and then immediately embedded into optimal cutting temperature compound (OCT). OCT-embedded liver sections were cryosectioned (10 μm) using a cryostat (Leica). Upon fixation with 4% formaldehyde at 4°C, washing, and dehydration in ethanol, tissue sections were boiled at 90°C-95°C for 1 minute in a pretreatment solution (Affymetrix-Panomics), followed by a 10-minute digestion in protease QF (Affymetrix-Panomics) at 40°C. Sections were then hybridized using specific probe sets targeting HBV (target region nucleotides 483-1473 of HBV [genotype D, GenBank V01460]) and human *MD2 1D1* (VA1-3013492-VC; Affymetrix-Panomics). Preamplification, amplification, and detection of bound probes were performed according to the manufacturer's instructions. Finally, pictures were acquired by confocal laser scanning microscopy (LSM710; Carl Zeiss Microscopy) and Zen2 software.

STATISTICAL ANALYSIS

Except where otherwise stated, cell culture experiments were performed at least 3 times in an independent manner. Statistical comparisons of the samples were performed using a two-tailed Mann-Whitney U test. For *in vivo* experiments, a two-tailed unpaired Student *t* test was performed for comparing gene expression from noninfected and HBV-infected mice. $^{*}P < 0.05$, $^{**}P < 0.01$, and $^{***}P < 0.001$ were considered significant. Significant *P* values are indicated by asterisks in the figures. Each digital multiplexed gene profiling experiment was performed using three biological replicates per condition, and the induction or repression of the gene set was analyzed using GSEA. FDR < 0.05 was considered statistically significant.

Results

EXPRESSION OF cGAS IN PHHs AND AN INFECTIOUS HBV CELL CULTURE MODEL

Prior to its functional characterization, we studied cGAS/*MB21D1* expression in primary hepatocytes and HBV permissive cell lines. cGAS protein expression was easily detectable in PHHs from three

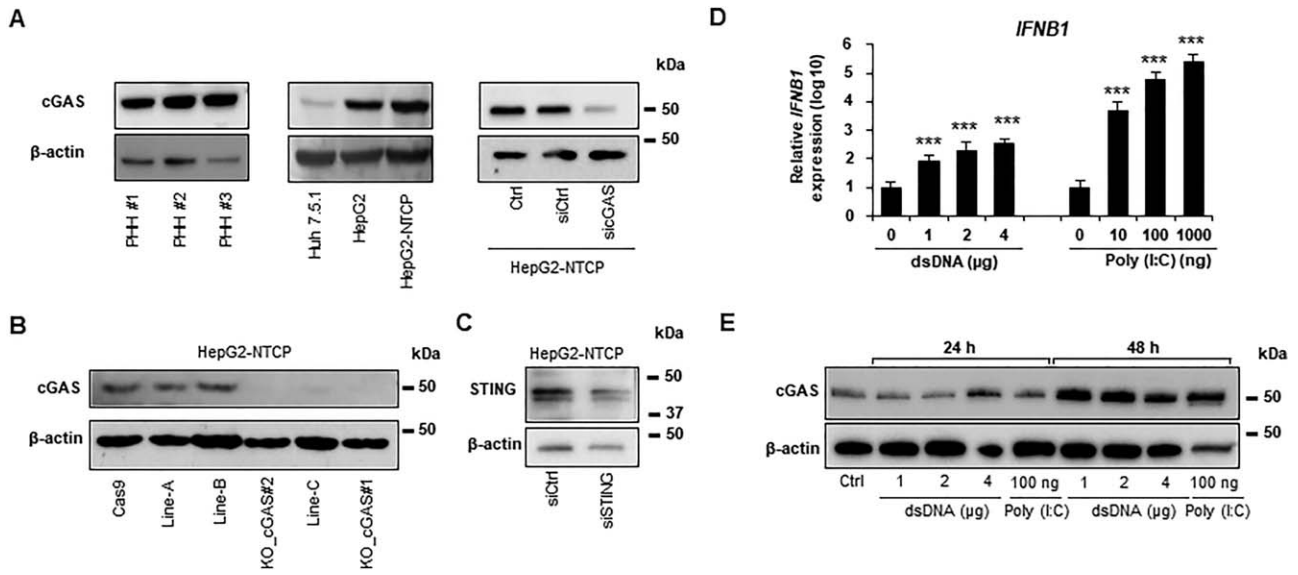

FIG. 1. cGAS expression and function in human hepatocytes and in a cell culture model for HBV infection. (A) Detection of endogenous cGAS protein expression in different cellular models by western blot. Cell lysates from PHHs from 3 independent donors, Huh7.5.1, HepG2, and HepG2-NTCP cells were used. HepG2-NTCP cells were reverse-transfected with siRNA targeting *MB21D1* (sicGAS) or a nontargeting siRNA control 2 days before cGAS detection. *β*-actin was used as a western blot control. Individual representative experiments are shown. (B) Generation of *MB21D1* KO cells. *MB21D1* KO HepG2-NTCP cell lines were generated through CRISPR/Cas9 technology. The absence or presence of cGAS protein was controlled by western blot using the HPA031700 anti-cGAS antibody in Cas9-expressing HepG2-NTCP cells (Cas9) and in different cell lines after transduction with the sgRNA targeting *MB21D1* (line-A, line-B, line-C, cGAS_KO#1, and cGAS_KO#2). One experiment is shown. (C) Detection of endogenous STING protein in HepG2-NTCP cells. siRNA targeting *TMEM173* (siSTING) or a nontargeting siRNA (siCtrl) was reverse-transfected into HepG2-NTCP cells. Silencing efficacy was assessed by western blot. One experiment is shown. (D,E) Poly(I:C) and dsDNA transfection induce *IFNB1* and *MB21D1* expression in HepG2-NTCP cells. HepG2-NTCP cells were transfected with increasing doses of poly(I:C) or calf thymus DNA at the indicated concentrations. *IFNB1* mRNA expression was quantified by quantitative RT-PCR 24 hours after transfection, and cGAS protein expression was assessed by western blot 24 and 48 hours after transfection. Quantitative RT-PCR data (D) are expressed as means ± SD relative to *IFNB1* expression (log10) compared to nontransfected control (0, set at 1) from four independent experiments performed in triplicate (dsDNA) or from three independent experiments performed in triplicate (poly I:C). One representative western blot experiment is shown (E).

independent donors (Fig. 1A). Because HBV infection of primary cells is highly variable and does not allow robust perturbation studies, we used an HBV infectious cell culture model based on differentiated hepatocyte-derived HepG2 cells overexpressing NTCP[30]—a key HBV entry factor. cGAS protein is expressed in HepG2-NTCP cells (Fig. 1A). We validated the specificity of cGAS detection using an siRNA specifically targeting the *MD21B1* expression (sicGAS) and western blots applying two antibodies (Fig. 1A; Supporting Fig. S1). Moreover, we generated CRISPR-mediated *MB21D1* KO cells using a specific sgRNA (Fig. 1B). Two cell lines, KO_cGAS#1 and KO_cGAS#2, were selected for further studies (Fig. 1B). Interestingly, the adaptor STING was also detected in HepG2-NTCP cells, suggesting a fully functional cGAS–STING pathway (Fig. 1C). To test the suitability of these cells as a model to analyze cGAS-mediated innate immune response after virus infection, we stimulated cells with different analogues of viral nucleic acids. Stimulation by poly(I:C) or dsDNA transfection elicited dose-dependent *IFNB1* expression in HepG2-NTCP cells (Fig. 1D). These results suggest that the cGAS sensing machinery is present and functional, even if it is less efficient than the RNA sensing complex. Moreover, cGAS protein expression was induced by both poly(I:C) and dsDNA stimulation, confirming an efficient IFN response through the upregulation of ISGs such as *MB21D1*[36] after RNA or DNA stimulation (Fig. 1E). Collectively, these data show that the HepG2-NTCP model is suitable to study innate immune responses.

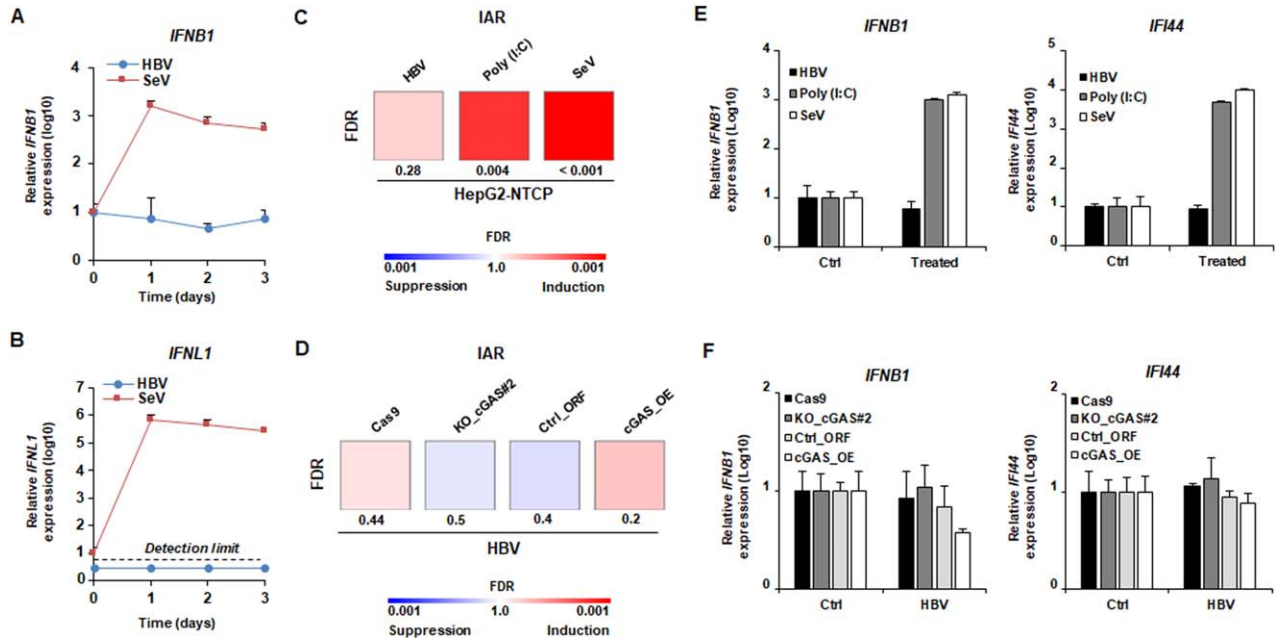

FIG. 2. Impaired cGAS-mediated sensing of HBV infection in HepG2-NTCP cells. (A,B) HBV infection does not induce *IFNB1* or *IFNL1* expression. HepG2-NTCP cells were infected with HBV (MOI, 500) or SeV (MOI, 10), and total RNA was extracted every day for 3 days. RNA extracted from naive cells before infection was used as a control (D0). *IFNB1* (A) and *IFNL1* (B) expression was then assessed by quantitative RT-PCR. Results are expressed as means ± SD *IFNB1/IFNL1* relative expression (log10) compared to controls (D0, all set at 1) from three independent experiments performed at least in duplicate (SeV) or four independent experiments performed in duplicate (HBV). No robust *IFNL1* expression was detected in HBV-infected samples (representative dots are presented under the "detection limit" dotted line). (C,E) cGAS-related ISGs are not affected by HBV infection. HepG2-NTCP cells were infected with HBV or SeV. Alternatively, HepG2-NTCP cells were transfected with poly(I:C) (100 ng). Two days after infection or transfection, total RNA was extracted. Gene expression of IAR signature was then analyzed using multiplexed gene profiling. Results were analyzed by GSEA compared to nontransfected or noninfected controls (C) or by *IFNB1* and *IFI44* gene expression (log10) compared to nontransfected or noninfected controls (set at 1) (E). One experiment performed in triplicate is shown. (D,F) The cGAS expression level does not affect the cellular response to HBV infection. HepG2-NTCP-Cas9 (Cas9), HepG2-NTCP-KO_cGAS#2 (Ko_cGAS#2), HepG2-NTCP-Ctrl_ORF (Ctrl_ORF), and HepG2-NTCP-cGAS_OE (cGAS_OE) were infected with HBV. Two days after infection, total RNA was extracted. Gene expression of IAR signature gene set was then analyzed using multiplexed gene profiling. Results were analyzed by GSEA compared to nontransfected or noninfected controls (D) or by *IFNB1* and *IFI44* gene expression (log10) compared to nontransfected or noninfected controls (set at 1) (F). One experiment performed in triplicate is shown.

HBV EVADES cGAS SENSING

Next, we investigated whether HBV was sensed in HBV permissive cells. To address this question, we infected HepG2-NTCP cells with recombinant HBV (MOI, 500 GEq/cell) and studied the expression of *IFNB1* at early time points after HBV infection. Because it has been described that HBV infection may induce the expression of type III IFN,[7] *IFNL1* expression was also quantified. The lack of increase in *IFNB1* and *IFNL1* expression despite efficient infection (Supporting Fig. S2) indicates poor or absent detection of HBV by cellular sensors (Fig. 2A,B). In contrast, SeV, known to induce a strong IFN response in hepatocytes,[13] strongly induced *IFNB1* and *IFNL1* expression (Fig. 2 A, B). Because cGAS has been shown to induce the expression of a large set of innate effector genes (such as *OAS2* and *IFI44*, see Schoggins et al.[20]), the analysis of expression of a single effector gene such as *IFNB1* may not be sufficient to evaluate cGAS sensing. Therefore, we designed a 36 IAR gene set, comprising 29 ISGs whose expression is modulated by cGAS activity described by Schoggins et al.[20] as well as seven established innate immune response effector genes (Supporting Table S2). We then infected HepG2-NTCP cells with HBV or SeV and measured the innate antiviral immune response at day 2 postinfection by analysis of IAR gene

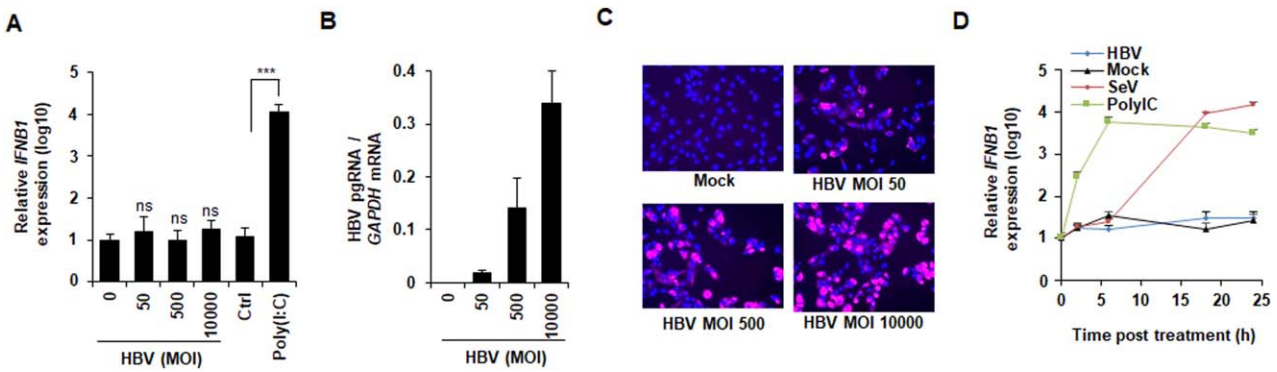

FIG. 3. Impaired sensing of HBV infection at high MOIs or early time points of infection. (A-C) HepG2-NTCP cells were infected with HBV at increasing MOIs (0, 50, 500, and 10,000 GEq/cell) or transfected with poly(I:C) (100 ng). Two days after infection or transfection, cells were lysed, total RNA was extracted, and *IFNB1* expression (A) as well as HBV pgRNA levels (B) were quantified by quantitative RT-PCR. (A) Results are expressed as means ± SD relative to *IFNB1* expression (log10) compared to mock infected cells (MOI 0, set at 1) from three independent experiments performed in triplicate. (B) Results are expressed means ± SD relative to HBV pgRNA levels compared to mock infected cells (MOI 0, set at 100%) from three independent experiments performed in triplicate. Alternatively, HBV infection was assessed at 10 days postinfection by immunofluorescence of HBsAg (C). One representative experiment is shown. (D) HBV infection does not induce *IFNB1* expression at early time points. HepG2-NTCP cells were either infected by HBV or SeV or transfected with poly(I:C). Total RNA was extracted at 2, 6, 18, and 24 hours postinfection/posttransfection, and *IFNB1* expression was assessed by quantitative PCR. Results are expressed as means ± SD relative to *IFNB1* expression (log10) compared to naive cells (0, set at 1) from three independent experiments performed in triplicate.

expression using digital multiplexed gene profiling (nCounter NanoString) and GSEA-based analysis. Whereas poly(I:C) transfection and SeV infection induced a marked modulation of cGAS effector/IAR gene expression (FDR, 0.004 and <0.001, respectively), no significant modulation of IAR gene expression was observed in HBV-infected cells (Fig. 2C), as further illustrated by the expression of *IFNB1* and *IFI44* (Fig. 2E). To measure the impact of cGAS expression on the cellular response to HBV infection, we then infected cGAS-depleted (KO_cGAS#2) and cGAS-overexpressing (cGAS_OE) HepG2-NTCP cells with HBV and analyzed the expression of the cGAS-related genes after infection. No significant modulation of the IAR signature was observed in HBV-infected samples (Fig. 2D), as further illustrated by absent modulation of *IFNB1* and *IFI44* expression (Fig. 2F).

To exclude the possibility that low HBV infection could be the reason for the absence of IFN induction, we performed additional experiments using increasing MOIs. No induction of *IFNB1* (Fig. 3A) was observed even at an MOI of 10,000, despite very high infection efficiency as shown by quantitation of pgRNA and immunofluorescence of HBsAg (Fig. 3B,C). To investigate whether IFN induction occurs potentially at a very early step of viral infection and was missed in the experimental design shown above, we performed a time course study of the IFN response to HBV within the first 24 hours postinfection. HBV infection did not induce a measurable IFN response during early steps of HBV infection (Fig. 3D). In contrast, SeV, an established inducer of IFN, showed robust induction of IFN responses in HepG2-NTCP cells (Fig. 3D). Taken together, these data suggest an absence of sensing of HBV infection by the cGAS–STING pathway in HepG2-NTCP cells.

Because the HBV genome is packaged into the nucleocapsid,[37] we investigated whether packaging shields virion DNA from cGAS recognition. We purified HBV genomic rcDNA from HBV infectious particles (Supporting Fig. S3) and transfected the naked viral genome into HepG2-NTCP cells (1 μg, corresponding to approximately 10^6-10^7 HBV DNA copies/μL). A significant (FDR, 0.02) induction of the IAR signature (illustrated by *IFNB1* and *IFI44* expression, Fig. 4B) was observed after both rcDNA and dsDNA transfection, suggesting sensing of the naked HBV genome (Fig. 4A). Interestingly, the number of cellular HBV DNA copies was higher in HBV-infected cells compared to rcDNA-transfected cells (Fig. 4C), confirming that the levels of HBV DNA in

HBV-infected cells are sufficient to trigger IFN signaling and that the absence of HBV sensing in infected cells was not due to low MOIs. Moreover, induction of IAR gene expression was absent in HepG2-NTCP-KO_cGAS#2 cells, suggesting a cGAS-specific activation of innate immunity by both dsDNA and rcDNA transfection in our model.

To validate these observations in a more physiological model, we infected PHHs with HBV and controlled cGAS gene expression after 2 days of infection. Interestingly, while SeV strongly induced IAR gene expression (Fig. 5B), a highly efficient HBV infection (Fig. 5A) did not induce the expression of IAR genes (Fig. 5B). In contrast, the transfection of rcDNA and dsRNA into PHHs from 4 different donors robustly triggered the expression of *IFNB1* and *IFNL1* (Fig. 5C), suggesting a robust sensing of viral DNA in human hepatocytes. Collectively, these data suggest that nonencapsidated HBV DNA is sensed by cGAS but that this sensing is impaired during HBV infection.

THE cGAS–STING PATHWAY EXHIBITS ROBUST ANTIVIRAL ACTIVITY AGAINST HBV INFECTION WITH REDUCTION OF cccDNA LEVELS

Because cGAS exhibits antiviral activity against a broad range of DNA and RNA viruses (even in the absence of direct viral sensing),[20] we then investigated the antiviral effect of the cGAS–STING signaling pathway in HBV infection. We silenced the expression *MB21D1*, *TMEM173* (encoding the STING protein), *TBK1*, and *IFI16* (another cytoplasmic DNA sensor able to directly activate STING[17]) in HepG2-NTCP cells prior to infection with HBV. Silencing of *MB21D1*, *TMEM173*, and *TBK1* expression induced a marked increase in HBV infection (Fig. 6A,B). In contrast, the silencing of *IFI16* had no effect on HBV infection. CRISPR/Cas9-mediated KO or overexpression of cGAS protein resulted in a marked increase or decrease in HBV infection and HBV cccDNA levels—the key viral nucleic acid responsible for viral persistence (Fig. 6C-E). Notably, overexpression of cGAS did not affect NTCP expression at the cell surface, suggesting that the susceptibilities of the different cell lines to HBV infection are equivalent (Supporting Fig. S4). Taken together, our results suggest that cGAS is functional and exerts antiviral activity in HBV permissive cells.

HBV INFECTION INDUCES REPRESSION OF cGAS AND ITS EFFECTOR GENE EXPRESSION IN CELL CULTURE AND IN LIVER CHIMERIC MICE

Because several reports have suggested that HBV proteins can inhibit IFN-signaling pathways,[16] we next investigated whether HBV infection interferes with the expression of cGAS-related genes by quantifying *MB21D1*/cGAS mRNA and protein expression (Fig. 7A,B). Interestingly, cGAS protein expression (Fig. 7B) as well as expression of *MB21D1*, *TMEM173*, and *TBK1* mRNA (Fig. 7C) were significantly inhibited in HBV-infected cells. To confirm this observation *in vivo*, we then investigated the expression of human *MB21D1* expression in HBV-infected human liver chimeric mice. *MB21D1* was expressed at low but detectable levels (Fig. 7D). *MB21D1* expression was significantly ($P = 0.013$) down-regulated in HBV-infected mice compared to noninfected control mice, confirming our results in the cell culture model (Fig. 7E). Importantly, *MB21D1* expression levels did not correlate with HBV genotype (Table 1). An absent correlation of human serum albumin with either *MB21D1* expression (Table 1 and Fig. 7E) or status of HBV infection (Table 1; *t* test HBV versus control, $P = 0.26$) largely excludes the possibility that the observed differences in cGAS expression are due to different human hepatocyte repopulation levels or to a decrease of human hepatocyte cell viability in individual animals. To investigate whether HBV modulates cGAS effector function, we analyzed virus-induced changes on cGAS effector gene expression using gene expression profiling in three control mice and the three HBV-infected mice exhibiting the lowest levels of *MB21D1* expression (Table 1). HBV infection resulted in a significant (FDR, 0.047) down-regulation of the expression of cGAS effector genes in human hepatocytes in chimeric mice (Fig. 7F). The data showed that HBV represses expression of cGAS and its effector genes *in vivo*.

Discussion

The interaction between HBV and the innate immune system is a complex process that remains elusive and controversial.[15] Collectively, our data demonstrate that in human hepatocytes (1) naked HBV genomic rcDNA is sensed in a cGAS-dependent manner, whereas the packaged HBV genome appears not

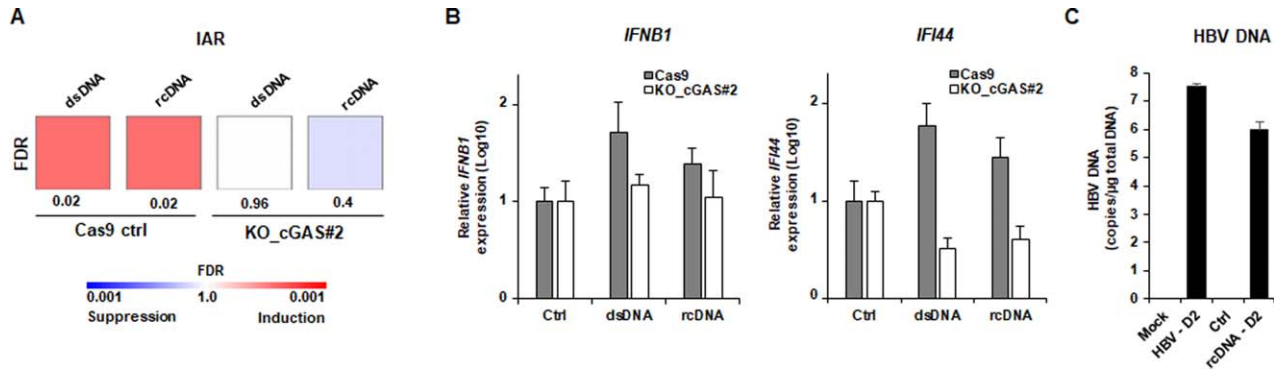

FIG. 4. Sensing of HBV rcDNA in HepG2-NTCP cells. (A,B) Transfection of purified HBV rcDNA genome induces a cGAS-mediated innate immune response. HBV rcDNA was extracted from recombinant HBV virions as described in Patients and Methods and quantified by quantitative PCR (Supporting Fig. S3). HBV rcDNA (1 μg) and positive control dsDNA (1 μg) were transfected into HepG2-NTCP-Cas9 and HepG2-NTCP-KO_cGAS#2 cells. Three days after transfection, total RNA was extracted. Gene expression of IAR set was then analyzed using multiplexed gene profiling. The transcripts were analyzed by GSEA compared to non-transfected control (A) or by *IFNB1* and *IFI44* gene expression (log10) compared to nontransfected control (set at 1) (B). One experiment in triplicate is shown. (C) HBV DNA in HepG2-NTCP cells after rcDNA transfection and HBV infection are similar. HepG2-NTCP cells were infected with HBV or transfected with HBV rcDNA (1 μg). At day 2 after transfection/infection, DNA was extracted and total HBV DNA was quantified by quantitative PCR. Results are expressed as means ± SD total DNA copies per microgram of total DNA (log10) from three independent experiments performed in triplicate (HBV infection) and two independent experiments performed in triplicate (HBV rcDNA transfection).

to be recognized during viral infection; (2) the cGAS–STING pathway exhibits antiviral activity against HBV infection including reduction of viral cccDNA levels; (3) HBV infection suppresses both cGAS expression and function in cell culture and humanized liver chimeric mice.

The detection of HBV DNA by the cellular sensors within infected cells is still poorly understood and

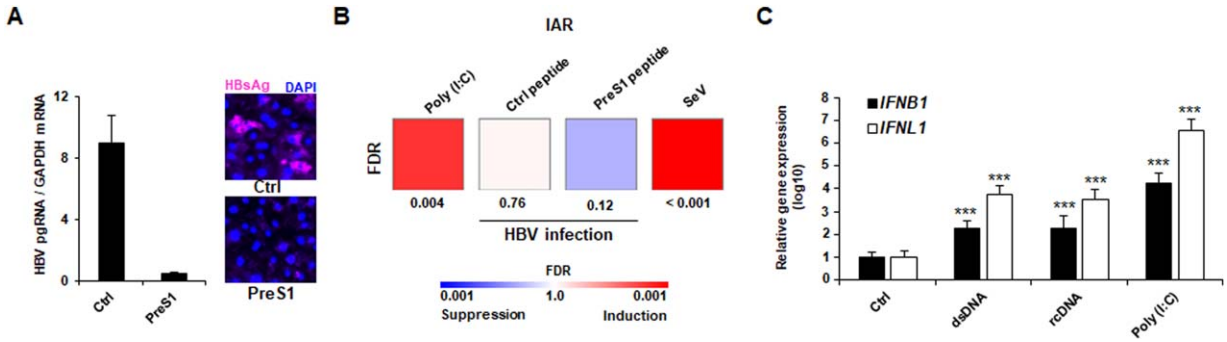

FIG. 5. Sensing of naked HBV rcDNA but not infectious HBV virions in PHHs. (A,B) HBV infection does not induce ISG expression in PHHs. PHHs were treated with a preS1 peptide or a scrambled peptide (control) for 1 hour before infection with HBV. As positive controls, PHHs were transfected with poly(I:C) (100 ng) or infected with SeV (MOI ~10). HBV infection of PHHs was assessed 10 days postinfection by quantitative RT-PCR (A, left panel) or immunofluorescence (A, right panel). Quantitative RT-PCR results are expressed as means ± SD ratio HBV pgRNA RNA/GAPDH mRNA from one experiment corresponding to the gene profiling experiment and performed in duplicate. Two days after infection, total RNA was extracted, and gene expression of IAR was then analyzed using multiplexed gene profiling. Results were analyzed by GSEA compared to nontransfected control (B). One experiment in triplicate is shown. (C) Induction of *IFBN1* and *IFNL1* expression in PHHs. PHHs were transfected with dsDNA (4 μg) or HBV rcDNA (4 μg). *IFNB1* and *IFNL1* expression was assessed 24 hours after transfection by quantitative RT-PCR. Results are expressed as means ± SD log10 *IFNB1* or *IFNL1* expression compared to nontransfected control cells (set at 1) from five independent experiments performed at least in duplicate. Abbreviation: DAPI, 4',6-diamidino-2-phenylindole.

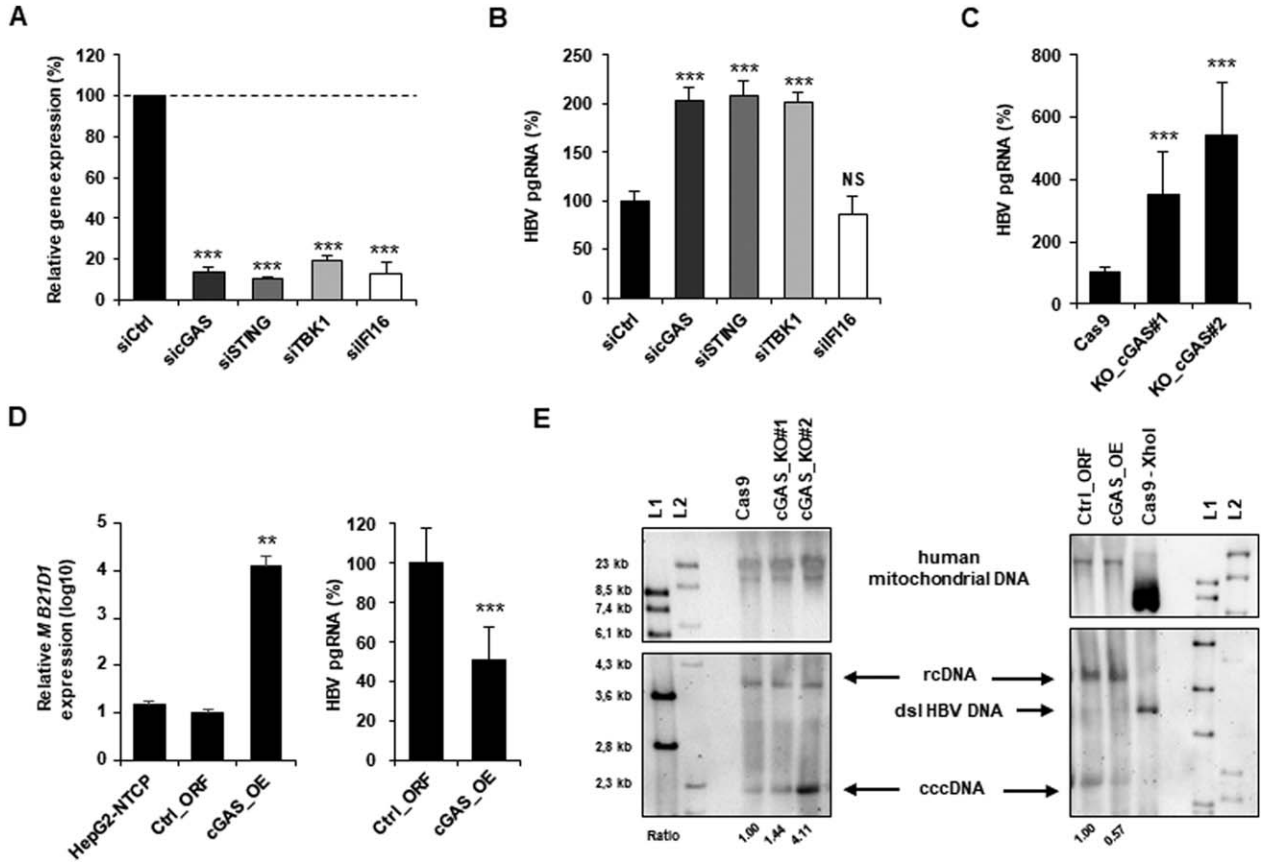

FIG. 6. Antiviral activity of cGAS results in reduction of HBV cccDNA. (A,B) Silencing of cGAS-related gene expression increases HBV infection. siRNA targeting *MB21D1* (sicGAS), *TMEM173* (siSTING), *TBK1* (siTBK1), or *IFI16* (siIFI16) or a nontargeting siRNA (siCtrl) were reverse-transfected into HepG2-NTCP cells 2 days prior to HBV infection. Silencing efficacy was assessed by quantitative RT-PCR 2 days after transfection (A). Results are expressed as means ± SD percentage gene expression relative to siCtrl (set at 100%) from four independent experiments performed in technical duplicate. HBV infection was assessed by quantification of HBV pgRNA by quantitative RT-PCR 10 days after infection (B). Results are expressed as means ± SD percentage HBV pgRNA expression relative to siCtrl (set at 100%) from four independent experiments performed in technical duplicate. (C) KO of *MB21D1* gene increases HBV infection. cGAS_KO#1, cGAS_KO#2, and control Cas9 cells were then infected with HBV; and viral infection was assessed 10 days after infection as described above. Results are expressed as means ± SD percentage HBV pgRNA expression relative to control cell line (Cas9, set at 100%) from three independent experiments performed in triplicate. (D) cGAS overexpression reduces HBV infection. HepG2-NTCP cells were transduced with lentivirus encoding either a control plasmid (Ctrl_ORF) or a plasmid encoding the full-length *MB21D1* ORF (cGAS_OE). *MB21D1* expression was assessed by quantitative RT-PCR (left panel). Results are expressed as means ± SD percentage relative *MB21D1* expression (log10) relative to control cell line (Ctrl_ORF, set at 1) from three independent experiments performed in duplicate. HepG2-NTCP, Ctrl_ORF, and cGAS_OE cells were then infected with HBV for 10 days, and HBV infection was assessed as described above. Results are expressed as means ± SD percentage HBV pgRNA expression relative to control cell line (Ctrl_ORF, set at 100%) from three independent experiments performed in triplicate. (E) Detection of HBV cccDNA by Southern blot. HepG2-NTCP-derived cGAS_KO or cGAS_overexpressing cell lines were infected for 10 days with HBV. Total DNA from indicated HBV-infected cells was extracted, and HBV DNA was detected by Southern blot. Two different DNA ladders (L1, L2) were used. *XhoI* digestion of DNA extracted from HBV-infected HepG2-NTCP-Cas9 cells was used as a control and resulted in a single 3.2-kb band (dsl HBV DNA). Mitochondrial DNA was detected as a loading control. One experiment is shown. Abbreviations: NS, nonsignificant; OE, overexpressing.

remains controversial. *In vitro* and *in vivo* data strongly suggest that HBV behaves like a stealth virus, unable to trigger any innate immune response.[8,9,11] Other studies have suggested that HBV-derived dsDNA fragments[25] and viral nucleocapsid destabilization and disassembly[38,39] could induce innate immune responses. Our results demonstrate that in human hepatocytes—the natural target cell of HBV infection—exposure of the naked HBV genome leads to the activation of innate antiviral immune

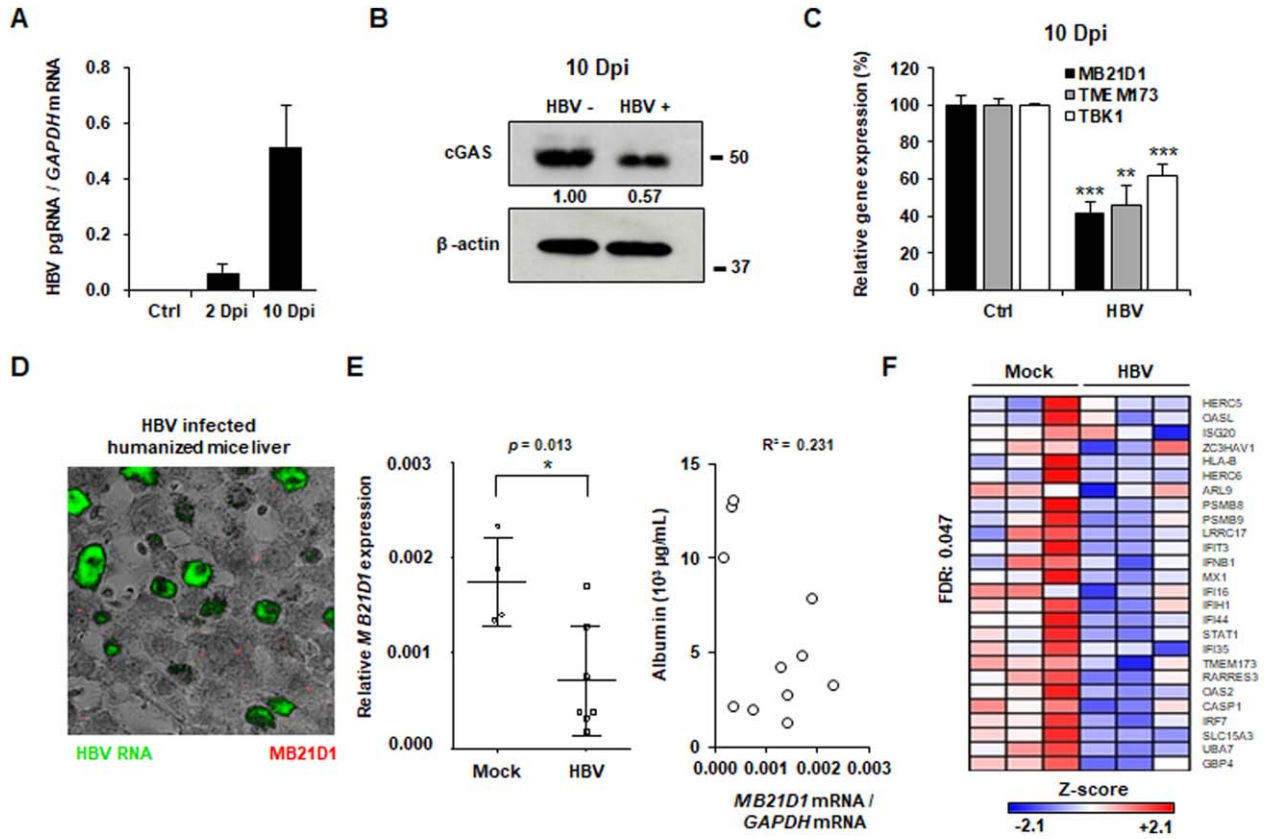

FIG. 7. HBV infection suppresses expression of the cGAS-related gene cell culture and humanized liver chimeric mice *in vivo*. (A-C) HepG2-NTCP cells were infected with HBV for 10 days. HBV infection was assessed by quantification of HBV pgRNA by quantitative RT-PCR. Results are expressed as means ± SD from three experiments performed in triplicate. cGAS protein expression was assessed 10 days after infection (B, one experiment is shown). Gene expression relative to noninfected control cells of *MB21D1*, *TMEM173*, and *TBK1* was assessed by quantitative RT-PCR at day 10 after infection (C). Results are expressed as means ± SEM from three independent experiments performed in triplicate. (D,E) *MB21D1* and IAR gene set expression is impaired in HBV-infected mice. uPA-SCID mice were infected with HBV for 16 weeks. Mice were then sacrificed, and HBV infection was assessed by HBV RNA–specific *in situ* hybridization (D) and quantification of HBV viral load in the serum (Table 1). Human *MB21D1* expression was detected in human hepatocytes by FISH from one HBV-infected mouse (D) and by quantitative RT-PCR from seven HBV-infected mice and four control mice (E, left panel). Results are expressed as the ratio *MB21D1* mRNA/*GAPDH* mRNA. All individual mice are presented as well as means ± SD for each group (mock and HBV-infected mice). The level of *MB21D1* expression was independent of the viability of engrafted human hepatocytes as indicated by an absent correlation between *MB21D1* expression and human serum albumin expression in humanized mice (R^2 = 0.231; E, right panel). (F) The IAR gene set was analyzed using the nCounter NanoString in mice 6472, 6251, and 6254 (mock infected mice, Table 1) and 4766, 4771, and 4847 (HBV-infected mice, Table 1). A significant down-regulation (FDR, 0.047) of the gene set was observed in HBV-infected mice compared to control mice. Individual Z scores for the genes significantly modulated between the two groups according to GSEA are presented. Negative Z score (blue) and positive Z score (red) correspond to repression and induction of the indicated genes, respectively. Abbreviation: Dpi, days postinfection.

responses. In contrast, sensing is largely absent during HBV infection, most likely due to packaging into the viral capsid. These results extend a previous observation in hepatoma cell lines transfected with replication-competent HBV DNA that the HBV genome itself can be recognized by the classical sensors.[25]

Interestingly, the capsid of HIV-1 also prevents the sensing of HIV cDNA by cGAS following reverse-transcription up to integration, whereas HIV-2 capsid may unmask the cDNA, leading to a stronger sensing by cGAS and a lower pathogenicity of the strain.[40]

Another explanation of this absence of sensing would be the lack a functional STING protein in hepatocytes, as has been recently reported.[41] In our study, rcDNA and dsDNA were sensed in a cGAS-dependent manner and able to activate the cGAS-

TABLE 1. cGAS Expression in HBV-Infected Human Liver Chimeric Mice

	Mouse	Albumin (μg/mL)	HBV (IU/mL)	*MB21D1* mRNA
Control	6410	1,280	—	1.40E-03
	6472	2,720	—	1.40E-03
	6251	3,240	—	2.30E-03
	6254	7,870	—	1.90E-03
HBV				
Gt E	4770	4,200	2.9E+07	1.30E-03
	4773	4,800	1.5E+08	1.70E-03
	4766	12,760	3.6E+06	3.20E-04
	4771	13,120	6.2E+05	3.70E-04
Gt D	4846	2,127	5.5E+05	3.80E-04
	4847	10,045	1.6E+08	1.70E-04
	4848	1,992	6.7E+06	7.50E-04

Levels of human albumin, HBV viral load, and *MB21D1* in liver tissue from HBV-infected and control mice are shown. *MB21D1* expression is normalized to *GAPDH* expression. The HBV genotype is indicated. Bold indicates mice used for multiplexed gene profiling.
Abbreviation: Gt, genotype.

mediated antiviral response in HepG2-NTCP cells (Fig. 4). Moreover, we detected STING at the protein level, in accordance with a recent study[42]; and specific silencing of *TMEM173* (STING) expression was associated with a significant increase in HBV infection (Fig. 6). Consequently, it is likely that STING is functionally active in HepG2 cells. The observed HBV DNA sensing in PHHs (Fig. 5) suggests that the foreign DNA detection pathways are active in PHHs as well. This observed innate immune response despite weak STING expression may suggest a STING-independent activity of cGAS, as has been recently reported,[43] including in hepatocytes.[44] To understand the impact of cGAS and STING expression on the innate immune response to HBV infection, it would be of further interest to analyze the HBV-induced modulation of gene expression in Kupffer cells following phagocytosis as they exhibit higher STING and cGAS levels compared to hepatocytes[41,45] and respond to HBV infection.[11] In the same vein, cGAMP has been shown to be packaged in viral particles.[46] It would be of interest to determine whether HBV particles can incorporate cGAMP during viral assembly and to test their ability to stimulate other cell types through this indirect pathway.

Moreover, our results show conclusively that cGAS basal expression has antiviral activity against HBV infection including reduction of viral cccDNA. This finding extends previous studies showing that cGAS exhibited antiviral activity against a broad range of RNA and DNA viruses[20] and that the cGAS–STING pathway can impair HBV replication and assembly in transfection studies.[24,25] Schoggins and colleagues proposed that expression of cGAS may be responsible for the establishment of a basal antiviral level in cells through its activation by an unknown ligand. cGAS-depleted cells may then be more susceptible to viral infections through the down-regulation of the basal level of innate antiviral genes.[20]

Given its antiviral function, cGAS is a target of choice for viruses in order to evade immune responses. It has been reported that the Kaposi's sarcoma–associated herpesvirus negatively regulated the cGAS-dependent signaling pathway.[47,48] In the same vein, HBV viral proteins have been shown to interfere with the Janus kinase–signal transducer and activator of transcription signaling pathway.[16] Our data suggest that HBV can repress expression of the cGAS and its related genes, such as *MB21D1*, *TMEM173*, and *TBK1*. More interestingly, *MB21D1* expression was down-regulated in the liver of HBV-infected mice, validating the relevance of these findings *in vivo*. It still needs to be determined whether HBV can directly target cGAS and cGAS-related factors for an active inhibition of this signaling pathway. A recent study elegantly demonstrated an active inhibition of the cGAS pathway by dengue virus through nonstructural protein 2B.[49] On the other hand, *MB21D1* (as a classical member of the ISGs[20,36]) down-regulation may be the consequence of global inhibition of the canonical IFN pathways by HBV, as suggested by some investigators[16,50] but not by others.[11,13,14] Given the antiviral activity of the cGAS-signaling pathway against HBV including reduction of HBV cccDNA (Fig. 6),[24,25] the virus-mediated restriction of *MB21D1* expression may play an additional role in HBV immune evasion.

Acknowledgment: We thank D. Garcin (University of Geneva, Geneva, Switzerland) for providing the SeV inoculum; D. Calabrese, S. Wieland, and M. Heim (University of Basel, Basel, Switzerland) for the FISH analyses and helpful discussions; F. Zhang (Broad Institute of MIT and Harvard, Cambridge, MA) for lentiCas9-Blast and lentiGuide-Puro plasmids; C. Thumann, N. Brignon, and M. Oudot (Inserm UMRS_1110) for excellent technical support; and J.M. Rousée (Laboratoire Schuh-groupement Bio 67, Strasbourg, France) for the quantification of HBV loads in sera of humanized mice.

REFERENCES

1) Trepo C, Chan HL, Lok A. Hepatitis B virus infection. Lancet 2014;384:2053-2063.
2) **Zeisel MB**, **Lucifora J**, Mason WS, Sureau C, Beck J, Levrero M, et al. Towards an HBV cure: state-of-the-art and unresolved questions-report of the ANRS workshop on HBV cure. Gut 2015;64:1314-1326.
3) Levrero M, Testoni B, Zoulim F. HBV cure: why, how, when? Curr Opin Virol 2016;18:135-143.
4) Verrier ER, Colpitts CC, Sureau C, Baumert TF. Hepatitis B virus receptors and molecular drug targets. Hepatol Int 2016;10: 567-573.
5) Nassal M. Hepatitis B virus cccDNA—viral persistence reservoir and key obstacle for a cure of chronic hepatitis B. Gut 2015;64: 1972-1984.
6) Lu HL, Liao F. Melanoma differentiation-associated gene 5 senses hepatitis B virus and activates innate immune signaling to suppress virus replication. J Immunol 2013;191:3264-3276.
7) **Sato S**, **Li K**, **Kameyama T**, **Hayashi T**, Ishida Y, Murakami S, et al. The RNA sensor RIG-I dually functions as an innate sensor and direct antiviral factor for hepatitis B virus. Immunity 2015;42:123-132.
8) Wieland S, Thimme R, Purcell RH, Chisari FV. Genomic analysis of the host response to hepatitis B virus infection. Proc Natl Acad Sci USA 2004;101:6669-6674.
9) Wieland SF, Chisari FV. Stealth and cunning: hepatitis B and hepatitis C viruses. J Virol 2005;79:9369-9380.
10) Fletcher SP, Chin DJ, Ji Y, Iniguez AL, Taillon B, Swinney DC, et al. Transcriptomic analysis of the woodchuck model of chronic hepatitis B. HEPATOLOGY 2012;56:820-830.
11) Cheng X, Xia Y, Serti E, Block PD, Chung M, Chayama K, et al. Hepatitis B virus evades innate immunity of hepatocytes but activates macrophages during infection. HEPATOLOGY 2017; 66:1779-1793.
12) **Luangsay S**, **Gruffaz M**, Isorce N, Testoni B, Michelet M, Faure-Dupuy S, et al. Early inhibition of hepatocyte innate responses by hepatitis B virus. J Hepatol 2015;63:1314-1322.
13) Suslov A, Boldanova T, Wang X, Wieland S, Heim MH. Hepatitis B virus does not interfere with innate immune responses in the human liver. Gastroenterology 2018;154:1778-1790.
14) Mutz P, Metz P, Lempp FA, Bender S, Qu B, Schoneweis K, et al. HBV bypasses the innate immune response and does not protect HCV from antiviral activity of interferon. Gastroenterology 2018;154:1791-1804.
15) Ferrari C. HBV and the immune response. Liver Int 2015; 35(Suppl. 1):121-128.
16) Bertoletti A, Ferrari C. Innate and adaptive immune responses in chronic hepatitis B virus infections: towards restoration of immune control of viral infection. Gut 2012;61:1754-1764.
17) Chan YK, Gack MU. Viral evasion of intracellular DNA and RNA sensing. Nat Rev Microbiol 2016;14:360-373.
18) Gao D, Wu J, Wu YT, Du F, Aroh C, Yan N, et al. Cyclic GMP-AMP synthase is an innate immune sensor of HIV and other retroviruses. Science 2013;341:903-906.
19) **Sun L**, **Wu J**, Du F, Chen X, Chen ZJ. Cyclic GMP-AMP synthase is a cytosolic DNA sensor that activates the type I interferon pathway. Science 2013;339:786-791.
20) Schoggins JW, MacDuff DA, Imanaka N, Gainey MD, Shrestha B, Eitson JL, et al. Pan-viral specificity of IFN-induced genes reveals new roles for cGAS in innate immunity. Nature 2014;505:691-695.
21) Xiao TS, Fitzgerald KA. The cGAS–STING pathway for DNA sensing. Mol Cell 2013;51:135-139.
22) **Zhang X**, **Shi H**, Wu J, Sun L, Chen C, Chen ZJ. Cyclic GMP-AMP containing mixed phosphodiester linkages is an endogenous high-affinity ligand for STING. Mol Cell 2013;51: 226-235.
23) **Wu J**, **Sun L**, Chen X, Du F, Shi H, Chen C, et al. Cyclic GMP-AMP is an endogenous second messenger in innate immune signaling by cytosolic DNA. Science 2013;339:826-830.
24) He J, Hao R, Liu D, Liu X, Wu S, Guo S, et al. Inhibition of hepatitis B virus replication by activation of the cGAS–STING pathway. J Gen Virol 2016;97:3368-3378.
25) Dansako H, Ueda Y, Okumura N, Satoh S, Sugiyama M, Mizokami M, et al. The cyclic GMP-AMP synthetase-STING signaling pathway is required for both the innate immune response against HBV and the suppression of HBV assembly. FEBS J 2016;283:144-156.
26) Verrier ER, Colpitts CC, Schuster C, Zeisel MB, Baumert TF. Cell culture models for the investigation of hepatitis B and D virus infection. Viruses 2016;8:E261.
27) Israelow B, Narbus CM, Sourisseau M, Evans MJ. HepG2 cells mount an effective antiviral interferon-lambda based innate immune response to hepatitis C virus infection. HEPATOLOGY 2014;60:1170-1179.
28) Mailly L, Xiao F, Lupberger J, Wilson GK, Aubert P, Duong FH, et al. Clearance of persistent hepatitis C virus infection in humanized mice using a claudin-1-targeting monoclonal antibody. Nat Biotechnol 2015;33:549-554.
29) **Lupberger J**, **Zeisel MB**, Xiao F, Thumann C, Fofana I, Zona L, et al. EGFR and EphA2 are host factors for hepatitis C virus entry and possible targets for antiviral therapy. Nat Med 2011; 17:589-595.
30) Verrier ER, Colpitts CC, Bach C, Heydmann L, Weiss A, Renaud M, et al. A targeted functional RNAi screen uncovers glypican 5 as an entry factor for hepatitis B and D viruses. HEPATOLOGY 2016;63:35-48.
31) **Sanjana NE**, **Shalem O**, Zhang F. Improved vectors and genome-wide libraries for CRISPR screening. Nat Methods 2014;11:783-784.
32) Lucifora J, Salvetti A, Marniquet X, Mailly L, Testoni B, Fusil F, et al. Detection of the hepatitis B virus (HBV) covalently-closed-circular DNA (cccDNA) in mice transduced with a recombinant AAV-HBV vector. Antiviral Res 2017;145:14-19.
33) Gao W, Hu J. Formation of hepatitis B virus covalently closed circular DNA: removal of genome-linked protein. J Virol 2007; 81:6164-6174.
34) Subramanian A, Tamayo P, Mootha VK, Mukherjee S, Ebert BL, Gillette MA, et al. Gene set enrichment analysis: a knowledge-based approach for interpreting genome-wide expression profiles. Proc Natl Acad Sci USA 2005;102:15545-15550.
35) Wieland S, Makowska Z, Campana B, Calabrese D, Dill MT, Chung J, et al. Simultaneous detection of hepatitis C virus and interferon stimulated gene expression in infected human liver. HEPATOLOGY 2014;59:2121-2130.
36) Schoggins JW, Wilson SJ, Panis M, Murphy MY, Jones CT, Bieniasz P, et al. A diverse range of gene products are effectors of the type I interferon antiviral response. Nature 2011;472:481-485.
37) Blondot ML, Bruss V, Kann M. Intracellular transport and egress of hepatitis B virus. J Hepatol 2016;64(1 Suppl.):S49-S59.
38) Cui X, Clark DN, Liu K, Xu XD, Guo JT, Hu J. Viral DNA-dependent induction of innate immune response to hepatitis B

virus in immortalized mouse hepatocytes. J Virol 2015;90:486-496.
39) Cui X, Luckenbaugh L, Bruss V, Hu J. Alteration of mature nucleocapsid and enhancement of covalently closed circular dna formation by hepatitis B virus core mutants defective in complete-virion formation. J Virol 2015;89:10064-10072.
40) **Lahaye X**, **Satoh T**, Gentili M, Cerboni S, Conrad C, Hurbain I, et al. The capsids of HIV-1 and HIV-2 determine immune detection of the viral cDNA by the innate sensor cGAS in dendritic cells. Immunity 2013;39:1132-1142.
41) Thomsen MK, Nandakumar R, Stadler D, Malo A, Valls RM, Wang F, et al. Lack of immunological DNA sensing in hepatocytes facilitates hepatitis B virus infection. HEPATOLOGY 2016;64:746-759.
42) **Cho CS**, **Park HW**, Ho A, Semple IA, Kim B, Jang I, et al. Lipotoxicity induces hepatic protein inclusions through TBK1-mediated p62/SQSTM1 phosphorylation. HEPATOLOGY 2017; doi:10.1002/hep.29742. [Epub ahead of print]
43) Yang H, Wang H, Ren J, Chen Q, Chen ZJ. cGAS is essential for cellular senescence. Proc Natl Acad Sci USA 2017;114:E4612-E4620.
44) Lei Z, Deng M, Yi Z, Sun Q, Shapiro RA, Xu H, et al. cGAS-mediated autophagy protects the liver from ischemia/reperfusion injury independent of STING. Am J Physiol Gastrointest Liver Physiol 2018; doi:10.1152/ajpgi.00326.2017. [Epub ahead of print]
45) Leong CR, Oshiumi H, Okamoto M, Azuma M, Takaki H, Matsumoto M, et al. A MAVS/TICAM-1-independent interferon-inducing pathway contributes to regulation of hepatitis B virus replication in the mouse hydrodynamic injection model. J Innate Immun 2015;7:47-58.
46) Gentili M, Kowal J, Tkach M, Satoh T, Lahaye X, Conrad C, et al. Transmission of innate immune signaling by packaging of cGAMP in viral particles. Science 2015;349:1232-1236.
47) **Wu JJ**, **Li W**, Shao Y, Avey D, Fu B, Gillen J, et al. Inhibition of cGAS DNA sensing by a herpesvirus virion protein. Cell Host Microbe 2015;18:333-344.
48) Li W, Avey D, Fu B, Wu JJ, Ma S, Liu X, et al. Kaposi's sarcoma-associated herpesvirus inhibitor of cGAS (KicGAS), encoded by ORF52, is an abundant tegument protein and is required for production of infectious progeny viruses. J Virol 2016;90:5329-5342.
49) Aguirre S, Luthra P, Sanchez-Aparicio MT, Maestre AM, Patel J, Lamothe F, et al. Dengue virus NS2B protein targets cGAS for degradation and prevents mitochondrial DNA sensing during infection. Nat Microbiol 2017;2:17037.
50) Ortega-Prieto AM, Skelton JK, Wai SN, Large E, Lussignol M, Vizcay-Barrena G, et al. 3D microfluidic liver cultures as a physiological preclinical tool for hepatitis B virus infection. Nat Commun 2018;9:682.

Author names in bold designate shared co-first authorship.

Supporting Information

Additional Supporting Information may be found at onlinelibrary.wiley.com/doi/10.1002/hep.30054/suppinfo.

4.4 Un criblage gain de fonction identifie CDKN2C comme un facteur d'hôte du VHB

L'objectif de cette étude était de tirer partie des différences de sensibilité à l'infection des deux modèles d'études majeurs utilisés au laboratoire. Ainsi, la surexpression de *SLC10A1* (qui code pour NTCP) dans les lignées hépatocytaires HepG2 leur confèrent une sensibilité à l'infection par le VHB et le VHD, quand les cellules Huh7 surexprimant le récepteur sont sensibles à l'infection par le VHD et très peu permissives à l'infection par le VHB (22). Les études préliminaires sur les deux lignées suggèrent un blocage du cycle viral entré l'entrée du virus dans la cellule et la transcription des ARN viraux médiée par l'ADNccc. Emettant l'hypothèse que l'absence d'un ou plusieurs facteurs proviral(aux) clé dans les cellules Huh7 était responsable de ce blocage, une approche de génomique à haut débit « gain de fonction » à l'échelle du génome a été réalisée. Le criblage a permis d'identifier un panel de candidats potentiellement impliqués dans le cycle viral du VHB, dont *HNF4A* qui code pour un facteur de transcription connu pour stimuler la réplication du virus (43). Les études de validation dans les différents modèles cellulaires, notamment des hépatocytes primaires humains (PHH) ont confirmé l'importance de *CDKN2C*, qui code pour un membre de la famille des inhibiteurs de kinases dépendantes des cyclines INK4 (Eller, Heydmann et al., en révision à Nat Commun, voir manuscrit ci-après). En particulier, CDKN2C interagit avec CDK4 et CDK6, provoquant un arrêt du cycle cellulaire en phase G1 (44). L'induction de l'arrêt en phase G1 corrélée à l'augmentation de l'infection par le VHB dans des cellules Huh7-NTCP traités avec des inhibiteurs de CDK4/6 suggèrent que la surexpression de *CDKN2C* stimule l'infection par le VHB *via* ce mécanisme d'arrêt du cycle en phase G1. Par ailleurs, l'analyse des transcrits viraux et des niveaux d'ADNccc dans les cellules infectées suggèrent que CDKN2C stimule la transcription des ARN viraux à partir de l'ADNccc. Largement surexprimé dans les cellules HepG2 en comparaison des cellules Huh7, *CDKN2C* pourrait donc être un des facteurs proviraux manquants dans la lignée Huh7 expliquant sa permissivité réduite à l'infection. Par ailleurs, la corrélation entre niveau d'expression de *CDKN2C* et la progression de la maladie hépatique dans des patients souffrant d'hépatite B chronique suggère un rôle de ce facteur dans le développement de la maladie hépatique viro-induite. Cette étude, qui identifie un facteur proviral ayant une pertinence clinique, confirme la robustesse des criblages de génomique fonctionnelle pour la compréhension des interactions VHB-hépatocytes.

Collaborations majeures : J. Lucifora (CRCL Lyon) ; M. Nassal (U. Freiburg, ALL) ; Y. Hoshida (U. Texas, Dalla, USA) ; D. Root (Broad Institute, Cambridge, USA) ; C. Sureau (INTS, Paris)

Etudiantes encadrées : Carla Eller & Laura Heydmann (doctorantes)

Publication associée : Eller, Heydmann et al., en révision (Nat Commun)

Eller C, Heydmann L, et al., en revision (Nat Commun)

A genome-wide gain-of-function screen identifies CDKN2C as a HBV host factor

Carla Eller[1,#], Laura Heydmann[1,#], Che C. Colpitts[1,2], Houssein El Saghire[1], Federica Piccioni[3], Frank Jühling[1], Karim Majzoub[1], Caroline Pons[4], Julie Lucifora[4], Joachim Lupberger[1], Michael Nassal[5], Glenn S. Cowley[3], Naoto Fujiwara[6], Sen-Yung Hsieh[7], Yujin Hoshida[6], Emanuele Felli[1,8], Patrick Pessaux[1,8], Camille Sureau[9], Catherine Schuster[1], David E. Root[3], Eloi R. Verrier[1,$]*, Thomas F. Baumert[1,8,10,$]*

[#]Contributed equally as first authors

[$]Contributed equally as last authors

[1]Université de Strasbourg, Inserm, Institut de Recherche sur les Maladies Virales et Hépatiques UMR_S1110, F-67000 Strasbourg, France; [2]Department of Biomedical and Molecular Sciences, Queen's University, Kingston, Canada; [3]Broad Institute of Massachusetts Institute of Technology and Harvard, Cambridge, MA, USA; [4]Inserm, U1052, Cancer Research Center of Lyon (CRCL), Université de Lyon (UCBL1), CNRS UMR_5286, Centre Léon Bérard, Lyon, France [5]Department of Internal Medicine II/Molecular Biology, University Hospital Freiburg, Freiburg, Germany; [6]Liver Tumor Translational Research Program, Simmons Comprehensive Cancer Center, Division of Digestive and Liver Diseases, Department of Internal Medicine, University of Texas Southwestern Medical Center, Dallas, Texas; [7]Department of Gastroenterology and Hepatology, Chang Gung Memorial Hospital, Taipei, Taiwan; [8]Institut Hospitalo-Universitaire, Pôle Hépato-digestif, Nouvel Hôpital Civil, 67000 Strasbourg, France; [9]INTS, Laboratoire de Virologie Moléculaire, Paris, France, [10] Institut Universitaire de France (IUF), Paris , France.

***Corresponding authors**: Prof. Thomas F. Baumert, MD and Dr Eloi R. Verrier; Inserm U1110, Institut de Recherche sur les Maladies Virales et Hépatiques, Université de Strasbourg, 3 Rue Koeberlé, 67000 Strasbourg, France; Phone: +33 3 68 85 37 03, Fax: +33 3 68 85 37 24, e-mail: thomas.baumert@unistra.fr; e.verrier@unistra.fr

Keywords: HBV, Genome-wide screen, host-dependency factors

Version révisée soumise à Nature Communications le 19 décembre 2019

ABSTRACT

Chronic HBV infection is a major cause of liver disease and cancer worldwide. While current therapies can suppress viral replication, approaches for cure are lacking, and the knowledge of virus-host interactions is still limited. Here, we performed a genome-wide gain-of-function screen, using a poorly permissive hepatoma cell line named Huh-106, to uncover host factors that enhance HBV infection. Validation studies in primary human hepatocytes identified *CDKN2C* as an important host factor for the HBV life cycle. Interestingly, *CDKN2C* is overexpressed in highly permissive cell lines and HBV-infected patients. Mechanistic studies unraveled a role of *CDKN2C* in inducing cell cycle G1 arrest through inhibition of CDK4/6 and stimulating HBV replication. A correlation between *CDKN2C* expression and disease progression in HBV-infected patients suggests a functional role in HBV-induced liver disease. Taken together, we identified a previously undiscovered clinically relevant HBV host factor, allowing the development of improved infectious model systems for drug discovery and the study of the HBV life cycle.

INTRODUCTION

Chronic infection by hepatitis B virus (HBV) is a major health problem and the leading cause of hepatocellular carcinoma (HCC) worldwide [1]. The global HBV burden persists despite the availability of an effective preventative vaccine and it is estimated that HBV chronically infects 250 million people. While current therapies based on nucleot(s)ide analogs (NUCs) suppress viral replication and reduce progression of liver disease, treatment is lifelong and viral cure is extremely rare [2]. Different curative strategies are urgently needed to address this global medical burden.

HBV is a small enveloped DNA virus in the *Hepadnaviridae* family [3]. The HBV surface antigen (HBsAg) mediates entry of the virus into hepatocytes via primary low-affinity interactions with heparan sulfate proteoglycans [4–6] and secondary specific binding to the sodium taurocholate cotransporting polypeptide (NTCP) [7,8], ultimately leading to fusion and release of the viral capsid into the cytoplasm. The capsid delivers the viral genome to the nucleus, where HBV relaxed circular DNA (rcDNA) is converted into episomal covalently closed circular DNA (cccDNA), in a process thought to be mediated by host DNA repair enzymes, such as tyrosyl-DNA-phosphodiesterase 2 (TDP2) [9] and DNA Polymerase kappa (POLK) [10]. The cccDNA is the reservoir for viral persistence and serves as a template for all viral transcripts. CccDNA is not affected by the NUC-based treatments targeting the viral reverse transcriptase, which converts viral pre-genomic RNA (pgRNA) into *de novo* genomic DNA, within newly formed nucleocapsids prior to virion budding [11].

Currently available drugs for the treatment of chronic HBV infection, such as NUCs, are direct-acting antiviral (DAAs) and allow the suppression of viral replication, but viral cure is rarely achieved. Innovative therapeutic strategies, such as host targeting agents (HTAs), have emerged as novel

candidates for the treatment of viral infections, including hepatotropic viruses [12–15]. However, this strategy requires a comprehensive understanding of virus-host interactions at the molecular level. In the context of HBV infection, the limited access to robust infection models has restrained for a long time the characterization of host factors involved in the viral entry process. The discovery of NTCP as a receptor for HBV has allowed the development of cell culture models suitable for the study of the full life cycle [7,16]. Indeed, exogenous expression of NTCP in human hepatoma cell lines (such as HepG2 and Huh7) confers susceptibility to HBV infection. However, NTCP-overexpressing Huh7 cells remain poorly permissive to HBV infection but support infection by hepatitis D virus (HDV), an HBV-satellite virus carrying HBV envelope proteins [16]. This suggests that after HBV entry, additional key factors are still limiting in these cells. Therefore, we hypothesized that characterization of differences between the two cell lines should allow the identification of previously undiscovered HBV host factors. Discovery of such host factors in human hepatoma cells would open avenues to develop new infection models, such as immunocompetent transgenic animal models that are fully susceptible to HBV. Indeed, a previous study suggests that the limited ability of HBV to replicate in mouse cells is caused by the lack of a host cell dependency factor [17]. Here, we performed a genome-wide gain-of-function screen using a weakly permissive NTCP-overexpressing Huh7-derived cell line termed Huh-106 cells [5] and a genome-scale lentiviral open reading frame (ORF) library [18], aiming to uncover HBV-related host-dependency factors. We expect that the identification of these previously undiscovered HBV factors will facilitate the development of improved infectious cell culture systems for the identification of innovative antiviral molecules.

RESULTS

A high-throughput screening strategy for the identification of HBV host factors by functional genomics. To characterize HBV infection in different hepatoma cell lines, we compared the susceptibility of two NTCP-overexpressing cell lines (Huh7-derived Huh-106 [5] and HepG2-NTCP) to HBV and HDV infection. Both cell lines were similarly susceptible to HDV infection, suggesting equivalent virus entry in both cell lines **(Fig. 1a)**. However, in contrast to HepG2-NTCP cells, Huh-106 cells appear poorly permissive to HBV infection **(Fig. 1a)**, despite their ability to bind HBV particles **(Fig. 1b)**. Furthermore, Huh-106 cells support the conversion of incoming HBV rcDNA to cccDNA, although to a much lesser extent than HepG2-NTCP cells **(Fig. 1c, d)**. Interestingly, the kinetics of cccDNA formation are similar in both cell lines **(Fig. 1e)**. Moreover, quantification of intracellular pgRNA and secreted antigens (HBsAg and HBeAg) during the course of infection revealed a severe restriction of the HBV life cycle in Huh-106 cells at different steps **(Fig. 1f-h)**. Taken together, these findings suggest that HBV infection is constrained in Huh-106 cells in a step between NTCP-mediated entry and cccDNA-mediated transcription.

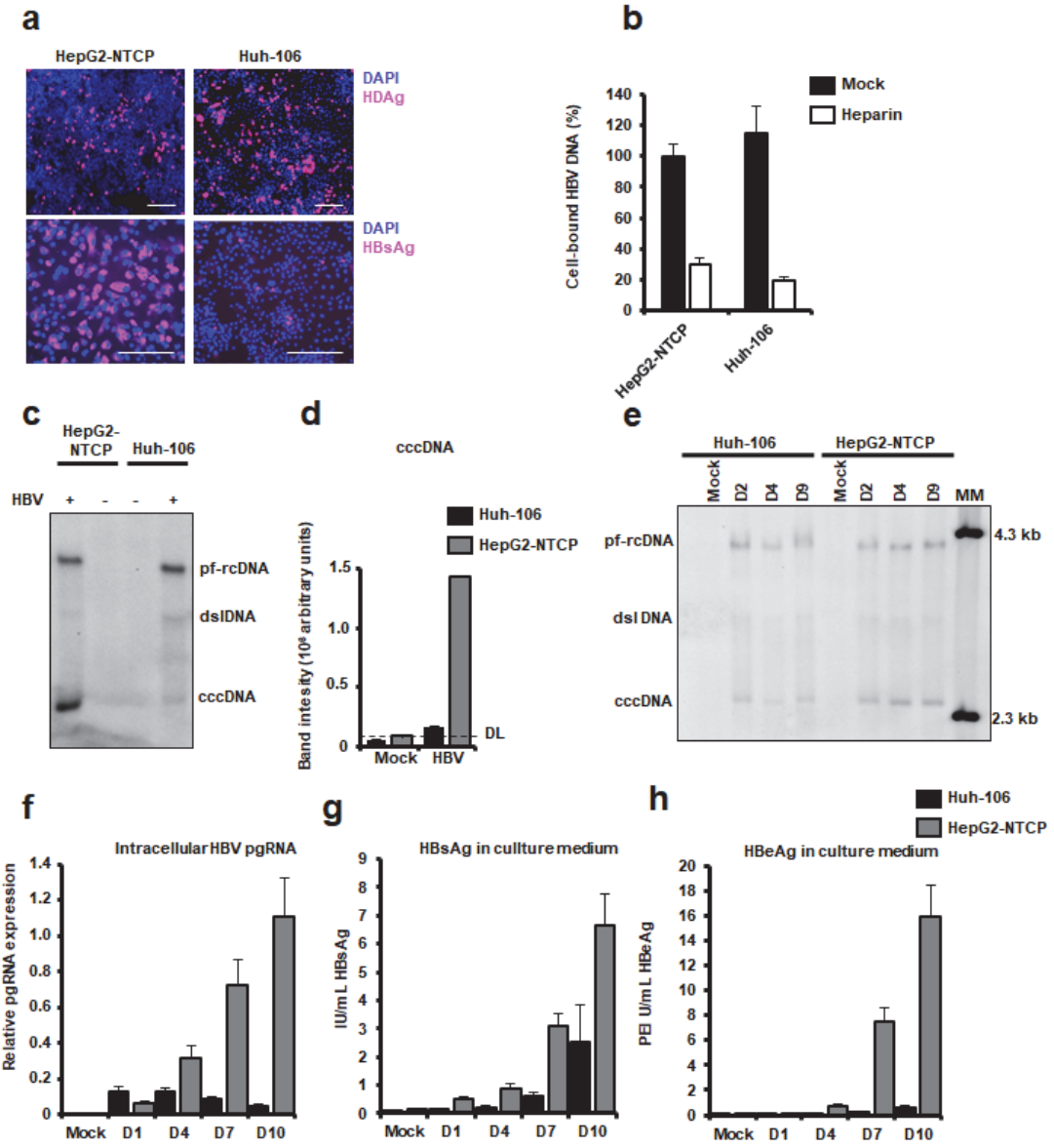

Figure 4.1. Huh-106 are less permissive to HBV infection than HepG2-NTCP. a HBV and HDV infection of HepG2-NTCP and Huh-106 cells and detection of HBsAg and HDAg by IF after 10 dpi. One representative experiment is shown. Scale bars: 100 µm. **b** Binding of HBV particles to HepG2-NTCP and Huh-106 cells**.** Results are expressed as means +/- SEM bound HBV genome copies (%) from 3 independent experiments (n=8). **c** Comparison of HBV cccDNA levels in HepG2-NTCP and Huh-106 cells detected by Southern blot. Protein-free relaxed circular DNA (pf-rcDNA), double stranded linear DNA (dsl DNA) and covalently closed circular DNA (cccDNA) are indicated. One representative experiment out of four is shown. **d** Quantification of cccDNA band intensity. Dashed line indicates the detection limit (DL). Results are expressed as means +/- SEM 10^6 band intensity (arbitrary units) from 4 independent experiments. **e** Time course experiment of HBV infection in Huh-106 and HepG2-NTCP. DNA was extracted from cells 2 (D2), 4 (D4) or 9 (Mock, D9) days post HBV infection and detected by Southern blot. Bands of pf-rcDNA, dsl DNA, and cccDNA were identified using a molecular marker (MM). One experiment is out of three shown. Quantification of cccDNA band intensities in Figure S5a. **f-h** Quantification of intracellular pgRNA by qRT-PCR (f) and secreted HBsAg (g) and HBeAg (h) by CLIA in Huh-106 and HepG2-NTCP cells 1 (D1), 4 (D4), 7 (D7) or 10 (Mock, D10) days post HBV infection. **f** Results are expressed as means +/- SEM relative pgRNA expression from 4 experiments (n=13). **g** Results are expressed as means +/- SEM IU/mL HBsAg from 4 experiments (n=12). **h** Results are expressed as means +/- SEM PEI U/mL HBeAg from 4 experiments (n=12).

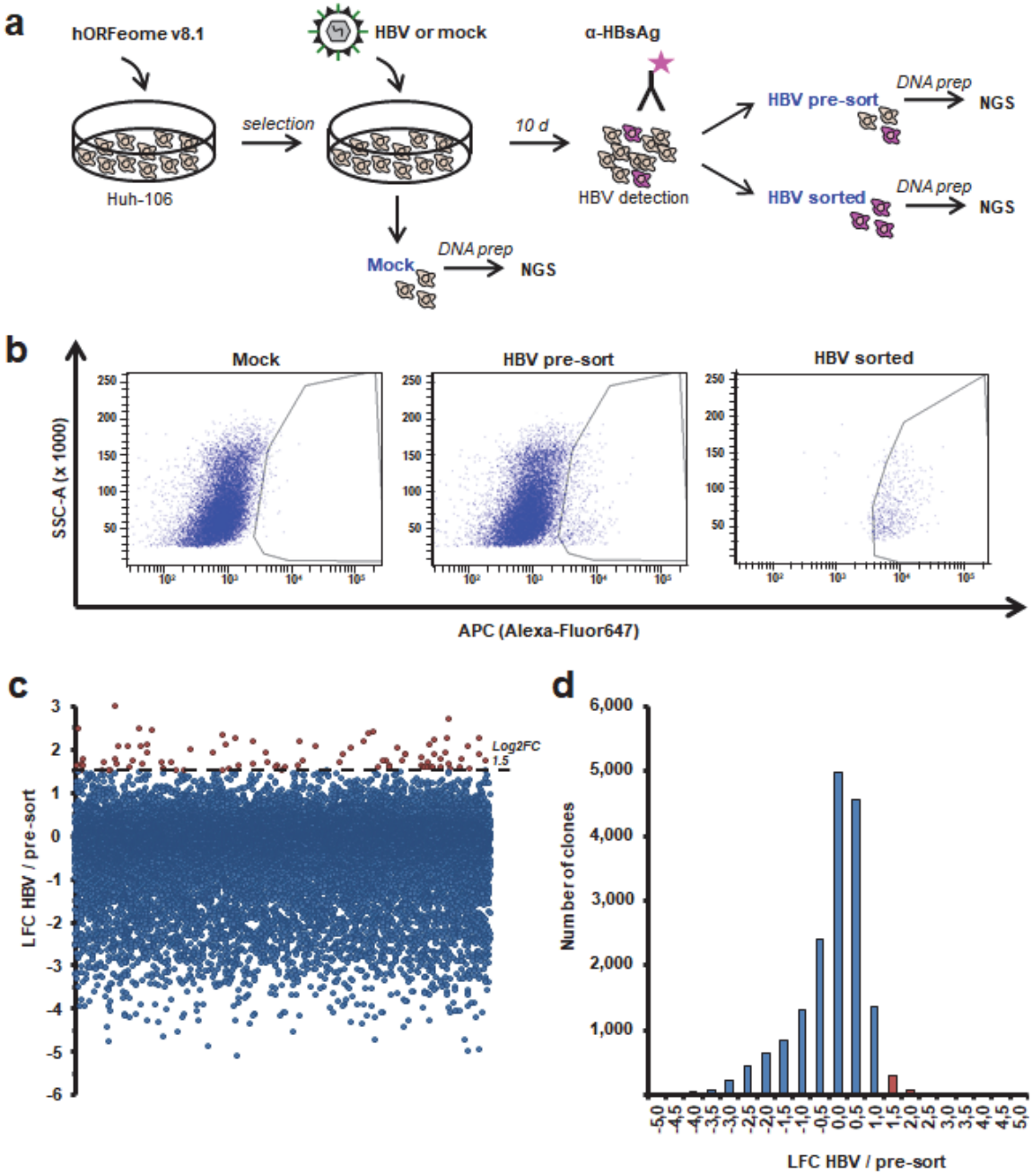

Figure 4.2. Gain-of-function (GOF) screen in Huh-106 cells for the identification of HBV host factors. **a** Schematic workflow of GOF-screen. **b** FACS for HBsAg-positive cells in Huh-106 transduced with an ORF-library (hORFeome v8.1) 10 days after HBV infection (HBV pre-sort). Flow-cytometric analysis of uninfected cells as gating control (Mock) and of the HBsAg-positive sorted population as sorting control (HBV sorted). **c-d** Primary screen candidates. ORFs with Log2FC > 1.5 were selected for validation.

Assuming that this restriction is due to the lack of key host factor(s) for HBV infection, we pursued a functional genomics approach to screen for factors that increase the susceptibility of Huh-106 cells to HBV infection. To this end, we performed a gain-of-function screen for HBV infection using Huh-106 cells and a genome-scale lentiviral expression library of more than 16,000 human ORFs [18]. Huh-106 cells were first transduced with the lentiviral hORFeome V8.1 [18], and then

inoculated with HBV **(Fig. 2a)**. Sorting for HBsAg-positive cells by fluorescence-activated cell sorting (FACS) 10 days post-infection allowed the collection of HBV-infected cells only (HBV sorted) for subsequent analysis to identify factors conferring susceptibility to HBV infection. Using Illumina next-generation sequencing (NGS) and deconvolution using PoolQ, we compared the infected pool of cells (HBV sorted, **Fig. 2a, b**) to the control population (HBV pre-sort, **Fig. 2a**, **b**) to determine which ORFs were enriched in HBs-positive cells. Candidate HBV host factors were identified based on an enrichment threshold of log2 fold change (Log2FC) > 1.5 **(Fig. 2c, d)**. Following an algorithm based on liver expression and the number of sequences per candidate to further filter the list (see Methods), 47 candidate genes were selected for validation **(Table S1)**. Among them was *HNF4A,* a gene encoding a transcription factor previously known to enhance HBV replication [19], supporting the ability of our screen to identify HBV host factors. Interestingly, another transcription factor stimulating HBV replication, *HLF* [20], scored a Log2FC = 1.49 just below the selection threshold. The remaining candidates therefore represent a list of putative new factors for HBV infection for further validation and study.

Identification of CDKN2C as an HBV host factor differentially expressed in HepG2- and Huh7-derived cell lines. To validate the candidate host factors identified above, we individually overexpressed the candidate ORFs in Huh-106 cells before infection with HBV for 10 days. Of the 47 identified ORFs, 35 were evaluated (see Methods), along with lentiviruses encoding *GFP*, *KRT80* and *CPA1* as negative controls **(Table S1)**. HBV infection was assessed by quantification of secreted HBV antigens in the cell culture supernatant of infected cells, indicating increased HBV infection versus controls for a majority of the candidates. Several had large effects on both secreted HBeAg and HBsAg, including the top scorers *ESRP1, SPATA24, U2AF1*, *CDKN2C*, and *GPR27* **(Fig. 3a)**. Importantly, the top candidate ESRP1 was not detected at the protein level in our systems (data not shown), suggesting a non-physiological effect on HBV infection. However, this construct was used as a technical positive control in further experiments. To systematically identify genes that are differentially expressed in the studied cell lines, we performed transcriptomic analyses using microarrays for gene expression profiling in HepG2-NTCP and Huh-106 cells. Pathway enrichment analysis identified a small number of signaling pathways that exhibited significantly different expression patterns between the two cell lines, although the vast majority of pathways were similarly expressed **(Fig. 3b)**. Notably, IFNα response gene expression was higher in HepG2 cells, consistent with previous observations that HepG2 cells are more competent for mounting an efficient innate immune response following viral infection compared to Huh7-derived cells [21,22].

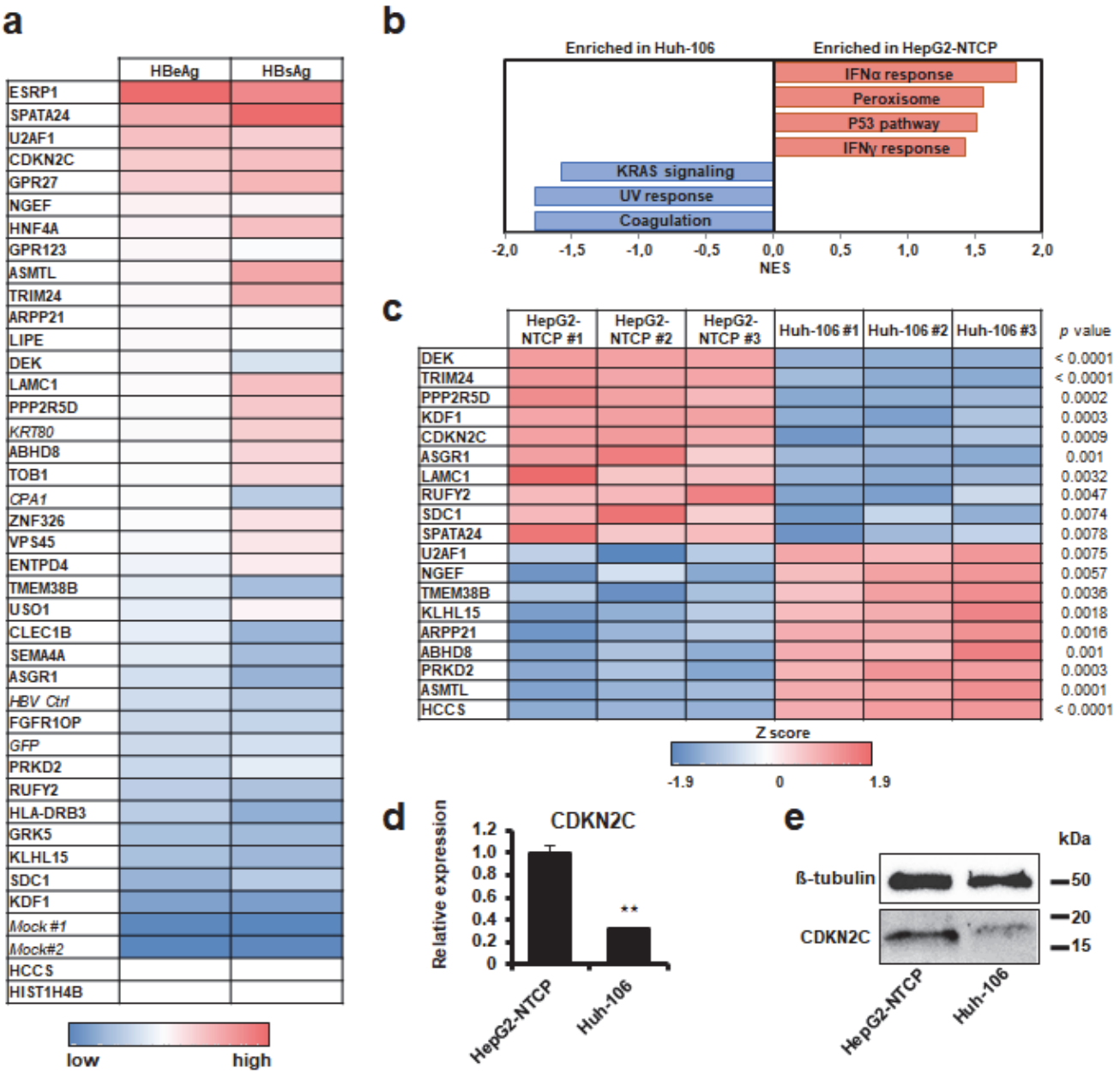

Figure 4.3. CDKN2C is differentially expressed in HepG2-NTCP and Huh-106 cells. a Heatmap of candidate validation. Huh-106 cells were transduced with the indicated ORF and infected with HBV. HBV infection was assessed at 10 dpi by CLIA quantification of secreted HBeAg and HBsAg. Results are expressed as means concentration of secreted HBeAg or HBsAg from 1 experiments (n=2). **b-c** Microarray for comparison of gene expression in HepG2-NTCP and Huh-106 cells. Analysis of differentially expressed pathways (**b**) and candidate host factors from the primary screen through Z score transformation (**c**) are presented. **d-e** CDKN2C is upregulated in HepG2-NTCP compared to Huh-106 cells. **d** *CDKN2C* mRNA expression in HepG2-NTCP and Huh-106 cells quantified by qRT-PCR. Results are expressed as means +/- SEM *CDKN2C* relative expression compared to HepG2-NTCP (set to 1) from 3 independent experiments (n=6). **e** Endogenous CDKN2C protein expression in HepG2-NTCP and Huh-106 cells detected by Western Blot. One representative experiment out of two is shown. ★★ $p < 0.01$

Comparing the expression of primary screen candidate genes from the microarray data, we identified *CDKN2C* and *SPATA24* as highly expressed genes in HepG2-NTCP versus Huh-106 cells **(Fig. 3c)**. Given the specific previously annotated function of SPATA24/T6441 in spermiogenesis [23] we focused instead on *CDKN2C* for further characterization. The higher expression of *CDKN2C* in HepG2-NTCP

versus Huh-106 cells was confirmed by qPCR and Western blot (**Fig. 3d, e)**. The involvement of *CDKN2C* in HBV infection in Huh-106 cells was confirmed by a 6-fold increase in viral pgRNA levels following overexpression of *CDKN2C* when compared to the empty control vector **(Fig. 4a)**.

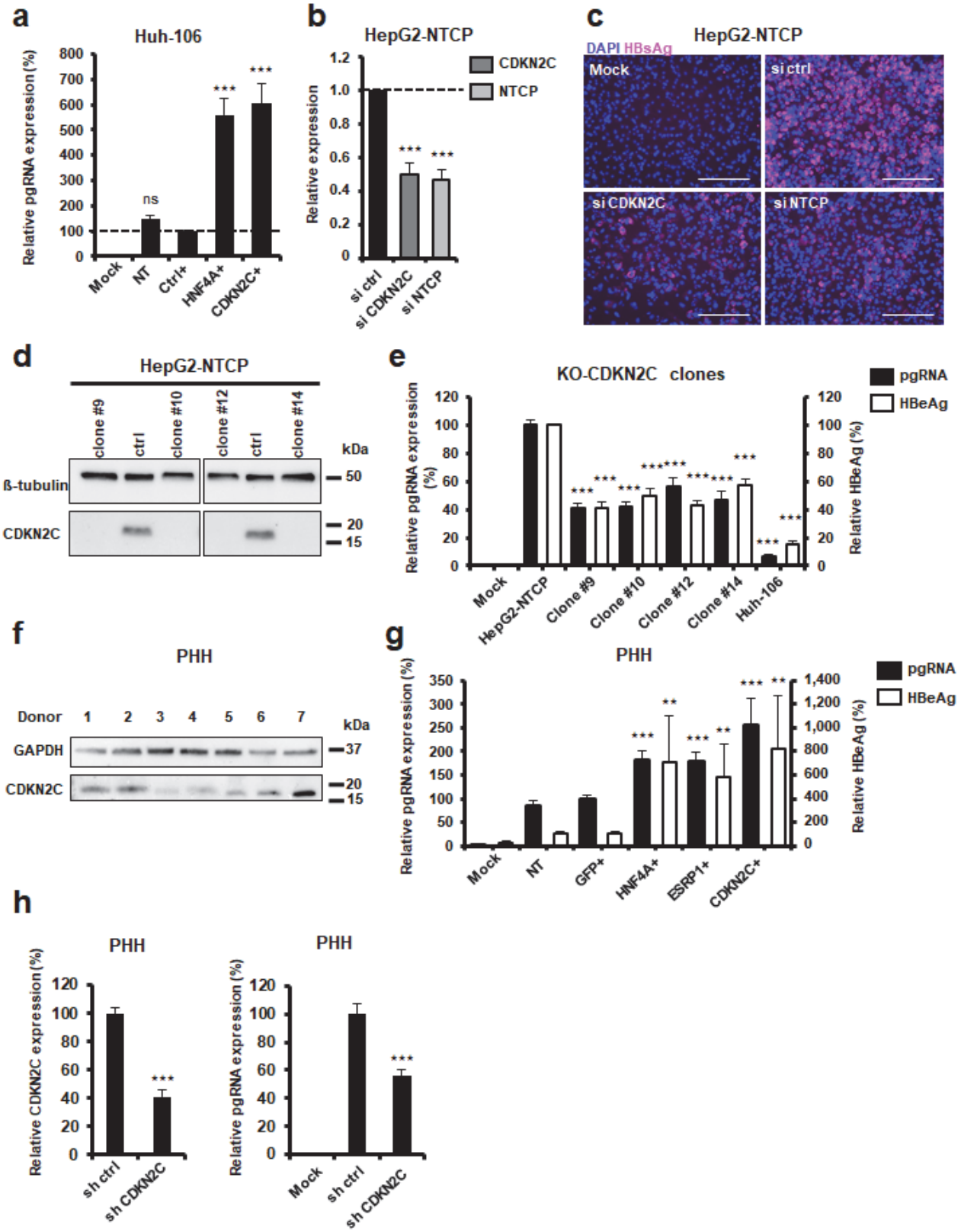

Figure 4.4. CDKN2C is a HBV host factor. a Individual ORF-overexpression in Huh-106 and HBV infection 3 days after transduction. Detection of HBV pgRNA by qRT-PCR 10 dpi. Results are expressed as means +/- SEM relative pgRNA expression (%) compared to ctrl (set as 100%) from 8 independent experiments (n=21). **b-c** Transfection of HepG2-NTCP cells with siRNAs targeting CDKN2C, NTCP or non-targeting control (si ctrl). **b** mRNA expression was quantified by qRT-PCR 2 days post transfection. Results are expressed as means +/- SEM relative expression compared to si ctrl (set to 1) from 4 independent experiments (n=8). **c** HBV infection of HepG2-NTCP cells 2 days post transfection and detection of HBsAg by IF 10 dpi. Scale bars: 100 µm. **d** Knockout of CDKN2C in HepG2-NTCP and clonal selection for production of KO-CDKN2C cell lines. CDKN2C expression was controlled by Western Blot for in HepG2-NTCP (ctrl) and KO-CDKN2C clones. **e** HBV infection of HepG2-NTCP, KO-CDKN2C clones and Huh-106. HBV infection was assessed at 10 dpi by quantification of HBV pgRNA by qRT-PCR (black) and quantification of secreted HBeAg by CLIA (white). Results are expressed as means +/- SEM % HBV infection compared to HepG2-NTCP (set as 100%) from 3 independent experiments (n=9 for pgRNA and n=12 for HBe CLIA). **f** Western Blot for detection of endogenous CDKN2C expression in primary human hepatocytes (PHH) from 7 different donors (1-7). One experiment is shown. **g** Validation studies in PHH from 3 different donors transduced with ORF lentivirus for 3 days and infected with HBV. HBV markers are detected 10 dpi. Total RNA was extracted and pgRNA was quantified by qRT-PCR (black). Concentration of secreted HBeAg in cell supernatant was assessed by CLIA (white). Results are expressed as means +/- SEM % HBV infection compared to ctrl (GFP) (set to 100%) from 3 independent experiments from different donors (n=12 for pgRNA; n=6 for HBeAg). **h** Silencing of *CDKN2C* expression decreases HBV infection in PHH. PHH from 3 independent donors were transduced with lentiviruses containing CDKN2C-targeting shRNA or non-targeting shRNA control (sh ctrl). Silencing efficacy was assessed after 3 days by qRT-PCR. Results are expressed as means +/- SEM % gene expression compared to sh ctrl (set to 100%) from 3 independent experiments from different donors (n=9). PHH were then infected with HBV and HBV infection was assessed by qRT-PCR quantification of HBV pgRNA 8 dpi. Results are expressed as means +/- SEM relative pgRNA expression compared to sh ctrl (set to 100%) from 3 independent experiments from different donors (n=9). ★ $p < 0.05$; ★★ $p < 0.01$; ★★★ $p < 0.001$

Taking advantage of high infection levels in HepG2-NTCP cells, we aimed to confirm the phenotypic effect of *CDKN2C* on HBV infection by a loss-of-function approach, using siRNA specifically targeting *CDKN2C* or *SLC10A1* (the gene encoding the HBV receptor NTCP) in susceptible HepG2-NTCP cells, as shown in **Figure 4b-c**. We observed a marked decrease in HBV infection in cells with silenced *CDKN2C* or *SLC10A1* expression. To rule out off-target effects, we used CRISPR-Cas9 to generate and clonally select four independent HepG2-NTCP CDKN2C knockout (KO) cell lines **(Fig. 4d)**. Functional analysis confirmed a marked decrease in both HBV pgRNA and secreted HBe antigen levels in HepG2-NTCP KO-CDKN2C cells compared to naïve HepG2-NTCP cells **(Fig. 4e)**. Finally, to validate the relevance of *CDKN2C* in a physiological model, we investigated CDKN2C-HBV interactions in primary human hepatocytes (PHH), the natural target cells for HBV infection, which express the protein at varying levels comparable to HepG2-NTCP cells **(Fig. 4f)**. Consistent with our previous observations, the overexpression of *HNF4A* and *CDKN2C* in PHH resulted in a significant and marked increase in HBV infection **(Fig. 4g)**. Moreover, the silencing of *CDKN2C* expression using target-specific shRNA induced a significant and robust decrease in HBV infection **(Fig. 4h)**. Taken together, our data support a role for *CDKN2C* in HBV infection. Therefore, the differential expression of this gene between the two cell lines suggests that a lack of *CDKN2C* expression may contribute to the limited susceptibility of Huh-106 cells to HBV infection.

CDKN2C stimulates HBV cccDNA-mediated transcription. To address the mechanism by which *CDKN2C* contributes to HBV infection, we performed additional experiments using alternative read-outs to identify the steps of the viral life cycle that may be affected by *CDKN2C* expression. Transduction efficacy was assessed by quantification of GFP expression in HBV-infected *GFP*-transduced cells after 10 days **(Fig. S2)**. Detection of intracellular HBsAg by immunofluorescence (IF) **(Fig. 5a)** and its quantification by flow cytometric analysis **(Fig. 5b)** revealed a significant increase in HBV infection levels in Huh-106 cells overexpressing *HNF4A, ESRP1* and *CDKN2C*. Notably, co-overexpression of *CDKN2C* and *ESRP1* leads to an even higher percentage of HBsAg positive cells **(Fig. 5b),** suggesting that the two factors affect HBV infection through independent pathways. Interestingly, overexpression of both factors in Huh-106 cells markedly increased HBV infection but failed to reach levels observed in HepG2-NTCP cells **(Fig. 5b, c**), suggesting the existence of additional differentially expressed factors in the two cell lines. To determine the step of the HBV life cycle affected by *CDKN2C* expression, we detected HBV DNA genome intermediates by Southern blot and HBV RNA levels by Northern blot. As shown in **Figure 5d-e**, no marked change in HBV cccDNA levels was observed when *CDKN2C* was overexpressed, suggesting no effect on HBV replication before cccDNA formation. Detection of viral RNAs by Northern blot revealed increased HBV RNA levels in cells overexpressing *HNF4A* and *CDKN2C* compared to *GFP*-overexpressing cells **(Fig. 5f-g)**. To determine whether CDKN2C has a direct effect on HBV RNA formation, we quantified nascent HBV RNAs using labelled uridine. Huh-106 cells overexpressing *CDKN2C* displayed a 3-fold increased level of newly synthesized HBV RNA **(Fig 5h)**. This suggests a role for CDKN2C in cccDNA-mediated transcription of HBV RNAs.

***CDKN2C* overexpression improves quality but not quantity of HBV virion production in HepAD38 cells.** To investigate whether modification of *CDKN2C* expression modulates the production of virus particles in HBV-expressing cells, we overexpressed *CDKN2C* and *HNF4A* in HepAD38 donor cells. 10 days after ORF-lentivirus transduction, we harvested supernatants and infected HepG2-NTCP acceptor cells with an adjusted MOI from supernatant from HepAD38 donor cells containing HBV particles **(Fig. 6a)**. While a slight increase in the secretion of HBsAg and HBeAg is observed, *CDKN2C* overexpression in HepAD38 donor cells did not affect the secretion of HBV DNA in the supernatant **(Fig. 6b, c)**. Interestingly, overexpression of *CDKN2C* in HepAD38 increased infection of HepG2-NTCP acceptor cells 3-fold, suggesting a role for CDKN2C in enhancing the formation of high-quality neo-virions **(Fig. 6d, e),** in line with the recent observation that virion production is enhanced in slow-proliferating HBV-replicating cells [24]. Collectively, our data identify CDKN2C as a previously undiscovered HBV host factor, which activates transcription from cccDNA in human hepatocytes.

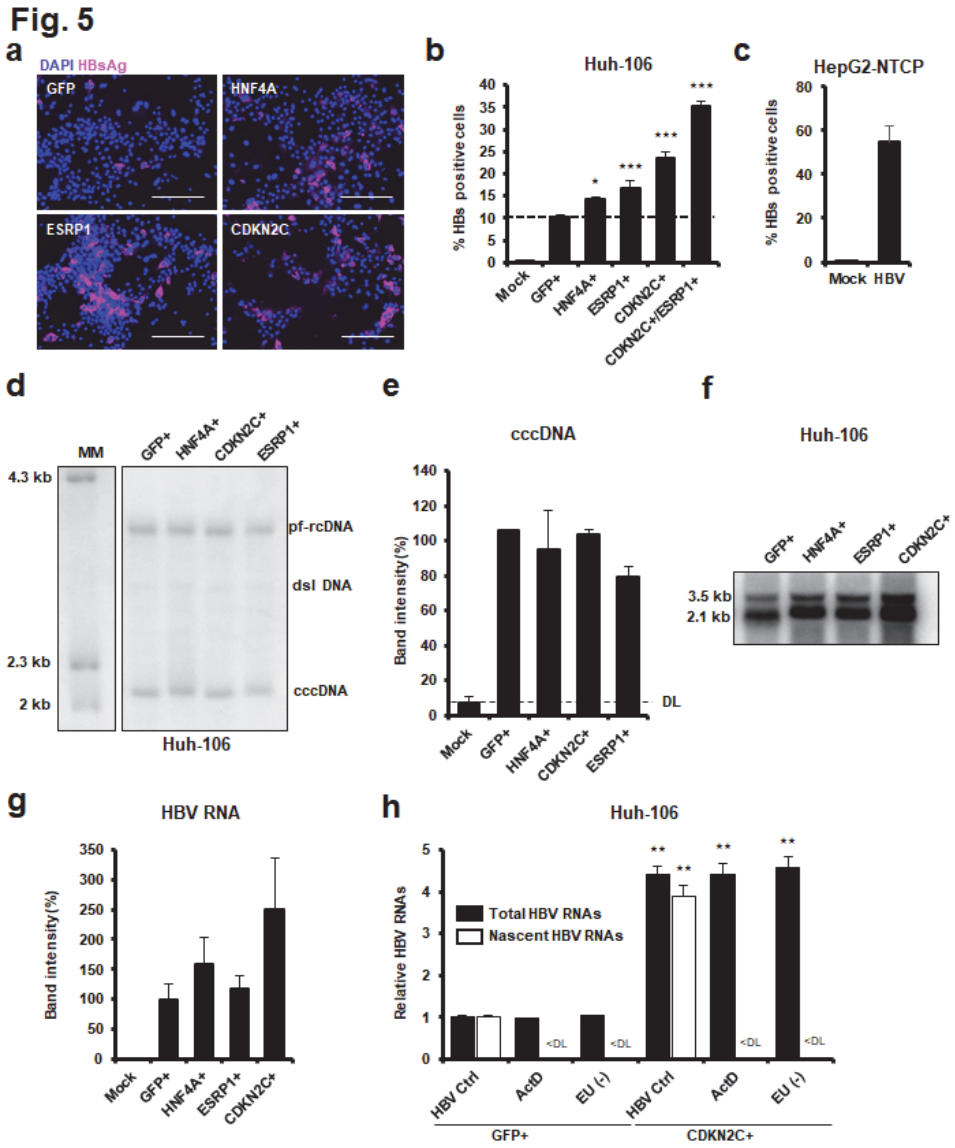

Figure 4.5. CDKN2C stimulates HBV cccDNA-mediated transcription. a-b, d-g Validation studies in Huh-106 overexpressing individual ORFs and infected with HBV for 10 days. **a** Detection of HBsAg by IF. Scale bars: 100 µm. **b** Flow-cytometric analysis for quantification of HBsAg-positive cells. Results are expressed as means +/- SEM % HBsAg positive cells compared to GFP from 5 independent experiments (n=13, n=11 for HNF4A) and 3 independent experiments (n=8) for CDKN2C+ESRP1 **c** Flow-cytometric analysis for quantification of HBsAg-positive cells in HBV-infected HepG2-NTCP cells. Results are expressed as means +/- SEM % HBsAg positive cells from 4 independent experiments (n=4) **d-e** Detection of HBV DNAs by Southern Blot in transduced and HBV infected Huh-106 4 dpi. **d** Southern Blot with indicated bands of HBV pf-rcDNA, dsl HBV DNA and HBV cccDNA. One representative experiment out of two is shown. **e** Quantification of cccDNA using Image Lab Version 5.2.1 (Bio-Rad). Results are expressed as means +/- SEM % band intensity compared to GFP (set to 100%) from 3 independent experiments (n=2). **f** Detection of HBV RNAs by Northern blot. The pgRNA (3,5 kb) and surface mRNAs of 2.1 to 2.4 kb (2.1 kb) are detected. One representative experiment out of two is shown. **g** Quantification of HBV RNA band intensity. Results are expressed as means +/- SEM % band intensity compared to GFP (set to 100%) from 4 independent experiments. **h** Analysis of nascent HBV RNA synthesis. Quantification of total HBV RNAs (4 dpi) and nascent HBV RNAs (d4pi, 120 minutes) in Huh-106 cells overexpressing CDKN2C using labelled uridine (EU). Actinomycin D (ActD) was used as negative control. Results are expressed as means +/- SEM % relative HBV RNAs compared to HBV Ctrl (Huh-106 GFP+ - set to 1) from 2 independent experiments (n=6). ★ $p < 0.05$; ★★★ $p < 0.001$

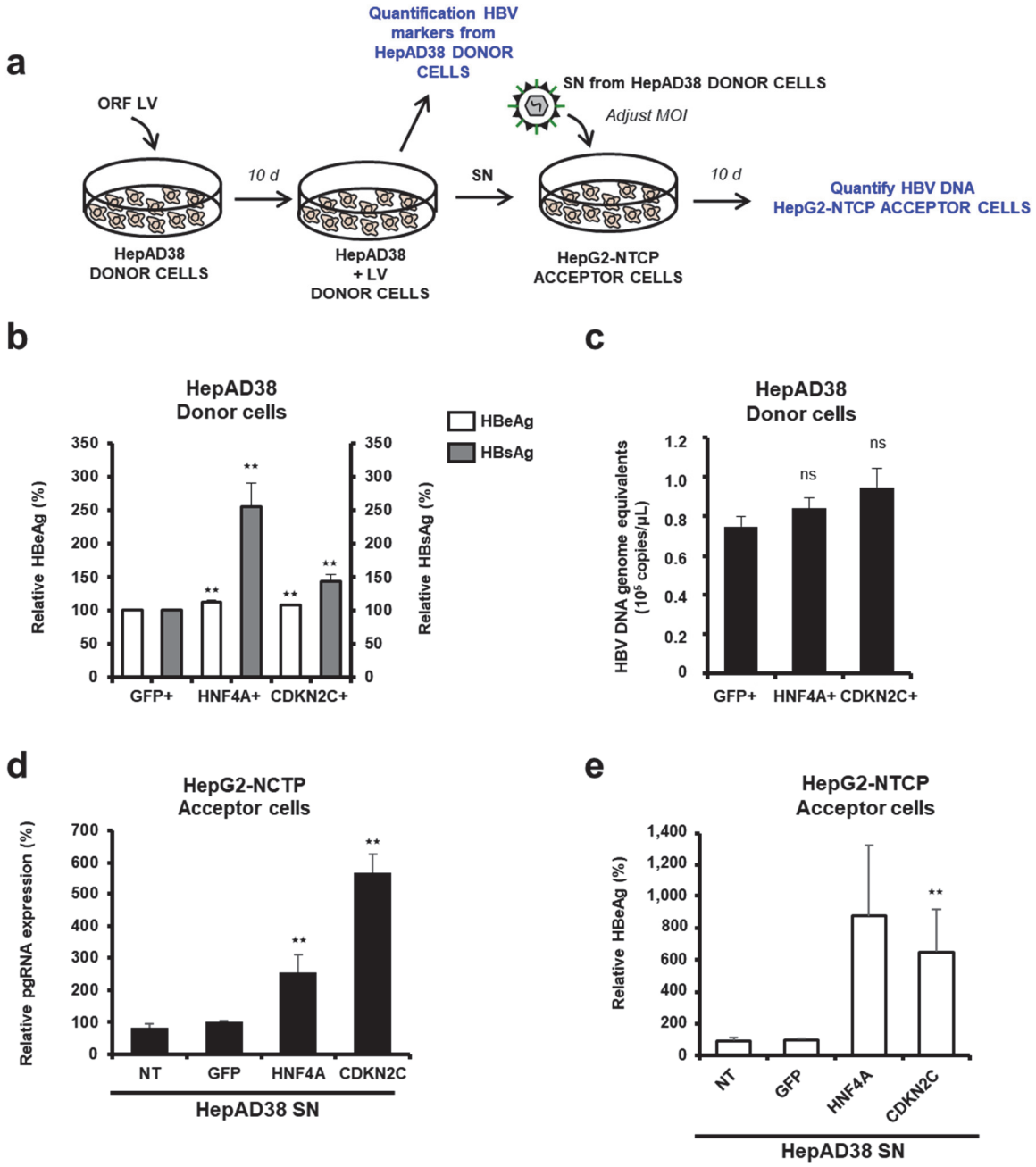

Figure 4.6. *CDKN2C* overexpression improves quality but not quantity of HBV virion production in HepAD38 cells. a Schematic workflow of experiments. HepAD38 cells in production medium (Donor cells) were non-transduced (NT) or transduced with ORF lentivirus for 10 days. **b-c** Supernatant (SN) from HepAD38 donor cells was harvested and HBV markers were quantified from SN. **b** HBeAg and HBsAg secretion was quantified by CLIA. Results are expressed as means +/- SEM % secreted HBeAg or % secreted HBsAg compared to NT (set to 100%) from 3 independent experiments (n=6). **c** HBV DNA level in the supernatant was determined by qPCR. Results are expressed as means +/- SEM HBV DNA genome equivalents from 3 independent experiments (n=6). **d-e** HepG2-NTCP (Acceptor cells) were infected with adjusted MOI from supernatant from HepAD38 donor cells. **d** HBV pgRNA expression was quantified by qRT-PCR 10 dpi. Results are expressed as means +/- SEM % relative pgRNA expression compared to NT (set at 100%) from 3 independent experiments (n=6). **e** HBeAg secretion was quantified by CLIA 10 dpi. Results are expressed as means +/- SEM % relative secreted HBeAg compared to NT (set at 100%) from 3 independent experiments (n=6). ★★ $p < 0.01$

CDKN2C-mediated stimulation of HBV transcription is correlated with a cell cycle arrest. *CDKN2C* encodes the cyclin dependent kinase inhibitor 2C (CDKN2C), a regulator of G1 cell cycle progression through interaction with cyclin dependent kinases 4 and 6 (CDK4/6). In fact, overexpression of *CDKN2C* induces G1 cell cycle arrest in Huh-106 cells **(Fig. S3)**. To determine if this known function of CDKN2C is responsible for enhancing HBV infection, we performed functional studies using two clinical CDK4/6-specific small molecule inhibitors, Palbociclib [25] and LEE011 [26]. We first confirmed that Palbociclib treatment of Huh7 and Huh-106 cells at non-toxic concentrations induced G1 cell cycle arrest as demonstrated by the accumulation of cells in G1 phase **(Fig. S4a-b)**. We then determined HBV infection levels in Huh-106 cells treated with either of the inhibitors before and after HBV infection **(Fig. 7a, e)**. Visualization of intracellular HBsAg revealed a marked increase in HBV infection levels after treatment with Palbociclib or LEE011 **(Fig. 7b)**.

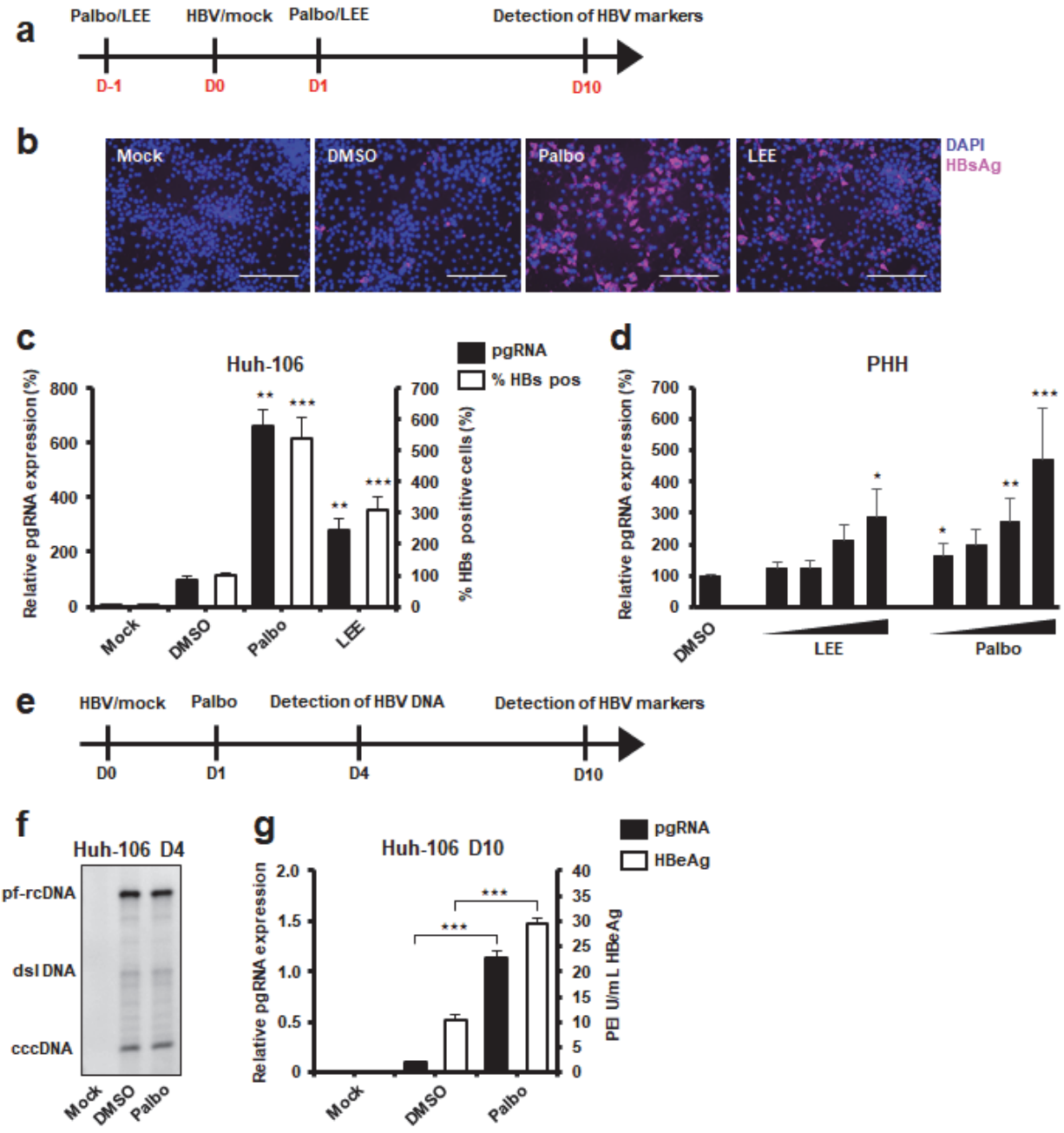

Figure 4.7. CDKN2C-mediated stimulation of HBV transcription is correlated with a cell cycle arrest. Effect of treatment with CDK4/6 inhibitors Palbociclib (Palbo) and LEE011 (LEE) on HBV infection. **a** Schematic workflow of experiments b-d. Detection of HBV markers in mock/HBV infected Huh-106 cells or PHH treated with DMSO or Palbo/LEE before (D-1 to D0) and after (D1 to D10) HBV infection 10dpi. **b-c** Detection of HBV markers 10 dpi in mock-treated of HBV infected Huh-106 cells treated with DMSO or 100 nM Palbo/LEE. **b** Detection of HBsAg by IF 10 dpi. Scale bars: 100 µm. **c** Quantification of HBV pgRNA by qRT-PCR (black). Quantification of HBsAg-positive cells by flow cytometric analysis (white). Results are expressed as means +/- SEM % HBV infection compared to DMSO (set to 100%) from 3 independent experiments (n=5) for pgRNA and from 4 independent experiments (n=12) for % HBs pos. **d** Quantification of HBV pgRNA10 dpi in mock-treated of HBV infected PHH treated with DMSO or 1-1000 nM Palbo/LEE. Results are expressed as means +/- SEM % relative pgRNA expression compared to DMSO (set to 100%) from 3 independent donors (n=9). **e** Schematic workflow of experiments f-h. Treatment of mock/HBV infected Huh-106 or HepG2-NTCP cells with 0 nM (DMSO) or 100 nM Palbociclib (Palbo) after HBV infection. **f** Detection of HBV DNA by Southern blot in Huh-106 cells 4 dpi. HBV pf-rcDNA, dsl DNA cccDNA bands are indicated. One representative experiment out of 3 is shown. Quantification of cccDNA bands in Figure S5b. **g** Detection of HBV markers in Huh-106 10 dpi. Quantification of HBV pgRNA by qRT-PCR (black) and of secreted HBeAg by CLIA (white). Results are expressed as means +/- SEM relative pgRNA expression (pgRNA) or as means +/- SEM PEI U/mL HBeAg from 3 independent experiments (n=9) for pgRNA and from 3 independent experiments (n=12) for HBeAg. ★ $p < 0.05$; ★★ $p < 0.01$; ★★★ $p < 0.001$

Furthermore, quantification of HBV pgRNA and HBsAg-positive cells revealed a significant increase in HBV infection upon both Palbociclib and LEE011 treatment **(Fig. 7c).** Similar results were obtained in PHHs treated with CDK4/6 inhibitors at different concentrations (1, 10, 100 and 1,000 nM) confirming the proviral effect of Palbociclib and LEE011 **(Fig. 7d)**. To investigate whether Palbociclib-mediated enhancement of infection is dependent on HBV entry, we treated HBV infected Huh-106 cells with 100 nM Palbociclib following removal of the HBV inoculum **(Fig. 7e)**. As shown in **Figure 7f**, Palbociclib treatment did not affect HBV cccDNA levels, suggesting no effect on the viral entry steps including cccDNA formation. However, pgRNA and secreted HBeAg levels were significantly increased in Palbociclib-treated cells, indicating that CDKs are important for post-entry steps of the viral life cycle **(Fig. 7g)**. Collectively, our data identify *CDKN2C* as a previously undiscovered HBV host factor, most likely acting through inhibition of CDK4/6, triggering a cell cycle G1 arrest and enhancing HBV transcription **(Fig. 8)**.

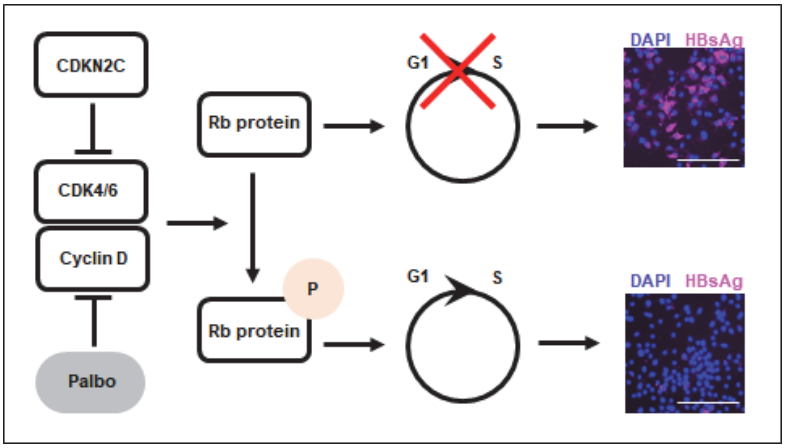

Figure 4.8. Schematic model of the effect of CDKN2C expression and Palbociclib (Palbo) treatment on HBV infection. CDKN2C and Palbociclib inhibit the CDK4/6 and Cyclin D mediated phosphorylation of Rb protein, leading to an accumulation of Rb protein in its unphosphorylated state. Unphosphorylated Rb protein induces a cell cycle G1 arrest resulting in increased HBV infection rates. Illustrative HBV infection pictures come from Fig. 7. Scale bars: 100 µm.

CDKN2C expression is associated with HBV-related chronic liver disease and survival in patients. To assess whether HBV infection directly affects *CDKN2C* expression, we infected PHH with HBV and evaluated *CDKN2C* gene expression. Interestingly, *CDKN2C* expression was upregulated upon HBV infection **(Fig. 9a)**. In line with this observation, the analysis of *CDKN2C* expression from patient liver tissues retrieved from the Gene Expression Omnibus database revealed an upregulation of *CDKN2C* in patients with active replication compared to patients with undetectable viral load and healthy patients **(Fig. 9b)**. Moreover, a correlation was observed between HBV viral load and *CDKN2C* expression in liver tissues from 9 HBV-infected patients **(Fig. S6a)**. Finally, *CDKN2C* expression appeared to be modulated in different stages of HBV infection **(Fig. 9c)**. Taken together, these data suggest that HBV infection modulates *CDKN2C* expression in chronically infected patients. To evaluate whether *CDKN2C* expression is associated with the development of virus induced liver disease, we analyzed *CDKN2C* expression in HBV patients with advanced liver disease and HCC. We first observed that patients with advanced fibrosis (F3) exhibit higher *CDKN2C* mRNA levels compared to patients with F1 or F2 fibrosis *CDKNC2* expression **(Fig. S6b)**. Moreover, *CDKN2C* expression was significantly higher in tumor tissues from HBV-derived HCC compared to adjacent tissue **(Fig. 9d)**. To assess the specificity of this correlation, we analyzed *CDKN2C* expression in HCC patients regardless the etiology. *CDKN2C* levels were markedly elevated in the tumor liver tissue of patients chronically infected with HCV or HBV and patients with alcoholic liver disease (Alc) or non-alcoholic fatty liver disease (NAFLD) as compared with non-tumor tissue **(Fig. 9e)**, suggesting that *CDKN2C* expression is upregulated in HCC in an etiology-independent manner. Finally, higher expression of *CDKN2C* in HCC patients was associated with significantly lower long-term overall survival **(Fig. 9f)**. Taken together, our data suggest that HBV infection modulates *CDKN2C* expression and that *CDKN2C* expression is associated with liver disease progression and poor survival.

DISCUSSION

Chronic hepatitis B is the most common form of severe viral hepatitis worldwide and a leading cause of hepatocellular carcinoma. To date, molecular details of HBV-host interactions are not fully understood. Using a functional genomics approach, we identified *CDKN2C* as a previously undiscovered host factor for HBV infection. The functional impact of this finding is confirmed by: (1) a marked increase or decrease in HBV infection after *CDKN2C* overexpression or knockout, respectively; (2) an increase in HBV markers following *CDKN2C* overexpression and (3) a significant pro-viral effect of CDK4/6 inhibitors correlated with cell cycle G1 arrest.

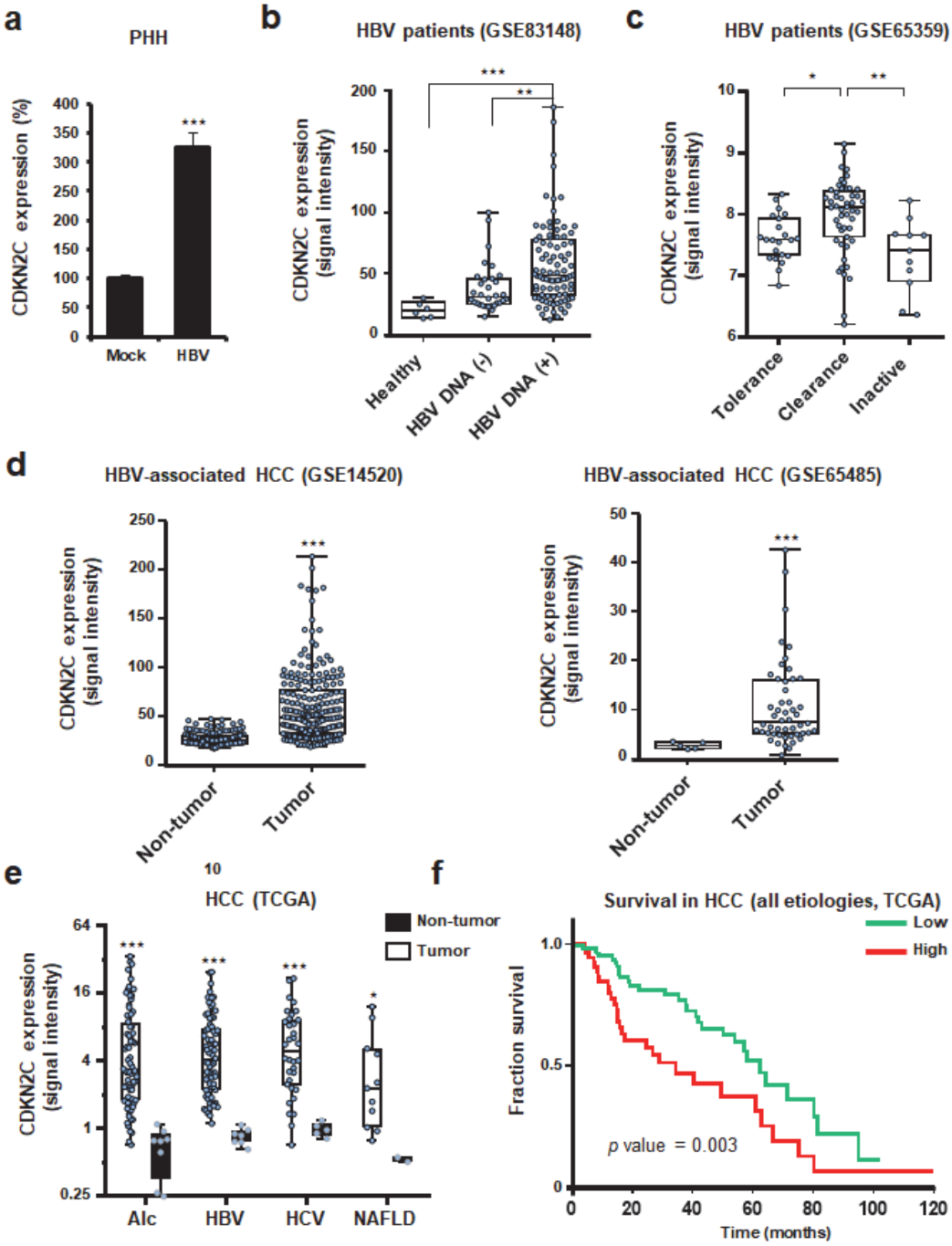

Figure 4.9. CDKN2C expression is associated with HBV infection, liver disease and survival in patients. a *CDKN2C* mRNA expression in HBV infected PHH from 3 different donors quantified by qRT-PCR. Results are expressed as means +/- SEM % relative CDKN2C expression compared to Mock (set to 100%) from 3 independent experiments (n=9). **b** *CDKN2C* expression in HBV-infected patients with undetectable (HBV DNA(-)) or detectable (HBV DNA(+)) HBV DNA compared to healthy patients(cohorts described in Methods). **c** *CDKN2C* expression in HBV-infected patients depending on the stage of virus infection (cohorts described in Methods). **d** *CDKN2C* expression in tumor and adjacent tissues in HCC patients from two independent cohorts (see Methods)**. e** *CDKN2C* expression in tumor and non-tumor (normal) liver tissue from HCV-infected patients, HBV-infected patients, patients with alcoholic liver disease (Alc) and patients with non-alcoholic fatty liver disease (NAFLD) extracted from TCGA database as described in Methods. **f** Survival analysis for HCC patients with low or high CDKN2C expression (cohort see Methods). ★ $p < 0.05$; ★★ $p < 0.01$; ★★★ $p < 0.001$.

The role of *CDKN2C* as an HBV host factor was identified in a gain-of-function approach combining a cell-based model system [5] with a genome-scale ORF library [18]. The ability of our screen to discover HBV host factors promoting different steps of the HBV life cycle is supported by the identification of *HNF4A* in the primary screen. *HNF4A* encodes a liver-specific transcription factor, hepatocyte nuclear factor 4 (HNF4), that has been shown to be important for HBV replication by enhancing transcription from the promoters of HBV core [27], major surface antigen and large surface antigen [19]. Hence, HNF4A is likely to be a key transcription factor that regulates the HBV replication cycle and contributes to hepatotropism [28,29]. Notably, the hepatic leukemia factor (HLF), another transcription factor playing a role in the regulation of the HBV core promoter via interaction with sites other than HNF4 [20], scored with a Log2FC value of 1.49 just below our threshold for selection of candidate host factors. This supports the ability of our screening strategy to detect HBV host factors. Notably, the screen and validation experiments identified *ESRP1* as the top candidate HBV host factor. *ESRP1* encodes a splicing regulator especially involved in a large splicing program critical for the development in mammals [30]. Importantly, ESRP1 protein expression was not detected in our systems, suggesting no or weak expression in hepatocytes. It is however likely that the splicing regulation of hepatocyte factors or the virus transcripts themselves (as it has been described, see [31]) explain the observed effect, even if not physiologically relevant.

While some pro- and anti-viral host factors have been described, many aspects of virus-host interactions remain poorly understood. Importantly, the correlation between HBV replication and cell cycle progression has long been a topic of investigation. For instance, in 1979, Aden *et al.* [32] demonstrated increased HBV antigen production in non-dividing tumor-derived cells with integrated HBV DNA sequences. Similar observations were made in an HBV-transfected hepatoma derived cell line [33]. Later, HBV replication was found to be inversely correlated to cellular DNA synthesis and to be enhanced in quiescent hepatocytes [34]. In fact, effective *in vitro* infection with HBV requires the presence of dimethyl sulfoxide (DMSO), known to enhance and prolong HBV infection by several mechanisms [16,35] and to decrease cell proliferation [36]. It has been previously described that HBV preferentially infects resting cells and that the virus is able to deregulate the infected cell cycle to favor its replication [37,38]. However, it remains unclear which host factors are involved in that process and whether cells arrested in G0/G1 or G2/M phase are more prone to HBV infection. Our data support the hypothesis that G1 cell cycle arrest is favorable for HBV replication and that CDKN2C is a key host factor mediating this virus-host interaction. A comparison of the proliferative ability of HepG2 cells with that of HepG2.2.15 (constitutively expressing HBV from integrated viral DNA), indicated that HBV induces a G1 phase arrest [37]. It has also been shown in PHH that HBV arrests infected cells in the G2/M phase and replicates more favorably during this cell cycle phase [38]. In eukaryotic cells, cyclin dependent kinases (CDKs) are key components of cell cycle regulation machinery. They form

complexes with cyclins to control the transition through cell cycle phases and therefore allow cell division of healthy cells [39]. Interactions of HBV with certain CDKs have been shown. For example, CDK2 is involved in the phosphorylation of HBc and might be incorporated into viral capsids [40]. Moreover, inhibitors of CDKs have been shown to modulate HBV infection with different outcomes. On the one hand, knockout or inhibition of CDK2 enhances HBV replication by phosphorylation and deactivation of the host restriction factor SAMHD1 [41]. On the other hand, the CDK9-inhibitor FIT039 prevents replication of HBV and other DNA viruses and is under consideration as an antiviral candidate against HBV [42,43]. These data suggest a link between the CDK-cyclin pathway and the HBV life cycle. However, the key components and mechanisms remain unclear.

Here, we identify CDK4/6 as additional players in the regulation of HBV infection and show that CDK4/6 inhibitors are beneficial for the viral life cycle. CDK4/6 promote the cell cycle G1/S transition by phosphorylating the retinoblastoma (Rb) protein, the gene product of a tumor suppressor gene, and a central regulator of cell cycle progression [44]. The cyclin dependent kinase inhibitor 2C (CDKN2C) interacts with CDK4/6 to block cell cycle G1 progression via Rb protein phosphorylation [45]. Here, we find that *CDKN2C* overexpression in HBV infected hepatocytes enhances replication in both NTCP-overexpressing hepatoma derived cell line and in PHH. Our results suggest an effect of CDKN2C on host cellular factors that are instrumental in HBV transcription. Overall, we identify CDKN2C as HBV host factor, acting through inhibition of CDK4/6 and prevention of G1 cell cycle progression.

The identification of *CDKN2C* as a host factor for HBV infection not only improves our understanding of the virus-host interactions, but also contributes to the explanation of the poor permissivity of NTCP-overexpressing Huh7 cells to this virus **(Fig. 1a)**. A detailed understanding of the molecular mechanisms underlying the varying susceptibility of currently available HBV infection models to HBV infection is crucial for the development of improved infectious cell culture models. The weak permissivity of Huh7-NTCP compared to HepG2-NTCP cells to HBV infection could be partially explained by lower *CDKN2C* expression levels **(Fig. 3d-e)**. However, the lower cccDNA levels in Huh7-NTCP compared to HepG2-NTCP are not caused by the lack of *CDKN2C* as its overexpression does not affect cccDNA formation **(Fig. 5d, e)**. Huh7-NTCP cells might therefore be useful to identify additional missing pro-viral host factors or restriction factors involved in cccDNA formation. Overall, a better understanding of virus-host interactions will facilitate the development of improved infectious model systems for drug discovery.

In patients, *CDKN2C* expression is accompanied with progression of HBV-associated fibrosis and is higher in HBV-associated cirrhotic and HCC tissues compared to tumor-adjacent tissues. In fact, *CDKN2C* is an etiology-independent marker of liver disease **(Fig. 9)** and part of a regulatory signature involved in liver regeneration [46]. This might explain the association of higher *CDKN2C* expression in

HCC patients with lower long-term survival **(Fig. 9)**. While the upregulation of CDK inhibitors in cancer cells may appear counterintuitive, our consistent observations of an association between *CDKN2C* expression and progressive liver disease and hepatocarcinogenesis in several independent cohorts (Fig. 9) are in line with a recent observation that the expression of the tumor suppressor and *CDKN2C* effector Rb, which is regularly inactivated in human cancer, was inversely correlated with *CDKN2A*, another CDK4/6 inhibitor [47].Given the positive correlation of CDKN2C expression and survival, it is likely that CDKN2C rather has procarcinogenic properties than a tumor suppressive function in HCC (Fig. 9). It is also interest to note that a recent study showed that pgRNA-positive HCCs were characterized by low levels of cell cycle and DNA repair markers and that pgRNA and cccDNA in tumors was correlated to the absence of tumorous microvascular invasion and to better patient survival [48]. Collectively, these observations provide a starting point for further studies investigating the functional role of CDKN2C is HBV-induced liver disease.

Interestingly, chemotherapeutic agents for cancer treatment cause immunosuppression and can lead to HBV reactivation in asymptomatic HBV carriers or patients with resolved HBV infection [49,50]. The list of chemotherapeutic agents associated with HBV reactivation is growing and includes anthracyclines, corticosteroids, platinum, vinca alkaloid, other small molecule agents, monoclonal antibodies and immune modulators [49]. Therefore, several professional societies, including AASLD and EASL, recommend HBV screening in all cancer patients undergoing chemotherapy and immunization with HBV vaccine or prophylactic antiviral therapy [49]. However, awareness of this serious clinical problem is limited [49] and needs to be considered in clinical trials for new treatments. CDK-inhibiting drugs are a novel class of cancer therapeutics and three CDK4/6 inhibitors, palbociclib, ribociclib (LEE011), and abemaciclib are FDA and EMA approved for the treatment of advanced hormone receptor positive (HR+) breast cancer and in clinical trials for other non-breast malignancies [51]. Palbociclib (PD-0332991) is now under evaluation for the treatment of different Rb protein positive cancers [52–54] and most importantly in clinical trials for the treatment of HCC [55,56]. Chronic HBV infection accounts for approximately 50% of cases of HCC worldwide [1]. In this study, we show that CDK4/6 inhibition by palbociclib enhances HBV replication by arresting cells in the G0/G1 phase of the cell cycle. Therefore, caution is warranted in the use of such agents for HCC treatment. Our findings have important clinical implications as they indicate that there might be a potential risk of HBV reactivation during therapy with a CDK4/6 inhibitor, such as palbociclib, currently evaluated for HCC treatment.

Taken together, our gain-of-function screening approach allowed the identification of key HBV host factors, such as CDKN2C, with clinical implications in patients. Our data pave the way for the development of more permissive infection systems for the study of virus host interactions and the identification of previously undiscovered antiviral targets urgently needed for viral cure.

METHODS

Human subjects. Human serum from patients with chronic HBV/HDV infection followed at the Strasbourg University Hospitals, Strasbourg, France was obtained with informed consent. PHH were obtained from liver tissue from patients undergoing liver resection for liver metastasis at the Strasbourg University Hospitals with informed consent. Protocols were approved by the local Ethics Committee of the Strasbourg University Hospitals (CPP) and the Ministry of Higher Education and Research of France (DC-2016-2616). Human samples from HBV infected patients followed at the Chang Gung Memorial Hospital (Taipei, Taiwan) were obtained with informed consent. Protocols were approved by the local Ethics Committee (Institutional Review Board 102-3825C).

Cell lines and viruses. NTCP-overexpressing Huh-106 and HepG2-NTCP cell lines [5,57] as well as human embryonic kidney 293T (HEK 293T) [58] cell line have been described. PHH were isolated and cultured as described [58]. Recombinant HDV production [5,57] as well as purification of infectious HBV particles from the inducible human hepatoblastoma HepAD38 has been described [5,59,60].

Reagents and plasmids. DMSO, polybrene and PEG 8000 (polyethylene glycol) were obtained from Sigma-Aldrich (Merck). DNA and RNA transfection at the indicated concentrations was performed using CalPhos Mammalian Transfection Kit (Clonetech) and Lipofectamine RNAiMAX (Thermo Scientific) according to the manufacturer's instructions, respectively. The ORF-encoding lentivirus constructs for validations were obtained from the RNAi Platform, Broad Institute of MIT and Harvard (Cambridge, MA, USA). Cell viability was assessed using PrestoBlue Cell Viability Reagent (Invitrogen) according to the manufacturer's instructions. Palbociclib and LEE011 (Ribociclib) were obtained from Synkinase and Sellekchem respectively.

HBV binding. The binding of HBV virions at the cell surface was assessed as described [5]. In brief, cells were incubated with pretreated HBV in the presence of 4% PEG for 24 hours at 16 ºC. Unbound virions were removed by three washes with PBS, and cells and bound virions were lysed. HBV total DNA was quantified by qPCR using a standard curve generated from known HBV genome copies.

HBV and HDV infections. For HBV infection, NTCP-overexpressing cell lines and PHH were infected by recombinant HBV in presence of 4% of PEG-8000 (GEq 500 or 1000 per cell) [5,60]. After infection, Huh7-106 and HepG2-NTCP cells were washed and culture in PMM medium with 2% or 3.5% of DMSO respectively for 10 days. HBV infection was assessed 10 days post infection (dpi) by immunofluorescence (IF) using a mouse monoclonal antibody targeting HBsAg (Bio-Techne, clone

1044/329) and Alexa Fluor 647-labelled secondary antibody targeting mouse IgGs (Jackson Research). Cell nuclei were stained with DAPI. Fluorescent imaging was performed using an Axio Observer Z1 microscope (Carl Zeiss, Germany). Alternatively, cells were lysed and total RNA was extracted using the ReliaPrep RNA Miniprep Systems (Promega) and qRT-PCR quantification of HBV pregenomic RNA (pgRNA) was assessed as described [5,60,61]. HBsAg and hepatitis B e antigen (HBeAg) secretion were quantified by chemiluminescence immunoassay (CLIA, Autobio) following the manufacturer's instructions. Southern blot detection of HBV cccDNA was performed using digoxigenin (DIG)-labeled (Roche) specific probes as described [62]. Total DNA from HBV-infected cells was extracted using the Hirt method as described [63]. Specific DIG-labeled probes for the detection of HBV and mitochondrial probes for the detection of HBV and mitochondrial DNAs were synthetized using the PCR DIG Probe Synthesis Kit (Roche) and the primers as described [60]. HBV total RNAs were detected by Northern blot. Total RNA was purified using ReliaPrep RNA Miniprep Systems (Promega). 5 µg of total RNA was subjected to electrophoresis through a 2.2 M formaldehyde, 1% agarose gel and transferred to a nylon membrane positively charged (Roche). The membrane-bound RNA was hybridized to a ^{32}P-labeled RNA probe specific for detection of HBV RNA of 1200 to 1944 bp of viral genome (3.5 kbp to 2.1 kbp). For HDV infection, NTCP-overexpressing cell lines were infected with recombinant HDV (GEq 100 per cell) as described [5,60]. HDV infection was assessed 7 days after infection by IF using an antibody targeting the hepatitis delta antigen (HDAg) purified from serum of an HBV/HDV co-infected patient [64] and AF647-labeled secondary antibody targeting human IgGs (Jackson Research) as described [5,65].

Genome-scale lentiviral expression library and gain-of function screen. hORFeome V8.1 library (Broad Institute of MIT and Harvard, Cambridge, MA, USA) containing a pool of 16,172 clonal ORFs (mapping 13,833 human genes) was cloned into a pLX_TRC317 vector. The establishment of the genome-scale ORFeome library has been described [18]. 30 million Huh-106 cells were transduced with the lentiviral ORFeome library in duplicate in the presence of polybrene (4 µg/ml). To avoid a cumulative effect of multiple ORFs, the LV volume was optimized to obtain 30% of transduced cells. Cells were then selected with puromycin (0.9 µg/ml) for 3 days. After amplification, transduced cells were infected with recombinant HBV at a MOI of 1000 GE/cell or mock-infected. At 10 days post infection, cells were stained for HBsAg expression and sorted by flow cytometry.

Gene expression analysis in HBV-infected Huh-106 after ORFeome transduction. HBV-infected cells were fixed in 100% methanol for at least 20 minutes at -20°C. Cells were then blocked and permeabilized using PBS 0.5% BSA and 0.05% saponin for 1 hour at RT. Cells were stained using an AF647-conjugated mouse monoclonal anti-HBsAg Ab (Bio-Techne, clone 1044/329) and resuspended

in 0.5% BSA. HBsAg positive cells were sorted by Fluorescence Activating Cell Sorting (FACS) (BD FACSAria Flow Cytometer). 20 million cells were taken from HBV-infected sample as pre-sort control and total genomic DNA (gDNA) was extracted from cell pellets using Qiagen kits according to the manufacturer's protocol (Qiagen). Additionally, gDNA was extracted from 20 million HBV positive sorted cells from two biological replicates, named HBV sorted. Extracted DNA was used as a template for PCR to amplify the barcode sequences that accompany every ORF in the library. The unique barcode associated with each ORF construct was determined by Sanger sequencing in an arrayed collection of all the ORF constructs prior to pooling. PCR and sequencing were performed as previously described [66,67]. The details of the PCR primers and conditions can be found here: https://portals.broadinstitute.org/gpp/public/resources/protocols. Samples were sequenced on a HiSeq2000 (Illumina). The resulting reads were matched to their barcodes and their associated ORFs using PoolQ (see https://portals.broadinstitute.org/gpp/public/resources/protocols for more information on PoolQ). For analysis, the read counts were normalized to reads-per-million and then log2 transformed. The log2 fold-change (Log2FC) of each ORF was determined relative to the initial time point for each biological replicate. 90 hits with Log2FC values above the threshold set at 1.5 were selected as candidates.

Flow cytometry. For further flow cytometry analysis of HBV-infected cells, cells were fixed in 100% methanol for at least 20 minutes at -20 ºC. Cells were then blocked and permeabilized using PBS 1% FBS, 0.05% saponin for 30 min at RT. HBsAg was stained using a mouse monoclonal anti-HBsAg Ab (Bio-Techne, clone 1044/329) for 30 minutes at 4 ºC and then with an AF647-labelled secondary antibody targeting mouse IgGs (Jackson Research) for 30 minutes at 4 ºC. For flow cytometry analysis of DNA content, cells were fixed in ice-cold 75% ethanol in water for 30 minutes at 4ºC. Cells were washed and resuspend and incubated in PBS 50 µg/mL propidium iodide (Invitrogen) and 50 µg/mL Ribonuclease A (Sigma) for 30 min at RT. Cells were subsequently washed and resuspended in PBS 5 µM EDTA prior to sorting through a CytoFLEX flow cytometer system (Beckman Coulter).

Candidate selection from the primary screen. The impact of gene over-expression on HBV infection was defined by a specific enrichment in cDNA sequences in HBV-positive sorted cells compared to the pre-sort population. For hit selection, a functional threshold of Log2FC = 1.5 compared to pre-sorted cells was applied, leading to a total of 90 candidates **(Table S1, Figure 2c-d)**. As multiple ORF sequences for one given gene are sometimes present in the library, individual sequences were analyzed. Candidate genes with multiple associated ORFs were selected only if clones presented significant differences in their sequences (truncations in Cter or Nter of the proteins) or if a at least two identical ORFs exhibited a Log2FC > 1. Candidate gene expression in the liver was then assessed through the

Human Protein Atlas (available from www.proteinatlas.org) [68]. Candidates with liver expression < 0.1 transcript per million (TPM) were removed from the analysis, leading to a final selection of 47 candidates **(Table S1)**. 47 ORF-containing lentiviruses were then obtained for individual validations, 35 of which met internal quality control based on lentiviral titration. In addition, lentiviruses encoding *GFP*, *KRT80* and *CPA1* cDNA sequences were obtained as negative controls from the primary screen.

Hit validation in Huh-106 cells and PHH. Individual ORFs were expressed from pLX-Blast-V5 (lentiviral) expression plasmids. Lentivirus particles were produced in HEK 293T cells by cotransfection of plasmids expressing the human immunodeficiency virus (HIV) gap-pol, the vesicular stomatitis virus glycoprotein (VSV-G) and the pLX-Blast-V5-ORF plasmids in the ratio of 10:3:10, using the CalPhos Mammalian Transfection kit as described [58]. Three days after transfection, supernatants were collected, pooled and clarified using 0.45 µm pore filters. Huh-106 were individually transduced with the 38 ORF-expressing lentivirus constructions and selected with 6 µg/mL of blasticidin 48 hours prior to HBV infection. HBV infection was assessed after ten days by quantification of HBeAg and HBsAg expression in the supernatant of infected cells as described above. For further validations, PHH and Huh-106 were transduced with individual ORF-containing lentivirus prior to HBV infection. Infection was assessed after ten days by Southern blot detection of HBV DNA, Northern blot and qRT-PCR detection of HBV RNAs, immunodetection of HBsAg, and quantification of HBeAg as described above.

CDKN2C HepG2-NTCP knockout generation.

To generate clonal HepG2-NTCP CDKN2C knock-outs, the following primers corresponding to guide RNAs targeting CDKN2C exons were cloned into the Zhang lab generated Cas9 expressing pX458 plasmid (Addgene plasmid #48138): guide 1; Forward primer: CACCGACACCGCCTGT-GATTTGGCC, Reverse primer: AAACGGCCAAATCACAGGCGGTGTC. guide 2; Forward primer: CACCGCACAGGCGGTGTCCCCCTTA, Reverse primer: AAACTAAGGGGGACACCG-CCTGTGC. pX458 plasmids encoding guide RNAs against CDKN2C were transfected into HepG2-NTCP cells using lipofectamine 3000 (Life technologies) according to manufactures guidelines. Transfected cells were single cell sorted based on + GFP expression into 96 well plates using the SONY SH800S cell sorter. Individual clones were expanded, and four clonal cell lines were eventually selected for further characterization.

RNAi loss-of-function studies. ON-TARGETplus small interfering RNA (siRNA) pools (Dharmacon) targeting the transcripts of *CDKN2C* and *SLC10A1* (NTCP) were reverse-transfected into HepG2-NTCP cells with Lipofectamine RNAiMAX (Invitrogen) as described. RNA was purified

from cells harvested 2 days after transfection, and gene expression was analyzed by qRT-PCR. For silencing of *CDKN2C* expression in PHH, PHH were transduced with lentiviral vectors containing *CDKN2C*-targeting shRNA (target sequence: GATGTTAACATCGAGGATAAT) or a scrambled shRNA control (target sequence: CCTAAGGTTAAGTCGCCCTCG) obtained from VectorBuilder. RNA was purified from PHH harvested 3 days after transduction, and gene expression was analyzed by qRT-PCR.

Comparative analysis of gene expression in Huh-106 and HepG2-NTCP cells. Huh-106 and HepG2-NTCP cells were lysed and total RNA from three biological replicates per cell line was then extracted as described above. Microarray analysis of gene expression in both cell lines was performed at the IGBMC GenomEast platform (Illkirch, France). Biotinylated single strand cDNA targets were prepared from 200 ng of total RNA using the Ambion WT Expression Kit (Cat # 4411974) and the Affymetrix GeneChip® WT Terminal Labeling Kit (Cat # 900671) according to Affymetrix recommendations. Following fragmentation and end-labeling, 3 µg of cDNAs were hybridized for 16 hours at 45°C on GeneChip® Human Gene 2.0 ST arrays (Affymetrix) interrogating over 40 0000 RefSeq transcripts and ~ 11000 LncRNAs. The chips were washed and stained in the GeneChip® Fluidics Station 450 (Affymetrix) and scanned with the GeneChip® Scanner 3000 7G (Affymetrix) at a resolution of 0.7 µm. Raw data (CEL Intensity files) were extracted from the scanned images using the Affymetrix GeneChip® Command Console (AGCC) version 4.1.2. CEL files were further processed with Affymetrix Expression Console software version 1.4.1 to calculate probe set signal intensities using Robust Multi-array Average (RMA) algorithms with default settings. Modulated molecular pathways were determined by using GSEA [69]. Individual differential gene expression of the selected candidates was evaluated through the Z score transformation. The dataset is publicly available in the NCBI Gene Expression Omnibus database (accession number GSE132638).

Analysis of gene expression using quantitative RT-PCR. RNA was extracted as described above and gene expression was assessed by qRT-PCR as described [60]. Gene expression was normalized to GADPH expression. Primers and TaqMan® probes for *GAPDH*, *CDKN2C* and *SLC10A1* mRNA detection were obtained from ThermoFisher (TaqMan® Gene Expression Assays).

Protein expression. The expression of CDKN2C and *β*-tubulin was assessed by Western blot as described [5] using a monoclonal rabbit anti-CDKN2C antibody (anti-p18 INK4c, ab192239, Abcam), a rabbit polyclonal anti-*β*-tubulin antibody (GTX101279, Gentex) and a rabbit polyclonal anti-GAPDH (ab9485, Abcam), respectively. Peroxidase-AffiniPure Goat Anti-Rabbit IgG (H+L) (Jackson

Research 111-035-144) was used as a secondary antibody. Protein expression was assessed using the ChemiDoc™ Imaging System (BioRad).

Analysis of nascent HBV RNA synthesis. Run-on assays were performed using Click-iT™ Nascent RNA Capture Kit from Thermofisher Scientific according to the manufacturer's instructions. HBV total and nascent RNA expression was assessed from HBV-infected Huh-106 cells overexpressing either *GFP* or *CDKN2C* by qRT-PCR four days after virus inoculation with 2 h of ethynyl uridine (EU) labeling. Actinomycin D (ActD, Sigma-Aldrich, Merck) was used as a negative control. Cells were pre-treated with ActD at 10 mg/mL for 20 min prior to EU labeling in presence of ActD. Specific primers and TaqMan® probes for total HBV RNAs (Pa03453406_s1) were purchased from Life Technologies. HBV RNA levels were normalized to *GUSB* expression using primers and TaqMan® probes from Life Technologies (Hs99999908_m1).

Analysis of *CDKN2C* expression in patients. For the analysis of *CDKN2C* mRNA expression in patients, *CDKN2C* mRNA expression was assessed in control healthy patients (n=6), HBV-infected patients with no detectable HBV DNA (n=32), HBV-infected patients with detectable HBV DNA (n=90) from GSE83148 [70]. Similarly, CDKN2C mRNA expression was assessed in HBV patients at different stages of virus infection including immune tolerant phase (n=22), immune clearance phase (n=50) and inactive carrier phase (n=11) from GSE65359. Alternatively, total RNA was extracted from liver tissue of 9 HBV-infected patients by using High Pure RNA Paraffin kit (Roche) according to the manufacturer's instruction, and gene expression analysis was performed by RNA-seq as previously reported [71]. To analyze the correlation between *CDKN2C* expression and the progression of liver disease in HBV-infected patients, *CDKN2C* mRNA expression was assessed in HBV-related liver fibrosis patients of different stages from GSE84044 [72] (n=37 score 0, n=33 score 1, n=34 score 2, n=15 score 3). Finally, *CDKN2C* expression in HBV-induced HCC patients was assessed from GSE65485 [73] (n=50 tumor tissue, n=5 non-tumor tissue) and from GSE14520 [74] (n=221 tumor tissue, n=199 non-tumor tissue). *CDKN2C* mRNA expression is shown as signal intensity values. For survival analysis, liver expression level of *CDKN2C* and survival data were derived from The Cancer Genome Atlas (TCGA, https://www.cancer.gov/about-nci/organization/ccg/research/structural-genomics/tcga) TCGA-LIHC database [75]. To analyze *CDKN2C* expression in liver tissue of patients with chronic liver disease, FPKM values and clinical data were retrieved from TCGA. This data set includes samples from HCV-infected patients (34 tumor samples including 5 paired tumor/non-tumor samples), HBV-infected patients (76 tumor samples including 7 paired tumor/non-tumor samples), patients with alcoholic liver disease (ALD) (72 tumor samples including 8 paired tumor/non-tumor samples) and

patients with non-alcoholic fatty liver disease (NAFLD) (11 tumor samples including 2 paired tumor/non-tumor samples).

Statistical information. For *in vitro* experiments, statistical analyses were performed using a two-tailed Mann-Whitney U test; $p < 0.05$ (*), $p < 0.01$ (**), and $p < 0.001$ (***) were considered statistically significant. Significant *p*-values are indicated by asterisks in the individual figures and figure legends. The number of tested replicates is indicated in the figure legends (n). For microarray analyses, two-tailed unpaired Student's t-test was performed by comparing the values from three biological replicates per cell line. $p < 0.01$ was considered statistically significant. For clinical data, Mann-Whitney U test was used when comparing two groups (Fig. 9d-e). For multiple group comparison (Fig. 9b-c), Kruskal–Wallis H test was used. Correlation between *CDKN2C* expression and HBV viral load in patients was assessed using Spearman's rank correlation coefficient (Spearman's rho). Survival functions depending on *CDKN2C* expression were obtained using the Kaplan–Meier estimator. *p*-value was calculated using log-rank test for comparisons of Kaplan-Meier survival. $p < 0.01$ was considered statistically significant.

REFERENCES

1. El-Serag, H. B. Epidemiology of Viral Hepatitis and Hepatocellular Carcinoma. *Gastroenterology* **142**, 1264–1273 (2012).
2. Trépo, C., Chan, H. L. Y. & Lok, A. Hepatitis B virus infection. *Lancet* **384**, 2053–2063 (2014).
3. Seeger, C. & Mason S., W. Molecular Biology of Hepatitis B Virus Infection. *Virology* **33**, 395–401 (2015).
4. Schulze, A., Gripon, P. & Urban, S. Hepatitis B Virus Infection Initiates With a Large Surface Protein-Dependent Binding to Heparan Sulfate Proteoglycans. *Hepatology* **46**, 1759–1768 (2007).
5. Verrier, E. R. *et al.* A targeted functional RNA interference screen uncovers glypican 5 as an entry factor for hepatitis B and D viruses. *Hepatology* **63**, 35–48 (2016).
6. Sureau, C. & Salisse, J. A Conformational Heparan Sulfate Binding Site Essential to Infectivity Overlaps with the Conserved Hepatitis B Virus a-Determinant. *Hepatology* **57**, 985–94 (2013).
7. Yan, H. *et al.* Sodium taurocholate cotransporting polypeptide is a functional receptor for human hepatitis B and D virus. *Elife* **1**, (2012).
8. Li, W. & Urban, S. Entry of hepatitis B and hepatitis D virus into hepatocytes: Basic insights and clinical implications. *J. Hepatol.* **64**, S32-40 (2016).
9. Königer, C. *et al.* Involvement of the host DNA-repair enzyme TDP2 in formation of the covalently closed circular DNA persistence reservoir of hepatitis B viruses. *PNAS* **111**, E4244–E4253 (2014).
10. Qi, Y. *et al.* DNA Polymerase K Is a Key Cellular Factor for the Formation of Covalently Closed Circular DNA of Hepatitis B Virus. *PLoS Pathog.* **12**, 1–26 (2016).
11. Nassal, M. HBV cccDNA: viral persistence reservoir and key obstacle for a cure of chronic hepatitis B. *Gut* **64**, 1972–1984 (2015).
12. Baumert, T. F., Verrier, E. R., Nassal, M., Chung, R. T. & Zeisel, M. B. Host-targeting agents for treatment of hepatitis B virus infection. *Curr. Opin. Virol.* **14**, 41–46 (2015).
13. Crouchet, E., Wrensch, F., Schuster, C., Zeisel, M. B. & Baumert, T. F. Host-targeting therapies for hepatitis C virus infection: current developments and future applications. *Ther Adv Gastroenterol* **11**, 1–15 (2018).

14. Xia, Y. & Liang, T. J. Development of Direct-acting Antiviral and Host-targeting Agents for Treatment of Hepatitis B Virus Infection. *Gastroenterology* **156**, 311–324 (2019).
15. Bekerman, E. & Einav, S. Combating emerging viral threats. *Science (80-.).* **348**, 282–283 (2015).
16. Ni, Y. *et al.* Hepatitis B and D viruses exploit sodium taurocholate co-transporting polypeptide for species-specific entry into hepatocytes. *Gastroenterology* **146**, 1070–1083 (2014).
17. Lempp, F. A., Qu, B., Wang, Y. & Urban, S. Hepatitis B Virus Infection of a Mouse Hepatic Cell Line Reconstituted with Human Sodium Taurocholate Cotransporting. *J. Virol.* **90**, 4827–4831 (2016).
18. Yang, X. *et al.* A public genome-scale lentiviral expression library of human ORFs. *Nat. Methods* **8**, 659–661 (2011).
19. Raney, A. K., Johnson, J. L., Palmer, C. N. A. & McLachlan, A. Members of the nuclear receptor superfamily regulate transcription from the hepatitis B virus nucleocapsid promoter. *J. Virol.* **71**, 1058–71 (1997).
20. Ishida, H. *et al.* Identification of multiple transcription factors, HLF, FTF, and E4BP4, controlling hepatitis B virus enhancer II. *J. Virol.* **74**, 1241–51 (2000).
21. Israelow, B., Narbus, C. M., Sourisseau, M. & Evans, M. J. HepG2 Cells Mount an Effective Antiviral Interferon-Lambda Based Innate Immune Response to Hepatitis C Virus Infection. *Hepatology* **60**, 1170–1179 (2014).
22. Devhare, P. B., Desai, S. & Lole, K. S. Innate immune responses in human hepatocyte-derived cell lines alter genotype 1 hepatitis E virus replication efficiencies. *Sci. Rep.* **6**, (2016).
23. Song, X.-X. *et al.* Cloning and characterization of a novel spermiogenesis-related gene, T6441, in rat testis. *Front. Biosci.* **11**, 143–150 (2006).
24. König, A. *et al.* Efficient long-term amplification of hepatitis B virus isolates after infection of slow proliferating HepG2-NTCP cells. *J. Hepatol.* **71**, 289–300 (2019).
25. Fry, D. W. *et al.* Specific inhibition of cyclin-dependent kinase 4/6 by PD 0332991 and associated antitumor activity in human tumor xenografts. *Mol. Cancer Ther.* **3**, 1427–1438 (2004).
26. Kim, S. *et al.* LEE011: An orally bioavailable, selective small molecule inhibitor of CDK4/6 – Reactivating Rb in cancer. *Mol. Cancer Ther.* **12**, PR02 (2013).
27. Guo, W., Chen, M. & Yen, T. S. B. Hepatocyte-Specific Expression of the Hepatitis B Virus Core Promoter Depends on Both Positive and Negative Regulation. *Mol. Cell. Biol.* **13**, 443–448 (1993).
28. Kim, D. H., Kang, H. S. & Kim, K.-H. Roles of hepatocyte nuclear factors in hepatitis B virus infection. *World J Gastroenterol* **22**, 7017–7029 (2016).
29. Tang, H. & McLachlan, A. Transcriptional regulation of hepatitis B virus by nuclear hormone receptors is a critical determinant of viral tropism. *Proc. Natl. Acad. Sci. U. S. A.* **98**, 1841–6 (2001).
30. Bebee, T. W. *et al.* The splicing regulators Esrp1 and Esrp2 direct an epithelial splicing program essential for mammalian development. *Elife* **4**, 1–27 (2015).
31. Candotti, D. & Allain, J. Biological and clinical significance of hepatitis B virus RNA splicing: an update. *Ann. Blood* **2**, 1–14 (2017).
32. Aden, D. P., Fogel, A., Plotkin, S., Damjanov, I. & Knowles, B. B. Controlled synthesis of HBsAg in a differentited human liver carcinoma-derived cell line. *Nature* **282**, 615–616 (1979).
33. Sureau, C., Romet-Lemonne, J.-L., Mullins, J. I. & Essex, M. Production of Hepatitis B Virus by a Differentiated Human Hepatoma Cell Line after Transfection with Cloned Circular HBV DNA. *Cell* **47**, 37–47 (1986).
34. Ozer, A. *et al.* Effect of Hepatocyte Proliferation and Cellular DNA Synthesis on Hepatitis B Virus Replication. *Gastroenterology* **110**, 1519–1528 (1996).
35. Schulze, A., Mills, K., Weiss, T. S. & Urban, S. Hepatocyte Polarization Is Essential for the Productive Entry of the Hepatitis B Virus. *Hepatology* **55**, 373–383 (2012).
36. De Abreu Costa, L. *et al.* Dimethyl Sulfoxide (DMSO) Decreases Cell Proliferation and TNF-α, IFN-γ, and IL-2 Cytokines Production in Cultures of Peripheral Blood Lymphocytes. *Molecules* **22**, (2017).

37. Wang, T. *et al.* Hepatitis B virus induces G1 phase arrest by regulating cell cycle genes in HepG2.2.15 cells. *Virol. J.* **8**, 1–8 (2011).
38. Xia, Y. *et al.* Hepatitis B virus deregulates cell cycle to promote viral replication and a premalignant phenotype. *J. Virol.* **92**, e00722-18 (2018).
39. Vermeulen, K., Bockstaele, D. R. Van & Berneman, Z. N. The cell cycle: a review of regulation, deregulation and therapeutic targets in cancer. *Cell Prolif.* **36**, 131–149 (2003).
40. Ludgate, L. *et al.* Cyclin-Dependent Kinase 2 Phosphorylates S/T-P Sites in the Hepadnavirus Core Protein C-Terminal Domain and Is Incorporated into Viral Capsids. *J. Virol.* **86**, 12237–12250 (2012).
41. Hu, J. *et al.* Cyclin E2-CDK2 mediates SAMHD1 phosphorylation to abrogate its restriction of HBV replication in hepatoma cells. *FEBS Lett.* **592**, 1893–1904 (2018).
42. Yamamoto, M. *et al.* CDK9 inhibitor FIT-039 prevents replication of multiple DNA viruses. *J. Clin. Invest.* **124**, 3479–3488 (2014).
43. Tanaka, T. *et al.* Inhibitory effect of CDK9 inhibitor FIT-039 on hepatitis B virus propagation. *Antiviral Res.* **133**, 156–164 (2016).
44. Burkhart, D. L. & Sage, J. Cellular mechanisms of tumour suppression by the retinoblastoma gene. *Nat. Rev. Cancer* **8**, 671–682 (2008).
45. Guan, K. *et al.* Growth suppression by p18, a p16- and p14-related CDK6 inhibitor, correlates with wild-type pRb function. *Genes Dev.* **8**, 2939–2952 (1994).
46. Sato, Y. *et al.* Regulatory signatures of liver regeneration distilled by integrative analysis of mRNA, histone methylation, and proteomics. *J. Biol. Chem.* **292**, 8019–8037 (2017).
47. Reiter, F. P. *et al.* Predictors of ribociclib-mediated antitumour effects in native and sorafenib-resistant human hepatocellular carcinoma cells. *Cell. Oncol.* **42**, 705–715 (2019).
48. Halgand, B. *et al.* Hepatitis B Virus Pregenomic RNA in Hepatocellular Carcinoma: A Nosological and Prognostic Determinant. *Hepatology* **67**, 86–96 (2018).
49. Kawsar, H. I., Shahnewaz, J., Gopalakrishna, K. V, Spiro, T. P. & Daw, H. A. Hepatitis B Reactivation in Cancer Patients : Role of Prechemotherapy Screening and Antiviral Prophylaxis. *Clin. Adv. Hematol. Oncol.* **10**, 370–378 (2012).
50. Galbraith, R. M., Eddleston, A. L. W. F., Williams, R., Zuckerman, A. J. & Bagshawe, K. D. Fulminant hepatic failure in leukaemia and choriocarinoma related to withdrawal of cytotoxic drug therapy. *Lancet* 528–530 (1975).
51. Vijayaraghavan, S. & Moulder, S. Inhibiting CDK in Cancer Therapy: Current Evidence and Future Directions. *Target. Oncol.* **13**, 21–38 (2018).
52. Konecny, G. E. *et al.* Expression of p16 and Retinoblastoma Determines Response to CDK4/6 Inhibition in Ovarian Cancer. *Clin Cancer Res.* **17**, 1591–1602 (2011).
53. Cen, L. *et al.* p16-Cdk4-Rb axis controls sensitivity to a cyclin-dependent kinase inhibitor PD0332991 in glioblastoma xenograft cells. *Neuro. Oncol.* **14**, 870–881 (2012).
54. Logan, J. E. *et al.* PD-0332991, a Potent and Selective Inhibitor of Cyclin-dependent Kinase 4/6, Demonstrates Inhibition of Proliferation in Renal Cell Carcinoma at Nanomolar Concentrations and Molecular Markers Predict for Sensitivity. *Anticancer Res.* **33**, 2997–3004 (2013).
55. Littman, S. J., Brus, C. & Burkart, A. A phase II study of palbociclib (PD-0332991) in adult patients with advanced hepatocellular carcinoma. *J. Clin. Oncol.* **33**, (2015).
56. Bollard, J. *et al.* Palbociclib (PD-0332991), a selective CDK4/6 inhibitor, restricts tumour growth in preclinical models of hepatocellular carcinoma. *Gut* **66**, 1286–1296 (2017).
57. Verrier, E. R. *et al.* Solute Carrier NTCP Regulates Innate Antiviral Immune Responses Targeting Hepatitis C Virus Infection of Hepatocytes. *Cell Rep.* **17**, 1357–1368 (2016).
58. Lupberger, J. *et al.* EGFR and EphA2 are host factors for hepatitis C virus entry and possible targets for antiviral therapy. *Nat. Med.* **17**, 589–595 (2011).
59. Ladner, S. K. *et al.* Inducible expression of human hepatitis B virus (HBV) in stably transfected hepatoblastoma cells: a novel system for screening potential inhibitors of HBV replication. *Antimicrob. Agents Chemother.* **41**, 1715–20 (1997).

60. Verrier, E. R. *et al.* Hepatitis B virus evasion from cGAS sensing in human hepatocytes. *Hepatology* 1–36 (2018). doi:10.1002/hep.30054
61. Verrier, E. R. *et al.* Combined small molecule and loss-of-function screen uncovers estrogen receptor alpha and CAD as host factors for HDV infection and antiviral targets. *Gut* 1–10 (2019). doi:10.1136/gutjnl-2018-317065
62. Lucifora, J. *et al.* Detection of the hepatitis B virus (HBV) covalently-closed-circular DNA (cccDNA) in mice transduced with a recombinant AAV-HBV vector. *Antiviral Res.* **145**, 14–19 (2017).
63. Gao, W. & Hu, J. Formation of Hepatitis B Virus Covalently Closed Circular DNA: Removal of Genome-Linked Protein. *J. Virol.* **81**, 6164–6174 (2007).
64. Habersetzer, F. *et al.* Loss of hepatitis B surface antigen in a real-life clinical cohort of patients with chronic hepatitis B virus infection. *Liver Int.* **35**, 130–9 (2015).
65. Hughes, S. A., Wedemeyer, H. & Harrison, P. M. Hepatitis delta virus. *Lancet* **378**, 73–85 (2011).
66. Doench, J. G. *et al.* Optimized sgRNA design to maximize activity and minimize off-target effects of CRISPR-Cas9. *Nat. Biotechnol.* **34**, 1–12 (2016).
67. Piccioni, F., Younger, S. T. & Root, D. E. Pooled Lentiviral-Delivery Genetic Screens. *Curr. Protoc. Mol. Biol.* **121**, 32.1.1-32.1.21 (2018).
68. Uhlén, M. *et al.* Tissue-based map of the human proteome. *Science (80-.).* **347**, 1260419 (2015).
69. Subramanian, A. *et al.* Gene set enrichment analysis : A knowledge-based approach for interpreting genome-wide. *PNAS* **102**, 15545–15550 (2005).
70. Zhou, W. *et al.* Predictive model for inflammation grades of chronic hepatitis B : scale analysis of clinical parameters and gene expressions. *Liver Int.* **37**, 1632–1641 (2017).
71. Nakagawa, S. *et al.* Molecular liver cancer prevention in cirrhosis by organ transcriptome analysis and lysophosphatidic acid pathway inhibition. *Cancer Cell* **30**, 879–890 (2016).
72. Wang, M. *et al.* Characterization of gene expression profiles in HBV-related liver fibrosis patients and identification of ITGBL1 as a key regulator of fibrogenesis. *Sci. Rep.* **7**, 43446 (2017).
73. Dong, H. *et al.* Identification of HBV-MLL4 Integration and Its Molecular Basis in Chinese Hepatocellular Carcinoma. *PLoS One* **10**, e0123175 (2015).
74. Roessler, S. *et al.* A Unique Metastasis Gene Signature Enables Prediction of Tumor Relapse in Early Stage Hepatocellular Carcinoma Patients. *Cancer Res.* **70**, 10202–10212 (2010).
75. Erickson, B. J. *et al.* Radiology Data from The Cancer Genome Atlas Liver Hepatocellular Carcinoma [TCGA-LIHC] collection. The Cancer Imaging Archive. (2016). doi:http://doi.org/10.7937/K9/TCIA.2016.IMMQW8UQ

Acknowledgments. We thank Claudine Ebel, Romain Kaiser and Muriel Phillips (IGBMC, Flow Cytometry platform, France) for excellent technical assistance. We thank Christelle Thibault for the microarray analysis (IGBMC, GenomEast platform, Illkirch, France). We thank our colleague Sarah Durand (U1110) for the excellent technical support. This work was supported by Inserm, the University of Strasbourg, the European Union (ERC-2014-AdG-671231-HEPCIR, Infect-ERA hepBccc, EU H2020 Hep-CAR 667273), the IHU Fondation ARC (French Cancer Agency) TheraHCC program IHU201301187 and IHU201901299, the Institut Universitaire de France and the Agence Nationale de Recherche sur le Sida et les hépatites virales (ANRS) and the National Institute of Allergy and Infectious Diseases of the National Institutes of Health under award number R03AI131066. CCC acknowledges fellowships from the Canadian Institutes of Health Research (201411MFE-338606-245517) and the Canadian Network on Hepatitis C. ERV acknowledges fellowship from ANRS (ECTZ50121).

Author contributions. ERV and TFB designed and supervised research. TFB initiated the study. CCC, GSC, DR, ERV and TFB designed the gain-of-function screen. LH, CCC, FP, GSC and DR performed and analyzed the screen. CE, LH and CCC performed the validation experiments. CE, LH,

CCC, KM, JLup, MN, CSc, CSu, ERV and TFB analyzed the validation data. HES and ERV analyzed the microarray data. HES, FJ, NF, SYH, YH and ERV analyzed the clinical data. CSu performed the HBV Northern blots. CP and JLuc performed and analyzed the run-on data. PP and EF provided human hepatocytes. CE, LH, ERV and TFB wrote the manuscript. CE and LH contributed equally to this work as first authors. ERV and TFB contributed equally to this work as senior authors.

Competing interests. The authors have no competing interests to disclose.

Materials & Correspondence. Material and correspondence requests should be addressed to Prof. Thomas F. Baumert (thomas.baumert@unistra.fr) and Dr Eloi R. Verrier (e.verrier@unistra.fr).

Data availability. The dataset generated in this study, including the results from the gain-of-function primary screen, are available within Supplementary information. The microarray dataset is publicly available in the NCBI Gene Expression Omnibus database (accession number GSE132638). The rest of the data is available through the corresponding authors upon reasonable request.

4.5 CAD est un acteur clé de la réplication du VHD et une cible antivirale potentielle

Les études précédentes ont mis en lumière l'intérêt de mon approche pour une meilleure compréhension des interactions hôte-virus dans le cadre de l'infection par le VHB. À la suite des recommandations d'intensifier les recherches sur le VHD, émises par les membres du conseil scientifique du LabEx HepSYS dont le laboratoire est porteur (07/2014), j'ai mis au point une double approche de criblage à haut débit pour l'identification des facteurs hépatiques impliqués dans l'infection par le VHD. A l'aide d'une banque de siRNA ciblant plus de 7500 gènes (« Druggable genome », Dharmacon), j'ai analysé l'impact de la diminution de l'expression de chacun de ces gènes sur l'infection par le VHD. Dans un second temps, j'ai réalisé un criblage chimique à l'aide de la banque Prestwick, contenant environ 1200 molécules possédant des autorisations de mise sur le marché, afin d'identifier de petites molécules inhibitrices de l'infection VHD. Parmi les 7567 gènes ciblés par la banque de siRNA, 191 candidats ayant un impact significatif sur l'infection VHD ont été retenus. L'analyse bio-informatique des candidats issus du criblage identifie notamment des gènes impliqués dans l'activité de l'ARN polymérase II (Pol II), enzyme cruciale pour le VHD, qui la détourne de son activité principale de transcription de l'ARN messager pour répliquer son ARN génomique (32). Ces résultats valident la capacité de notre stratégie de criblage à identifier des protéines cellulaires impliquées spécifiquement dans la réplication du VHD dans les hépatocytes. Parmi les voies de signalisation mises en lumière, la biosynthèse des pyrimidines semble jouer un rôle important dans l'infection VHD. Notamment, la diminution de l'expression des gènes codant pour le récepteur des œstrogènes α (*ESR1*) et l'enzyme CAD (carbamoyl-phosphate synthetase 2, aspartate transcarbamylase, and dihydroorotase) induit une diminution significative du niveau d'infection VHD (45). ESR1 est un récepteur hormonal nucléaire exprimé principalement dans le tissu épithélial de la glande mammaire et l'appareil reproducteur féminin, mais aussi dans les poumons, le système vasculaire et le foie (46). Dans le foie, le polymorphisme du gène *ESR1* a notamment été associé à la sensibilité à l'infection chronique par le VHB (47). Par ailleurs, ESR1 se lie au facteur de transcription SP1 dans le noyau, induisant l'expression de *CAD* (48), qui code pour une enzyme catalysant les trois premières étapes de la biosynthèse des pyrimidines, dont plusieurs acteurs importants sont identifiés dans notre criblage. L'analyse du criblage chimique effectué en parallèle m'a permis d'établir une liste de molécules inhibant l'infection VHD. Le Fulvestrant, un inhibiteur bien connu d'ESR1, inhibe de manière dose dépendante l'infection VHD dans notre modèle, confirmant ainsi les résultats de notre criblage siRNA. L'activité antivirale du Fulvestrant est corrélée à une inhibition de l'expression de l'enzyme CAD, confirmant le lien fonctionnel entre ESR1 et CAD. Cibler ESR1, molécule ayant de nombreux effets sur la cellule, peut se révéler risqué. Par conséquent, la suite de ce travail s'est focalisée sur le potentiel antiviral de CAD. Nous avons fait synthétiser, en partenariat avec le

Laboratoire de Synthèse, Réactivité Organiques et Catalyse de l'Institut de Chimie de Strasbourg (Prof. P. Pale) un inhibiteur spécifique de l'enzyme CAD, l'acide sparfosique ou PALA, non disponible sur le marché. Le PALA montre une activité antivirale marquée contre le VHD, dans notre modèle cellulaire et dans les hépatocytes primaires, confirmant l'intérêt de cibler CAD dans le cadre de nouvelles stratégies antivirales. L'analyse des différentes formes d'ARN du VHD indique que le PALA inhibe toutes les étapes de la réplication, y compris la synthèse de l'ARN antigénomique. De plus, la complémentation du milieu de culture à l'aide d'uridine ou de DHO (produit de CAD) annule l'effet antiviral du PALA, confirmant l'importance de la fonction physiologique de CAD dans la réplication du VHD.

L'ensemble de ces résultats valident l'intérêt d'une double approche de criblage pour identifier des facteurs cellulaires impliqués dans l'infection virale, et de petites molécules antivirales. La stratégie mise en œuvre a permis d'identifier ESR1 et CAD comme des acteurs majeurs de la réplication du VHD, et des cibles thérapeutiques potentielles pour le développement de nouveaux traitements contre cette infection incurable.

Collaborations majeures : L. Brino (IGBMC, Illirch) ; P. Pale (Institut de Chimie, Université de Strasbourg, Strasbourg).

Publication associée : Verrier ER et al., Gut 2020;69:158–167

Verrier ER et al., Gut 2020;69:158–167

OPEN ACCESS

ORIGINAL ARTICLE

Combined small molecule and loss-of-function screen uncovers estrogen receptor alpha and CAD as host factors for HDV infection and antiviral targets

Eloi R Verrier,[1] Amélie Weiss,[2] Charlotte Bach,[1] Laura Heydmann,[1] Vincent Turon-Lagot,[1] Arnaud Kopp,[2] Houssein El Saghire,[1] Emilie Crouchet,[1] Patrick Pessaux ,[1,3] Thomas Garcia,[4] Patrick Pale,[4] Mirjam B Zeisel,[1] Camille Sureau,[5] Catherine Schuster,[1] Laurent Brino,[2] Thomas F Baumert [1,3,6]

[1]Université de Strasbourg, Inserm, Institut de Recherche sur les Maladies Virales et Hépatiques UMR_S1110, F-67000 Strasbourg, France
[2]IGBMC, Plateforme de Criblage Haut-débit, UMR7104 CNRS U1258 Inserm, Illkirch, France
[3]Institut Hospitalo-universitaire, Pôle Hépato-digestif, Nouvel Hôpital Civil, Strasbourg, France
[4]Laboratoire de Synthèse, Réactivité Organiques et Catalyse, Institut de Chimie, UMR 7177 CNRS, Université de Strasbourg, Strasbourg, France
[5]INTS, Laboratoire de Virologie Moléculaire, Paris, France
[6]Institut Universitaire de France, Paris, France

Correspondence to
Dr Eloi R Verrier and Pr Thomas F Baumert, Inserm UMR_S1110, Institut de Recherche sur les Maladies Virales et Hépatiques, 3 rue Koeberlé, 67000 Strasbourg, France;
e.verrier@unistra.fr, thomas.baumert@unistra.fr

Received 26 June 2018
Revised 24 January 2019
Accepted 10 February 2019
Published Online First 4 March 2019

To cite: Verrier ER, Weiss A, Bach C, *et al*. *Gut* 2020;**69**:158–167.

ABSTRACT

Objective Hepatitis D virus (HDV) is a circular RNA virus coinfecting hepatocytes with hepatitis B virus. Chronic hepatitis D results in severe liver disease and an increased risk of liver cancer. Efficient therapeutic approaches against HDV are absent.

Design Here, we combined an RNAi loss-of-function and small molecule screen to uncover host-dependency factors for HDV infection.

Results Functional screening unravelled the hypoxia-inducible factor (HIF)-signalling and insulin-resistance pathways, RNA polymerase II, glycosaminoglycan biosynthesis and the pyrimidine metabolism as virus-hepatocyte dependency networks. Validation studies in primary human hepatocytes identified the carbamoyl-phosphatesynthetase 2, aspartate transcarbamylase and dihydroorotase (CAD) enzyme and estrogen receptor alpha (encoded by *ESR1*) as key host factors for HDV life cycle. Mechanistic studies revealed that the two host factors are required for viral replication. Inhibition studies using N-(phosphonoacetyl)-L-aspartic acid and fulvestrant, specific CAD and ESR1 inhibitors, respectively, uncovered their impact as antiviral targets.

Conclusion The discovery of HDV host-dependency factors elucidates the pathogenesis of viral disease biology and opens therapeutic strategies for HDV cure.

Significance of this study

What is already known on this subject?
- Chronic hepatitis D is the most severe form of viral hepatitis.
- Efficient therapeutic strategies are absent.
- Hepatitis D virus is a small hepatitis B virus satellite virus.
- Knowledge about HDV–hepatocyte interactions is limited.
- HDV host-dependency factors are largely unknown.

What are the new findings?
- A RNAi screen identified oestrogen receptor 1 (ESR1) and CAD as novel host factors for HDV infection.
- The inhibition of CAD restricts HDV infection through uridine depletion.
- ESR1 and CAD are functionally linked by transcriptional activation of gene expression.
- ESR1 and CAD inhibitors fulvestrant and PALA, respectively, specifically inhibit HDV replication in a dose-dependent manner in human hepatocytes.
- CAD and ESR1 are previously undiscovered targets for antiviral therapies.

How might it impact on clinical practice in the foreseeable future?
- The discovery of HDV host-dependency factors opens the door for novel therapeutic strategies against chronic hepatitis D - a major unmet medical need.
- Fulvestrant and PALA-like molecules are candidate compounds for HDV antivirals to enter preclinical development.

INTRODUCTION

Hepatitis delta virus (HDV) infects human hepatocytes and causes acute acerbation of liver disease in patients chronically infected with hepatitis B virus (HBV).[1] Among HBV-infected patients, 5%–10% are coinfected with HDV.[2] HDV coinfection or surinfection in HBV carriers induces more severe disease compared with infection with HBV alone. This includes a greater likelihood of experiencing liver failure and a more rapid progression to liver cirrhosis, with a markedly increased risk of developing hepatocellular carcinoma.[3] Consequently, chronic hepatitis D is considered as one of the most severe forms of viral hepatitis. Treatment with HBV nucleos(t)ide analogues is not effective at reducing HDV replication or disease. Moreover, the virus is only poorly controlled by the current interferon (IFN)-based therapies.[3] To date, no treatment allows efficient cure of hepatitis D with eradication of the virus and its associated disease.[4–6] Thus, there is a major unmet medical need for curative therapies.

HDV is a small, circular RNA HBV satellite virus related to plant viroids using HBV envelope proteins to assemble its infectious particles.[1 5 6] Consequently, it can only be propagated by HBV-infected

hepatocytes producing HBV envelope proteins (Hepatitis B surface antigen or HBsAg). The HDV genome is a circular 1.7 kb single-stranded negative-sense RNA molecule (for a review on HDV virology and pathogenesis, see ref 5). The HDV life cycle starts with virus entry into hepatocyte after attachment to heparan sulfate proteoglycans (HSPG) at the cell surface.[5 7] As HBV and HDV share the same envelope proteins, they appear to share the same entry pathway and receptor(s), including the sodium taurocholate cotransporting polypeptide (NTCP) and glypican 5 (reviewed in refs 5 6 8). The HDV genome is then imported in the nucleus, and three types of RNAs are transcribed by the host RNA polymerase II: replication is initiated by synthesis of an antigenomic RNA that serves as a template for the production of new HDV genomic RNA and HDV mRNA from genomic RNA.[5] mRNA transcripts contain one unique open reading frame encoding the hepatitis delta antigen (HDAg) that exists in two forms (small version [S-HDAg] and large version [L-HDAg]) which play differential roles in the HDV life cycle.[5 6] Indeed, S-HDAg is essential to HDV replication, while prenylation of L-HDAg leads to the inhibition of HDV replication and is crucial for binding to HBV envelope proteins and virion assembly.[6] In the nucleus, L-HDAgs bind to the de novo HDV genomic RNA to form a new ribonucleoprotein, which is exported to the cytoplasm and interacts with HBsAgs at the endoplasmic reticulum to form new infectious virions that are then secreted to propagate further rounds of HDV infection.[6] While the molecular virology of HDV has been elucidated, the role of host-dependency factors for HDV infection remains largely unknown.[5]

A unique feature of HDV is the apparent lack of non-structural protein encoded by the viral genome (including viral polymerase), making it highly dependent of the host machinery for its replication. Targeting host factors is an emerging concept in the treatment of infectious diseases including hepatitis viruses.[9–12] Two host compounds targeting HDV factors have been developed up to clinical proof of concept: these include Myrcludex B, a small peptide targeting HBV/HDV entry factor NTCP, and the prenylation inhibitor lonafranib.[4 13 14] Both compounds demonstrated a significant clinical antiviral effect in chronically infected patients,[4 13 14] supporting the validity of the concept of host-targeting antivirals for HDV infection. However, data on long-term safety, potential resistance in subsets of patients and sustained virological response remain to be determined. Thus, complementary approaches targeting other host factors and/or steps of the HDV life cycle are needed for curative therapies.

Taking advantage of our recently developed robust HDV infection system for the study of HDV–host factor interactions[7] combined with a dual screening approach, we aimed to uncover HDV host-dependency factors as antiviral targets.

RESULTS

A high-throughput RNAi loss-of-function screen uncovers hepatocyte host-dependency factors required for HDV infection

To identify host factors required for HDV infection, we performed a high-throughput loss-of-function screen using the HDV-susceptible cell line Huh-106.[7] Since one key goal was the discovery of druggable host targets, we used a library comprising siRNAs targeting 7567 genes, which have been selected as targets for therapeutics, including kinases, proteases, phosphatases, G protein-coupled receptor, ion channels, ubiquitin ligases, proteins involved in senescence, autophagy, DNA repair and targetable nuclear receptors. Huh-106 cells were transfected with siRNAs pools 48 hours before inoculation with HDV (figure 1A) with an optical immunostaining-based viral protein (HDAg) readout 7 days after infection. The silencing of expression of HDV host factor NTCP was used as functional positive control (figure 1B-C). The results of the primary screen are presented in online supplementary table S1 .

Using the hit selection algorithm described in online supplementary material and methods and figure 1E, we identified 191 host factor genes showing a robust correlation between gene silencing and level of HDV infection, moderate toxicity of gene-specific siRNA and their expression in the liver (figure 1D,E and online supplementary table S2). The threshold of hit selection (described in figure 1E) was based on the functional effect of *SLC10A1* silencing (approximately 45% decrease in HDV infection, online supplementary table S1). The hit rate of 191 genes corresponds to 2.5% of total genes, which is similar to screens for other virus host factor-dependency screens.[15 16]

Functional pathway analysis using KEGG pathways identified a network of host factors belonging to HSPG biosynthesis, including *EXT1* and *EXT2* (figure 2A,B). These genes encode two major exostosins, key HSPG-related enzymes exhibiting glycosyltransferase activities and involved in the elongation of heparan sulfate chains.[17] Moreover, several subunits of the RNA polymerase II were identified in our screen (figure 2B), including specific subunits such as *POLR2G* or *POLR2I*, encoding Rpb7 and Rpb9, which play key roles in the initiation of transcription and binding to DNA template for an accurate selection of the transcription start sites, respectively.[18 19] The identification of HSPG enzymes and RNA polymerase II as known HDV-related pathways[5 7] validates our approach for host factor discovery (figure 2). Importantly, the screen identified several previously unknown HDV-related networks, such as the hypoxia inducible factor 1 alpha (HIF-1α) signalling pathway, known to enhance the replication of several RNA and DNA viruses such as Epstein-Barr virus and HIV.[20 21] Interestingly, the HIF-1α signalling pathway also plays a key role in hepatocarcinogenesis and liver tumour progression[22 23] through its ability to target the expression of oncogenic genes such as the proliferation-specific transcription factor Forkhead box M1.[24] HIF-1α overexpression in HCC has been correlated with worse clinical outcomes and is considered as a poor prognosis factor and molecular target for liver disease therapy.[24] Interestingly, the highly significant scoring of insulin resistance-related pathways highlights the importance of hepatocyte metabolism as host-dependency factors on HDV infection (figure 2).

Finally, we identified several host factors involved in the biosynthesis of pyrimidine, including *CANT1*, *ENTPD5* and *CAD*.

The pyrimidine biosynthesis enzyme CAD is a key host factor for HDV infection and antiviral target in human hepatocytes

Given its high impact on HDV infection, functional relevance, liver expression and targetability, we focused on *CAD*, encoding the carbamoyl-phosphate synthetase 2, aspartate transcarbamylase and dihydroorotase (CAD), an enzyme playing a key role in the pyrimidine biosynthesis (online supplementary table S2; figure 2).[25] Silencing of *CAD* led to a robust decrease in HDV infection (figure 3A). CAD is a trifunctional enzyme catalysing the first steps of pyrimidine biosynthesis.[26] Interestingly, *CAD* expression is known to be regulated by activated estrogen receptor alpha (or estrogen receptor 1, ESR1), which binds to the transcription factor SP1,[27] two other host-dependency factors uncovered by the RNAi screen (figure 3A). These data

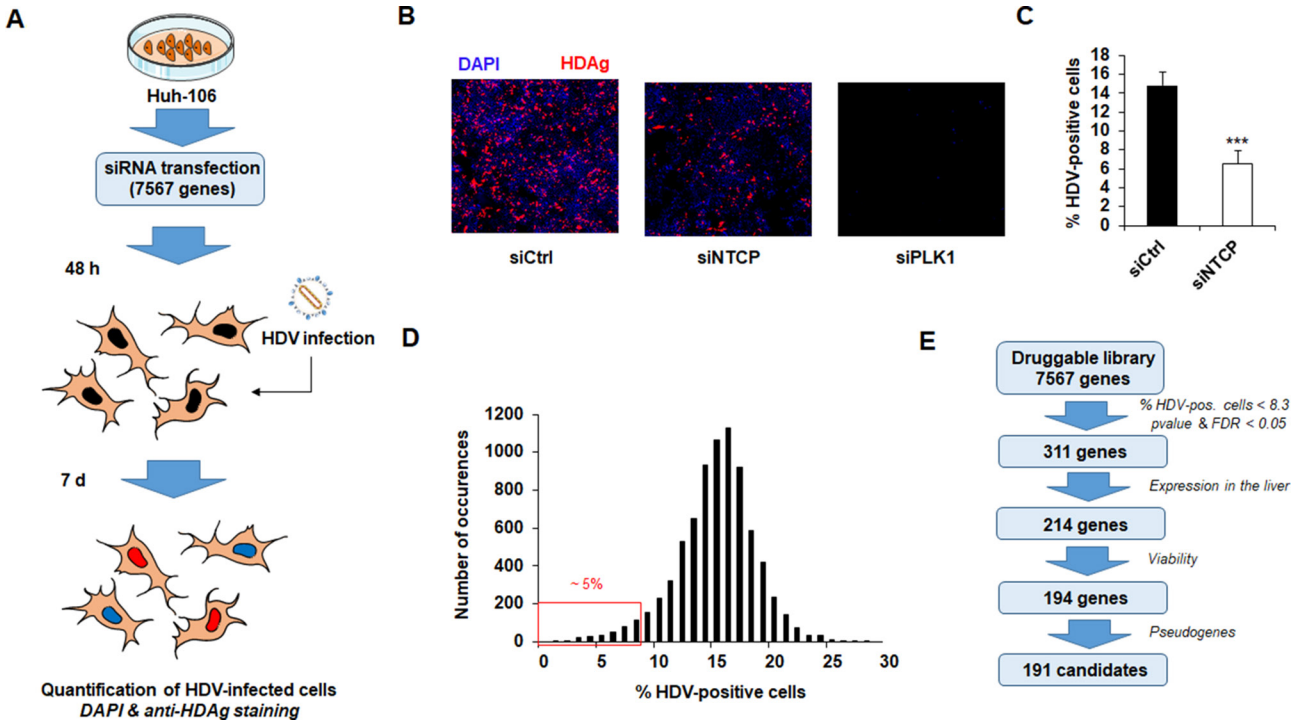

Figure 1 Identification of host-dependency factors for HDV infection using a high-throughput RNAi screen. (A). Approach with flow chart of the screen. NTCP-overexpressing Huh7 cells (termed Huh-106) were transfected with pools of four siRNAs per target of the Dharmacon 'Druggable genome' library 48 hours before HDV infection. Infection was assessed after 7 days by immunofluorescence. Each siRNA pool was tested in triplicate. As controls, Huh-106 cells were transfected with a non-targeting siRNA control (siCtrl), siRNA targeting *SLC10A1* (siNTCP) and *PLK1* (siPLK1, lethal for the cells) expression. Representative images of HDV infection in Huh-106 cells from the primary screen are shown in B. As readout for infection, cells were stained with an anti-HDAg antibody and cell nuclei were stained with 4′,6-diamidino-2-phenylindole (DAPI). (C) General effect of the siNTCP on HDV infection at the screen level. Results are expressed as means ± SD % HDV-positive cells from siCtrl-treated cells (n=318) and siNTCP-treated cells (n=265). ***p value <0.001 (unpaired Student's t-test). (D). Distribution of host-factor candidates according to their inhibitory effect on HDV infection. The top 5% (% HDV positive cells <8.3) were selected as candidates for further work-up. (E). Selection of candidate genes from the primary screen. From the 311 genes inducing a >45% decrease in HDV infection after silencing, candidate genes were selected depending on their robustness (p value and false discoery rate (FDR) <0.05), their expression in the liver (Illumina Body Map tool) and their toxicity. Toxicity was evaluated as the percentage of viability compared with the siCtrl, quantified by counting the DAPI-positive nuclei in the wells at the end of infection. From the 194 selected candidates, *RNF130* was present twice (subset 8 and subset 10), and two pseudogenes (tAKR/*AKR1C6P* and *LOC402164*) were removed. One hundred and ninety-one candidates (top 2.5%) were further worked up. HDV, hepatitis D virus; NTCP, sodium taurocholate cotransporting polypeptide.

suggest a key role of the pyrimidine biosynthesis pathway and its associated nuclear proteins for the HDV life cycle.

We next investigated the functional role of CAD in HDV infection. We first performed additional silencing studies using individual *CAD*-specific siRNA. As shown in figure 3B–D, a strong reduction of HDV RNA was observed after transfection of Huh-106 cells with the four individual siRNAs composing the siRNA pool, validating the key role of *CAD* expression in HDV infection. Notably, *CAD* expression was not significantly affected by HDV infection (figure 3E).

Aiming to characterise the potential of CAD as an antiviral target, we synthetised a specific inhibitor of CAD, sparfosic acid or N-(phosphonoacetyl)-L-aspartic acid (PALA).[26] PALA is an aspartic acid derivative, which inhibits the aspartate carbamoyltransferase activity of the enzyme. We then investigated the antiviral activity of PALA in HDV-infected Huh-106 cells. As shown in figure 3F, PALA dose dependently inhibits HDV infection with an IC_{50}=1.2 µM. Notably, a decrease in cell viability was observed after 7 days of culture.

To validate this result in the most physiological model for HDV infection, we investigated the antiviral activity of PALA using HDV infection of primary human hepatocytes (PHHs). Interestingly, while no toxicity was observed in PHH even at high doses (100 µM), the IC_{50} of PALA was slightly higher in PHH (figure 3G), which may reflect differences in uridine pools and/or *CAD* expression in rapidly dividing Huh7-based cells versus non-dividing PHH in cell culture.[28]

To investigate the mechanism of action of CAD–HDV interaction, we performed a rescue experiment using PALA and uridine-supplemented medium. Northern blot detection of HDV genomic RNA in infected cells revealed that the addition of uridine in PALA-treated cells restored HDV infection, validating the functional relevance of pyrimidine pathway for HDV replication (figure 4A). Notably, PALA at a concentration of 2.5 µM induced a strong decrease in HDV infection, which was efficiently rescued by uridine treatment (figure 4B,C). This dose was then selected for further functional studies. Importantly, no direct interaction was observed between CAD and the HDV antigens (figure 4D). As the inhibition of pyrimidine pathway has been shown to stimulate the innate antiviral response with subsequent inhibition of viral propagation,[29] we next assessed the expression of *IFNB1* following PALA treatment in Huh-106 cells. As shown in figure 4E, no *IFNB1* induction was observed after treatment with either PALA or Brequinar, targeting dihydroorotate dehydrogenase (DHODH), suggesting an absence of innate immune stimulation by pyrimidine inhibitors in hepatocyte-derived cells.

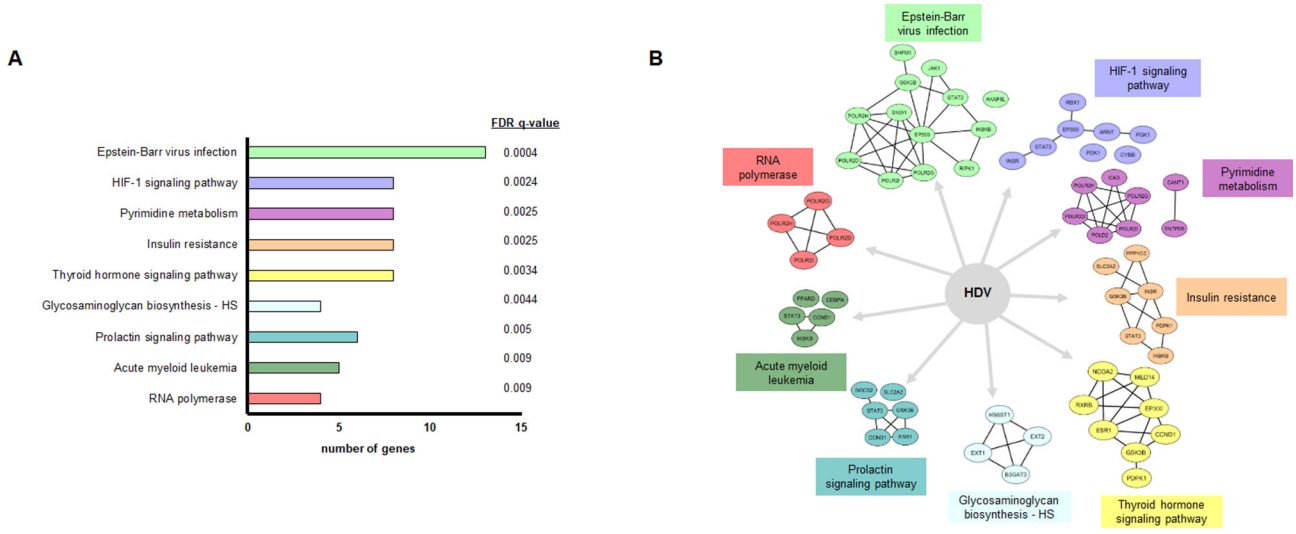

Figure 2 Pathway analysis of HDV host factors identified within the RNAi screen. The identified host genes were subjected to functional enrichment pathway analysis through ToppGene Suite (https://toppgene.cchmc.org) using Kyoto Encyclopedia of Genes and Genomes (KEGG) database. Pathways scoring at a FDR value of < 0.05 were considered significant. (A) Representation of the number of genes and FDR values of different KEGG pathways significantly enriched within the primary siRNA screen candidates. (B) Individual genes contributing to the enrichment of the significant KEGG pathways were further analyzed for protein-protein interactions using STRING database. Interaction networks were represented using Cytoscape 3.6.0.

To further validate the involvement of the biological function of CAD in HDV infection, cell culture medium was then complemented using either glutamine (Glu; the initial substrate of CAD) or dihydroorotate (DHO; the final product of CAD) (figure 5A, as described in ref 25). As shown in figure 5B and online supplementary figure S1, while Glu treatment had no effect on intracellular HDV RNA, DHO treatment in PALA-treated cells restored HDV RNA to non-treated levels, suggesting that PALA antiviral activity is linked to CAD physiological function.

To map the replication steps mediated by CAD and targeted by PALA, we performed northern blot analyses of HDV RNA allowing to quantify the HDV genome and antigenome in the presence or absence of PALA. As shown in figure 5C, PALA treatment effectively decreased the levels of both HDV genomic and antigenomic RNAs. Moreover, this inhibition was already observed during the early stages of viral replication (online supplementary figure S1). These data demonstrate that PALA inhibits all the steps of HDV replication including the synthesis of antigenomic RNA (figure 5C).

Next, we performed kinetic studies adding PALA preinfection, peri-infection and HDV postinfection (figure 5D). PALA potently inhibited HDV infection given at any time before, during and following initiation of replication. Interestingly, the inhibitory effect was most pronounced when PALA was added prior or during initiation of replication. Finally, to exclude effects on other steps of the early HDV life cycle, we studied the effect of PALA treatment on HDV binding to the Huh-106 cell surface. The absent effect on HDV binding further confirms HDV replication as the life cycle step targeted by PALA (figure 5E).

To test the specificity of the pyrimidine pathway for HDV infection, we treated HBV-producing HepAD38 cells with PALA. As shown in figure 5F, PALA did not modulate HBV antigen production as shown by an absent effect on HBeAg and HBsAg secretion. While tenofovir (TFV) treatment dose-dependently inhibited HBV replication, PALA had no effect on HBV DNA in the supernatant of HepAD38 cells (figure 5G). Finally, the silencing of *CAD* expression did not affect HBV infection in HepG2-NTCP cells (figure 5H). These results suggest that the pyrimidine/CAD pathway is relevant for HDV but not HBV replication. Collectively, our results identify CAD as a key HDV host factor involved in HDV replication and target for antiviral therapy.

A small molecule screen uncovers ESR1 inhibitor fulvestrant as host targeting agent

Next, we performed a small molecule screen using the Prestwick library, containing 1280 drugs approved by the Food and Drug Administration (FDA) (figure 6A). Among the molecules exhibiting an antiviral activity against HDV, we identified fluvastatin and cyclosporin A, two well-described NTCP inhibitors (online supplementary table S3), confirming the validity of the screen. Interestingly, ribavirin, a broad antiviral nucleoside analogue[30] previously used for the treatment of chronic hepatitis C[31] exhibits a marked antiviral activity against HDV (online supplementary table S3). In the same vein, nelfinavir, a protease inhibitor presenting antiretroviral activity[32] was also identified in the drug screen (online supplementary table S3).

Given our discovery of ESR1 as HDV host-dependency factor, we next focused on ESR1-targeting agents. The library includes several agonists and antagonists of ESR1, as well as characterised targets for endocrine therapy in breast cancer.[33] Interestingly, the ESR1 antagonist fulvestrant exhibited a marked, significant and dose-dependent antiviral effect against HDV, whereas tamoxifen and toremifen, two ESR1 modulators with oestrogenic effects in the liver[34] increased HDV infection, validating the importance of ESR1 in HDV infection (figure 6B-C). Interestingly, a 48-hour treatment started after virus inoculation induced a marked decrease in HDV-infected cells (figure 5D), suggesting an effect on HDV replication.

Next, we aimed investigate the mechanism of action of the antiviral activity of fulvestrant by investigating a functional link of ESR1 and CAD suggested by protein/protein interaction studies.[27] To address this question, CAD expression was analysed in Huh-106 cells and PHH in the presence or absence of the ESR1 antagonist (figure 6E-G). As shown in figure 6G,

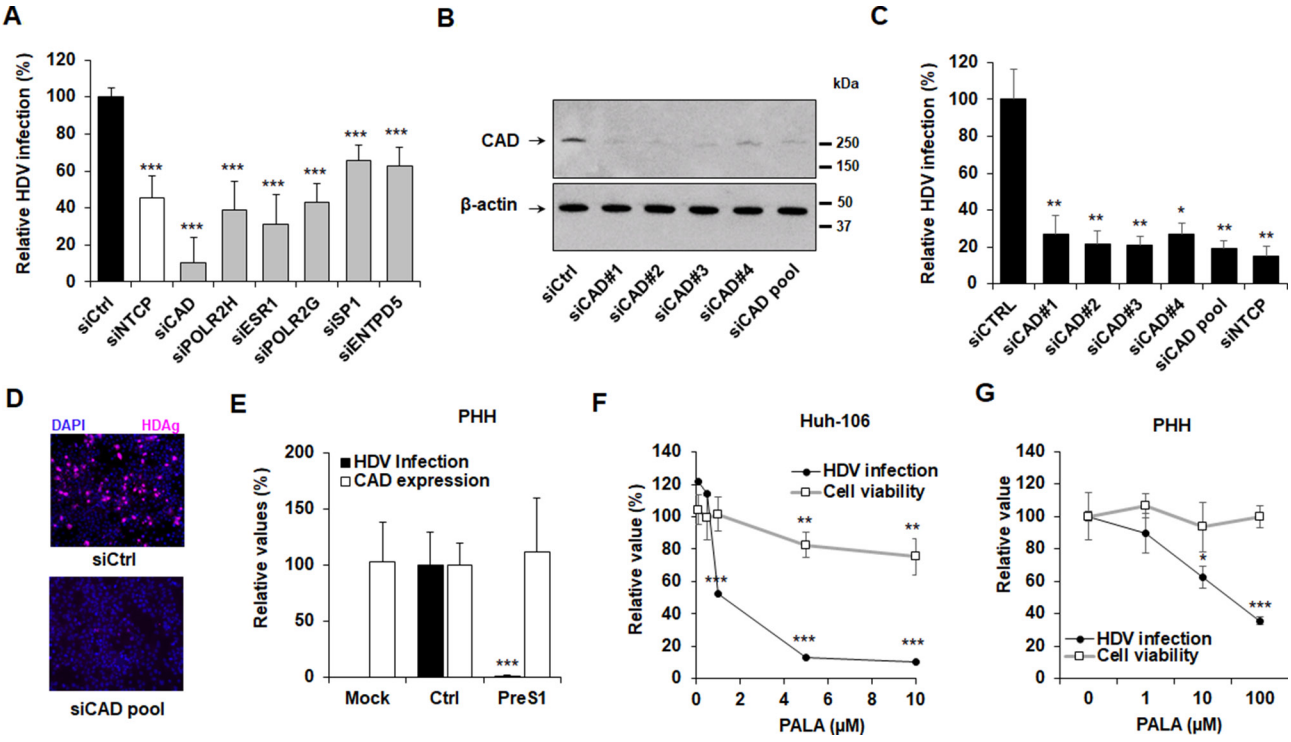

Figure 3 CAD is a key host factor required for HDV infection. (A) Functional validation of host factors belonging to the pyrimidine biosynthesis using perturbation studies. Results are presented as means ± SD % HDV infection compared with control siRNA (siCtrl, set at 100%) from three independent screens (n=9, primary screen and two validation screens performed in triplicate). ***p value <0.001 (unpaired Student's t-test compared with siCtrl samples). (B–D) CAD is required for HDV infection. Huh-106 cells were reverse-transfected with four individual siRNAs targeting *CAD* mRNA or with the pool of four siRNAs. Silencing efficacy was assessed by western blot after 2 days. (B) One representative experiment is shown. Cells were then infected with HDV, and virus infection was assessed after 7 days by quantitative reverse transcription (qRT)-PCR. Results are expressed as means ± SEM % HDV infection compared with siCtrl (set at 100%) from three independent experiments (n=8). (C) Alternatively, HDV infection was assessed by immunofluorescence (IF) using a patient-derived anti-HDAg antibody. (D) One representative experiment using the pool of siCAD is shown. (E) HDV infection has no effect on CAD expression in PHH. PHH were treated with preS1 peptide (preS1) or a peptide control (Ctrl) for 1 hour prior to infection with HDV for 7 days. Results are expressed as means ± SD % HDV infection (assessed by HDV RNA levels) or *CAD* expression compared with control peptide-treated cells (Ctrl, set at 100%) from four independent experiments (n=8). (F–G) The CAD inhibitor PALA dose-dependently inhibits HDV infection in Huh-106 cells (F) and PHH (G). Cells were treated with PALA at the indicated concentrations 24 hours before infection with HDV. Cells were then cultured for 7 days in presence of PALA. HDV infection was assessed by qRT-PCR. Cell viability was assessed by Presto Blue. Results are expressed as means ± SD % HDV infection or cell viability compared with untreated cells (0, set at 100%) from three independent experiments (Huh-106 [F], n=9) or as means ± SEM % HDV infection or cell viability from three independent experiments (PHH [G], n=8). CAD, carbamoyl-phosphate synthetase 2, aspartate transcarbamylase and dihydroorotase; HDV, hepatitis D virus; PALA, N-(phosphonoa cetyl)-L-aspartic acid; PHH, primary human hepatocyte.

fulvestrant treatment resulted in a loss of CAD protein expression in both Huh-106 cell line and PHH, suggesting that the antiviral activity of ESR1-inhibitor fulvestrant is mediated by ESR1-mediated downregulation of *CAD* expression, which in turn is required for HDV replication, confirming the previous observations with PALA.

Taken together, our dual screening approach uncovers the pyrimidine pathway and its associated and regulatory proteins as host factors for HDV infection and targets for antiviral therapy.

DISCUSSION

Chronic hepatitis D is the most severe form of viral hepatitis, and at present time, no treatment allows robust viral clearance. Using a dual screening approach, we identified *ESR1* and *CAD* as host factors and antiviral targets for HDV infection. The functional impact of the pyrimidine biosynthesis for HDV replication is corroborated by: (1) a marked decrease in HDV infection after *CAD* and *ESR1* silencing; (2) a significant antiviral effect of CAD and ESR1 inhibitors PALA and fulvestrant; and (3) kinetic experiments mapping viral replication as the step of the viral life cycle mediated by these host factors and targeted by the antiviral (4) validation studies in primary human hepatocytes.

Whereas the molecular virology of HDV is well described, the molecular interactions between the virus and liver host factors are still largely unknown.[5] In mammalian cells, the pyrimidine biosynthesis pathway leads to the production of de novo nucleotides and plays a key role in RNA and DNA production, as well as protein glycosylation or cell membrane assembly.[25] Moreover, uridine nucleotides and derivatives regulate key physiological processes, such as lipid metabolism, regulation of normal central nervous system activity or modulation of reproduction,[35] making this pathway a major actor of important metabolic processes. As a source of nucleotides for HDV RNA, this pathway is likely to be required for optimal virus replication. Moreover, as a key regulator of viral glycosylation,[25] an alteration of this pathway may alter post-translational modification of host or viral proteins, disrupting viral infection.

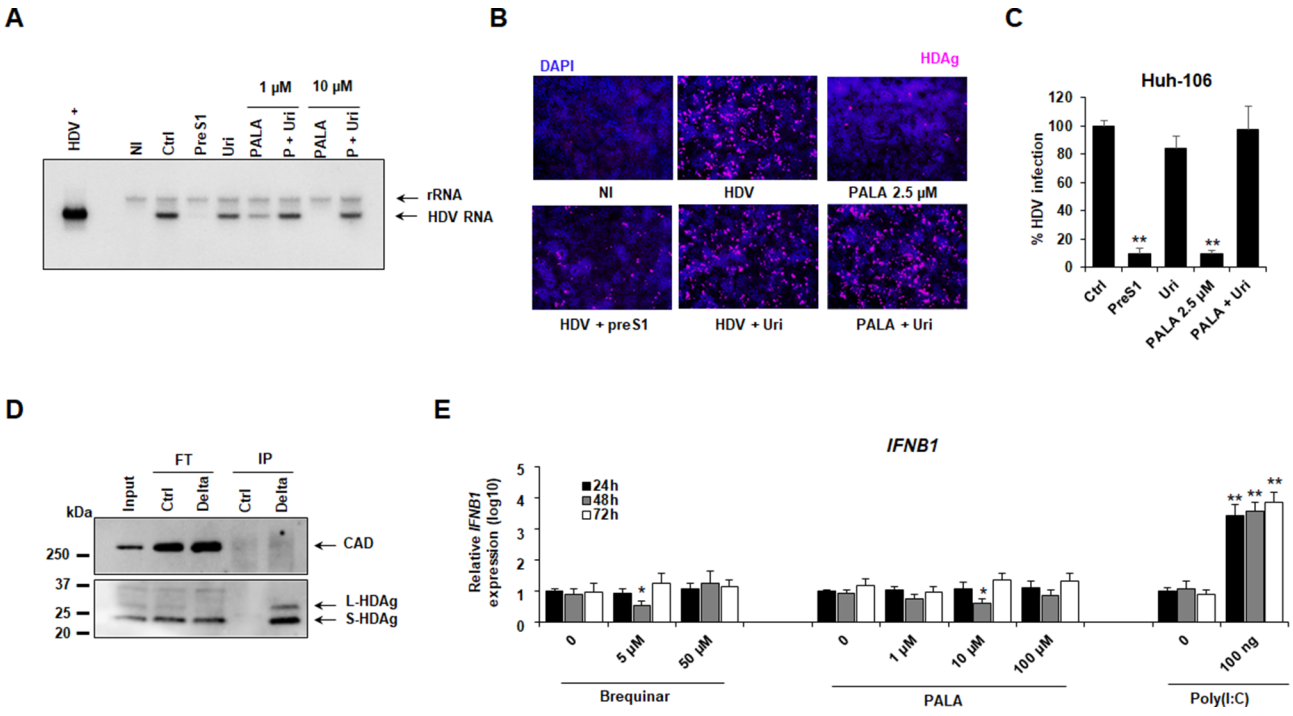

Figure 4 Characterisation of CAD–HDV functional interaction. (A–C) Uridine complementation restores HDV infection in PALA-treated cells. Huh-106 cells were treated with PALA (1 µM or 10 µM) in presence or absence of 30 µM uridine 24 hours prior to infection with HDV, and compound treatment was maintained for 7 days. HDV infection was assessed by northern blot (A). HDV+ corresponds to approximately 5.10^7 HDV RNA genome equivalents extracted from HDV particles produced in Huh7 cells. rRNA corresponds to ribosomal RNA. One representative experiment is shown. Alternatively, Huh-106 cells were treated with PALA 2.5 µM in presence or absence of 30 µM uridine. HDV infection was assessed after 7 days by IF (B) or qRT-PCR (C). Results are expressed as means ± SEM % HDV infection compared with HDV-infected untreated cells (Ctrl, set at 100%) from three independent experiments (n=6). (D) Absent direct interaction between HDV antigens and CAD. Huh-106 were transfected with pSVL(D3) plasmid encoding the HDV genome. Three days after transfection, cells were lysed, and HDAg-specific co-immunoprecipitation (co-IP) was performed using an anti-HDAg antibody (Delta) or with a control antibody (Ctrl). HDV antigens and CAD expression in the original cell lysate (input), in Flow-through control samples (FT) and in IP eluates (IP) were assessed by western blot. One experiment is shown. (E) No IFN induction after inhibition of pyrimidine biosynthesis in Huh-106 cells. Huh-106 cells were treated with Brequinar or PALA at the indicated concentrations. Alternatively, Huh-106 cells were reverse-transfected with Poly(I:C) (100 ng). Cells were then lysed every day for 3 days, and *IFNB1* expression was assessed by qRT-PCR. Results are expressed as means ± SD relative *IFNB1* expression (log10) compared with untreated or non-transfected cells (0, all set at 1) from three independent experiments (n=6). CAD, carbamoyl-phosphate synthetase 2, aspartate transcarbamylase and dihydroorotase; HDV, hepatitis D virus; PALA, N-(phosphonoacetyl)-L-aspartic acid.

CAD is a multifunctional enzyme exhibiting carbamoylphosphate synthetase, aspartate transcarbamoylase and dihydroorotase activities catalysing the three first steps of the pyrimidine biosynthesis pathway,[36] playing a key role in HDV infection as such. The observed antiviral activity of the CAD-specific inhibitor PALA validates the importance of this factor and pathway in HDV infection. It is of interest to note that another enzyme of the pyrimidine biosynthesis pathway DHODH, which catalyses the production of orotate from DHO, has been described as an antiviral target by small molecule GSK983.[37] Here, we confirmed that the CAD-mediated DHO and uridine starvation is responsible for the observed antiviral effect (figures 4 and 5). Interestingly, HSPG synthesis has been shown to be dependent on the pyrimidine synthesis pathway in a CAD-defective animal model.[38] However, we did not observe any effect of CAD inhibition on either HBV infection or HDV entry (figure 5E–H). While recent studies have suggested that the inhibition of pyrimidine biosynthesis can stimulate innate antiviral responses,[29] no induction of IFN expression was observed in our model (figure 4E). Thus, it is likely that the modulation of CAD activity or expression affects HDV infection through its classical enzymatic activity linked to pyrimidine metabolism, mainly affecting viral replication through uridine starvation, affecting both genomic and antigenomic HDV RNAs. In this context, our study suggests that the first steps of replication are particularly susceptible to PALA. These results are consistent with the timing of HDV RNA amplification, much more pronounced during the early phase of replication, before L-HDAg-mediated slowdown of replication.[5]

Among the genes regulating the pyrimidine pathway, we identified *ESR1* as a HDV host-dependency factor and antiviral target. ESR1 is a nuclear hormone receptor expressed in the mammary gland and female reproductive track and also in lung and liver.[39] In our mechanistic analyses, we show that ESR1 inhibition by fulvestrant led to a decrease in CAD protein expression, which most likely explains the antiviral effect of the molecule.

Our screening strategy also identified small molecules exhibiting significant antiviral activity against HDV infection. Among them was found ribavirin, a nucleoside analogue previously used for the treatment of chronic HCV infection.[40] Given its concentration in the primary screen (10 µM), HDV inhibition is most likely due to the ability of ribavirin to inhibit de novo synthesis of GTP as recently suggested as a possible mechanism for the inhibition of hepatitis E virus (HEV) replication in Huh7 cells (IC_{50} of 18.9 µM for GTP depletion; EC_{50} of 3 µM for HEV replication[41]). However, clinical attempts to treat hepatitis D using ribavirin were largely unsuccessful.[4]

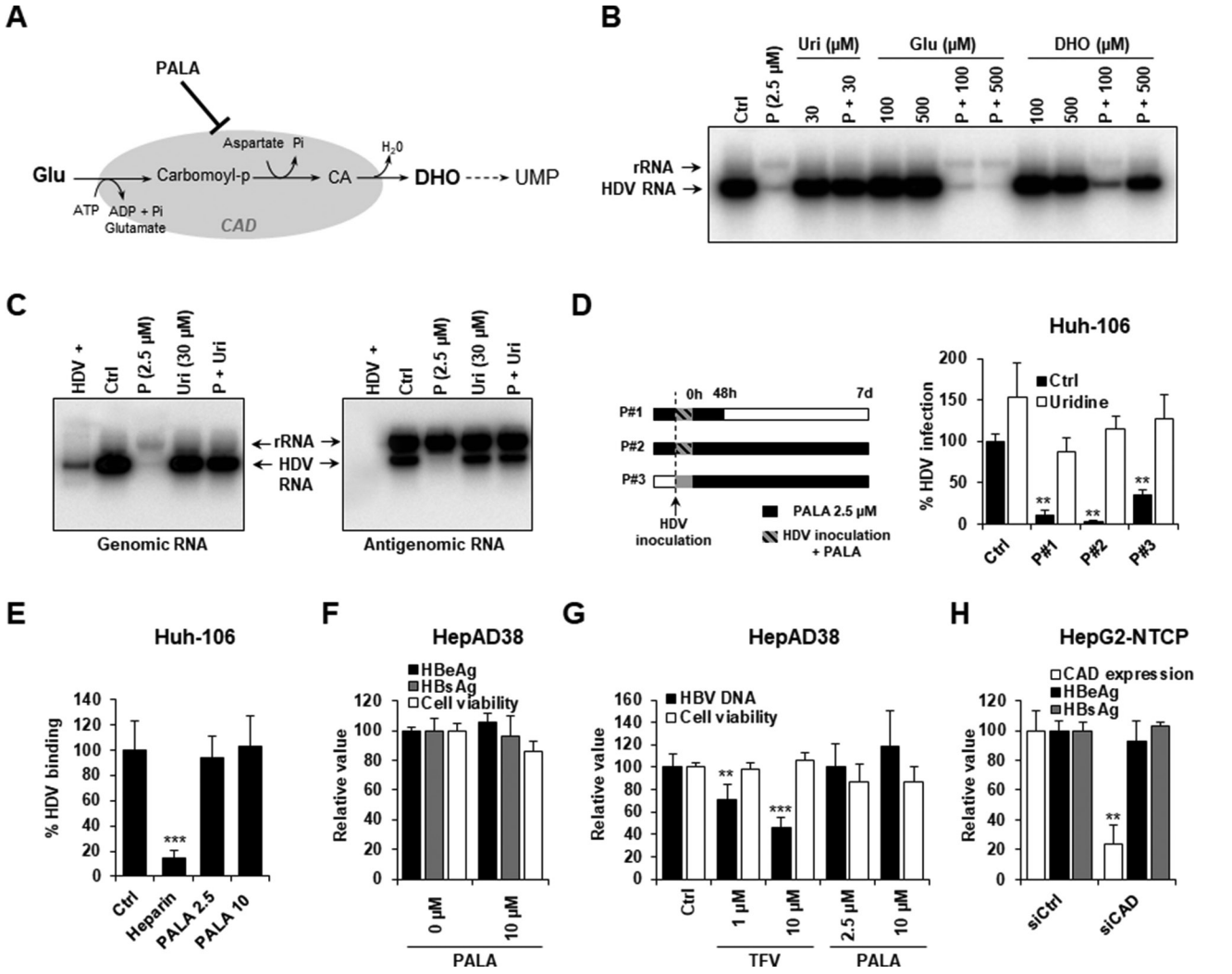

Figure 5 PALA specifically inhibits HDV replication by targeting CAD biological function. (A) Schematic representation of reactions catalysed by CAD enzyme. (B) DHO treatment restores HDV infection in PALA-treated cells. Huh-106 cells were treated with PALA 2.5 µM and infected with HDV in presence or absence of L-glutamine (Glu) or DHO at the indicated concentrations. Infection was assessed after 7 days by northern blot detection of HDV genomic RNA. rRNA corresponds to ribosomal RNA. One experiment is shown. (C) PALA inhibits both HDV genomic and antigenomic production. Huh-106 cells were treated with PALA 2.5 µM 24 hours prior to infection with HDV. HDV genomic and antigenomic RNAs were detected by northern blot using specific probes 7 days after infection. HDV+ corresponds to approximately 5.10^7 HDV RNA genome equivalents extracted from HDV particles produced in Huh7 cells. One experiment is shown. (D) Kinetics of HDV infection by PALA. Huh-106 cells were pretreated with PALA at 2.5 µM and infected with HDV (conditions P#1 and P#2). Cells were then cultured in presence of PALA for 48 hours (P#1) or for 7 days (P#2) in presence or absence of uridine (30 µM). Alternatively, Huh-106 cells were infected with HDV with no PALA pretreatment (P#3). Sixteen hours after viral inoculation, cells were cultured in presence of PALA 2.5 µM with or without uridine (30 µM). HDV infection was assessed after 7 days by qRT-PCR. Results are expressed as means ± SEM % HDV infection compared with HDV-infected untreated cells (Ctrl, set at 100%) from three independent experiments (n=6). (E) PALA does not affect HDV binding. Huh-106 cells were cultured for 24 hours at 16°C in presence of HDV particles, which were pretreated or not with heparin (30 µg/mL). HDV binding was measured by qRT-PCR quantification of total HDV RNA bound to cells after 24 hours. Results are expressed as means ± SD % HDV binding relative to control untreated cells (Ctrl, set at 100%) from three independent experiments (n=9). (F–H) CAD inhibition or silencing does not affect HBV infection and replication. (F) HBV-producing HepAD38 cells were treated with PALA (10 µM) for 3 days. HBeAg and HBsAg secretion in culture supernatant was then quantified by chemiluminescent immunoassay (CLIA). Cell viability was assessed by Presto Blue. Results are expressed as means ± SEM % HBeAg production, HBsAg production or cell viability compared with untreated cells (0 µM, all set at 100%) from three independent experiments (n=6). (G) HepAD38 cells were treated with either tenofovir (TFV) or PALA at the indicated concentrations for 3 days. HBV replication was assessed by quantification of HBV DNA copies in the supernatant of treated cells by qPCR. Results are expressed as means ± SD % HBV DNA in the supernatant or cell viability compared with untreated cells (Ctrl, all set at 100%) from three independent experiments (n=9). (H) HepG2-NTCP cells were reverse-transfected with siCAD or siCtrl for 2 days prior to infection with HBV. HBV infection was assessed after 10 days by quantification of HBeAg and HBsAg production using chemiluminescent immunoassay (CLIA). Results are expressed as means ± SD % CAD expression, HBeAg production or HBsAg production compared with siCtrl-transfected cells (siCtrl, all set at 100%) from three independent experiments (n=6). CA, Carbamoyl aspartic acid; CAD, carbamoyl-phosphate synthetase 2, aspartate transcarbamylase and dihydroorotase; DHO: dihydroorotate; Glu, glutamine; HBV, hepatitis B virus; HDV, hepatitis D virus; PALA, N-(phosphonoacetyl)-L-aspartic acid; Pi, inorganic phosphate; UMP, uridine monophosphate.

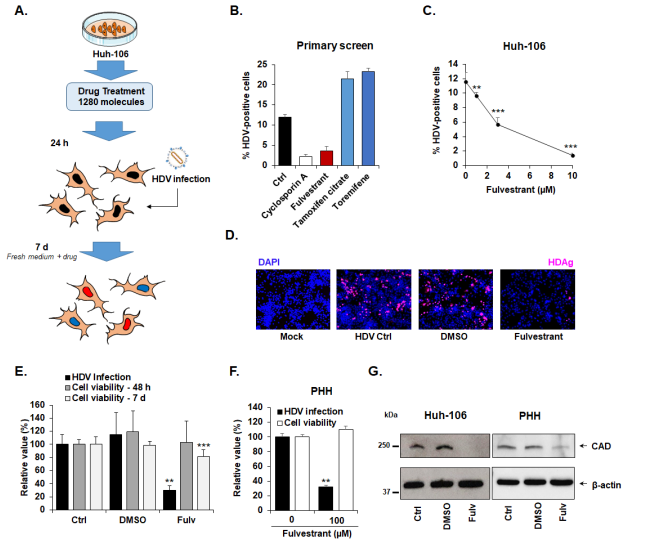

Figure 6 ESR1 inhibitor fulvestrant inhibits HDV replication by suppression of CAD expression. (A) Small molecule screen flow chart. Huh-106 cells were treated with individual compounds belonging to the Prestwick chemical library (10 µM) 1 day prior to infection with HDV. Infection was assessed after 7 days by immunofluorescence. Every compound was tested in triplicate. (B). ESR1 modulators affect HDV infection. From the primary screen, fulvestrant (an ESR1 inhibitor) from the one hand, and tamoxifen and toremifen from the other hand (two agonists/modulators of ESR1) exhibited antiviral or proviral activity against HDV, respectively. Results are presented as means ± SD % HDV infected cells (n=3). (C). Fulvestrant dose-dependently inhibits HDV infection. Huh-106 cells were treated with fulvestrant at the indicated concentrations and then infected with HDV for 7 days. Results are expressed as means ± SD % HDV infected cells from three independent experiments (n=9). (D) Short fulvestrant treatment for 48 hours following virus inoculation inhibits HDV infection. Huh-106 cells were infected with HDV and then treated with fulvestrant (10 µM) or dimethyl sulfoxide (DMSO) for 48 hours. Cells were then cultured in absence of drug and infection was assessed after 7 days by IF. One representative experiment is shown. (E) Fulvestrant antiviral activity is associated with slight cytotoxicity. Cell viability was assessed after 48 hours and after 7 days by Presto blue. HDV infection was assessed after 7 days by qRT-PCR. Results are expressed as means ± SD % HDV infection (HDV RNA) or cell viability compared with untreated HDV-infected cells (Ctrl, set at 100%) from three independent experiments (n=9). (F) Fulvestrant antiviral activity in PHH. PHH were infected with HDV, and then treated with fulvestrant for 48 hours at the indicated concentrations. Results are expressed as means ± SD % HDV infection (HDV RNA) or cell viability compared with untreated HDV-infected PHH (Ctrl, set at 100%) from two independent experiments (n=6). (G) Fulvestrant inhibits CAD expression. Huh-106 cells and PHH were treated with fulvestrant (Fulv, 10 µM) or DMSO for 72 hours. CAD expression was assessed by western blot. CAD, carbamoyl-phosphate synthetase 2, aspartate transcarbamylase and dihydroorotase; HDV, hepatitis D virus; ESR1, estrogen receptor 1; PHH, primary human hepatocyte.

Collectively, we identified previously undiscovered pathways and host factors for HDV infection and antiviral targets. Host-targeting agents are a promising approach for the development of new antiviral treatments, notably because they limit the emergence of resistant variants.[8–10 42] In particular for RNA viruses, which do not integrate into the genome, host-targeting agents hold promise for viral cure.[43] Indeed, in chronic HCV infection antibodies targeting a viral host entry factor claudin-1 cure viral infection in a state-of-the-art mouse model,[12] and a miRNA-122 antagonist has been shown to cure chronic HCV infection in monotherapy in a subset of patients.[44] Two host compounds targeting HDV factors have been developed up to clinical proof of concept: these include Myrcludex B, a small peptide-targeting HBV/HDV entry factor NTCP and the prenylation inhibitor lonafranib.[4 13 14] In randomised clinical trials, both compounds demonstrated a significant and robust antiviral effect in chronically infected patients,[4 13 14] supporting the validity of the concept of host-targeting antivirals for HDV infection. However, long-term safety, potential resistance in subsets of patients and data on sustained virological response remain to be determined. The discovery of novel host factors described in this study may overcome these limitations by complementary, safer and more efficient approaches. Compounds targeting essential host factors of the viral replication step may be conceptually superior to entry or prenylation inhibitors by targeting the most vulnerable step of the viral life cycle. Indeed, viral replication is the target of many effective clinically licenced antiviral therapies such as nucleoside analogues for HBV infection or polymerase/protease inhibitors for HIV and HCV infection.

A theoretical disadvantage of HTA is their putative adverse effects on physiological processes mediated by the host factors. In this context, given that an HDV treatment will occur in a context of diseased liver, assessment of safety will be a major parameter in development. In this regard, it is of interest to note that pyrimidine synthesis inhibitors, such as leflunomide or teriflunomide, are currently used for the treatment of rheumatoid arthritis and multiple sclerosis.[45 46] The safety profile of these compounds suggests that pyrimidine biosynthesis is a targetable pathway for antiviral strategies. Indeed, the FDA-approved leflunomide, targeting DHODH, induces uridine starvation at concentrations similar to PALA concentrations we used in this study (0–100 µM).[47] Although detailed toxicity analyses in animal model and human tissues will be required to assess the therapeutic window of PALA, the dose–response effects of leflunomide suggests that PALA doses required to inhibit HDV infection are most likely in a range that will have an acceptable clinical safety profile.

In conclusion, by uncovering key host factors for HDV infection our results significantly improve the understanding of the HDV life cycle and contribute to the development of novel antiviral strategies for HDV cure.

MATERIAL AND METHODS

Human subjects

Human serum from patients with chronic HBV/HDV infection followed at the Strasbourg University Hospitals, Strasbourg, France, was obtained with informed consent. PHHs were obtained from liver tissue from patients undergoing liver resection for liver metastasis at the Strasbourg University Hospitals with informed consent.

Cell lines and human hepatocytes

Huh-106,[7] HepAD38[7] and HepG2-NTCP[7] cells have been described. PHHs were isolated and cultured as described.[48]

Key reagents

Fulvestrant (I4409), DL-dihydroorotic acid (DHO, D7003), L-glutamine (59 202C), uridine (U3003) and TFV (1643601) were purchased from Sigma-Aldrich (Merck). Sparfocid acid (L-Aspartic acid, N-(phosphonoacetyl)-, disodium salt (9 CI) or PALA, NSC: 224131) was first obtained from the Drug Synthesis

and Chemistry Branch, Developmental Therapeutics Program, Division of Cancer Treatment and Diagnosis, National Cancer Institute, National Institute of Health, Bethesda, Maryland, USA. For further analyses, PALA was synthetised at the Institute of Chemistry, University of Strasbourg, as described in online supplementary material and methods. PreS1 peptide was synthetised by Bachem.[7]

HDV and HBV production and infection

The production of recombinant HDV and HBV infectious virus as well as the protocol for HDV infection of Huh-106 cells and PHHs and for HBV infection of HepG2-NTCP cells have been described.[7 49 50] A detailed protocol is presented in online supplementary material and methods.

RNAi loss-of-function and small molecule screens

Screening was performed at the High Throughput Screening platform of the Institut de Génétique et de Biologie Moléculaire et Cellulaire in Illkirch, France. The Human ON-TARGETplus 'Druggable Genome' siRNA Library was used for gene expression silencing. For the small molecule screen, the Chemical Library (PCL) containing 1280 FDA-approved molecules was obtained from Prestwick. Detailed information about both screening strategies as well as the algorithm for selection of HDV-dependency candidates are presented in online supplementary material and methods.

Validation of CAD as a HDV host factor using individual siRNAs

Huh-106 cells were reverse-transfected with the four individual siRNAs from the siCAD pool, a pool of siRNA targeting SLC10A1 (siNTCP) or a non-targeting siRNA control (siCtrl) using lipofectamin RNAi max as described.[7 50] Gene expression was assessed, 2 days after transfection, by western blot detection of CAD protein using a rabbit monoclonal anti-CAD antibody (Abcam ab40800) as previously described.[7 50] β-actin expression was assessed as a loading control using a mouse monoclonal anti-β-actin antibody (Sigma, A5441). Two days after transfection, cells were infected by HDV, and infection was assessed after 7 days as described in online supplementary material and methods.

Statistical analysis

All experiments were performed at least twice in an independent manner. Statistical analyses were performed using a two-tailed Mann-Whitney U test unless otherwise stated; $p<0.05$ (*), $p<0.01$ (**) and $p<0.001$ (***) were considered statistically significant. Significant p values are indicated by asterisks in the individual figures and figure legends. The number of biological replicates is indicated in the figure legends (n).

Additional methodological information are available in online supplementary material.

Acknowledgements We would like to thank J Taylor (Fox Chase Cancer Center) for the gift of the HDV expression plasmid (pSVL(D3)) and our colleagues S Durand and M Renaud for excellent technical support. We thank the INGESTEM infrastructure for access to the IGBMC high-throughput high-content screening workstation.

Contributors TB initiated the study. TB and ERV designed and supervised research. ERV, AW, LB and TB set up, designed and performed the siRNA and small molecule screens. TG and PPa produced the sparfosic acid. ERV, CB, LH, VT-L and EC performed the validation experiments. CSu performed the HDV northern blots. PPe provided human hepatocytes. ERV, AW, CB, LH, EC, MBZ, CSu, CSc, LB and TB analysed the data. ERV, HES and AK performed the bioinformatical analyses of the screens. EV and TB wrote the manuscript. All the authors approved the study.

Funding This work was supported by Inserm, the University of Strasbourg, the European Union (Infect-ERA hepBccc, ERC-2014-AdG-671231-HEPCIR and Horizon 2020 research and innovation programme under grant agreement 667273 - HEPCAR), Agence Nationale de Recherches sur le Sida et les Hépatites Virales (ANRS 15/1099) and the French Cancer Agency (ARC IHU201301187). This work has been published under the framework of the LabEx ANR-10-LAB-28 and benefits from a funding from the state managed by the French National Research Agency as part of the Investments for the Future (Investissements d'Avenir) programme. ERV is the recipient of an ANRS fellowship (ECTZ50121).

Competing interests None declared.

Ethics approval Protocols were approved by the local Ethics Committee of the Strasbourg University Hospitals (CPP) and the Ministry of Higher Education and Research of France (DC 2016 2616).

Provenance and peer review Not commissioned; externally peer reviewed.

Data sharing statement The datasets generated in this study, including the results from both RNAi and small molecule primary screens, are available within online supplementary material files. The rest of the data are available from the corresponding authors on reasonable request.

ORCID iDs
Patrick Pessaux http://orcid.org/0000-0001-5635-7437
Thomas F Baumert http://orcid.org/0000-0002-9022-5611

REFERENCES

1 Taylor JM. Virology of hepatitis D virus. *Semin Liver Dis* 2012;32:195–200.
2 Fattovich G, Giustina G, Christensen E, *et al*. Influence of hepatitis delta virus infection on morbidity and mortality in compensated cirrhosis type B. The European concerted action on viral hepatitis (Eurohep). *Gut* 2000;46:420–6.
3 Hughes SA, Wedemeyer H, Harrison PM. Hepatitis delta virus. *The Lancet* 2011;378:73–85.
4 Rizzetto M. Investigational drugs in development for Hepatitis D. *Expert Opin Investig Drugs* 2017;26:999–1005.
5 Sureau C, Negro F. The hepatitis delta virus: replication and pathogenesis. *J Hepatol* 2016;64:S102–16.
6 Webb CT, Lupták A. Kinetic parameters of trans scission by extended hdv-like ribozymes and the prospect for the discovery of genomic trans-cleaving RNAs. *Biochemistry* 2018;57:1440–50.
7 Verrier ER, Colpitts CC, Bach C, *et al*. A targeted functional RNA interference screen uncovers glypican 5 as an entry factor for hepatitis B and D viruses. *Hepatology* 2016;63:35–48.
8 Verrier ER, Colpitts CC, Sureau C, *et al*. Hepatitis B virus receptors and molecular drug targets. *Hepatol Int* 2016;10:567–73.
9 Baumert TF, Verrier ER, Nassal M, *et al*. Host-targeting agents for treatment of hepatitis B virus infection. *Curr Opin Virol* 2015;14:41–6.
10 Colpitts CC, Verrier ER, Baumert TF. Targeting viral entry for treatment of Hepatitis B and C virus infections. *ACS Infect Dis* 2015;1:420–7.
11 Harak C, Meyrath M, Romero-Brey I, *et al*. Tuning a cellular lipid kinase activity adapts hepatitis C virus to replication in cell culture. *Nat Microbiol* 2016;2:16247.
12 Mailly L, Xiao F, Lupberger J, *et al*. Clearance of persistent hepatitis C virus infection in humanized mice using a claudin-1-targeting monoclonal antibody. *Nat Biotechnol* 2015;33:549–54.
13 Koh C, Canini L, Dahari H, *et al*. Oral prenylation inhibition with lonafarnib in chronic hepatitis D infection: a proof-of-concept randomised, double-blind, placebo-controlled phase 2A trial. *Lancet Infect Dis* 2015;15:1167–74.
14 Bogomolov P, Alexandrov A, Voronkova N, *et al*. Treatment of chronic hepatitis D with the entry inhibitor myrcludex B: first results of a phase Ib/IIa study. *J Hepatol* 2016;65:490–8.
15 Li Q, Brass AL, Ng A, *et al*. A genome-wide genetic screen for host factors required for hepatitis C virus propagation. *Proc Natl Acad Sci U S A* 2009;106:16410–5.
16 Brass AL, Dykxhoorn DM, Benita Y, *et al*. Identification of host proteins required for HIV infection through a functional genomic screen. *Science* 2008;319:921–6.
17 Busse-Wicher M, Wicher KB, Kusche-Gullberg M. The exostosin family: proteins with many functions. *Matrix Biol* 2014;35:25–33.
18 Sharma N, Kumari R. Rpb4 and Rpb7: multifunctional subunits of RNA polymerase II. *Crit Rev Microbiol* 2013;39:362–72.
19 Hull MW, McKune K, Woychik NA. RNA polymerase II subunit RPB9 is required for accurate start site selection. *Genes Dev* 1995;9:481–90.
20 Kraus RJ, Yu X, Cordes BA, *et al*. Hypoxia-inducible factor-1α plays roles in Epstein-Barr virus's natural life cycle and tumorigenesis by inducing lytic infection

through direct binding to the immediate-early BZLF1 gene promoter. *PLoS Pathog* 2017;13:e1006404.
21 Morinet F, Parent M, Pillet S, *et al*. Hypoxia inducible factor one alpha and human viral pathogens. *Curr Res Transl Med* 2017;65:7–9.
22 Chiu DK, Tse AP, Xu IM, *et al*. Hypoxia inducible factor HIF-1 promotes myeloid-derived suppressor cells accumulation through ENTPD2/CD39L1 in hepatocellular carcinoma. *Nat Commun* 2017;8:517.
23 Luo D, Wang Z, Wu J, *et al*. The Role of Hypoxia Inducible Factor-1 in Hepatocellular Carcinoma. *Biomed Res Int* 2014;2014:1–11.
24 Lin D, Wu J. Hypoxia inducible factor in hepatocellular carcinoma: a therapeutic target. *World J Gastroenterol* 2015;21:12171–8.
25 Evans DR, Guy HI. Mammalian pyrimidine biosynthesis: fresh insights into an ancient pathway. *J Biol Chem* 2004;279:33035–8.
26 Löffler M, Fairbanks LD, Zameitat E, *et al*. Pyrimidine pathways in health and disease. *Trends Mol Med* 2005;11:430–7.
27 Wang Y, Wang Z, Liu T, *et al*. Effects of flanking regions on HDV cotranscriptional folding kinetics. *RNA* 2018;24:1229–40.
28 Swyryd EA, Seaver SS, Stark GR. N-(phosphonacetyl)-L-aspartate, a potent transition state analog inhibitor of aspartate transcarbamylase, blocks proliferation of mammalian cells in culture. *J Biol Chem* 1974;249:6945–50.
29 Lucas-Hourani M, Dauzonne D, Jorda P, *et al*. Inhibition of pyrimidine biosynthesis pathway suppresses viral growth through innate immunity. *PLoS Pathog* 2013;9:e1003678.
30 Reyes GR. Ribavirin: recent insights into antiviral mechanisms of action. *Curr Opin Drug Discov Devel* 2001;4:651–6.
31 Sulkowski MS, Cooper C, Hunyady B, *et al*. Management of adverse effects of Peg-IFN and ribavirin therapy for hepatitis C. *Nat Rev Gastroenterol Hepatol* 2011;8:212–23.
32 Perry CM, Frampton JE, McCormack PL, *et al*. Nelfinavir: a review of its use in the management of HIV infection. *Drugs* 2005;65:2209–44.
33 Jeselsohn R, Buchwalter G, De Angelis C, *et al*. ESR1 mutations—a mechanism for acquired endocrine resistance in breast cancer. *Nat Rev Clin Oncol* 2015;12:573–83.
34 Ellmén J, Hakulinen P, Partanen A, *et al*. Estrogenic effects of toremifene and tamoxifen in postmenopausal breast cancer patients. *Breast Cancer Res Treat* 2003;82:103–11.
35 Connolly GP, Duley JA. Uridine and its nucleotides: biological actions, therapeutic potentials. *Trends Pharmacol Sci* 1999;20:218–25.
36 Lee L, Kelly RE, Pastra-Landis SC, *et al*. Oligomeric structure of the multifunctional protein CAD that initiates pyrimidine biosynthesis in mammalian cells. *Proc Natl Acad Sci U S A* 1985;82:6802–6.
37 Deans RM, Morgens DW, Ökesli A, *et al*. Parallel shRNA and CRISPR-Cas9 screens enable antiviral drug target identification. *Nat Chem Biol* 2016;12:361–6.
38 Franks DM, Izumikawa T, Kitagawa H, *et al*. C. elegans pharyngeal morphogenesis requires both de novo synthesis of pyrimidines and synthesis of heparan sulfate proteoglycans. *Dev Biol* 2006;296:409–20.
39 Droog M, Mensink M, Zwart W. The estrogen receptor α-cistrome beyond breast cancer. *Mol Endocrinol* 2016;30:1046–58.
40 Loustaud-Ratti V, Debette-Gratien M, Jacques J, *et al*. Ribavirin: past, present and future. *World J Hepatol* 2016;8:123–30.
41 Debing Y, Emerson SU, Wang Y, *et al*. Ribavirin inhibits in vitro hepatitis E virus replication through depletion of cellular GTP pools and is moderately synergistic with alpha interferon. *Antimicrob Agents Chemother* 2014;58:267–73.
42 Levrero M, Testoni B, Zoulim F. HBV cure: why, how, when? *Curr Opin Virol* 2016;18:135–43.
43 Zeisel MB, Baumert TF. Clinical development of hepatitis C virus host-targeting agents. *Lancet* 2017;389:674–5.
44 van der Ree MH, de Vree JM, Stelma F, *et al*. Safety, tolerability, and antiviral effect of RG-101 in patients with chronic hepatitis C: a phase 1B, double-blind, randomised controlled trial. *Lancet* 2017;389:709–17.
45 Zhang C, Chu M. Leflunomide: a promising drug with good antitumor potential. *Biochem Biophys Res Commun* 2018;496:726–30.
46 Bar-Or A, Pachner A, Menguy-Vacheron F, *et al*. Teriflunomide and its mechanism of action in multiple sclerosis. *Drugs* 2014;74:659–74.
47 Baumann P, Mandl-Weber S, Volkl A, *et al*. Dihydroorotate dehydrogenase inhibitor A771726 (leflunomide) induces apoptosis and diminishes proliferation of multiple myeloma cells. *Mol Cancer Ther* 2009;8:366–75.
48 Lupberger J, Zeisel MB, Xiao F, *et al*. EGFR and EphA2 are host factors for hepatitis C virus entry and possible targets for antiviral therapy. *Nat Med* 2011;17:589–95.
49 Verrier ER, Yim SA, Heydmann L, *et al*. Hepatitis B virus evasion from cyclic guanosine monophosphate-adenosine monophosphate synthase sensing in human Hepatocytes. *Hepatology* 2018;68:1695–709.
50 Verrier ER, Colpitts CC, Bach C, *et al*. Solute Carrier NTCP Regulates innate antiviral immune responses targeting Hepatitis C virus infection of hepatocytes. *Cell Rep* 2016;17:1357–68.

PROJETS DE RECHERCHE

5. CONTEXTE INTERNATIONAL

L'infection chronique par le VHB et la co-infection par le VHD sont deux causes majeures de maladies hépatiques et de cancer du foie, et sont aujourd'hui incurables. Plusieurs programmes internationaux et consortiums se sont mis en place pour promouvoir les projets de recherche sur cette thématique (16, 49-51). Notamment, une coalition internationale pour promouvoir la recherche de traitement anti-VHB curatif, ICE-HBV a récemment été établie (50). Au niveau national, l'Inserm et l'entreprise Sanofi se sont associés en 2017 dans un programme spécifique « HBV cure », soutenu par l'ANRS. Un axe de recherche important est l'identification des facteurs cellulaires impliqués dans les cycles viraux pour une meilleure compréhension des interactions moléculaires virus-hôte. Cette recherche a longtemps été freinée par l'absence de modèles robustes supportant les cycles infectieux complets. Notre laboratoire a été l'un des premiers au monde à mettre en place et publier des projets basés sur les nouveaux modèles récemment développés (37, 38), et dispose ainsi d'une position privilégiée au sein des équipes de recherche travaillant sur cette thématique. J'ai été recruté comme Chargé de Recherche Classe Normale (CRCN) Inserm en novembre 2018 et affecté à l'Unité UMR_S1110 du professeur Baumert pour poursuivre les recherches engagées dans la caractérisation des interactions hépatocytes-VHB/VHD. L'activité principale de l'unité Inserm U1110 est la compréhension des interactions hôte-virus dans le cadre des infections du foie par le VHB et le VHC pour la caractérisation de nouvelles cibles thérapeutiques (recherche translationnelle). Historiquement, l'unité a une très forte expertise dans la caractérisation des facteurs hépatiques impliqués dans l'entrée du VHC (52-56). L'expertise du laboratoire dans la découverte de nouvelles cibles thérapeutiques et des stratégies de traitements innovantes ciblant les facteurs du foie est illustrée par la mise en place d'un essai clinique phase I/II avec la molécule Erlotinib qui cible un des facteurs d'entrée du VHC (NCT NCT01835938 ; Hôpitaux Universitaires de Strasbourg) et la démonstration préclinique sur un modèle murin qu'un anticorps anti-CLDN1 (un récepteur du VHC) permet l'éradication du virus (57). Le présent projet de recherche s'inscrit dans une dynamique du laboratoire visant à identifier et caractériser de nouvelles cibles thérapeutiques de l'hôte pour le traitement de ces infections majeures du foie, et est donc en parfaite synergie avec les activités du laboratoire. Pour l'exécution des travaux, les méthodes ont été établies et décrites au laboratoire (38). Les collaborations avec les plateformes techniques ou les unités de recherche sont également mises en place et financées. Ces projets sont articulés autour d'un groupe que je coordonne composé d'une technicienne de recherche (C. Bach), d'une assistance ingénieure apprentie (S. Jachez), une assistante ingénieure / étudiante en thèse (L. Heydmann), un étudiant en thèse (V. Turon-Lagot), une étudiante M2 (M. Heuschkel) et un chercheur postdoctoral (G. Ligat).

6. NOUVELLES CIBLES THERAPEUTIQUES CONTRE LE VHD

6.1 Financement

- ANRS projet ECTZ104527 (2020-2022) – **PI** ; 126k€
- ANRS projet ECTZ102776 (2020-2022) – **Partenaire** (PI : J. Lucifora) ; 18,5k€
- *ANR JCJC 2020 Projet DELTArget (2021-2014) – **PI** ; 300k€ (demande en cours)*

6.2 Personnel impliqué

C. Bach (technicienne supérieure de recherche Inserm)
V. Turon-Lagot (doctorant – ATER Unistra)
S. Jachez (étudiante L3 en apprentissage Inserm)
M. Heuschkel (étudiante M2 Inserm)

6.3 Collaborations majeures

Unités de recherche :	J. Lucifora (CRCL, Lyon)
	P. Pale (Université de Strasbourg)
	C. Sureau (INTS, Paris)
Plateformes :	A. Weiss (IGBMC, Illkirch)
	J. Weber (IOCB, Prague, CZO)
	Y. Hoshida (University of Texas, Dallas, USA)
	P. Hammann (IBMC, Strasbourg)

6.4 Introduction

L'hépatite D chronique, forme la plus sévère d'hépatite virale chronique, est un problème de santé publique Mondial, probablement sous-estimé (58, 59) pour lequel aucune solution thérapeutique satisfaisante n'est disponible (29). Une caractéristique unique du VHD est le manque de protéines non structurales codées par le génome viral (y compris une polymérase virale), ce qui le rend très fortement dépendant de la machinerie cellulaire pour sa réplication (29). Cibler les facteurs de l'hôte est un concept émergent dans le traitement des maladies infectieuses, y compris les hépatites virales (57, 60-62). Dans ce contexte, la double approche de criblage récemment publiée par notre groupe a permis de caractériser CAD comme un facteur clé de la réplication du VHD et une cible antivirale potentielle, et a démontré l'intérêt de nos démarches à haut débit dans l'identification de nouvelles cibles

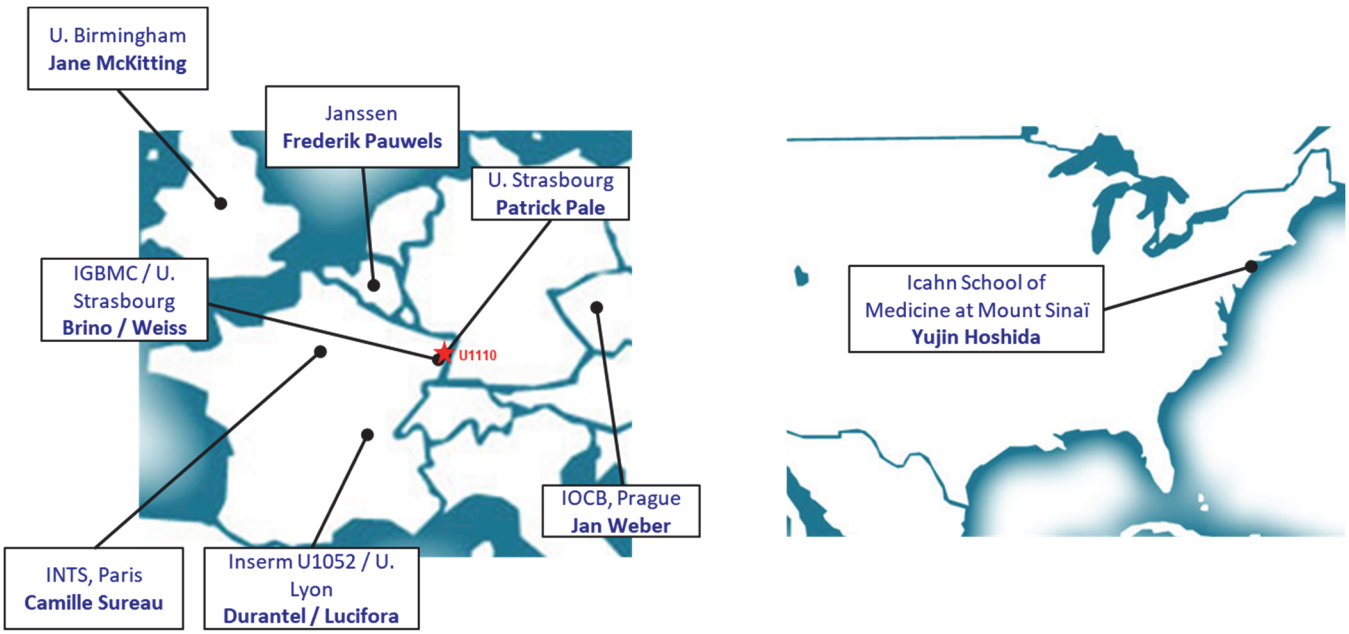

Figure 6.1. Principales collaborations nationales et internationales de l'U1110 avec des unités de recherche et des plateformes technologiques dans le cadre des projets VHD depuis 2013.

thérapeutiques (45). Un des objectifs majeurs que je souhaite poursuivre est la caractérisation des facteurs hépatiques impliqués dans le cycle viral du VHD pour le développement de nouvelles stratégies de traitement. Dans cette optique, les stratégies ciblant les facteurs de l'hôte – par le risque intrinsèque qu'elles comportent – nécessitent une connaissance précise et exhaustive des mécanismes moléculaires mis en jeu dans les interactions entre le virus et sa cible. Dans ce contexte, le groupe thématique au sein de l'unité U1110 saura s'appuyer sur un réseau international pluridisciplinaire constitué autour de la thématique VHD au cours des sept dernières années à notre initiative. Ce réseau comporte des experts mondialement reconnus dans la biologie du VHD (C. Sureau, J. Lucifora) et les maladies hépatiques (Y. Hoshida), mais également des chimistes (P. Pale, J. Weber), des plateformes techniques (L. Brino / A. Weiss, P. Hammann), et des acteurs de l'industrie pharmaceutique (Janssen). Par ailleurs, les modèles animaux établis dans notre laboratoire sont des outils appropriés pour la caractérisation des candidats dans des modèles physiologiques (57, 63). L'accomplissement de ce programme permettra une description exhaustive des interactions VHD-hépatocytes et la caractérisation de nouvelles cibles pour la clairance virale.

6.5 Validation de l'effet antiviral du PALA dans des études pré-cliniques.

Notre double approche de criblage a identifié PALA comme un candidat majeur pour les études pré-cliniques. Le premier objectif de ce programme sera de valider PALA dans des modèles VHD *in vivo*. Notamment, un modèle de souris « knock-in » humanisé exprimant une version chimérique de NTCP et sensible à l'infection VHD (64) est disponible dans l'animalerie A3 de l'unité (L. Mailly). Les premières études démontrent pour la première fois l'effet anti-VHD du PALA *in vivo* (Figure 6.2).

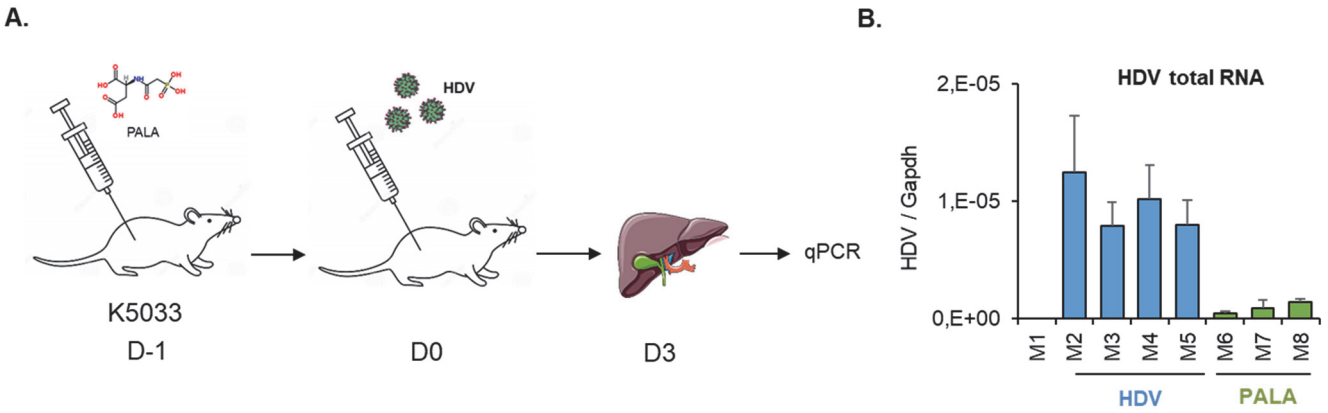

Figure 6.2: Activité antivirale du PALA *in vivo*. Les souris K5033 exprimant une version chimérique du récepteur NTCP les rendant sensibles à l'infection par le VHD ont reçu une injection péritonéale de PALA (100mg/kg) 24h avant d'être infectées par le VHD recombinant. Trois jours après l'infection, les souris ont été sacrifiées, les ARN totaux extraits depuis le foie et l'infection par le VHD a été quantifiée par qRT-PCR. Les résultats présentent les moyennes de trois réplicats biologiques par souris. M1 : souris non traitée, non infectée. M2-M5 : souris non traitées, infectées par le VHD. M6-M8 : souris traitées au PALA puis infectées par le VHD.

Le PALA a été synthétisé par notre collaborateur de l'Institut de Chimie de Strasbourg, (Pr. P. Pale). Ce résultat sera confirmé dans un autre modèle murin supportant la co-infection VHD/VHB, les souris chimériques uPA-SCID ou FRG-NOD qui sont disponibles dans notre unité Inserm (63). Nous prévoyons de coinfecter des souris FRG-NOD avec du VHD et du VHB puis de les traiter avec PALA, afin d'évaluer son effet antiviral sur l'infection HDV in vivo et sa toxicité potentielle chez la souris. Adaptant les protocoles de la littérature (65), le PALA sera injecté toutes les deux semaines par voie intrapéritonéale à des souris FRG-NOD coinfectées par le VHB / HDV à la dose initiale de 100 mg / kg. L'infection VHD sera contrôlée toutes les deux semaines pendant 6 semaines par quantification de l'ARN VHD dans le sérum de souris par qRT-PCR. De plus, une immunodétection de l'antigène HDAg dans des échantillons de foie sera effectuée à la fin de l'étude. L'IC90 du PALA sera ensuite déterminé par dose-réponse. Pour évaluer la toxicité du PALA *in vivo*, des souris Balb / C recevront une injection de PALA à 100 mg / kg. Les paramètres biochimiques sériques seront surveillés pendant 4 semaines (ALT, AST, urée, créatinine, protéines totales, albumine, bilirubine totale, LDH, ALP), une numération globulaire complète sera effectuée et l'histopathologie des organes sera analysée comme décrit précédemment par l'unité (57). L'amélioration des propriétés antivirales du PALA et la réduction de ses effets indésirables potentiels seront évaluées par la synthèse de composés dérivés, dans le cadre de notre collaboration avec le professeur Patrick Pale. Ces composés seront ensuite criblés et évalués en parallèle du PALA dans des modèles *in vitro* (hépatocytes primaires humains) et murins. Par ailleurs, les liens étroits entre notre unité et le CHU de Strasbourg nous permettent d'envisager, à plus long terme, la mise en place d'un essai clinique (phase I / phase IIa) après identification d'une molécule prometteuse via le Centre d'Investigation Clinique 'Investigation Clinique Centre (Inserm CIC 1434). La validation de PALA et de ses dérivés dans des modèles précliniques nous aidera à évaluer son potentiel antiviral pour le développement d'une nouvelle stratégie thérapeutique.

6.6 Validation et caractérisation de nouveaux facteurs impliqués dans l'infection VHD

Le criblage siRNA a permis l'identification de 191 candidats impliqués dans le cycle viral VHD (45). Une sélection des «33 meilleurs » présentant l'effet le plus prononcé sur l'infection à HDV, une toxicité modérée et une reproductibilité acceptable parmi les criblages secondaires a été conservée pour une analyse plus approfondie. En plus de *CAD* et *SLC10A1* (codant pour NTCP), des gènes codant pour des protéines transmembranaires (*TMPRSS9*, *LPXL*…), des transporteurs nucléaires (*NXT1*), une phosphatase (*PPP1CC*) ont été identifiés, suggérant un large panel de candidats impliqués dans différentes étapes du cycle viral. L'objectif de ce projet, mené par un étudiant en thèse du groupe (V. Turon-Lagot) est de valider le l'impication de ces facteurs cellulaires dans l'infection VHD à l'aide de stratégie « perte de fonction » alternatives donc des lignées *knock-out* CRISPR-Cas9 pour les gènes ciblés, système bien établi au sein du groupe (63) comme illustré en Figure 6.3.

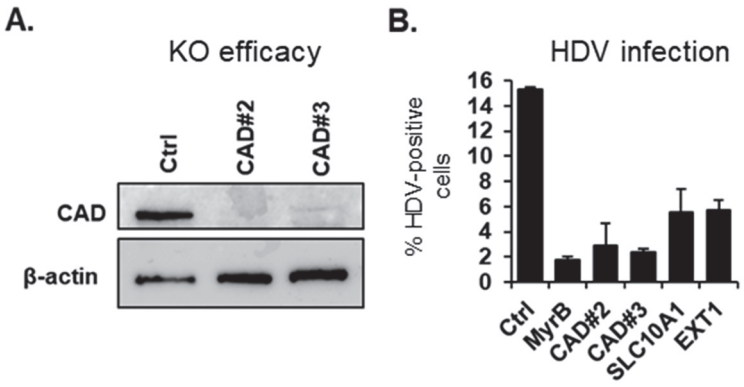

Figure 6.3: Validation de l'implication des candidats dans l'infection VHD à l'aide de lignées KO CRISPR-Cas9. Les cellules Huh-106 surexprimant la protéine cas9 ont été transduites avec des guides (sg) ciblant *CAD*, *SLC10A1* ou *EXT1* ou un guide contrôle. L'efficacité du KO a été contrôlée par Western blot (A). L'infection VHD a été quantifiée par immunodétection de l'antigène HDAg. Le Myrcludex B (MyrB) a été utilisé comme contrôle.

A l'aide d'une approche biochimique et pharmacologique, les mécanismes et le potentiel antiviral des ciblés identifiées sera étudié dans des modèles physiologiques d'infection comme les hépatocytes primaires. Des analyses cinétiques complémentaires et des méthodes de quantification de l'infection alternatives (détection par Northern blot de différentes formes d'ARN HDV par exemple) permettront de cibler l'étape du cycle viral impactée. Nous ambitionnons ainsi une caractérisation plus complète des interactions VHD-hépatocytes et la caractérisation de nouvelles cibles antivirales.

6.7 Caractérisation de l'interactome d'HDAg

Pour poursuivre la caractérisation des interactions moléculaires en le VHD et les hépatocytes, nous envisageons d'identifier les protéines cellulaires interagissant avec l'antigène delta HDAg. En collaboration avec P Hammann (IBMC, Strasbourg), une première analyse par spectrométrie de masse après co-immunoprécipitation (coIP) à l'aide d'un anticorps anti-HDAg à partir d'extraits protéiques de cellules Huh7-NTCP (clone Huh-106) infectées ont permis d'établir une première liste de candidats. Parmi ces candidats, l'hélicase MOV-10, précédemment décrite comme un partenaire de HDAg impliquée dans la réplication du VHD (66) ainsi qu'une sous unité de l'ADN polymérase II (POLR2H) ont été identifiées. Parmi les autres candidats, l'identification de PABPC1, connue pour interagir avec la protéine virale ICP27 du virus de l'herpès (HSV) stimulant la production de protéines virales (67, 68) suggère qu'un mécanisme similaire impliquant HDAg pourrait ainsi être impliqué dans la réplication du VHD.

A.

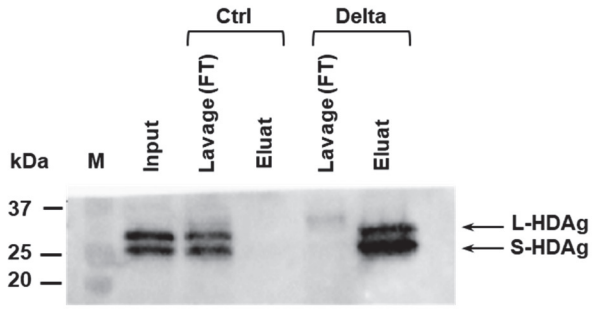

B.

Nom	Gène	Log2FC	*p*-value
Antigène delta		8.28	2.7E-94
Y-box-binding protein 1	YBX1	2.53	1.2E-07
Polyadenylate-binding protein 1	PABPC1	1.50	8.7E-07
Y-box-binding protein 3	YBX3	4.15	3.2E-06
Helicase MOV-10	MOV10	1.64	5.2E-04
DNA-directed RNA polymerases I, II, and III subunit RPABC3	POLR2H	3.18	1.8E-02

Figure 6.4 : Identification des partenaires cellulaires de HDAg. A. Modèle de la coIP. Après transfection avec le plasmide pSVL(D3) codant pour le génome du VHD, les cellules Huh-106 ont été lysées et une co-IP a été réalisées à l'aide d'un anticorps ciblant HDAg (Delta) ou un anticorps contrôle. L'expression des deux formes de HDAg est détectée par Western blot dans le lysat d'origine (input), dans les échantillons contrôles (FT) et dans les éluats d'IP (Eluat) **B**. Identification des partenaires de HDAg par spectrométrie de masse. Les CoIP ont été réalisées comme précédemment dans des cellules Huh-106 infectées par le VHD. Les peptides interagissant avec HDAg ont été analysés par chromatographie liquide - spectrométrie de masse. Parmi les candidats, la forme longue de l'antigène delta (« L-HDAg ») ainsi que les protéines codées par *YBX1*, *PABPC1*, *YBX3*, *MOV10* et *POLR2H* sont représentées, avec le taux d'enrichissement des peptides dans l'échantillon « Eluat Delta » par rapport aux contrôles et la *p*value associée. M : marqueur.

Des coIP additionnelles seront réalisées pour confirmer ces résultats préliminaires, notamment sur des modèles d'infection alternatifs en collaboration avec J. Lucifora du CRCL de Lyon (cellules HepaRG entre autres). Les listes de candidats seront comparées et analysées et croisées avec les résultats du criblage siRNA primaire à la recherche de candidats communs. Des validations individuelles par Western blot et des stratégies « perte de fonction » permettront de sélectionner les candidats d'intérêt pour une caractérisation plus précise.

6.8 Criblage haut débit pour l'identification de nouvelles molécules antivirales

En collaboration avec L. Brino (IGBMC), le criblage de la banque de molécules Prestwick sur un modèle d'infection VHD a permis l'identification de nouveaux composés antiviraux, dont le Fulvestrant (45). Etant donné le succès de ce criblage pilote, nous envisageons d'étendre le nombre de composés testés en réalisant un criblage haut débit pour l'identification de nouveaux composés antiviraux. Dans ce contexte, nous envisageons de cribler la banque « IOCB library of molecules », mise à disposition par J. Weber (Institute of Organic Chemistry and Biochemistry, Prague, CEZ) et disponible à la plateforme de l'IGBMC. Cette banque contient 3872 molécules synthétisées au sein de l'institut IOCB sans présélection, et contient notamment des composés basés sur la chimie des analogues de nucléos(t)ides et molécules dérivées de produits naturels (69-71). En particulier, certains antiviraux ont été identifiés au sein de la banque lors de criblage pour des inhibiteurs de VHC, virus de la dengue ou rhinovirus humain (72, 73).

Le criblage sera réalisé par A. Weiss de la plateforme de criblage haut débit de l'IGBMC. La stratégie de criblage impliquera le modèle d'infection Huh-106/VHD décrit précédemment (45) qui a été adapté au format plaques 384 puits. L'infection VHD sera quantifiée par immunodétection de l'antigène HDAg dans les cellules infectées. Les molécules antivirales les plus pertinentes (effet sur l'infection, toxicité…) selon sélectionnées pour validation et caractérisation de leur mode d'action et de leur potentiel antiviral à l'aide d'hépatocytes primaires humains.

6.9 Conclusion

Etant données nos premiers résultats et l'expertise de longue date du laboratoire dans l'étude des interactions hôte virus, l'approche développée dans ce programme est réaliste et je suis confiant quant à la réalisation des objectifs dans les cinq ans à venir. J'attends de ce programme qu'il accroisse notre compréhension de l'infection par le VHD par l'identification de nouveaux candidats impliqués dans le cycle viral. De plus, la caractérisation de ces candidats fournira de nouvelles cibles pour la clairance virale. Collectivement, les découvertes et le développement d'agents thérapeutiques induits par les résultats de ce programme permettront un pas en avant vers une approche multimodale pour éradiquer cette menace majeure de santé publique.

7. CIBLER l'ADNccc, RESERVOIR DU VHB

7.1 Financement

- ANRS projet ECTZ87384 (2019-2021) – **co-PI** (co-PI : T. Baumert) ; 132k€
- ANRS allocation postdoctorale (2019-2021) – G. Ligat

7.2 Personnel impliqué

G. Ligat (chercheur postdoctoral Inserm – allocataire ANRS)
L. Heydmann (assistante ingénieure Unistra – doctorante)
S. Jachez (étudiante L3 en apprentissage Inserm)

7.3 Collaborations majeures

Unité de recherche :	M. Nassal (U. Freiburg, ALL)
	J. Lucifora (CRCL, Lyon)
	P. Bielawski (U. Gdansk, POL)
Plateforme :	L. Brino (IGBMC, Illkirch)

7.4 Introduction

L'ADNccc du VHB est un intermédiaire de réplication, qui sert de matrice à la synthèse des ARN VHB. Il est formé dans le noyau au cours de l'infection à partir de l'ADN génomique du VHB, ADNrc partiellement double brin de 3,2 kb lié de façon covalente à la polymérase virale (27). Ce « minichromosome » est responsable de la chronicité et de la persistance de l'infection dans les hépatocytes et n'est pas ciblé par les traitements actuels (27). Dans la perspective du programme international « HBV Cure », il est admis qu'une éradication totale du virus passe par l'élimination de l'ADNccc dans les hépatocytes infectés (« guérison complète », (16)). Un effort substantiel est donc attendu par la communauté pour comprendre la formation et l'activité de cet ADNccc et si possible développer de nouvelles stratégies pour l'éliminer ou l'inactiver. La formation et la régulation de cet ADNccc sont encore peu connues. Cependant, certains indices conceptuels des mécanismes permettant la formation d'ADNccc à partir de l'ADNrc proviennent des différences structurelles entre les deux ADN. Notamment, la conversion de l'ADNrc partiellement double brin en ADNccc est susceptible

d'impliquer la machinerie cellulaire de réparation de l'ADN (74). La polymérase kappa (POLK) a été récemment identifiée comme une enzyme clé de la synthèse d'ADNccc (75). Un objectif majeur de mon programme sera la compréhension de la conversion de l'ADNccc à partir de l'ADNrc pour enrayer sa formation et inhiber la réplication virale. Dans cette optique, l'U1110 est à l'origine, avec M. Nassal de l'Université de Fribourg, d'un consortium européen Infect-ERA impliquant des unités de recherche de Pologne (University of Gdansk, POL) et de Belgique (J. Neyts, University of Leuven, BEL) et la plateforme de criblage de l'IGBMC et dont un objectif majeur est la mise au point d'un criblage cellulaire pour l'identification de nouveaux facteurs impliqués dans la formation de l'ADNccc. En collaboration avec M. Nassal, nous avons mis au point une lignée rapportrice HA2/3.

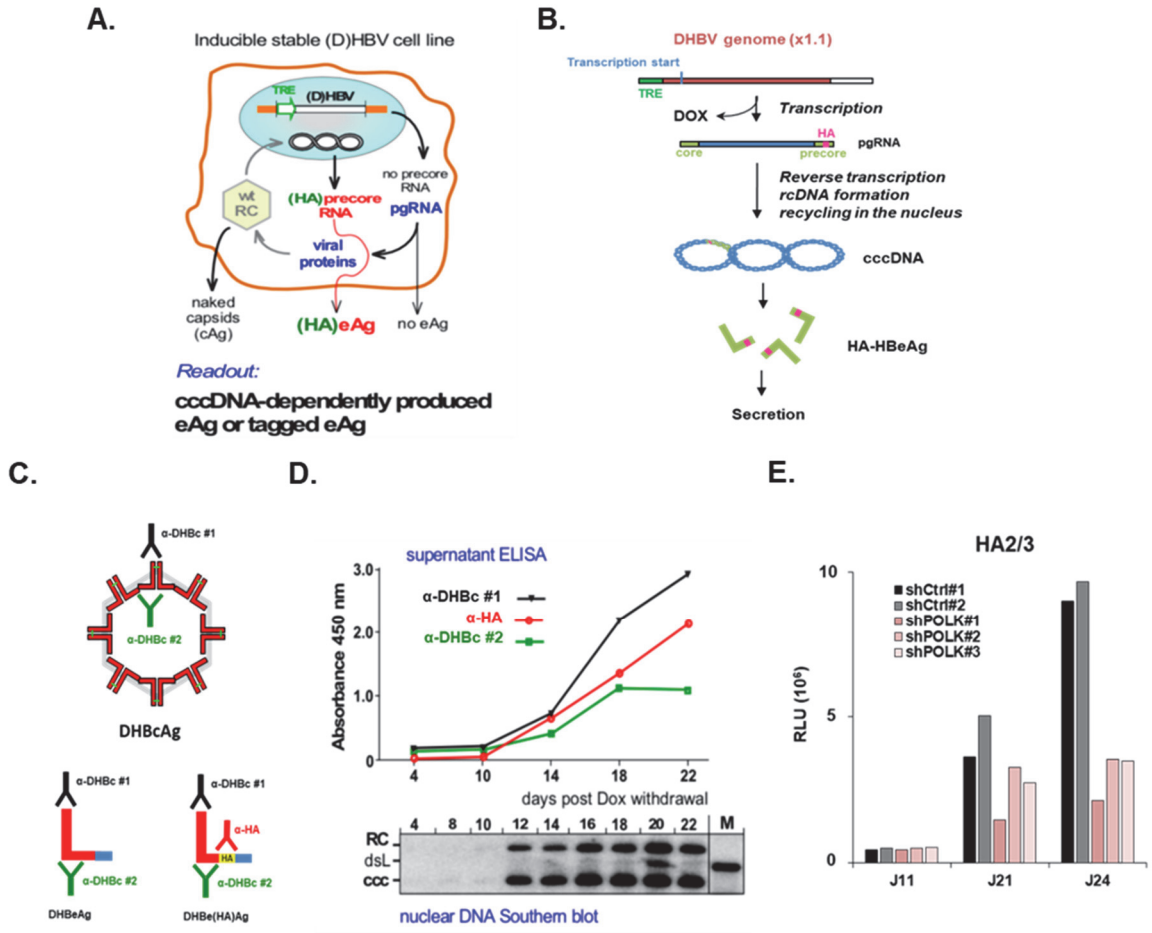

Figure 7.1. Lignée cellulaire inductible HA2/3 exprimant le VHB de canard (DHBV pour *duck hepatitis B virus*). **A-C**. La lignée cellulaire HA2/3 exprime de manière stable la protéine transactivatrice de la tétracycline et une version du génome du DHBV à partir de laquelle l'ARN prégénomique (pg) est transcrit à partir d'un promoteur inductible (TRE) qui ne permet pas la transcription directe de la région « précore » après suppression de la doxycycline (DOX). Ainsi, l'antigène « DHBeAg » du DHBV, ou protéine précore n'est pas produite à partir du transgène. La formation d'ADNccc après recyclage de l'ARNpg dans le noyau induit alors la synthèse de l'ARN précore et de DHBeAg. La production de DHBeAg soluble est donc un marqueur de l'activité de l'ADNccc dans cette lignée. Pour assurer la spécificité de la détection de DHBeAg (qui partage la majorité de sa séquence avec l'antigène core « DHBcAg », (**C**)), un tag HA a été introduit dans la région précore. La sécrétion de l'antigène HA (« HA-HBeAg ») peut être quantifiée par ELISA anti-HA (α-HA) (**D**). D. La sécrétion d'HA-HBeAg est corrélée à la synthèse d'ADNccc (**D**). La sécrétion d'HA-HBeAg est inhibée par la diminution de l'expression de *POLK*, jouant un rôle clé dans la formation de l'ADNccc. (**E**). A,C : adapté de (74).

Cette lignée inductible « Tet-OFF » exprime le génome du VHB de canard (DHBV, produisant beaucoup plus d'ADNccc humain (74)) et secrète un antigène DHBe (ou prortéine « precore ») marqué HA uniquement en présence d'un ADNccc fonctionnel (76). La quantification de la production de cet antigène par ELISA permet d'évaluer donc l'activité de l'ADNccc (Figure 7.1). L'exploitation de ce modèle unique d'étude de l'activité spécifique de l'ADNccc permettra l'identification et la caractérisation de nouveaux facteurs cellulaires impliqués dans sa formation. Pour la réalisation de ce programme, financé par l'ANRS dans la continuité du consortium Infect-ERA, le groupe s'appuiera également sur des collaborations internationales d'experts en biologie du VHB (D. Durantel et J. Lucifora) mais également des plateformes techniques du Broad Institute of MIT and Harvard (Cambridge, USA) (Figure 7.2) avec lesquels l'unité collabore dans le cadre de ses projets VHB.

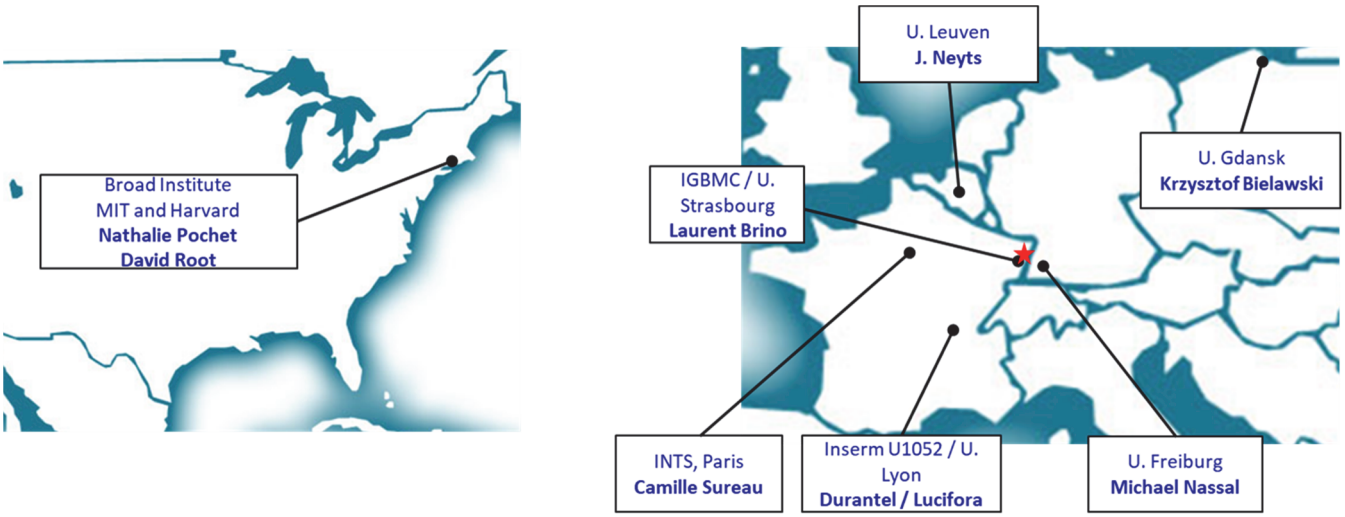

Figure 7.2. Principales collaborations nationales et internationales de l'U1110 avec des unités de recherche et des plateformes technologiques dans le cadre des projets VHB depuis 2013.

7.5 Résultats préliminaires

Etant donné l'importance supposée de la machinerie de réparation de l'ADN dans la formation de l'ADNccc, nous avons appliqué à la lignée cellulaire HA2/3 un criblage perte de fonction à l'aide d'une banque de shRNA ciblant 239 gènes appartenant à la réponse aux dommages de l'ADN (DDR pour *DNA damage response*) a été réalisé en collaboration avec la plateforme de criblage à haut débit de l'IGBMC (L. Brino). La banque a été synthétisée à façon par la « Genetic Perturbation Platform » du Broad Institute of MIT and Harvard (Cambridge, USA). Après transduction, la production d'ADNccc dans les cellules HA2/3 après suppression de la doxycycline dans le milieu a été quantifiée par ELISA HA (Figure 7.3). Après sélection des candidats comme défini dans la Figure 7.3, le criblage a permis l'identification d'un panel de 27 facteurs potentiels impliqués dans la formation de l'ADNccc. Parmi ces candidats, l'identification de *POLK* (75), *TDP2* (77) et *FEN1* (78), connus pour leur

implication dans la formation de l'ADNccc, valident notre approche. Le but de ce programme est de valider et caractériser les candidats issus du criblage, et d'exploiter le modèle cellulaire pour l'identification d'inhibiteur de l'ADNccc. Avec l'achèvement de ce programme, nous ambitions de comprendre la formation de l'ADNccc dans les hépatocytes infectés et de proposer des stratégies pour éliminer ce réservoir du virus dans les cellules.

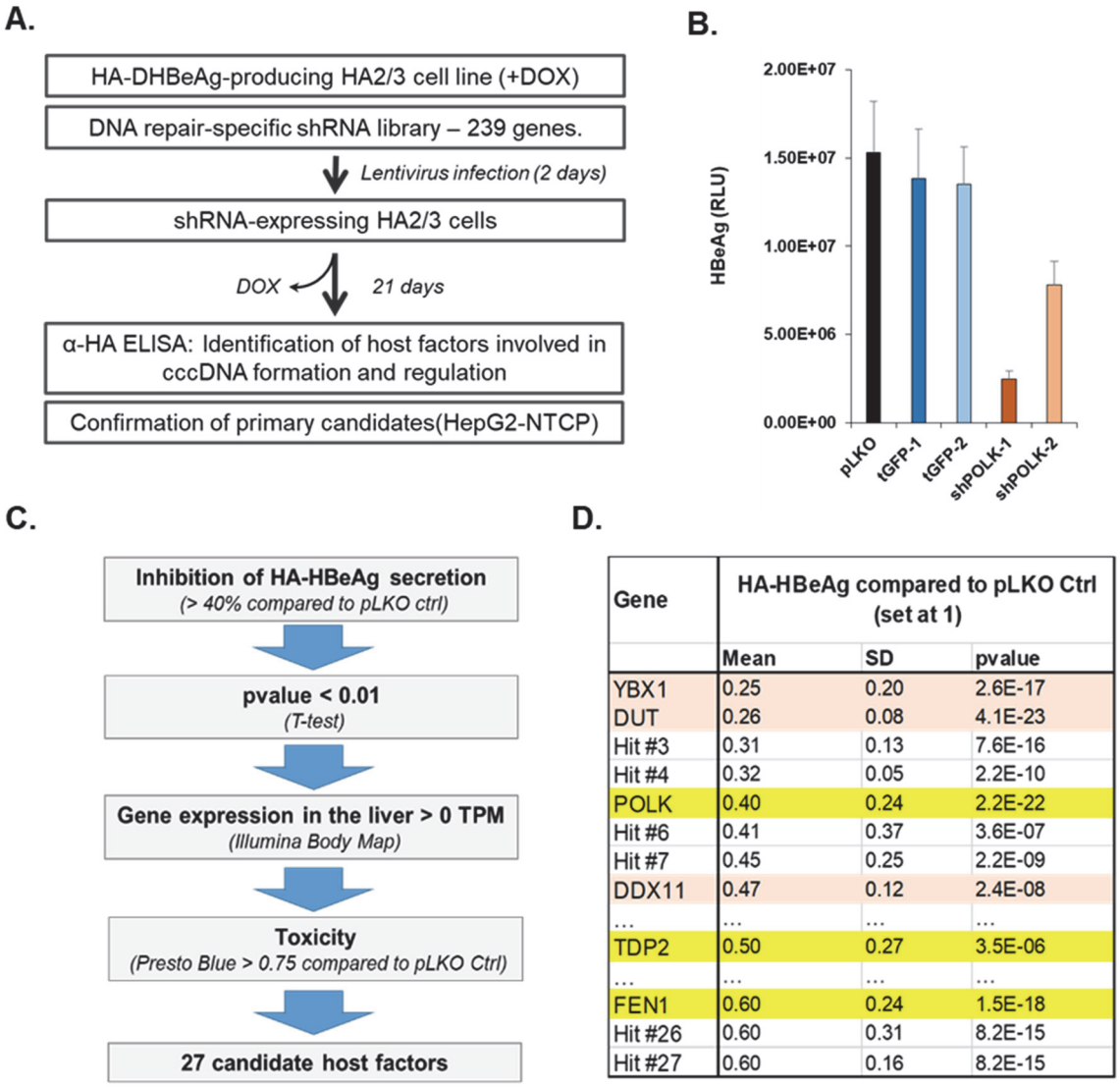

Gene	HA-HBeAg compared to pLKO Ctrl (set at 1)		
	Mean	SD	pvalue
YBX1	0.25	0.20	2.6E-17
DUT	0.26	0.08	4.1E-23
Hit #3	0.31	0.13	7.6E-16
Hit #4	0.32	0.05	2.2E-10
POLK	0.40	0.24	2.2E-22
Hit #6	0.41	0.37	3.6E-07
Hit #7	0.45	0.25	2.2E-09
DDX11	0.47	0.12	2.4E-08
…	…	…	…
TDP2	0.50	0.27	3.5E-06
…	…	…	…
FEN1	0.60	0.24	1.5E-18
Hit #26	0.60	0.31	8.2E-15
Hit #27	0.60	0.16	8.2E-15

Figure 7.3. Mise au point d'un criblage shRNA ciblant la machinerie de réparation de l'ADN. A. Présentation de la stratégie de criblage. **B**. deux shRNA ciblant l'expression de *POLK* ont été utilisés comme contrôle positif sur chaque plaque du criblage. **C**. Le criblage shRNA a permis l'identification de candidats induisant une diminution de la sécrétion d'HA-HBeAg. Après sélection en fonction de la robustesse des réplicats, de l'expression dans la fois et la viabilité cellulaire après transduction, 27 candidats ont été sélectionnés. **D**. Parmi ces candidats, *POLK, TDP2* et *FEN1*, déjà connus pour leur implication dans la formation de l'ADNccc ont été identifiés.

7.6 Caractérisation des candidats du criblage

Le criblage primaire a fourni une liste de facteurs hôtes candidats impliqués dans la formation d'ADNccc de DHBV. Comme la lignée cellulaire HA2/3 exprime le génome du DHBV, la première

étape de validation consistera à confirmer les résultats du criblage primaire dans des modèles impliquant le VHB humain. Ce projet sera réalisé par un chercheur postdoctoral, financé par une allocation nominative de recherche de l'ANRS. Pour ce faire, nous profiterons des modèles d'infection établis au laboratoire (38, 63). Le modèle HepG2-NTCP supporte le cycle viral complet du VHB, y compris la formation d'ADNccc fonctionnel (voir Eller, Heydmann et al., en révision à Nat Commun ci-dessus). Ainsi, l'objectif de ce projet est de définir une liste comparative des facteurs de réparation de l'ADN impliqués dans la formation d'ADNccc du VHB et du DHBV dans les systèmes infectieux humains, y compris *in fine* les hépatocytes primaires humains ainsi que les modèles murins disponibles au laboratoire, dont le modèle uPA-SCID chimérique qui supporte l'infection par le VHB (63). Pour les études de perte de fonction, les souris seront pré-injectées 14 jours avant l'infection par le VHB avec des vecteurs viraux adéno-associés recombinants (rAAV) optimisés pour le modèle de xénogreffe humaine (comme décrit dans (79)) et exprimant un shRNA spécifique du candidat sélectionné. L'expression du gène cible sera évaluée par immunofluorescence in situ ou Western blot 14 et 28 jours après l'injection de rAAV (79). L'infection par le VHB sera évaluée à la fois par la mesure de la charge virale du VHB dans le sérum murin (82) et par la détection directe de l'ADNccc par Southern blot dans les lysats de cellules hépatiques. Par ailleurs, les inhibiteurs des candidats sélectionnés seront testés sur des hépatocytes primaires humains et les souris infectées par le VHB. Si aucun inhibiteur des candidats sélectionnés n'est disponible sur le marché, une collaboration avec l'Institut de Chimie de l'Université de Strasbourg (Prof Patrick Pale) pour produire et tester de petites molécules d'intérêt peut être envisagée (voir (45)).

Parmi les candidats, *YBX1* a été identifié comme le candidat le plus prometteur (Figure 7.3). *YBX1* code pour la protéine multifonctionnelle YB-1 (*Y-Box-binding Protein 1*), capable de se lier aux ADN et aux ARN et impliquée dans de nombreux processus cellulaires y compris la régulation de la transcription et de la traduction, l'épissage des pré-ARNm et la réparation de l'ADN (80). En raison de ses capacités de liaison aux acides nucléiques, YB-1 pourrait interagir directement avec l'ADNccc du VHB, affectant sa formation ou son activité. Des tests d'immunoprécipitation de la chromatine utilisant des anticorps ciblant YB-1 seront effectués pour répondre à cette question. Dans le même ordre d'idées, l'interactome de YB-1 sera caractérisé, en particulier son interaction potentielle avec les protéines du VHB telles que HBx, connue pour réguler l'activité de l'ADNccc (27). Des études cinétiques à l'aide des shRNA permettront également de cibler l'étape du cycle viral dans laquelle intervient YB-1.

Collectivement, notre approche validera et caractérisera les candidats et fournira un panel de cibles antivirales validées *in vivo* comme point de départ pour le développement de nouvelles stratégies de traitement ciblant l'ADNccc.

7.7 Pertinence clinique des candidats sélectionnés.

Afin de confirmer l'importance des facteurs identifiés dans la biologie du VHB, nous proposons de tester la pertinence clinique des candidats chez les patients chroniquement infectés par le VHB. Pour ce faire, les polymorphismes de nos gènes candidats seront étudiés et l'association entre le fond génétique des patients et leur sensibilité à l'infection et la progression de la malade hépatique seront analysées. Ce projet est réalisé en collaboration avec le professeur P. Bielawski de l'Université de Gdansk (POL). Le polymorphisme des gènes sélectionnés sera analysé par désorption-ionisation laser assistée par matrice suivie d'une analyse par spectrométrie de masse à temps de vol (MALDI-TOF MS) couplée à une PCR SBE (*single-base extension*) pour la détection de SNP (*single-nucleotide polymorphism*) à haut débit (81). Des échantillons d'ADN et des données cliniques de 600 patients infectés de façon chronique par le VHB ainsi que de 60 patients qui ont spontanément éliminés le VHB (groupe témoin) provenant de la cohorte française ANRS CO22 HEPATHER ont été fournis par l'ANRS et sont déjà disponibles dans le laboratoire de notre collaborateur de l'Université de Gdansk. La distribution des génotypes sera comparée entre le contrôle (clairance spontanée) et le groupe d'étude (hépatite B chronique) pour évaluer l'effet du polymorphisme des gènes candidats sur la sensibilité à l'infection chronique par le VHB. Pour analyser les associations entre génotypes et lésions hépatiques, des données concernant l'histopathologie hépatique des patients seront incluses (inflammation, fibrose, cirrhose, stéatose, carcinome hépatocellulaire). Par cette approche nous ambitionnons de valider chez les patients l'importance des facteurs étudiés dans le cycle viral du VHB et évaluer leur potentiel thérapeutique.

7.8 Adaptation de la lignée cellulaire pour le criblage de petites molécules.

Etant donné le succès de la première approche de criblage, notre objectif est de mettre au point un modèle de criblage haut débit à l'aide de la lignée cellulaire HA2/3 pour l'identification de molécules ciblant l'ADNccc. En collaboration avec la plateforme de criblage de l'IGBMC, la culture des cellules et la détection de DHBe seront adaptées en plaques 384 puits pour permettre le criblage de larges banques de molécules. Comme criblage pilote, la banque « DNA Damage/DNA Repair compound Library » de SelleckChem sera testée sur les lignées HA2/3. Cette banque contient 179 molécules ciblant la machinerie de réparation de l'ADN, notamment des topoisomérases, des histones désacétylases et des facteurs impliqués dans la synthèse d'ADN et d'ARN. Ce premier criblage apportera un premier panel de molécules potentiellement inhibitrices de la synthèse d'ADNccc qui seront ensuite validés dans nos modèles d'infection. En fonction des résultats, le modèle de criblage

sera étendu à des banques beaucoup plus larges et non limitées à la machinerie de réparation de l'ADN, à la recherche de nouveaux inhibiteurs de l'ADNccc.

7.9 Conclusion

La formation et la régulation de l'ADNccc dans les hépatocytes infectés sont encore largement méconnus. Nos résultats préliminaires confirment la pertinence de notre approche pour l'identification de nouveaux facteurs cellulaires impliqués dans la production de la ADNccc. Ce programme permettra d'évaluer la pertinence clinique des facteurs identifiés et d'en estimer le potentiel antiviral. Collectivement, les résultats de ce programme proposeront des solutions nouvelles pour l'éradication de l'ADNccc chez les patients chroniquement infectés par le VHB.

8. REFERENCES

1. Verrier ER, Langevin C, Quillet E, Boudinot P. Genetic analysis of resistance to rhabdovirus infection in rainbow trout (Oncorhyncus mykiss). Virologie 2013;17:426-441.

2. Thorgaard GH, Bailey GS, Williams D, Buhler DR, Kaattari SL, Ristow SS, Hansen JD, et al. Status and opportunities for genomics research with rainbow trout. Comp Biochem Physiol B Biochem Mol Biol 2002;133:609-646.

3. Wolf K, Rumsey G. The Representative Research Animal: Why Rainbow Trout (Salmo gairdneri Rich.)? J Appl Ichtyol 1985;1:131-138.

4. Crane M, Hyatt A. Viruses of fish: an overview of significant pathogens. Viruses 2011;3:2025-2046.

5. Verrier ER, Dorson M, Mauger S, Torhy C, Ciobotaru C, Hervet C, Dechamp N, et al. Resistance to a rhabdovirus (VHSV) in rainbow trout: identification of a major QTL related to innate mechanisms. PLoS One 2013;8:e55302.

6. Quillet E, Dorson M, Aubard G, Torhy C. In vitro viral haemorrhagic septicaemia virus replication in excised fins of rainbow trout: correlation with resistance to waterborne challenge and genetic variation. Dis Aquat Organ 2001;45:171-182.

7. Quillet E, Dorson M, Le Guillou S, Benmansour A, Boudinot P. Wide range of susceptibility to rhabdoviruses in homozygous clones of rainbow trout. Fish Shellfish Immunol 2007;22:510-519.

8. Verrier ER, Langevin C, Tohry C, Houel A, Ducrocq V, Benmansour A, Quillet E, et al. Genetic resistance to rhabdovirus infection in teleost fish is paralleled to the derived cell resistance status. PLoS One 2012;7:e33935.

9. Langevin C, Aleksejeva E, Passoni G, Palha N, Levraud JP, Boudinot P. The antiviral innate immune response in fish: evolution and conservation of the IFN system. J Mol Biol 2013;425:4904-4920.

10. Verrier ER, Langevin C, Benmansour A, Boudinot P. Early antiviral response and virus-induced genes in fish. Dev Comp Immunol 2011;35:1204-1214.

11. Palti Y, Gahr SA, Purcell MK, Hadidi S, Rexroad CE, 3rd, Wiens GD. Identification, characterization and genetic mapping of TLR7, TLR8a1 and TLR8a2 genes in rainbow trout (Oncorhynchus mykiss). Dev Comp Immunol 2010;34:219-233.

12. Verrier ER, Genet C, Laloe D, Jaffrezic F, Rau A, Esquerre D, Dechamp N, et al. Genetic and transcriptomic analyses provide new insights on the early antiviral response to VHSV in resistant and susceptible rainbow trout. BMC Genomics 2018;19:482.

13. Verrier ER, Ehanno A, Biacchesi S, Le Guillou S, Dechamp N, Boudinot P, Bremont M, et al. Lack of correlation between the resistances to two rhabdovirus infections in rainbow trout. Fish Shellfish Immunol 2013;35:9-17.

14. Purcell MK, Lapatra SE, Woodson JC, Kurath G, Winton JR. Early viral replication and induced or constitutive immunity in rainbow trout families with differential resistance to Infectious hematopoietic necrosis virus (IHNV). Fish Shellfish Immunol 2010;28:98-105.

15. Berthelot C, Brunet F, Chalopin D, Juanchich A, Bernard M, Noel B, Bento P, et al. The rainbow trout genome provides novel insights into evolution after whole-genome duplication in vertebrates. Nat Commun 2014;5:3657.

16. Zeisel MB, Lucifora J, Mason WS, Sureau C, Beck J, Levrero M, Kann M, et al. Towards an HBV cure: state-of-the-art and unresolved questions-report of the ANRS workshop on HBV cure. Gut 2015;64:1314-1326.

17. Trepo C, Chan HL, Lok A. Hepatitis B virus infection. Lancet 2014;384:2053-2063.

18. Chemin I, Zoulim F. Hepatitis B virus induced hepatocellular carcinoma. Cancer Lett 2009;286:52-59.

19. Seeger C, Mason WS. Molecular biology of hepatitis B virus infection. Virology 2015;479-480:672-686.

20. Sureau C, Salisse J. A conformational heparan sulfate binding site essential to infectivity overlaps with the conserved hepatitis B virus a-determinant. Hepatology 2013;57:985-994.

21. Schulze A, Gripon P, Urban S. Hepatitis B virus infection initiates with a large surface protein-dependent binding to heparan sulfate proteoglycans. Hepatology 2007;46:1759-1768.

22. Ni Y, Lempp FA, Mehrle S, Nkongolo S, Kaufman C, Falth M, Stindt J, et al. Hepatitis B and D viruses exploit sodium taurocholate co-transporting polypeptide for species-specific entry into hepatocytes. Gastroenterology 2014;146:1070-1083.

23. Yan H, Zhong G, Xu G, He W, Jing Z, Gao Z, Huang Y, et al. Sodium taurocholate cotransporting polypeptide is a functional receptor for human hepatitis B and D virus. Elife 2012;1:e00049.

24. Verrier ER, Colpitts CC, Sureau C, Baumert TF. Hepatitis B virus receptors and molecular drug targets. Hepatol Int 2016;10:567-573.

25. Eller C, Heydmann L, Colpitts CC, Verrier ER, Schuster C, Baumert TF. The functional role of sodium taurocholate cotransporting polypeptide NTCP in the life cycle of hepatitis B, C and D viruses. Cell Mol Life Sci 2018;75:3895-3905.

26. Verrier ER, Heydmann L, Baumert TF, Schuster C. Solute carrier NTCP, a key actor in liver infections by hepatitis viruses and a promising antiviral target. Virologie 2018;22:55-66.

27. Nassal M. HBV cccDNA: viral persistence reservoir and key obstacle for a cure of chronic hepatitis B. Gut 2015;64:1972-1984.

28. Fattovich G, Giustina G, Christensen E, Pantalena M, Zagni I, Realdi G, Schalm SW. Influence of hepatitis delta virus infection on morbidity and mortality in compensated cirrhosis type B. The European Concerted Action on Viral Hepatitis (Eurohep). Gut 2000;46:420-426.

29. Turon-Lagot V, Saviano A, Schuster C, Verrier ER. Hepatitis D virus: viral cycle and new therapeutic approaches. Virologie (Montrouge) 2019;23:149-159.

30. Taylor JM. Virology of hepatitis D virus. Semin Liver Dis 2012;32:195-200.

31. Lempp FA, Urban S. Hepatitis Delta Virus: Replication Strategy and Upcoming Therapeutic Options for a Neglected Human Pathogen. Viruses 2017;9:E172.

32. Sureau C, Negro F. The hepatitis delta virus: Replication and pathogenesis. J Hepatol 2016;64:S102-116.

33. Hughes SA, Wedemeyer H, Harrison PM. Hepatitis delta virus. Lancet 2011;378:73-85.

34. Verrier ER, Colpitts CC, Schuster C, Zeisel MB, Baumert TF. Cell Culture Models for the Investigation of Hepatitis B and D Virus Infection. Viruses-Basel 2016;8:E261.

35. Chung RT, Baumert TF. Curing chronic hepatitis C--the arc of a medical triumph. N Engl J Med 2014;370:1576-1578.

36. Verrier ER, Tawar RG, Schuster C, Brino L, Bach C, Heydmann L, Habersetzer F, et al. A high-throughput HDV infection model system for screening of antivirals and host-targeting compounds. J Hepatol 2014;60:S128-S129.

37. Verrier ER, Colpitts CC, Bach C, Heydmann L, Xiao F, Thumann C, Crouchet E, et al. Solute Carrier NTCP Regulates Innate Antiviral Immune Responses Targeting Hepatitis C Virus Infection of Hepatocytes. Cell Rep 2016;17:1357–1368.

38. Verrier ER, Colpitts CC, Bach C, Heydmann L, Weiss A, Renaud M, Durand SC, et al. A targeted functional RNAi screen uncovers Glypican 5 as an entry factor for hepatitis B and D viruses. Hepatology 2016;63:35–48.

39. Konstantinou D, Deutsch M. The spectrum of HBV/HCV coinfection: epidemiology, clinical characteristics, viralinteractions and management. Ann Gastroenterol 2015;28:221-228.

40. Rehermann B, Nascimbeni M. Immunology of hepatitis B virus and hepatitis C virus infection. Nat Rev Immunol 2005;5:215-229.

41. Gao D, Wu J, Wu YT, Du F, Aroh C, Yan N, Sun L, et al. Cyclic GMP-AMP synthase is an innate immune sensor of HIV and other retroviruses. Science 2013;341:903-906.

42. Schoggins JW, MacDuff DA, Imanaka N, Gainey MD, Shrestha B, Eitson JL, Mar KB, et al. Pan-viral specificity of IFN-induced genes reveals new roles for cGAS in innate immunity. Nature 2014;505:691-695.

43. Raney AK, Johnson JL, Palmer CN, McLachlan A. Members of the nuclear receptor superfamily regulate transcription from the hepatitis B virus nucleocapsid promoter. J Virol 1997;71:1058-1071.

44. Guan KL, Jenkins CW, Li Y, Nichols MA, Wu X, O'Keefe CL, Matera AG, et al. Growth suppression by p18, a p16INK4/MTS1- and p14INK4B/MTS2-related CDK6 inhibitor, correlates with wild-type pRb function. Genes Dev 1994;8:2939-2952.

45. Verrier ER, Weiss A, Bach C, Heydmann L, Turon-Lagot V, Kopp A, El Saghire H, et al. Combined small molecule and loss-of-function screen uncovers estrogen receptor alpha and CAD as host factors for HDV infection and antiviral targets. Gut 2020;69:158-167.

46. Droog M, Mensink M, Zwart W. The Estrogen Receptor alpha-Cistrome Beyond Breast Cancer. Mol Endocrinol 2016;30:1046-1058.

47. Deng G, Zhou G, Zhai Y, Li S, Li X, Li Y, Zhang R, et al. Association of estrogen receptor alpha polymorphisms with susceptibility to chronic hepatitis B virus infection. Hepatology 2004;40:318-326.

48. Khan S, Abdelrahim M, Samudio I, Safe S. Estrogen receptor/Sp1 complexes are required for induction of cad gene expression by 17beta-estradiol in breast cancer cells. Endocrinology 2003;144:2325-2335.

49. Block TM, Alter H, Brown N, Brownstein A, Brosgart C, Chang KM, Chen PJ, et al. Research priorities for the discovery of a cure for chronic hepatitis B: Report of a workshop. Antiviral Res 2017;150:93-100.

50. Revill P, Testoni B, Locarnini S, Zoulim F. Global strategies are required to cure and eliminate HBV infection. Nat Rev Gastroenterol Hepatol 2016;13:239-248.

51. Alter H, Block T, Brown N, Brownstein A, Brosgart C, Chang KM, Chen PJ, et al. A research agenda for curing chronic hepatitis B virus infection. Hepatology 2018;67:1127-1131.

52. Lupberger J, Zeisel MB, Xiao F, Thumann C, Fofana I, Zona L, Davis C, et al. EGFR and EphA2 are host factors for hepatitis C virus entry and possible targets for antiviral therapy. Nat Med 2011;17:589-595.

53. Zona L, Lupberger J, Sidahmed-Adrar N, Thumann C, Harris HJ, Barnes A, Florentin J, et al. HRas signal transduction promotes hepatitis C virus cell entry by triggering assembly of the host tetraspanin receptor complex. Cell Host Microbe 2013;13:302-313.

54. Zeisel MB, Koutsoudakis G, Schnober EK, Haberstroh A, Blum HE, Cosset FL, Wakita T, et al. Scavenger receptor class B type I is a key host factor for hepatitis C virus infection required for an entry step closely linked to CD81. Hepatology 2007;46:1722-1731.

55. Zahid MN, Turek M, Xiao F, Thi VL, Guerin M, Fofana I, Bachellier P, et al. The postbinding activity of scavenger receptor class B type I mediates initiation of hepatitis C virus infection and viral dissemination. Hepatology 2013;57:492-504.

56. Fofana I, Krieger SE, Grunert F, Glauben S, Xiao F, Fafi-Kremer S, Soulier E, et al. Monoclonal anti-claudin 1 antibodies prevent hepatitis C virus infection of primary human hepatocytes. Gastroenterology 2010;139:953-964, 964 e951-954.

57. Mailly L, Xiao F, Lupberger J, Wilson GK, Aubert P, Duong FH, Calabrese D, et al. Clearance of persistent hepatitis C virus infection in humanized mice using a claudin-1-targeting monoclonal antibody. Nat Biotechnol 2015;33:549-554.

58. Miao Z, Zhang S, Ou X, Li S, Ma Z, Wang W, Peppelenbosch MP, et al. Estimating the global prevalence, disease progression and clinical outcome of hepatitis delta virus infection. J Infect Dis 2019; In press (doi: 10.1093/infdis/jiz633).

59. Chen HY, Shen DT, Ji DZ, Han PC, Zhang WM, Ma JF, Chen WS, et al. Prevalence and burden of hepatitis D virus infection in the global population: a systematic review and meta-analysis. Gut 2019;68:512-521.

60. Baumert TF, Verrier ER, Nassal M, Chung RT, Zeisel MB. Host-targeting agents for treatment of hepatitis B virus infection. Curr Opin Virol 2015;14:41-46.

61. Colpitts CC, Verrier ER, Baumert TF. Targeting viral entry for treatment of hepatitis B and C virus infections. ACS Infect Dis 2015;1:420–427.

62. Thomas D, Zoulim F. New challenges in viral hepatitis. Gut 2012;61 Suppl 1:i1-5.

63. Verrier ER, Yim SA, Heydmann L, El Saghire H, Bach C, Turon-Lagot V, Mailly L, et al. Hepatitis B Virus Evasion From Cyclic Guanosine Monophosphate-Adenosine Monophosphate Synthase Sensing in Human Hepatocytes. Hepatology 2018;68:1695-1709.

64. Winer BY, Shirvani-Dastgerdi E, Bram Y, Sellau J, Low BE, Johnson H, Huang T, et al. Preclinical assessment of antiviral combination therapy in a genetically humanized mouse model for hepatitis delta virus infection. Sci Transl Med 2018;10:eaap9328.

65. Wyde PR, Moore DK, Pimentel DM, Blough HA. Evaluation of the antiviral activity of N-(phosphonoacetyl)-L-aspartate against paramyxoviruses in tissue culture and against respiratory syncytial virus in cotton rats. Antiviral Res 1995;27:59-69.

66. Haussecker D, Cao D, Huang Y, Parameswaran P, Fire AZ, Kay MA. Capped small RNAs and MOV10 in human hepatitis delta virus replication. Nat Struct Mol Biol 2008;15:714-721.

67. Fontaine-Rodriguez EC, Taylor TJ, Olesky M, Knipe DM. Proteomics of herpes simplex virus infected cell protein 27: association with translation initiation factors. Virology 2004;330:487-492.

68. Fontaine-Rodriguez EC, Knipe DM. Herpes simplex virus ICP27 increases translation of a subset of viral late mRNAs. J Virol 2008;82:3538-3545.

69. Mejdrova I, Chalupska D, Kogler M, Sala M, Plackova P, Baumlova A, Hrebabecky H, et al. Highly Selective Phosphatidylinositol 4-Kinase IIIbeta Inhibitors and Structural Insight into Their Mode of Action. J Med Chem 2015;58:3767-3793.

70. Naus P, Caletkova O, Perlikova P, Postova Slavetinska L, Tloustova E, Hodek J, Weber J, et al. Synthesis and biological profiling of 6- or 7-(het)aryl-7-deazapurine 4'-C-methylribonucleosides. Bioorg Med Chem 2015;23:7422-7438.

71. Tichy M, Pohl R, Tloust'ova E, Weber J, Bahador G, Lee YJ, Hocek M. Synthesis and biological activity of benzo-fused 7-deazaadenosine analogues. 5- and 6-substituted 4-amino- or 4-alkylpyrimido[4,5-b]indole ribonucleosides. Bioorg Med Chem 2013;21:5362-5372.

72. Jagtap PR, Ford L, Deister E, Pohl R, Cisarova I, Hodek J, Weber J, et al. Highly functionalized and potent antiviral cyclopentane derivatives formed by a tandem process consisting of organometallic, transition-metal-catalyzed, and radical reaction steps. Chemistry 2014;20:10298-10304.

73. Mejdrova I, Chalupska D, Plackova P, Muller C, Sala M, Klima M, Baumlova A, et al. Rational Design of Novel Highly Potent and Selective Phosphatidylinositol 4-Kinase IIIbeta (PI4KB) Inhibitors as Broad-Spectrum Antiviral Agents and Tools for Chemical Biology. J Med Chem 2017;60:100-118.

74. Schreiner S, Nassal M. A Role for the Host DNA Damage Response in Hepatitis B Virus cccDNA Formation-and Beyond? Viruses 2017;9:E125.

75. Qi Y, Gao Z, Xu G, Peng B, Liu C, Yan H, Yao Q, et al. DNA Polymerase kappa Is a Key Cellular Factor for the Formation of Covalently Closed Circular DNA of Hepatitis B Virus. PLoS Pathog 2016;12:e1005893.

76. Doernbrack K, Verrier E, Heydmann L, Wrensch F, Maglott-Roth A, Brino L, Nassal M, et al. Defining hos DNA repair factors in the formation of the hepatitis B virus covalentrly close circular DNA persistence reservoir. Journal of Hepatology 2018;68:S788-S788.

77. Koniger C, Wingert I, Marsmann M, Rosler C, Beck J, Nassal M. Involvement of the host DNA-repair enzyme TDP2 in formation of the covalently closed circular DNA persistence reservoir of hepatitis B viruses. Proc Natl Acad Sci U S A 2014;111:E4244-4253.

78. Kitamura K, Que L, Shimadu M, Koura M, Ishihara Y, Wakae K, Nakamura T, et al. Flap endonuclease 1 is involved in cccDNA formation in the hepatitis B virus. PLoS Pathog 2018;14:e1007124.

79. Lisowski L, Dane AP, Chu K, Zhang Y, Cunningham SC, Wilson EM, Nygaard S, et al. Selection and evaluation of clinically relevant AAV variants in a xenograft liver model. Nature 2014;506:382-386.

80. Lyabin DN, Eliseeva IA, Ovchinnikov LP. YB-1 protein: functions and regulation. Wiley Interdiscip Rev RNA 2014;5:95-110.

81. Rybicka M, Stalke P, Dreczewski M, Smiatacz T, Bielawski KP. High-throughput matrix-assisted laser desorption ionization-time of flight mass spectrometry as an alternative approach to monitoring drug resistance of hepatitis B virus. J Clin Microbiol 2014;52:9-14.

9.1 Verrier ER et al., Virologie 2013;17:426-441

Virologie 2013, 17 (6) : 426-41

Analyse génétique de la résistance aux *rhabdovirus* chez la truite arc-en-ciel (*Oncorhynchus mykiss*)

Éloi R. Verrier[1,2,3]
Christelle Langevin[1]
Edwige Quillet[2]
Pierre Boudinot[1]

[1] Inra,
UR892,
virologie et immunologie moléculaire,
Domaine de Vilvert,
78350 Jouy-en-Josas,
France
<pierre.boudinot@jouy.inra.fr>
[2] Inra,
UMR1313,
génétique animale et biologie intégrative, Domaine de Vilvert
78350 Jouy-en-Josas,
France
[3] AgroParisTech,
16, rue Claude-Bernard,
75005 Paris
France
<eloi.verrier@unistra.fr>

Résumé. La truite arc-en-ciel (*Oncorhynchus mykiss*) est une espèce d'intérêt aquacole majeur en Europe et notamment en France. Le système immunitaire de cette espèce est également l'un des mieux connus au sein des poissons téléostéens. Différentes maladies virales affectent la truite arc-en-ciel, en particulier deux rhabdoviroses, causées par le virus de la septicémie hémorragique virale (VSHV) et par le virus de la nécrose hématopoïétique infectieuse (VNHI), qui sont à l'origine de pertes importantes dans les élevages. Une variabilité significative de la résistance naturelle à ces infections a été décrite chez la truite arc-en-ciel, entre et au sein des populations. L'étude de cette variabilité génétique est à la fois pertinente pour améliorer les approches de sélection d'individus naturellement résistants à ces virus, et pour progresser dans la dissection des mécanismes sous-jacents. Les méthodes employées, et les premiers résultats de l'analyse des bases génétiques de la résistance de la truite arc-en-ciel à la septicémie hémorragique virale sont présentés ici, de l'identification d'un QTL majeur à l'étude du rôle des interférons.

Mots clés : architecture génétique, truite arc-en-ciel, *rhabdovirus*, résistance aux infections

Abstract. The rainbow trout (*Oncorhynchus mykiss*) is one of most significant model in fish immunology, as well as a key species in European aquaculture. Two well-known *Novirhabdoviruses*, the viral haemorrhagic septicemia virus (VHSV) and the infectious hematopoietic necrosis virus (IHNV) cause serious damage in fish farms and represent a significant threat for aquaculture in a number of countries. A significant variability of resistance to these infections – intra- and inter-populations – has been described in rainbow trout. This genetic variability is not only relevant for the selection of fish naturally resistant to these viruses, but also for the dissection of the mechanisms of fish antiviral immunity. The methods used to analyze the genetic bases of the trout resistance to VHSV, and primary results are reported here from the identification of a major QTL to the impact of type I interferons.

Key words: genetic architechture, rainbow trout, *rhabdovirus*, resistance to infections

Introduction

Chez les animaux domestiques, le développement et l'intensification des systèmes d'élevage ont créé des niches favorables pour les agents pathogènes, dont la propagation est facilitée par le regroupement des animaux dans un espace restreint. La fréquence et la gravité des épisodes infectieux s'en trouvent augmentées. De plus, la circulation des animaux, des gamètes ou des œufs est un facteur important de propagation des maladies à travers le monde. Les maladies infectieuses peuvent causer de sérieux dommages et des pertes économiques importantes dans les élevages. Le coût des pertes dues aux seules infections virales pour

Tirés à part : É. R. Verrier

doi:10.1684/vir.2013.0541

Pour citer cet article : Verrier ÉR, Langevin C, Quillet E, Boudinot P. Analyse génétique de la résistance aux *rhabdovirus* chez la truite arc-en-ciel (*Oncorhynchus mykiss*). *Virologie* 2013; 17(6) : 426-41 doi:10.1684/vir.2013.0541

l'ensemble des filières animales est estimé à 17 % du chiffre d'affaire dans les pays développés [1]. Ces infections ont également un impact sur la sécurité alimentaire des produits et sur le bien-être des animaux. Les stratégies de contrôle des maladies incluent des mesures prophylactiques (pratiques d'élevage, vaccination), réglementaires (contrôles de la circulation des animaux) et/ou curatives (traitements sanitaires et antibiotiques). Ces mesures sont parfois coûteuses à mettre en place et rencontrent des limites, comme l'apparition sur le long terme d'agents pathogènes résistants aux traitements antibiotiques. Les stratégies vaccinales sont encore peu développées en raison de l'importance des coûts de production et de la difficulté technique de mise en place de telles stratégies par les éleveurs. Une méthode alternative consiste à sélectionner des animaux naturellement résistants aux maladies infectieuses. En effet, l'origine génétique des différences de résistance à de nombreux agents infectieux a été démontrée dans les populations d'animaux d'élevage [2]. Cette variabilité génétique a été exploitée avec succès dans des schémas de sélection pour la résistance à divers types d'agents pathogènes, conventionnels (virus, bactéries et parasites) ou non (prions). Les perspectives d'amélioration de la résistance par sélection sont donc prometteuses, d'autant que la montée en puissance des outils génomiques est susceptible de faciliter sa mise en œuvre pour des caractères complexes comme la résistance aux maladies et d'améliorer son efficacité.

Comme les filières animales terrestres, la pisciculture doit faire face à des maladies infectieuses qui affectent toutes les espèces d'élevage, marines ou d'eau douce. Le développement des vaccins a connu de remarquables succès, en particulier contre des maladies bactériennes, conduisant à une réduction spectaculaire de l'utilisation des antibiotiques dans les élevages industriels de saumon en Norvège et en Écosse. En revanche, les vaccins prévenant les maladies virales n'ont souvent donné que des résultats en demi-teinte. Ils sont souvent coûteux et particulièrement difficiles à administrer lorsque la protection associée nécessite l'injection individuelle à de très jeunes animaux. Les vaccins élaborés à partir de virus atténués sont généralement efficaces mais non dénués de risques. Les vaccins à ADN semblent dans ce contexte plus adaptés puisqu'ils sont particulièrement efficaces, notamment chez les salmonidés [3]. Leur utilisation demeure toutefois expérimentale et se heurte à la perception négative des OGM par les consommateurs et les médias. Ainsi, le développement de stratégies de sélection exploitant les résistances naturelles apparaît comme une alternative intéressante pour l'élevage piscicole.

Dans cette perspective, un nombre croissant de travaux vise à caractériser les bases génétiques de la résistance aux agents pathogènes chez les poissons. Au-delà des retombées finalisées (sélection de cheptels plus résistants), ces travaux ont aussi pour objectif de comprendre l'origine de la variabilité individuelle de résistance et d'identifier les mécanismes sous-jacents. La comparaison d'individus ou de groupes de résistance contrastée (sensibles/résistants) facilite souvent les investigations, comme l'illustrent de façon remarquable les avancées obtenues avec les lignées consanguines de souris [4]. L'utilisation de ces lignées a, entre autres, permis la mise en évidence des facteurs de restriction aux rétrovirus murins [5]. Dans les espèces où les outils fonctionnels disponibles pour l'étude des mécanismes immunitaires sont encore peu développés, cette approche permet en outre de développer des analyses sans *a priori* permettant la mise en évidence de mécanismes potentiellement nouveaux propres à l'espèce étudiée (et non pas l'étude par extrapolation de mécanismes décrits chez les espèces les plus étudiées).

Après un bref rappel des méthodes de description de la variabilité génétique de la résistance aux maladies, nous illustrerons cette démarche en présentant les avancées récentes obtenues dans la description des mécanismes de résistance virale chez un poisson téléostéen, la truite arc-en-ciel (*Oncorhynchus mykiss*). Notre modèle d'étude est la septicémie hémorragique virale, une des principales maladies de cette espèce.

Méthodes de description des bases génétiques de la résistance aux maladies chez les poissons téléostéens

Mise en évidence de la variabilité génétique de la résistance aux maladies chez les poissons

Comme dans les autres espèces d'élevage, la variabilité génétique de la résistance aux maladies chez les poissons a d'abord été décrite grâce aux méthodes classiques de la génétique quantitative. Ces méthodes incluent la comparaison de performances entre des populations ou des souches d'histoire ou d'origine géographique différentes, la comparaison de groupes d'individus apparentés issus d'une même population, et la mesure des réponses obtenues après des sélections expérimentales [6].

Les premiers travaux ont souvent cherché à démontrer l'existence d'un contrôle génétique de la résistance par comparaison des performances de populations distinctes. Parfois fructueuse, cette approche est néanmoins compliquée chez les poissons par l'absence assez générale d'information sur la différenciation génétique entre les groupes testés (la notion de souches ou populations est souvent incertaine) et par le fait que les performances sont, au moins au départ, évaluées dans des environnements

différents. Une phase de comparaison dans un même milieu, voire de croisement entre origines, est donc indispensable pour valider les conclusions. Une autre approche consiste à tester l'efficacité d'une sélection pour la résistance au sein d'une population donnée. Parmi les exemples documentés, on peut citer la production d'une lignée de truite arc-en-ciel résistante au virus de la nécrose pancréatique infectieuse (VNPI) par sélection des poissons rescapés de l'infection par le virus, avec une mortalité dans la lignée sélectionnée d'environ 5 % contre quasiment 100 % dans la population de référence [7]. De même, chez la carpe commune (*Cyprinus carpio*), une réponse à la sélection pour la résistance à l'hydropisie infectieuse (en partie due au *Rhabdovirus carpio*) est observée après neuf générations de sélection individuelle [8].

Un paramètre central pour quantifier la part des facteurs génétiques dans la variabilité d'un caractère et déterminer les possibilités d'amélioration de ce caractère par sélection est l'héritabilité. L'héritabilité indique en effet dans quelle mesure les performances pour ce caractère sont transmissibles d'une génération à l'autre. Elle peut être estimée à partir du progrès obtenu à l'issue de la sélection pour le caractère d'intérêt (voir ci-dessus). On parle alors d'héritabilité « réalisée ». Plusieurs générations de sélection sont en général nécessaires pour estimer l'héritabilité réalisée et une méthode plus rapide consiste à comparer la performance d'individus apparentés (parents/enfants, familles de frères-sœurs). Néanmoins, pour obtenir des estimations fiables de l'héritabilité par cette méthode, il est nécessaire de travailler avec un nombre élevé de familles, ce qui a longtemps été un frein au développement de ces travaux chez les poissons, malgré l'importance des problèmes de santé dans les élevages. En effet, la très petite taille des juvéniles (de l'ordre du centimètre pour un alevin de truite ou de saumon, du millimètre pour de nombreuses espèces marines) ne permet pas un marquage précoce des individus, indispensable pour tracer les généalogies, ce qui impose un élevage séparé des familles, nécessairement coûteux en installations. Cela a longtemps constitué un obstacle aux analyses génétiques chez les poissons et n'a été résolu que récemment, grâce au développement des empreintes génétiques. De plus, la résistance aux maladies est un caractère difficile à mesurer. Un bon modèle infectieux suppose une connaissance suffisamment approfondie de l'agent pathogène pour permettre une bonne répétabilité des infections expérimentales. Par ailleurs, les risques pour l'environnement imposent de pratiquer les épreuves infectieuses dans des installations confinées coûteuses. Enfin, il est difficile de sélectionner des reproducteurs sur leurs performances de résistance propre à cause des risques de mortalité et de transmission verticale de l'agent pathogène, ce qui alourdit le processus de sélection (la valeur génétique des reproducteurs doit être évaluée indirectement, à partir des performances de leurs apparentés, frères-sœurs ou descendants le plus souvent).

Des valeurs modérées à fortes (> 0,4) de l'héritabilité de la résistance ont été rapportées dans de nombreuses espèces de poissons après infection par différents pathogènes, dont des virus, des bactéries, des parasites et des champignons [9] (*tableau 1* pour les virus). Il existe donc chez les poissons, comme chez les espèces terrestres, une importante variabilité génétique de la résistance aux agents pathogènes. L'étape suivante consiste à préciser l'architecture de la variabilité génétique ainsi mise en évidence, l'étape ultime étant l'identification des gènes et des mutations responsables de la sensibilité/résistance.

L'apport des marqueurs moléculaires pour disséquer la variabilité génétique

Les avancées technologiques en biologie moléculaire ont permis le développement et l'utilisation facile de marqueurs

Tableau 1 Héritabilité de la résistance aux viroses chez les poissons.

Virus	Hôte	Phénotype	h^2	Références
VSHV	Truite arc-en-ciel	Survie	0,63	[10]
VSHV	Truite arc-en-ciel	Survie, DS[a]	0,57 ; 0,21	[11]
VNHI	Truite arc-en-ciel	Survie	0,05-0,51	[12]
VNHI	Saumon sockeye	Survie	0,27-0,38	[13]
VNPI	Saumon atlantique	Survie	0,15-0,5	[14]
VNPI	Morue de l'Atlantique	Survie	0,43-0,75	[15]
ISAV	Saumon atlantique	Survie	0,13	[16]
VMPS	Saumon atlantique	Survie	0,21	[17]
KHV	Carpe commune	Survie à 50 %[b]	0,79	[18]

Morue de l'Atlantique : *Gadus morhua L.* Saumon sockeye : *Oncorhynchus nerka.* VSHV : virus de la septicémie hémorragique virale ; VNHI : virus de nécrose hématopoïétique infectieuse ; VNPI : virus de la nécrose pancréatique infectieuse ; VMPS : virus de la maladie pancréatique du saumon ; KHV : *koi herpes virus.*

[a] DS : durée de survie après infection.

[b] Survie (oui/non) du poisson lorsque la mortalité du lot atteint 50 %.

génétiques. Les plus couramment utilisés sont les microsatellites et les *single nucleotide polymorphisms* (SNP). Le polymorphisme à ces marqueurs peut être utilisé pour détecter des variations génomiques à l'origine des variations de performance individuelle pour les caractères d'intérêt.

La détection de QTL

Il est possible de tester l'effet des différentes régions du génome sur la variabilité d'un caractère *via* l'utilisation de ces marqueurs moléculaires, qui sont utilisés comme des balises permettant de localiser la zone du génome étudiée. L'association entre les allèles aux marqueurs et la variabilité d'un caractère quantitatif définit une région du génome à l'intérieur de laquelle se trouvent un (ou plusieurs) facteur(s) responsable(s) de la variation phénotypique observée. Ces zones, appelées *Quantitative Trait Locus/loci* (QTL), sont de taille variable et contiennent un ou plusieurs gènes, responsables de la variation du caractère d'intérêt. Le principe de la détection de QTL est présenté sur la *figure 1*. On voit notamment que cette approche nécessite de travailler avec des structures familiales connues.

Peu d'études de détection de QTL de résistance aux virus existent chez les poissons, mais leur nombre est en augmentation rapide. Chez la truite arc-en-ciel, des QTL pour la résistance au virus de la nécrose hématopoïétique infectieuse (VNHI) et au VNPI ont par exemple été identifiés [19, 20]. Chez le cardeau hirame (*Paralichtys olivaceus*), un locus majeur responsable de 50 % de la survie des poissons après infection par un iridovirus a été détecté [21]. Chez le saumon atlantique (*Salmo salar*), enfin, un QTL majeur de résistance au VNPI a été identifié indépendamment par deux équipes (norvégienne et écossaise), à partir de populations commerciales. Ce QTL contrôle la résistance à la maladie en eau douce comme en eau de mer et explique jusqu'à 83 % de la variance génétique observée [22, 23]. Ce résultat suggère fortement l'existence d'un gène (ou d'un cluster de gènes) majeur responsable d'une large part de la variation de résistance au virus. Si les recherches s'intensifient dans ce sens, le gène responsable et la mutation causale ne sont pas encore identifiés.

Lorsque le nombre de marqueurs devient très important, il est possible de travailler directement à l'échelle des populations, sans passer par l'utilisation de généalogies (on parle d'études d'association). L'étude consiste alors à rechercher les marqueurs pour lesquels il existe un déséquilibre de liaison, à savoir une association préférentielle, entre un allèle au marqueur et le niveau de performance pour le caractère d'intérêt. Dans le cas de la résistance à l'IPNV chez le saumon atlantique par exemple, un marqueur présentant un allèle systématiquement associé à la résistance dans la population a ainsi été identifié. La détection de QTL constitue une première étape dans l'identification du/des gène(s) et la/les mutation(s) responsable(s) d'un phénotype, en confinant la zone du génome à explorer.

L'approche « gène candidat »

Si l'on connaît parfaitement la cascade de mécanismes moléculaires qui régissent le caractère étudié, on peut directement chercher à identifier parmi les gènes sous-tendant ces mécanismes ceux qui sont susceptibles d'avoir un impact sur les variations de performance. Cette approche dite « gène candidat » consiste alors à chercher du polymorphisme au sein de ces gènes, de leurs promoteurs ou de leurs régions régulatrices et à l'associer aux variations de valeurs phénotypiques observées (polymorphisme causal). Par exemple, des variations dans la séquence du gène *Mx*, impliqué dans la réponse interféron, ont été corrélées à des niveaux de résistance différents à l'infection par le VNHI chez la truite arc-en-ciel [24]. De même, les résistances au virus de l'anémie infectieuse du saumon (*Infectious Salmon Anemia Virus* [ISAV]) et au VNHI sont en partie liées au polymorphisme de certains gènes du complexe majeur d'histocompatibilité, indiquant un rôle de l'immunité spécifique dans la sensibilité à ces infections [25, 26].

L'ensemble de ces travaux démontre sans équivoque l'existence de bases génétiques contrôlant la résistance aux agents infectieux. L'analyse de la variabilité génétique de la résistance aux maladies et de ses composantes chez les poissons est un domaine en plein essor. Motivées par l'importance économique de certaines espèces de poissons d'élevage et le coût associé aux épisodes infectieux, les recherches sur les facteurs génétiques responsables de ces variations sont en forte progression depuis quelques années. La cartographie de QTL constitue un premier pas vers l'identification de la (des) mutation(s) causale(s) induisant des variations de résistance. En focalisant la recherche de gènes candidats à la zone du (ou des) QTL, ce type de démarche facilite le repérage des gènes clés de la résistance et permet de progresser dans la compréhension des mécanismes de la réponse antivirale du modèle, et des vertébrés en général.

La truite arc-en-ciel et le virus de la septicémie hémorragique virale (VSHV) : un modèle pour l'étude des bases génétiques de la résistance aux virus chez les poissons

La truite arc-en-ciel est un poisson d'aquaculture d'importance mondiale. Avec près de 34 000 tonnes produites chaque année, la France est le quatrième producteur

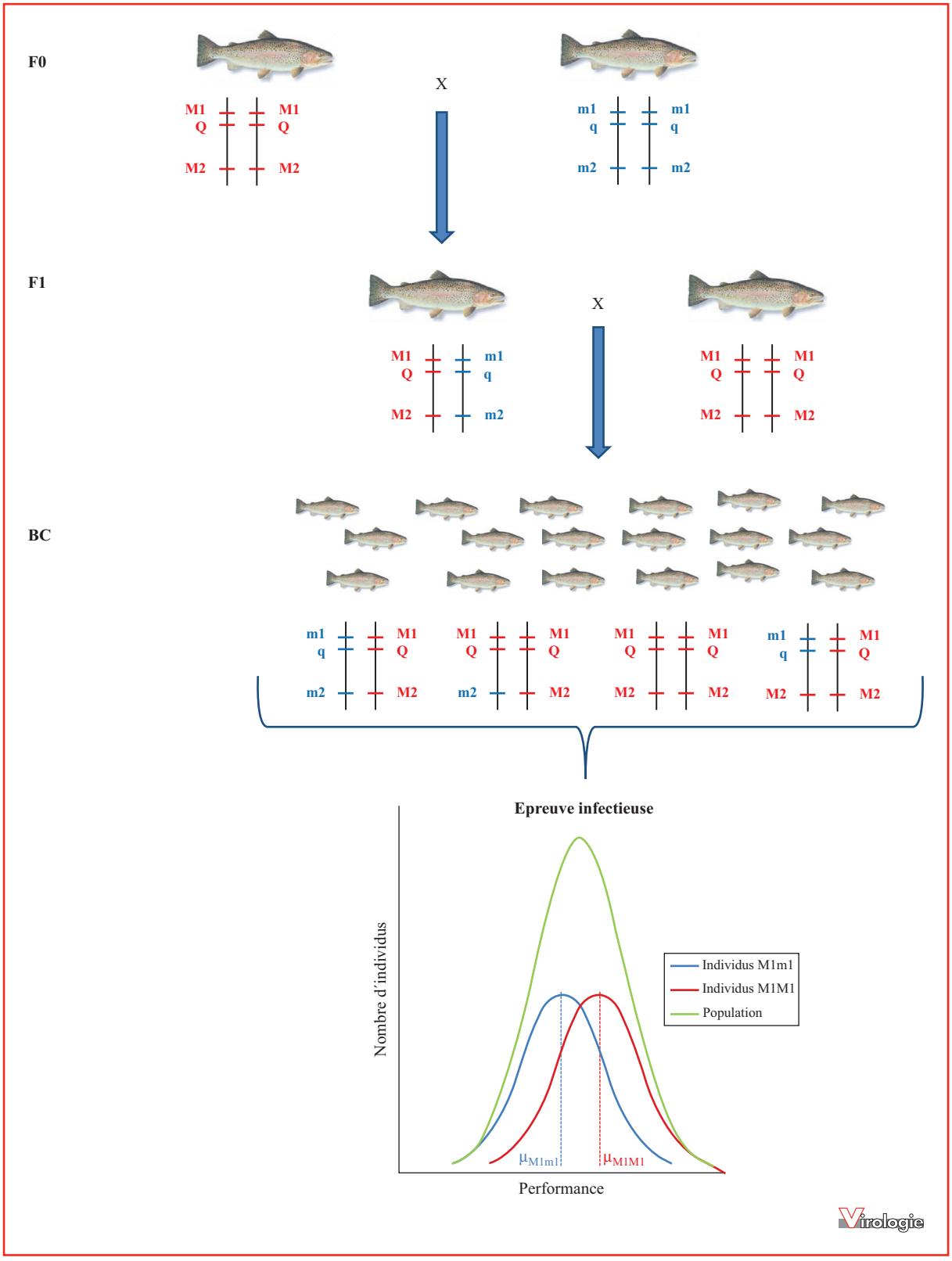

Figure 1.

mondial. Le fort développement de la filière s'accompagne d'une évolution des contraintes, avec notamment un plus grand risque d'épizooties pouvant sévir dans les élevages. Ainsi, le VSHV cause l'une des plus sérieuses maladies pouvant affecter les élevages de truites arc-en-ciel en Europe [27]. L'importance des conséquences économiques associées a motivé l'accumulation de connaissances sur ce virus et fait du couple truite arc-en-ciel/VSHV un bon modèle pour l'étude des interactions hôte-pathogène.

La truite arc-en-ciel, un modèle d'étude de l'immunité des poissons téléostéens

Une espèce de poisson téléostéen plutôt bien étudiée

Parmi les différentes espèces de poissons largement étudiées (poisson zèbre, fugu, Tétraodon, épinoche…), la truite arc-en-ciel est l'une de celles dont le système immunitaire et la réponse immunitaire face aux infections virales sont les mieux caractérisés, en partie en raison de son importance en aquaculture et en pêche sportive [28], mais pas uniquement. En effet, même si elle est plus coûteuse à maintenir dans une structure expérimentale que d'autres espèces de poissons, elle est relativement simple à élever. Sa reproduction est de plus bien maîtrisée [29], et sa taille relativement importante a beaucoup facilité certaines explorations. Enfin, les populations naturelles de truite arc-en-ciel ont également été largement étudiées, faisant de cette espèce un bon sujet d'étude pour certaines questions d'évolution, en particulier celles relatives à la domestication [30]. De plus, les agents viraux responsables des infections de cette espèce ont été très bien caractérisés (VSHV, VNHI et VNPI notamment).

Des outils génomiques en expansion

Malgré ces différents atouts, la truite arc-en-ciel ne figure pas encore dans la liste des espèces de poissons pour lesquelles une séquence génomique de référence est disponible. La principale raison à cela est l'existence d'un épisode supplémentaire de duplication complète du génome (4R), survenu chez l'ancêtre des salmonidés après la duplication 3R commune à tous les poissons téléostéens [31, 32]. Le génome des salmonidés est donc nettement plus grand que celui de la plupart des espèces de poissons modèles (environ 2 400 Mb). Il est, en outre, très riche en séquences répétées dispersées (environ 50 %), et, l'épisode de duplication 4R [33, 34] étant relativement récent à l'échelle évolutive, 25 à 50 % des locus possèdent encore un locus paralogue dont la séquence d'ADN est encore très conservée. Cette grande ressemblance entre des régions situées sur des chromosomes différents complique considérablement l'assemblage de ces génomes [35-37]. Deux projets exploitant les *Next Generation Sequencing* (NGS) [38, 39] sont en cours et devraient fournir très prochainement une première séquence génomique complète pour cette espèce. Une première version de la séquence d'un des projets a d'ailleurs été mise en ligne très récemment (voir http://www.animalgenome.org/repository/aquaculture/).

De nombreuses ressources génomiques sont cependant disponibles : on compte en particulier de nombreuses banques de *Bacterial Artificial Chromosome* (BAC) qui ont permis la construction d'une carte physique (basée sur les distances absolues en paires de base entre les marqueurs), ainsi qu'une base de données d'environ 200 000 séquences d'extrémités de BACs (ou *BAC end sequences* [BES]) [36, 37], un grand nombre d'*Expressed Sequenced Tag* (EST ou étiquette de séquence exprimée) et plusieurs transcriptomes de référence [40-42]. Une carte génétique (ensemble de marqueurs ordonnés sur le génome) synthétique reprenant les données de trois cartes génétiques établies indépendamment est aussi disponible [34], ainsi que des SNPs en nombre croissant [43, 44].

Des ressources génétiques originales

La fécondation externe et la grande plasticité biologique des poissons permettent, par ailleurs, de contrôler les évènements entourant la fin de la méiose et la fécondation. En modifiant la composition chromosomique des individus, il est possible d'obtenir des groupes de structure

Figure 1. *Suite*

Principe de la détection de QTL. Des parents (F0) de performance connue (par exemple sensible/résistant à un agent pathogène donné) sont croisés pour obtenir la génération F1. Les reproducteurs utilisés peuvent être issus de lignées sélectionnées, ou de lignées isogéniques caractérisées. Le génotype des F0 est connu aux marqueurs M1 et M2. Chaque parent est supposé homozygote aux marqueurs, et porte des allèles différents (M, m). Un individu F1 est à son tour croisé avec un des parents F0 pour donner la génération BC (croisement en retour ou *back-cross*), ce qui permet la ségrégation des allèles issus des parents F0 lors de la méïose du parent F1. Les descendants F2 sont ensuite mesurés pour le caractère et génotypés aux différents marqueurs. Pour chaque marqueur, on compare la performance moyenne des individus porteurs de l'un ou l'autre allèle (M1 contre m1, M2 contre m2). Dans cet exemple, il existe à proximité du marqueur M1 un QTL pour le caractère mesuré (deux allèles au QTL : Q/q, Q est l'allèle dominant et améliore la performance). Les descendants porteurs de l'allèle M1 au marqueur M1 auront donc une probabilité élevée d'être également porteurs de l'allèle Q au QTL, et donc, auront une résistance moyenne supérieure à celle des descendants porteurs de l'allèle m1. Pour un QTL d'effet donné, plus le marqueur est proche du QTL (fort déséquilibre de liaison), plus l'association allèle au marqueur/performance est forte, et plus la probabilité de détection du QTL est élevée. La cartographie de QTL doit donc être réalisée avec un nombre élevé de marqueurs (quelques centaines à quelques milliers), distribués de façon homogène sur l'ensemble du génome.

génétique tout à fait originale (polyploïdes, descendances uniparentales gynogénétiques ou uniparentales androgénétiques). Les lignées isogéniques haploïdes doublés obtenues par gynogenèse constituent notamment un matériel particulièrement intéressant pour la dissection génétique des caractères. La gynogenèse est une forme particulière de parthénogenèse, c'est-à-dire de développement d'un zygote pluriploïde à partir d'un gamète femelle non fécondé. Dans le cas de la gynogenèse, le développement de l'œuf est stimulé par la présence de sperme, sans contribution génétique du pronucléus mâle. Certains poissons comme le carassin *Carassius auratus gibelio* se reproduisent naturellement par gynogenèse dans certaines conditions [45]. La maîtrise de la fécondation *in vitro* a permis d'induire expérimentalement la gynogenèse dans différentes espèces de poisson, dont la truite arc-en-ciel. Dans ce cas, le matériel génétique des spermatozoïdes est inactivé par rayons ionisants (rayons gamma, ou le plus souvent rayons UV [46]) et l'état diploïde, indispensable à la survie de l'embryon, est restauré par application de chocs thermiques ou hyperbares peu après l'activation de l'ovule. Deux types de gynogenèse différents peuvent être induits, en fonction du processus utilisé pour restaurer l'état diploïde de l'embryon (*figure 2*), les produits obtenus présentant des caractéristiques génétiques différentes. L'utilisation combinée des deux types de gynogenèse a permis la production de lignées gynogénétiques isogéniques homozygotes (ce qui est assez rare chez les vertébrés) chez différentes espèces de poissons [47-49] (dont la truite arc-en-ciel) ; de telles lignées sont très pertinentes pour l'étude des caractères quantitatifs complexes, en particulier pour la résistance aux maladies et la caractérisation des réponses associées à des haplotypes particuliers.

Les lignées isogéniques sont constituées de poissons tous homozygotes à l'ensemble des locus et tous génétiquement identiques au sein d'une lignée. Ces lignées isogéniques sont en quelque sorte un équivalent génétique (obtenu en seulement deux générations) des lignées consanguines de souris. L'homozygotie des individus à tous les locus favorise l'expression de phénotypes plus contrastés que dans une population classique et permet en particulier d'augmenter la fréquence (et donc l'identification) d'individus porteurs d'allèles récessifs rares à des locus importants. Un autre avantage très important est la constance du matériel animal d'une génération à l'autre, ce qui facilite énormément la comparaison rigoureuse d'études non simultanées et permet d'accumuler les informations sur un même fond génétique. En outre, les individus étant homozygotes à tous les locus, l'analyse de leur polymorphisme permet de faire la différence entre variants alléliques d'un même locus et locus dupliqués (paralogues ou familles de gènes). Cette distinction est particulièrement intéressante dans le cas de la truite arc-en-ciel, dont le génome est issu d'une duplication ancestrale spécifique aux salmonidés, comme nous l'avons indiqué ci-dessus. Enfin, les individus d'une même lignée sont histocompatibles, ce qui est un avantage critique dans l'étude des réponses immunitaires [50, 51]. Les lignées isogéniques sont néanmoins difficiles à produire et à entretenir et ne sont de ce fait disponibles que dans un petit nombre d'espèces. En ce qui concerne la truite, elles n'ont été produites que par quelques laboratoires (un au Japon, un aux États-Unis et un en France).

Le virus de la SHV, un rhabdovirus pathogène chez la truite arc-en-ciel

L'importance économique de certains virus, capables de causer de sérieux dommages dans les élevages piscicoles, a conduit à leur étude approfondie. Le virus de la septicémie hémorragique virale (VSHV) constitue un des modèles viraux les mieux connus chez cette espèce.

Le virus de la SHV appartient à l'ordre des *Mononegavirales*, à la famille des *Rhabdoviridae* et au genre des *Novirhabdovirus*. Cette famille comprend environ 160 espèces de virus réparties en six genres (*Vesiculovirus*, *Lyssavirus*, *Éphémérovirus*, *Novirhabdovirus*, *Cytorhabdovirus*, et *Nucléorhabdovirus*) ayant une large diversité d'hôtes parmi les plantes et les animaux – dont les poissons téléostéens – et possédant des caractéristiques morphologiques et génétiques relativement proches [52]. Le génome viral est constitué d'un ARN simple brin anti-sens de 12 kb [53] codant pour cinq protéines structurales : une nucléoprotéine (N), une phosphoprotéine (P), une protéine de matrice (M), une glycoprotéine (G) et une polymérase (L pour « large ») et une protéine non structurale, la protéine NV impliquée dans la pathogénicité de ces virus chez la truite arc-en-ciel [54-58]. Le génome viral associé à la polymérase L et à son cofacteur la phosphoprotéine P constitue la nucléocapside. La protéine de matrice M est localisée à l'interface entre la nucléocapside et la surface du virus composée de trimères de protéine G. Cette glycoprotéine, unique protéine virale exprimée à la surface du virus est responsable du tropisme viral par la reconnaissance d'un récepteur spécifique à la surface des cellules cible et constitue l'antigène majeur contre lequel sont dirigés les anticorps neutralisants. Le cycle du VSHV est détaillé sur la *figure 3*. Ce virus compte parmi les trois *rhabdovirus* à déclaration obligatoire infectant les poissons (avec le virus de la virémie printanière de la carpe et le VNHI, autre *novirhabdovirus* majeur infectant les truites arc-en-ciel) listés par l'Office international des épizooties (OIE) [59].

Le VSHV est l'agent causal de la septicémie hémorragique virale. Identifiée dès le début du xx^{e} siècle, la maladie a longtemps été considérée comme une maladie spécifique des truites arc-en-ciel en Europe, jusqu'à ce que le virus soit détecté sur un saumon à la fin des années 1980.

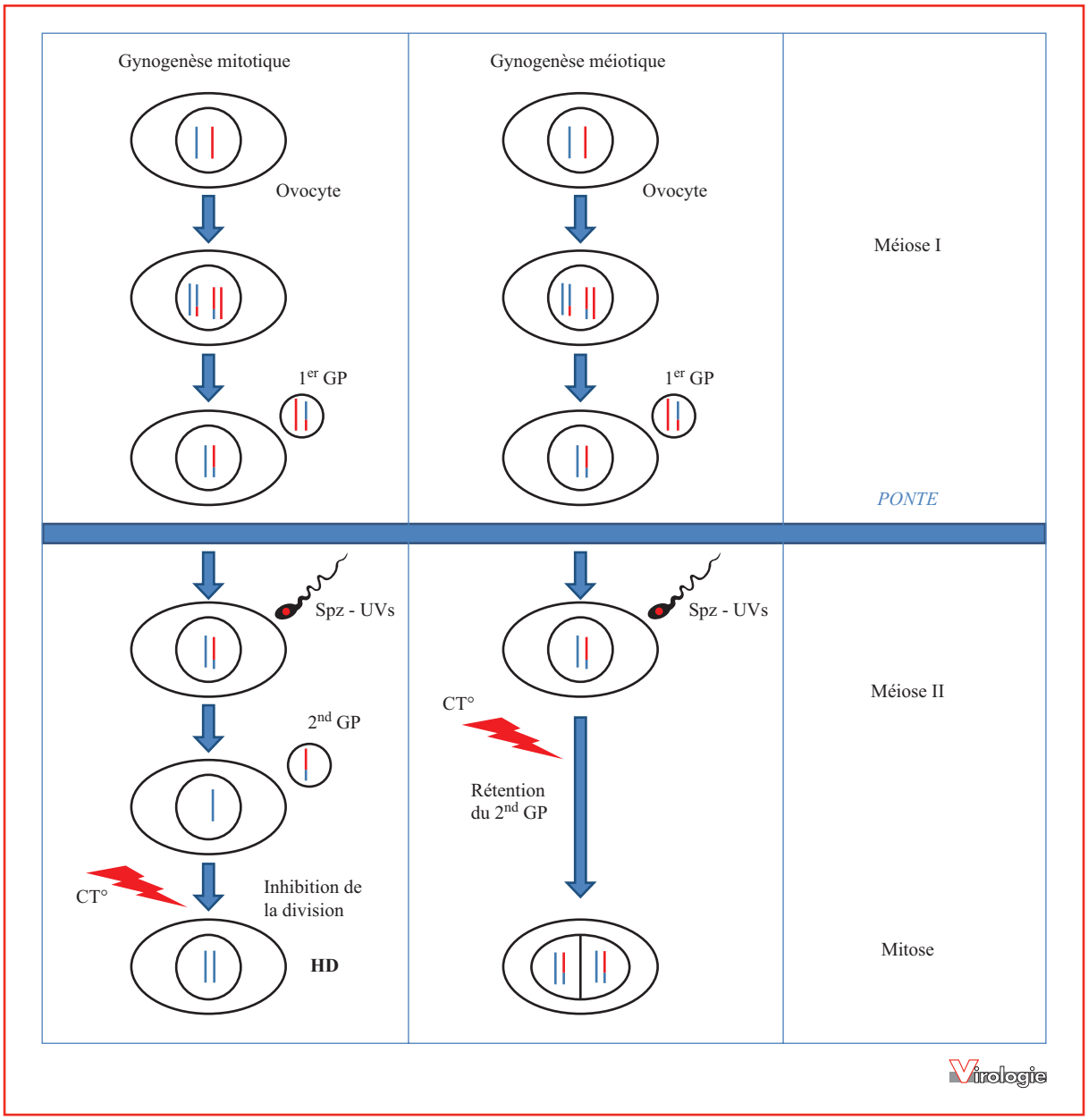

Figure 2. Les deux types de gynogenèse induite chez la truite. Le spermatozoïde est irradié aux UV (Spz-UV) afin d'inactiver le matériel génétique du pronucléus mâle. En l'absence de traitement complémentaire, on obtient un individu gynogénétique haploïde inviable. L'état diploïde viable peut ensuite être restauré de deux manières. Dans le cas de la gynogenèse mitotique, un choc thermique ou hyperbare est appliqué pour inhiber la première division cellulaire du zygote. On obtient un zygote haploïde doublé (HD), entièrement homozygote. Dans le cas de la gynogenèse méiotique, le traitement de diploïdisation bloque la deuxième division de méiose et induit la rétention du second globule polaire (2nd GP). Le zygote obtenu reste hétérozygote à certains locus, en fonction des recombinaisons survenues pendant la méiose de la femelle. On peut également obtenir des haploïdes doublés androgénétiques en irradiant l'ovule, puis en bloquant la première division embryonnaire. Pour obtenir des lignées isogéniques homozygotes à partir d'une population standard, deux générations de gynogenèse sont nécessaires. Une première génération de gynogenèse mitotique permet l'obtention d'individus HD. À la génération suivante, la reproduction par gynogenèse méiotique de chaque femelle HD permet d'obtenir des descendants génétiquement identiques entre eux, et identiques à la femelle HD. La descendance de chaque femelle HD constitue une lignée isogénique, contenant uniquement des individus femelles, compte tenu du mode de déterminisme du sexe chez la truite (XX-XY). Pour entretenir les lignées, le sexe de certains individus est inversé par traitement hormonal précoce. Les néomâles XX (femelle génétique de phénotype mâle) ainsi obtenus permettent de reproduire les lignées à l'identique à chaque génération par croisement intra-lignée (à l'exception des réarrangements chromosomiques ou des mutations).

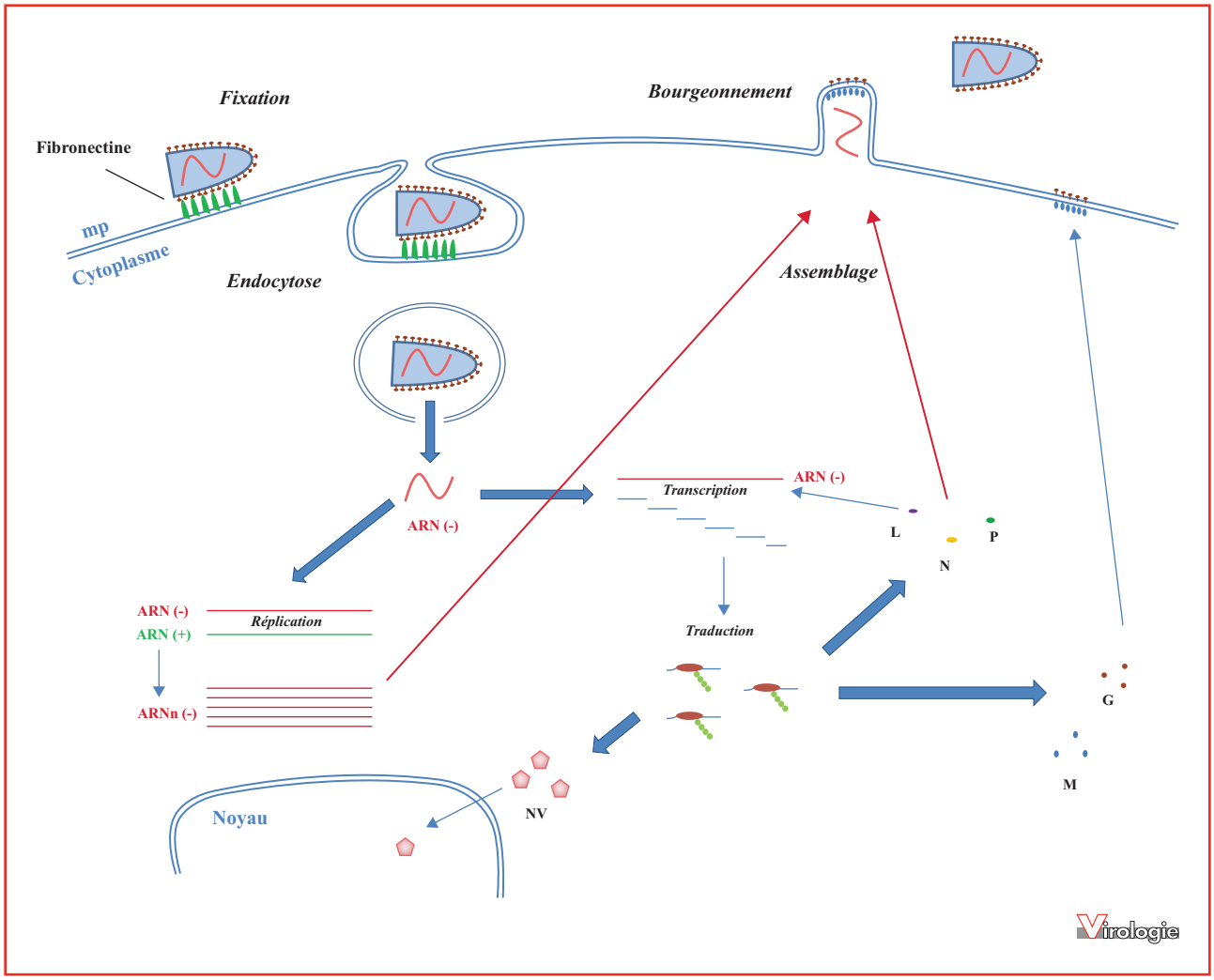

Figure 3. Cycle du VSHV : le cycle d'infection du VSHV fait intervenir les cinq protéines structurales : la fixation de la glycoprotéine G avec un récepteur membranaire (fibronectine) de la cellule cible entraîne l'entrée du virus par endocytose. Les membranes du virus et de l'endosome fusionnent, et la nucléocapside virale est libérée dans le cytoplasme de la cellule. Les gènes viraux sont alors transcrits à l'aide de la polymérase et les protéines sont traduites à l'aide de la machinerie de la cellule hôte. De nouveaux génomes complets viraux sont synthétisés à partir d'un ARN viral brin +. Les protéines L, N et P sont synthétisées à l'aide de ribosomes libres de la cellule situés dans le cytoplasme. Elles se lient à de nouvelles copies d'ARN antisens pour former la ribonucléoprotéine (RNP), qui s'associe à la protéine M pour former le complexe RNP-M. La glycoprotéine G, après avoir été glycosylée dans l'appareil de Golgi, est adressée au niveau de la membrane plasmique de la cellule hôte. Le complexe RNP-M migre vers les régions membranaires enrichies en protéines G virales pour former un nouveau *rhabdovirus* complètement enveloppé qui bourgeonne à la surface de la cellule hôte. La protéine NV d'un autre novirhabdovirus (VNHI) possède une séquence d'adressage au noyau responsable d'une localisation nucléocytoplasmique dans un contexte de surexpression.

L'origine de cette souche n'était pas européenne, mais nord-américaine [60, 61]. Cette maladie affecte en réalité de nombreuses espèces de poissons, marines ou d'eau douce, dont différents salmonidés, des clupéidés (comme le hareng d'Atlantique *Clupea harengus*) et des pleuronectidés [59], en Europe et ailleurs. Quatre génotypes majeurs (de I à IV) (et de nombreuses souches par génotype) ont été décrits à ce jour, correspondant à des zones géographiques distinctes (respectivement : eaux douces et mers d'Europe, mer Baltique, océan Atlantique nord, Amérique du nord/Japon/Corée) [62, 63]. Trois formes d'infection au virus de la SHV ont été décrites : la forme aiguë provoque chez les poissons de sérieuses lésions de type hémorragique, avec des épanchements sanguins sous l'épiderme, des saignements ponctuels dans les muscles, le tissu adipeux et la cavité ventrale, des branchies pâles, une coloration plus

foncée et une exophtalmie. Elle peut conduire à d'importantes pertes dans les élevages : la mortalité varie généralement de 30 à 70 % chez les adultes, et peut atteindre 100 % chez les alevins [64]. La forme chronique entraîne moins de mortalité et des signes cliniques moins marqués [65]. Enfin, une forme nerveuse a été rapportée, avec peu de mortalité et des symptômes plutôt moins marqués [66]. La diversité des souches virales, des hôtes et des interactions hôtes-pathogènes rend difficile la mise en place de programmes types de contrôle sanitaire de cette maladie. L'absence de traitement disponible contre ce virus rend le vide sanitaire indispensable pour éradiquer localement la maladie. Les programmes de destruction de cheptels après détection de la maladie se sont révélés efficaces au Royaume-Uni, en Norvège et au Danemark [59]. Aujourd'hui, la prophylaxie sanitaire couplée à une police sanitaire de contrôle de la circulation des gamètes et des animaux reste le seul moyen de prévenir efficacement les infections virales. En France, le fonctionnement d'une pisciculture est soumis à un agrément sanitaire d'élevage, et aujourd'hui, tout le territoire français est considéré indemne de SHV [67]. Cependant, obtenir des poissons résistants à ce virus demeure un enjeu significatif pour différentes raisons. En effet, le risque de réémergence est réel, les côtes françaises ne peuvent évidemment pas être considérées comme indemnes puisque différentes espèces marines sont sensibles au virus, et la France exporte des œufs/alevins vers des pays qui ne sont pas indemnes.

Variabilité génétique de la résistance à la SHV chez la truite arc-en-ciel

L'existence d'une variabilité génétique de la résistance aux infections pas le VSHV chez les salmonidés est connue depuis plusieurs décennies. Différentes souches de VSHV induisent, par ailleurs, des signes cliniques de sévérité variable en fonction des espèces de salmonidés. Ainsi, certains sérotypes très virulents chez la truite arc-en-ciel ne provoquent pas d'infection chez deux espèces voisines, le saumon coho (*Oncorhynchus kisutch*) et l'omble de fontaine (*Salvelinus fontinalis*). Le croisement entre la truite et ces deux espèces ne produit que quelques descendants hybrides viables, qui conservent la résistance du parent mâle saumon coho ou omble de fontaine après infection par les souches de VSHV virulentes chez la truite arc-en-ciel [10, 68-70].

Au sein de l'espèce truite arc-en-ciel, la variabilité génétique de la résistance a pu être mise en évidence par sélection expérimentale, certaines femelles résistantes au VSHV transmettant la résistance à leurs descendants gynogénétiques [10]. Des héritabilités modérées à élevées (supérieures à 0,5) ont également été mesurées [10, 11]. Enfin, la comparaison de lignées isogéniques précédemment décrites montre clairement l'importance du génotype de l'hôte dans l'issue de l'infection au virus, avec des mortalités après infection expérimentale variant de 100 % à moins de 5 % selon la lignée [48]. Récemment, une recherche de QTL de résistance a permis d'obtenir une première description de l'architecture génétique de la réponse au virus [71]. Au total, sept régions génomiques gouvernant la survie des juvéniles après une infection par bain ont été découvertes. De façon remarquable, une de ces régions joue un rôle majeur dans la résistance puisqu'elle explique jusqu'à 65 % de la variance phénotypique observée. Les autres QTL identifiés expliquent une part beaucoup plus réduite de la variation de résistance et ne sont en général retrouvés que dans l'une des deux familles analysées en détail dans cette étude. En revanche, le principal QTL a été retrouvé dans plusieurs autres familles testées en parallèle, ce qui confirme l'importance de cette région du génome dans la variation de résistance au sein de la population étudiée. De plus, ce QTL contrôle à la fois la survie des poissons après infection par balnéation et la croissance virale *in vitro* sur explant de nageoire, confirmant au niveau du génome les premières observations qui montraient une corrélation entre le test de multiplication virale *in vitro* et la survie [72]. Ce résultat important suggère que les mécanismes majeurs de résistance au VSHV sont de nature non adaptative.

Ce résultat représente une première étape vers l'identification des mécanismes responsables des différences inter individuelles de résistance au virus de la SHV. Il indique clairement le rôle majeur des mécanismes innés de la réponse antivirale dans la résistance à l'infection par le VSHV, ce qui a motivé l'exploration approfondie de ces mécanismes chez la truite arc-en-ciel.

Confirmation fonctionnelle de l'importance des mécanismes innés dans la résistance au VSHV chez la truite arc-en-ciel

Parallélisme entre résistance des poissons et résistance cellulaire dans le cas du VHSV.

Une première étude parue en 2007 a révélé une grande diversité de résistance des lignées isogéniques à l'infection par le virus de la SHV [48]. Des lignées cellulaires (fibroblastiques) ont été dérivées à partir d'ovaires de truites issues de ces mêmes lignées isogéniques (*figure 4*). La caractérisation de ces lignées cellulaires a montré une très bonne corrélation entre la résistance cellulaire et la résistance des poissons desquels la lignée est issue. Cette corrélation est observable très rapidement après l'infection (nombre de

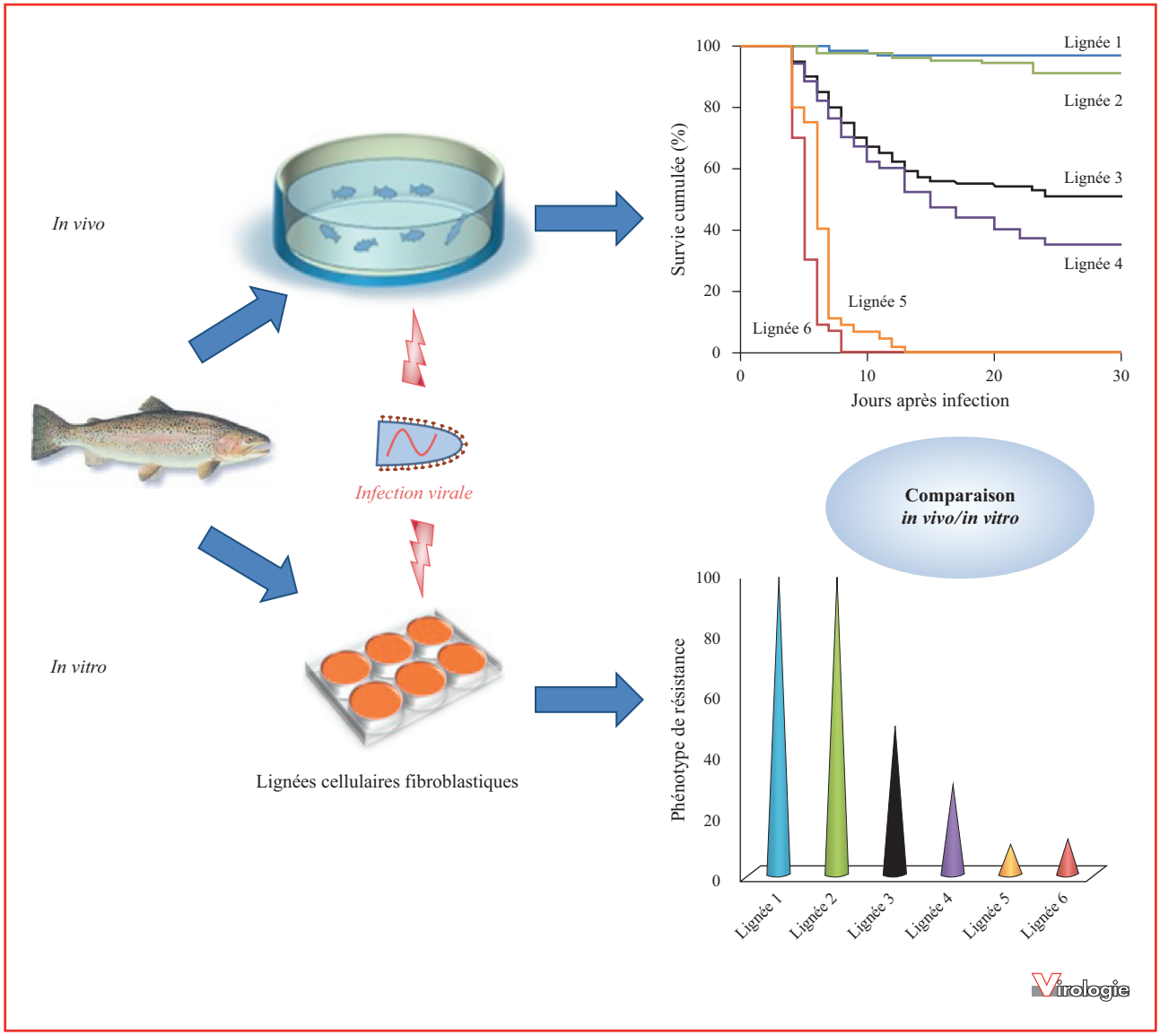

Figure 4. Utilisation des lignées isogéniques de truite arc-en-ciel pour comparer la résistance *in vivo* et *in vitro* à l'infection par le VSHV 07-71. Les lignées isogéniques de truite sont celles décrites dans [48] et [73]. Les lignées cellulaires fibroblastiques ont été dérivées d'ovaires de truites appartenant aux différentes lignées isogéniques. Les cellules peuvent être infectées *in vitro*. Un phénotype permettant de caractériser la résistance des lignées cellulaires peut par exemple être la destruction du tapis cellulaire après incubation avec du virus. La résistance *in vivo* des lignées isogéniques est quantifiée à partir de l'analyse des courbes de mortalité au cours d'une infection expérimentale par immersion (analyse de survie).
adaptée de [73].

transcrits viraux dans les cellules quatre heures après infection) [73]. Cela confirme sans équivoque le rôle majeur des mécanismes innés dans la résistance à cette infection et montre l'importance des phases précoces dans l'issue de l'infection, laissant supposer que la réponse interféron (IFN) peut être en cause dans les variations de résistances observées.

Comme chez les mammifères, les IFN sont des médiateurs d'une réponse antivirale précoce et non spécifique chez les poissons. L'activation de la réponse IFN est un facteur clé de l'inhibition de la réplication du virus. La particularité des IFNs viro-induits de poissons (ou « IFNφs » ou « type I ») est qu'ils possèdent à la fois des caractéristiques des IFN de type I et des IFN de type III mammaliens : ils sont

composés de cinq exons, alors que leurs structure tridimensionnelle est clairement similaire à celle des IFN de type I des mammifères [74-76]. Les récepteurs des IFNφs de poissons évoquent par ailleurs des récepteurs d'IFNs de type III mammaliens [75, 77].

L'expression des IFNφ est sujette à un niveau supplémentaire de régulation : il a été montré chez le saumon atlantique, le poisson zèbre et la truite arc-en-ciel que l'infection virale induisait l'expression d'un transcrit alternatif (par utilisation alternative de promoteur) pourvu d'un peptide signal et donc fonctionnel, contrairement au transcrit original exprimé constitutivement, et dépourvu de peptide signal [75, 78, 79]. Les IFNφ sont divisés en deux groupes en fonction de leurs cystéines : le groupe I comprend les IFN contenant deux cystéines, ce groupe étant conservé entre poissons cartilagineux et mammifères. Le groupe II contient des IFN possédant quatre cystéines. Ce groupe est spécifique des poissons et diffère du groupe des IFN de mammifères par la position de ces acides aminés [80].

L'implication des IFNφ dans la réponse aux infections à rhadbovirus a été largement démontrée chez les salmonidés. Ainsi, l'induction du système IFN *via* le Poly(I:C) protège les salmonidés contre le VSHV et le VNHI [81], tout comme les surnageants cellulaires contenant de l'IFN [82] ou l'IFN recombinant [77, 83]. Avant même la description des gènes des IFN de poissons, on savait que le système IFN et en particulier des ISG typiques (comme Mx) étaient impliqués dans la réponse précoce aux infections par VSHV et VNHI chez la truite arc-en-ciel [84-86]. On en sait un peu plus aujourd'hui sur les différents IFN de poissons et leur rôle dans la réponse aux *rhabdovirus* : les gènes des deux groupes d'IFNφ sont induits par les infections à *rhabdovirus*, mais leurs actions semblent assez différentes. Si l'on savait que les IFNφ recombinants du groupe I inhibaient la réplication virale, une récente étude chez le poisson zèbre a montré que les IFNφ du groupe II entraînent une induction rapide mais transitoire des ISG. Les IFN-φ du groupe I, eux, induisent l'expression des ISG et de certaines cytokines pro-inflammatoires de manière plus lente, mais plus durable pour la lutte contre l'infection [87]. L'IFN-γ joue également un rôle dans la réponse précoce à l'infection par les deux virus, qui est partiellement dépendant des IFN de type I [88]. L'IFN-γ semble pouvoir induire directement l'expression des ISG [88], et même celle des IFN-φ [66].

L'infection par ces deux *rhabdovirus* induit donc une réponse IFN classique. Ses effecteurs chez la truite arc-en-ciel sont des ISGs dont l'activité antivirale est, pour certains, décrite, comme pour la vipérine/vig-1, vig-2, isg15 ou Mx [89]. Chez les poissons infectés, la réponse IFN est souvent corrélée à la charge virale dans les tissus, et non à la protection des poissons contre l'infection [66]. Cette observation suggère une course critique entre la vitesse de réplication du virus, d'une part, et la cinétique d'expression des molécules antivirales, d'autre part, ce qui est confirmé par des études liant la vitesse de réplication de certaines souches du VNHI et leur pathogénicité [90, 91]. En revanche, l'inhibition précoce de la réplication virale, due à l'immunité innée ou à des barrières intrinsèques des cellules, a été associée à la résistance à l'infection chez la truite arc-en-ciel : ainsi, une plus faible charge virale après 24 heures d'infection est retrouvée dans des descendants de truites relativement résistantes à la NHI, par rapport à la charge virale retrouvée sur des descendants de familles plus sensibles [91, 92]. De plus, la résistance à l'infection par bain au virus de la SHV chez la truite arc-en-ciel est corrélée à la faible réplication virale *in vitro* sur des explants de nageoires [72]. L'étude publiée récemment par [73] confirme l'importance des mécanismes intrinsèques dans le contrôle de l'infection. Par ailleurs, cette étude a montré que dans une des lignées cellulaires au moins, l'induction précoce d'IFNφ1 était associée à la résistance, cette augmentation d'expression n'étant pas retrouvée dans les premières heures post-infections dans les lignées sensibles. La présence des gènes *tlr7/8* dans la zone du QTL majeur précédemment décrit [71, 93] pourrait correspondre à l'implication d'un facteur inné dépendant de l'IFN et intervenant dans les premières étapes de l'infection dans la résistance au VSHV. Cependant, il est à noter que dans une autre lignée, une forte résistance à l'infection n'est pas corrélée à une induction précoce d'IFNφ1, suggérant l'existence de différents mécanismes indépendants de résistance à l'infection par le VSHV [73].

Généralisation de l'importance des mécanismes innés à d'autres rhabdovirus

Une autre approche pour mieux comprendre la résistance aux infections aux *rhabdovirus* chez la truite arc-en-ciel est d'étudier les variations de mécanismes de virulence entre espèces de *rhabdovirus* étroitement apparentées comme le VSHV et le VNHI. Un certain nombre d'études démontrent clairement le rôle de mécanismes non spécifiques précoces dans la résistance à ces deux infections [71, 73, 92, 94]. Pour des applications pratiques, il est aussi important de s'intéresser à la fois à ces deux virus dans la mesure où ils induisent des pathologies présentant des symptômes très semblables chez les jeunes poissons. Les mécanismes innés, « non spécifiques » *a priori*, qui permettent la résistance à l'infection par le VSHV, pourraient assez naturellement conduire à une résistance au VNHI. En réalité, l'étude comparée de différentes lignées isogéniques de truites infectées avec les deux virus a conclu à l'absence de corrélation entre les résistances à ces deux virus [93, 95].

Ainsi, certaines lignées sont apparues extrêmement résistantes au VNHI mais extrêmement sensibles au VSHV. Les premiers résultats en culture cellulaire semblent indiquer que la résistance au VNHI dans les lignées isogéniques précédemment décrites dépend également de facteurs innés, mais correspond bien à la résistance des animaux : en effet, la résistance des lignées cellulaires (estimée par la destruction du tapis après infection) est également bien corrélée à la survie des poissons (Verrier, données non publiées). Cela suggère l'existence de modalités distinctes d'élaboration de la résistance, mais confirme l'importance de l'immunité innée dans la réponse à ces infections.

Conclusion

Même si les composantes du système de défense antivirale semblent globalement assez conservées entre mammifères et poissons téléostéens, les mécanismes précis de la réponse antivirale sont encore assez mal connus chez ces derniers. La dissection de l'architecture génétique de la résistance aux maladies, et notamment la description fine des individus naturellement résistants, est une approche sans *a priori* qui permettra de progresser vers la description complète des mécanismes antiviraux critiques mis en jeu chez les poissons. En démontrant le rôle primordial des mécanismes innés dans la résistance aux *rhabdovirus*, la comparaison des lignées isogéniques de truites arc-en-ciel après infection par le VSHV a permis l'obtention de résultats originaux, qui constituent une référence pour aborder l'analyse de la réponse antivirale précoce et progresser dans la compréhension de l'évolution des interactions hôtes-virus chez les vertébrés.

Avec l'accumulation d'informations sur la séquence du génome de la truite arc-en-ciel, il sera possible d'aller explorer plus précisément le contenu en gènes de la région du QTL majeur, afin d'identifier le gène (ou les gènes) responsable(s) de la variation de résistance observée et la (les) mutation(s) causale(s). L'outil cellulaire permettra en parallèle de valider fonctionnellement les différents candidats positionnels ainsi identifiés. Il sera également possible de rechercher du polymorphisme dans les gènes impliqués dans la réponse antivirale précoce, et ainsi de clarifier les liens entre ces mécanismes et la résistance à la SHV dans différents fonds génétiques.

L'identification d'un QTL à effet fort sur la résistance à la SHV ouvre également des perspectives en matière d'amélioration génétique pour la résistance. Chez les poissons, les programmes de sélection ont pour objectif initial l'amélioration de la croissance, objectif commun à toutes les filières d'élevage [9]. Les autres objectifs de sélection (résistance aux maladies, qualité de chair. . .) sont ensuite introduits progressivement en fonction des espèces, de la maturité des programmes de sélection et des moyens dont ils disposent. L'existence de QTL à effet fort comme ceux qui ont été identifiés pour le VNPI chez le saumon atlantique ou pour le VSHV chez la truite, facilite l'introduction de caractères de résistance aux maladies dans les programmes de sélection. La sélection assistée par marqueurs (SAM) utilise l'information moléculaire apportée par les allèles aux marqueurs proches des QTL pour préciser la valeur génétique des candidats à la sélection et améliorer l'efficacité de la sélection. Le bénéfice apporté par l'information au QTL est d'autant plus important que le QTL a un effet important sur le caractère (jusqu'à ce que l'allèle favorable au QTL soit fixé dans la population). L'inconvénient à terme d'une sélection ciblée sur un unique QTL majeur est que si le virus évolue et contourne la résistance associée au QTL, ce qu'il peut sans doute faire dans la mesure où il mute beaucoup et où les poissons sauvages représentent un réservoir non contrôlable, l'ensemble de la population sera touchée. La connaissance approfondie des mécanismes de défense sera alors nécessaire pour cibler les étapes clé de la défense antivirale et construire des résistances multifactorielles, plus difficiles à contourner.

Ces études montrent clairement l'intérêt de combiner approche positionnelle (cartographie de QTL et gènes candidats) et approche fonctionnelle (analyse des voies de signalisation et de leur régulation) pour progresser dans la description des réponses antivirales chez les vertébrés. Elles constituent également un premier pas vers la découverte de mécanismes de résistance aux virus potentiellement spécifiques des poissons téléostéens, qui permettraient de mieux comprendre l'évolution des interactions hôtes-virus chez les vertébrés.

Liens d'intérêts : les auteurs déclarent n'avoir aucun lien d'intérêt en rapport avec l'article.

Références

1. Bishop SC, Chesnais J, Stear MJ. Breeding for disease resistance: issues and opportunities. In : *Proceedings of the 7th World Congress on Genetics Applied to Livestock Production*, 2002 (Session 13).

2. Bishop SC, Axford RFE, Nicholas FW, Owen JB. *Breeding for disease resistance in farm animals*, 3rd Ed. Wallingford, UK : CABI, 2010.

3. Adams A, Thompson KD. Biotechnology offers revolution to fish health management. *Trends Biotechnol* 2006 ; 24 : 201-5.

4. Peltz G, Usuka J. From mouse genetics to human therapeutics. *Curr Opin Drug Discov Devel* 2005 ; 8 : 253-61.

5. Vidal SM, Malo D, Marquis JF, Gros P. Forward genetic dissection of immunity to infection in the mouse. *Annu Rev Immunol* 2008 ; 26 : 81-132.

6. Falconer D, MacKay T. *Introduction to quantitative genetics*, 4th Ed. Harlow, Essex, UK : Longmans Green, 1996.

7. Okamoto N, Tayama T, Kawanobe M, Fujiki N, Yasuda Y, Sano T. Resistance of a rainbow trout strain to infectious pancreatic necrosis. *Aquaculture* 1993 ; 117 : 71-6.

8. Kirpichnikov V. *Genetics and breeding of common carp*. Paris : INRA Editions, 1999.

9. Quillet E, Boudry P, Lapegue S. Variabilité génétique de la réponse aux organismes pathogènes : un outil pour améliorer la santé des mollusques et poissons d'élevage. *Prod Animales* 2007 ; 20 : 239-51.

10. Dorson M, Quillet E, Hollebecq MG, Torhy C, Chevassus B. Selection of rainbow trout resistant to viral haemorrhagic septicaemia virus and transmission of resistance by gynogenesis. *Vet Res* 1995 ; 26 : 361-8.

11. Henryon M, Berg P, Olesen NJ, *et al*. Selective breeding provides an approach to increase resistance of rainbow trout (*Onchorhynchus mykiss*) to the diseases, enteric redmouth disease, rainbow trout fry syndrome, and viral haemorrhagic septicaemia. *Aquaculture* 2005 ; 250 : 621-36.

12. Sanjyo S, Sato R, Kohara M, Tahara H. Estimation of the heritability for resistance to infectious haematopoieticnecrosis in rainbow trout. *Nippon Suisan Gakkaishi Bull Japan Soc Sci Fish* 1991 ; 57 : 1519-22.

13. McIntyre JD, Amend DF. Heritabilityof tolerance for infectious hematopoietic necrosis in sokeye salmon (*Oncorhynchus nerka*). *Trans Am Fish Soc* 1978 ; 107 : 305-8.

14. Midtlyng PJ, Storset A, Michel C, Slierendrecht WJ, Okamoto N. Breeding for disease resistance in fish. *Bull Eur Assoc Fish Pathol* 2002 ; 22 : 166-72.

15. Ødegård J, Sommer AI, Præbel AK. Heritability of resistance to viral nervous necrosis in Atlantic cod (*Gadus morhua L.*). *Aquaculture* 2010 ; 300 : 59-64.

16. Gjøen HM, Refstie T, Ulla O, Gjerde B. Genetic correlations between survival of Atlantic salmon in challenge and field tests. *Aquaculture* 1997 ; 158 : 277-88.

17. Norris A, Foyle L, Ratcliff J. Heritability of mortality in response to a natural pancreas disease (SPDV) challenge in Atlantic salmon, *Salmo salar L.*, post-smolts on a West of Ireland sea site. *J Fish Dis* 2008 ; 31 : 913-20.

18. Ødegård J, Olesen I, Dixon P, *et al*. Genetic analysis of common carp (*Cyprinus carpio*) strains. II: Resistance to *koi herpesvirus* and *Aeromonas hydrophila* and their relationship with pond survival. *Aquaculture* 2010 ; 304 : 7-13.

19. Palti Y, Parsons JE, Thorgaard GH. Identification of candidate DNA markers associated with IHN virus resistance in backcrosses of rainbow (*Oncorhynchus mykiss*) and cutthroat trout (*O. clarki*). *Aquaculture* 1999 ; 173 : 81-94.

20. Ozaki A, Sakamoto T, Khoo S, *et al*. Quantitative trait loci (QTLs) associated with resistance/susceptibility to infectious pancreatic necrosis virus (IPNV) in rainbow trout (*Oncorhynchus mykiss*). *Mol Genet Genomics* 2001 ; 265 : 23-31.

21. Fuji K, Kobayashi K, Hasegawa O, Coimbra MRM, Sakamoto T, Okamoto N. Identification of a single major genetic locus controlling the resistance to lymphocystis disease in Japanese flounder (*Paralichthys olivaceus*). *Aquaculture* 2006 ; 254 : 203-10.

22. Houston RD, Gheyas A, Hamilton A, *et al*. Detection and confirmation of a major QTL affecting resistance to infectious pancreatic necrosis (IPN) in Atlantic salmon (*Salmo salar*). *Dev Biol* 2008 ; 132 : 199-204.

23. Moen T, Baranski M, Sonesson AK, Kjøglum S. Confirmation and fine-mapping of a major QTL for resistance to infectious pancreatic necrosis in Atlantic salmon (*Salmo salar*): population-level associations between markers and trait. *BMC Genomics* 2009 ; 10 : 368.

24. Trobridge GD, LaPatra SE, Kim CH, Leong JC. Mx mRNA expression and RFLP analysis of rainbow trout *Oncorhynchus mykiss* genetic crosses selected for susceptibility or resistance to IHNV. *Dis Aquat Organ* 2000 ; 40 : 1-7.

25. Grimholt U, Larsen S, Nordmo R, *et al*. MHC polymorphism and disease resistance in Atlantic salmon (*Salmo salar*); facing pathogens with single expressed major histocompatibility class I and class II loci. *Immunogenetics* 2003 ; 55 : 210-9.

26. Miller KM, Winton JR, Schulze AD, Purcell MK, Ming TJ. Major histocompatibility complex loci are associated with susceptibility of atlantic salmon to infectious hematopoietic necrosis virus. *Environ Biol Fishes* 2004 ; 69 : 307-16.

27. Wolf K. *Fish viruses, fish viral diseases*. London, UK : Cornell University Press, 1988.

28. Wolf K, Rumsey G. The representative research animal: why rainbow trout (*Salmo gairdneri Rich.*)? *J Appl Ichthyol* 1985 ; 1 : 131-8.

29. Thorgaard GH, Bailey GS, Williams D, *et al*. Status and opportunities for genomics research with rainbow trout. *Comp Biochem Physiol B Biochem Mol Biol* 2002 ; 133 : 609-46.

30. Hershberger W. Genetic variability in rainbow trout populations. *Aquaculture* 1992 ; 100 : 51-71.

31. Allendorf F, Thorgaard GH. Tetraploidy and the evolution of salmonid fishes. In: Turner B, editor. *Evolutionary Genetics of Fishes*. New York : Springer US, 1984, p. 1-46.

32. Ohno S, Wolf U, Atkin NB. Evolution from fish to mammals by gene duplication. *Hereditas* 1968 ; 59 : 169-87.

33. Palti Y, Gahr SA, Hansen JD, Rexroad CE. Characterization of a new BAC library for rainbow trout: evidence for multi-locus duplication. *Anim Genet* 2004 ; 35 : 130-3.

34. Guyomard R, Boussaha M, Krieg F, Hervet C, Quillet E. A synthetic rainbow trout linkage map provides new insights into the salmonid whole genome duplication and the conservation of synteny among teleosts. *BMC Genet* 2012 ; 13 : 15.

35. Davidson WS, Koop BF, Jones SJM, *et al*. Sequencing the genome of the Atlantic salmon (*Salmo salar*). *Genome Biol* 2010 ; 11 : 403.

36. Palti Y, Genet C, Luo MC, *et al*. A first generation integrated map of the rainbow trout genome. *BMC Genomics* 2011 ; 12 : 180.

37. Genet C, Dehais P, Palti Y, *et al*. Analysis of BAC-end sequences in rainbow trout: content characterization and assessment of synteny between trout and other fish genomes. *BMC Genomics* 2011 ; 12 : 314.

38. Projet GenoTrout: http://www4.rennes.inra.fr/lpgp_eng/Programs/Genotrout.

39. Projet ARS: http://www.ars.usda.gov/research/publications/publications.htm?seq_no_115=162319.

40. Rexroad CE, Lee Y, Keele JW, *et al*. Sequence analysis of a rainbow trout cDNA library and creation of a gene index. *Cytogenet Genome Res* 2003 ; 102 : 347-54.

41. Govoroun M, Le Gac F, Guiguen Y. Generation of a large scale repertoire of Expressed Sequence Tags (ESTs) from normalised rainbow trout cDNA libraries. *BMC Genomics* 2006 ; 7 : 196.

42. Salem M, Rexroad CE, Wang J, Thorgaard GH, Yao J. Characterization of the rainbow trout transcriptome using Sanger and 454-pyrosequencing approaches. *BMC Genomics* 2010 ; 11 : 564.

43. Boussaha M, Guyomard R, Cabau C, Esquerré D, Quillet E. Development and characterisation of an expressed sequence tags (EST)-derived single nucleotide polymorphisms (SNPs) resource in rainbow trout. *BMC Genomics* 2012 ; 13 : 238.

44. Palti Y. Communication personnelle.

45. Chourrout D. La gynogenèse chez les vertébrés. *Reprod Nutr Dev* 1982 ; 22 : 713-34.

46. Chourrout D, Quillet E. Induced gynogenesis in the rainbow trout: sex and survival of progenies production of all-triploid populations. *Theor Appl Genet* 1982 ; 63 : 201-5.

47. Yamamoto E. Studies on sex-manipulation and production of cloned populations in hirame, *Paralichthys olivaceus* (Temminck et Schlegel). *Aquaculture* 1999 ; 173 : 235-46.

48. Quillet E, Dorson M, Le Guillou S, Benmansour A, Boudinot P. Wide range of susceptibility to *rhabdoviruses* in homozygous clones of rainbow trout. *Fish Shellfish Immunol* 2007 ; 22 : 510-9.

49. Komen H, Thorgaard GH. Androgenesis, gynogenesis and the production of clones in fishes: a review. *Aquaculture* 2007 ; 269 : 150-73.

50. Boudinot P, Boubekeur S, Benmansour A. *Rhabdovirus* infection induces public and private T cell responses in teleost fish. *J Immunol* 2001 ; 167 : 6202-9.

51. Fischer U, Utke K, Somamoto T, Köllner B, Ototake M, Nakanishi T. Cytotoxic activities of fish leucocytes. *Fish Shellfish Immunol* 2006 ; 20 : 209-26.

52. Fu Z. Genetic comparison of the *rhabdoviruses* from animals and plants. *Curr Top Microbiol Immunol* 2005 : 1-24.

53. Schütze H, Mundt E, Mettenleiter TC. Complete genomic sequence of viral hemorrhagic septicemia virus, a fish *rhabdovirus*. *Virus Genes* 1999 ; 19 : 59-65.

54. Basurco B, Benmansour A. Distant strains of the fish *rhabdovirus* VHSV maintain a sixth functional cistron which codes for a nonstructural protein of unknown function. *Virology* 1995 ; 212 : 741-5.

55. Benmansour A, Paubert G, Bernard J, De Kinkelin P. The polymerase-associated protein (M1) and the matrix protein (M2) from a virulent and an avirulent strain of viral hemorrhagic septicemia virus (VHSV), a fish *rhabdovirus*. *Virology* 1994 ; 198 : 602-12.

56. Bernard J, Lecocq-Xhonneux F, Rossius M, Thiry ME, De Kinkelin P. Cloning and sequencing the messenger RNA of the *N* gene of viral haemorrhagic septicaemia virus. *J Gen Virol* 1990 ; 71 : 1669-74.

57. Thiry M, Lecoq-Xhonneux F, Dheur I, Renard A, De Kinkelin P. Sequence of a cDNA carrying the glycoprotein gene and part of the matrix protein M2 gene of viral haemorrhagic scepticaemia virus, a fish *rhabdovirus*. *Biochim Biophys Acta* 1991 ; 1090 : 345-7.

58. Thoulouze M-I, Bouguyon E, Carpentier C, Brémont M. Essential role of the NV protein of *Novirhabdovirus* for pathogenicity in rainbow trout. *J Virol* 2004 ; 78 : 4098-107.

59. Crane M, Hyatt A. Viruses of fish: an overview of significant pathogens. *Viruses* 2011 ; 3 : 2025-46.

60. Batts W, Arakawa C, Bernard J, Winton J. Isolates of viral hemorrhagic septicemia virus from North America and Europe can be detected and distinguished by DNA probes. *Dis Aquat Organ* 1993 ; 17 : 67-71.

61. Oshima K, Higman K, Arakawa C, *et al*. Genetic comparison of viral hemorrhagic septicemia virus isolates from North America and Europe. *Dis Aquat Organ* 1993 ; 17 : 73-80.

62. Benmansour A, Basurco B, Monnier AF, Vende P, Winton JR, De Kinkelin P. Sequence variation of the glycoprotein gene identifies three distinct lineages within field isolates of viral haemorrhagic septicaemia virus, a fish *rhabdovirus*. *J Gen Virol* 1997 ; 78 : 2837-46.

63. OIE. *Manual of diagnostic tests for aquatic animals*, 6th ed. Paris, France : OIE, 2009.

64. Skall HF, Olesen NJ, Mellergaard S. Viral haemorrhagic septicaemia virus in marine fish and its implications for fish farming–a review. *J Fish Dis* 2005 ; 28 : 509-29.

65. Ghittino P. Viral hemorrhagic septicemia (VHS) in rainbow trout in Italy. *Ann N Y Acad Sci* 1965 ; 126 : 468-78.

66. Purcell MK, Laing KJ, Winton JR. Immunity to fish *rhabdoviruses*. *Viruses* 2012 ; 4 : 140-66.

67. Ministère de l'Agriculture. *Maladie des animaux aquatiques*, 2010.

68. Ord WM, LeBerre M, De Kinkelin P. Viral hemorrhagic septicemia – comparative susceptibility of rainbow-trout (*Salmo-gairdneri*) and hybrids (*Salmo-gairdneri* × *Oncorhynchus-kisutch*) or experimental infection. *J Fish Res Board Can* 1976 ; 33 : 1205-8.

69. Dorson M, Chevassus B, Torhy C. Comparal ve susceptibility of three species of char and of rairbow trout × char triploid hybrids to several pathogenic salmonid viruses. *Dis Aquat Organ* 1991 ; 11 : 217-24.

70. Dorson M, Chevassus B. Étude de la réceptivité d'hybrides triploïdes truite arc-en-ciel × saumon coho à la nécrose pancréatique infectieuse et à la septicémie hémorragique virale. *Bull Fr Peche Piscic* 1985 ; 296 : 29-34.

71. Verrier ER, Dorson M, Mauger S, *et al*. Resistance to a *rhabdovirus* (VHSV) in rainbow trout: identification of a major QTL related to innate mechanisms. *PLoS One* 2013 ; 8 : e55302.

72. Quillet E, Dorson M, Aubard G, Torhy C. *In vitro* viral haemorrhagic septicaemia virus replication in excised fins of rainbow trout: correlation with resistance to waterborne challenge and genetic variation. *Dis Aquat Organ* 2001 ; 45 : 171-82.

73. Verrier ER, Langevin C, Tohry C, *et al*. Genetic resistance to *rhabdovirus* infection in teleost fish is paralleled to the derived cell resistance status. *PLoS One* 2012 ; 7 : e33935.

74. Lutfalla G, Roest Crollius H, Stange-Thomann N, Jaillon O, Mogensen K, Monneron D. Comparative genomic analysis reveals independent expansion of a lineage-specific gene family in vertebrates: the class II cytokine receptors and their ligands in mammals and fish. *BMC Genomics* 2003 ; 4 : 29.

75. Levraud JP, Boudinot P, Colin I, *et al*. Identification of the zebrafish IFN receptor: implications for the origin of the vertebrate IFN system. *J Immunol* 2007 ; 178 : 4385-94.

76. Hamming OJ, Lutfalla G, Levraud JP, Hartmann R. Crystal structure of Zebrafish interferons I and II reveals conservation of type I interferon structure in vertebrates. *J Virol* 2011 ; 85 : 8181-7.

77. Aggad D, Mazel M, Boudinot P, *et al*. The two groups of zebrafish virus-induced interferons signal *via* distinct receptors with specific and shared chains. *J Immunol* 2009 ; 183 : 3924-31.

78. Bergan V, Steinsvik S, Xu H, Kileng Ø, Robertsen B. Promoters of type I interferon genes from Atlantic salmon contain two main regulatory regions. *FEBS J* 2006 ; 273 : 3893-906.

79. Purcell MK, Laing KJ, Woodson JC, Thorgaard GH, Hansen JD. Characterization of the interferon genes in homozygous rainbow trout reveals two novel genes, alternate splicing and differential regulation of duplicated genes. *Fish Shellfish Immunol* 2009 ; 26 : 293-304.

80. Zou J, Tafalla C, Truckle J, Secombes CJ. Identification of a second group of type I IFNs in fish sheds light on IFN evolution in vertebrates. *J Immunol* 2007 ; 179 : 3859-71.

81. Eaton W. Anti-viral activity in four species of salmonids following exposure to poly inosinic: cytidylic acid. *Dis Aquat Organ* 1990 ; 9 : 193-8.

82. De Kinkelin P, Dorson M, Hattenberger-Baudouy AM. Interferon synthesis in trout and carp after viral infection. *Dev Comp Immunol* 1982 ; Suppl2 : 167-74.

83. Ooi EL, Verjan N, Haraguchi I, *et al*. Innate immunomodulation with recombinant interferon-alpha enhances resistance of rainbow trout (*Oncorhynchus mykiss*) to infectious hematopoietic necrosis virus. *Dev Comp Immunol* 2008 ; 32 : 1211-20.

84. Trobridge GD, Chiou PP, Leong JA. Cloning of the rainbow trout (*Oncorhynchus mykiss*) Mx2 and Mx3 cDNAs and characterization of trout Mx protein expression in salmon cells. *J Virol* 1997 ; 71 : 5304-11.

85. Boudinot P, Massin P, Blanco M, Riffault S, Benmansour A. *vig-1*, a new fish gene induced by the *rhabdovirus* glycoprotein, has a virus-induced homologue in humans and shares conserved motifs with the MoaA family. *J Virol* 1999 ; 73 : 1846-52.

86. O'Farrell C, Vaghefi N, Cantonnet M, Buteau B, Boudinot P, Benmansour A. Survey of transcript expression in rainbow trout leukocytes reveals a major contribution of interferon-responsive genes in the early response to a *rhabdovirus* infection. *J Virol* 2002 ; 76 : 8040-9.

87. López-Muñoz A, Roca FJ, Meseguer J, Mulero V. New insights into the evolution of IFNs: zebrafish group II IFNs induce a rapid and transient expression of IFN-dependent genes and display powerful antiviral activities. *J Immunol* 2009 ; 182 : 3440-9.

88. Sun B, Skjæveland I, Svingerud T, Zou J, Jørgensen J, Robertsen B. Antiviral activity of salmonid gamma interferon against infectious pancreatic necrosis virus and salmonid alphavirus and its dependency on type I interferon. *J Virol* 2011 ; 85 : 9188-98.

89. Verrier ER, Langevin C, Benmansour A, Boudinot P. Early antiviral response and virus-induced genes in fish. *Dev Comp Immunol* 2011 ; 35 : 1204-14.

90. Park JW, Moon CH, Wargo AR, Purcell MK, Kurath G. Differential growth of U and M type infectious haematopoietic necrosis virus in a rainbow trout-derived cell line, RTG-2. *J Fish Dis* 2010 ; 33 : 583-91.

91. Wargo AR, Kurath G. *In vivo* fitness associated with high virulence in a vertebrate virus is a complex trait regulated by host entry, replication, and shedding. *J Virol* 2011 ; 85 : 3959-67.

92. Purcell MK, Lapatra SE, Woodson JC, Kurath G, Winton JR. Early viral replication and induced or constitutive immunity in rainbow trout families with differential resistance to Infectious hematopoietic necrosis virus (IHNV). *Fish Shellfish Immunol* 2010 ; 28 : 98-105.

93. Palti Y, Gahr SA, Purcell MK, *et al*. Identification, characterization and genetic mapping of *TLR7*, *TLR8a1* and *TLR8a2* genes in rainbow trout (*Oncorhynchus mykiss*). *Dev Comp Immunol* 2010 ; 34 : 219-33.

94. Peñaranda MMD, Purcell MK, Kurath G. Differential virulence mechanisms of infectious hematopoietic necrosis virus in rainbow trout (*Oncorhynchus mykiss*) include host entry and virus replication kinetics. *J Gen Virol* 2009 ; 90 : 2172-82.

95. Verrier ER, Ehanno A, Biacchesi S, *et al.* Lack of correlation between the resistances to two *rhabdovirus* infections in rainbow trout. Fish Shellfish Immunol 2013 ; 35 : 9-17.

9.2 Verrier ER et al., BMC Genomics 2018;19:482

Verrier et al. BMC Genomics (2018) 19:482
https://doi.org/10.1186/s12864-018-4860-1

BMC Genomics

RESEARCH ARTICLE Open Access

Genetic and transcriptomic analyses provide new insights on the early antiviral response to VHSV in resistant and susceptible rainbow trout

Eloi R. Verrier[1,2,5], Carine Genet[2,6], Denis Laloë[2], Florence Jaffrezic[2], Andrea Rau[2], Diane Esquerre[3], Nicolas Dechamp[2], Céline Ciobotaru[2], Caroline Hervet[2,7], Francine Krieg[2], Luc Jouneau[1], Christophe Klopp[4], Edwige Quillet[2*] and Pierre Boudinot[1*]

Abstract

Background: The viral hemorrhagic septicemia virus (VHSV) is a major threat for salmonid farming and for wild fish populations worldwide. Previous studies have highlighted the importance of innate factors regulated by a major quantitative trait locus (QTL) for the natural resistance to waterborne VHSV infection in rainbow trout. The aim of this study was to analyze the early transcriptomic response to VHSV inoculation in cell lines derived from previously described resistant and susceptible homozygous isogenic lines of rainbow trout to obtain insights into the molecular mechanisms responsible for the resistance to the viral infection.

Results: We first confirmed the presence of the major QTL in a backcross involving a highly resistant fish isogenic line (B57) and a highly susceptible one (A22), and were able to define the confidence interval of the QTL and to identify its precise position. We extended the definition of the QTL since it controls not only resistance to waterborne infection but also the kinetics of mortality after intra-peritoneal injection. Deep sequencing of the transcriptome of B57 and A22 derived cell lines exposed to inactivated VHSV showed a stronger response to virus inoculation in the resistant background. In line with our previous observations, an early and strong induction of interferon and interferon-stimulated genes was correlated with the resistance to VHSV, highlighting the major role of innate immune factors in natural trout resistance to the virus. Interestingly, major factors of the antiviral innate immunity were much more expressed in naive B57 cells compared to naive A22 cells, which likely contributes to the ability of B57 to mount a fast antiviral response after viral infection. These observations were further extended by the identification of several innate immune-related genes localized close to the QTL area on the rainbow trout genome.

Conclusions: Taken together, our results improve our knowledge in virus-host interactions in vertebrates and provide novel insights in the molecular mechanisms explaining the resistance to VHSV in rainbow trout. Our data also provide a collection of potential markers for resistance and susceptibility of rainbow trout to VHSV infection.

Keywords: Rainbow trout, VHSV, Antiviral resistance, Transcriptome deep sequencing, QTL

* Correspondence: edwige.quillet@inra.fr; pierre.boudinot@inra.fr
[2]GABI, INRA, AgroParisTech, Université Paris-Saclay, 78350 Jouy-en-Josas, France
[1]VIM, INRA, Université Paris-Saclay, 78350 Jouy-en-Josas, France
Full list of author information is available at the end of the article

Background

Viral outbreaks are a major global problem for aquaculture industry and fisheries, with important economic consequences [1, 2]. Novirhabdovirus are responsible for severe hemorrhagic diseases with significant fish mortality [3]. VHSV (viral hemorrhagic septicemia virus) infects farmed rainbow trout with severe consequences since no treatment or prophylactics allows to cure or prevent these major virus infections [4]. It also causes outbreaks in a number of wild finfish species in fresh and marine water worldwide [5] and is listed as a notifiable disease in many nations and international organizations [6]. VHSV is a single-stranded RNA virus containing a non-segmented RNA genome of approximately 12,000 nucleotides (nt) coding for five structural proteins and a sixth functional cistron which codes for a non-structural protein (NV), a feature specific of novirhabdoviridae. In rainbow trout, a high heritability of resistance to VHSH (from 0.57 to 0.63) has been reported in two independent studies [7, 8]. In the same line, a wide range of susceptibility to VHSV has been reported, with the existence of fish lines fully resistant to waterborne infection [9], suggesting that host genetics plays a key role in virus susceptibility. Several lines of evidence suggest that rainbow trout VHSV resistance implicates innate mechanisms. First, the correlation between fish survival and virus load in infected fin explants [10, 11] strongly suggests the contribution of innate or intrinsic virus resistance cellular factors. Another striking evidence was the exquisite correlation between both the resistance to waterborne VHSV infection of rainbow trout isogenic lines and of the fibroblast-like cell lines derived from these fish [12]. Finally, the identification in resistant x susceptible crossed trout families of a major genomic region Quantitative Trait Loci (QTL) controlling both fish survival and viral growth in fin tissue which further supports the crucial role of innate or intrinsic VHSV resistance factors [13]. Interestingly, the differences observed in the type-I interferon (IFN) induction between resistant and susceptible cell lines suggests that an early activation of the innate antiviral response is well correlated with the resistance to infection [12]. However, the detailed mechanisms of antiviral resistance remain to be determined. As in mammals, type-I IFN are responsible for the induction of a high number of genes (Interferon Stimulated genes, ISG) after virus infection in fish and especially in rainbow trout, including conserved antiviral genes such as *rsad2/viperin* [14], *mxa* [15], and *isg15* [16, 17], which constitute the first cellular line of defense against viral infection [18–21]. A differential induction of ISG based on genetic background, in kinetics or amplitude, may explain variation in the outcome of a viral infection. In this context, a comparison of transcriptome responses at an early stage of VHSV infection between resistant and susceptible fish would help to understand the resistance mechanisms.

With the recent development of next-generation sequencing, an increasing number of high-throughput transcriptomic studies allowed the description of fish response to virus infection [22–26]. Interestingly, transcriptomic analyses in resistant and susceptible Atlantic salmon (*Salmo salar*) after infectious pancreatic necrosis virus (IPNV) infection highlights significant differences in the immune responses to infection [27].

In this study, we aimed to gain new insights on the VHSV infection response mechanisms of cells from fish with resistant and susceptible genetic backgrounds. To do so, we took advantage of two rainbow trout homozygous isogenic lines exhibiting highly contrasted levels of susceptibility to virus infection: the resistant line B57 and the susceptible line A22 [9]. Using B57 and A22 derived offspring infected with VHSV, we first confirmed through a genetic study that the major QTL, which we previously identified on rainbow trout chromosome 3 (RT31 linkage group) [13], was effectively present in these genetic backgrounds. Using B57 and A22 derived fibroblastic cell lines, respectively resistant and susceptible as fish from which they derived, we therefore performed a genome-wide characterization of the transcriptome response to the virus through RNA deep sequencing. Both cells responded to the stimulation, but the activation of the type I IFN pathway was more intense in resistant cells, with many classical ISGs upregulated in the B57 cell line, but not in A22. Moreover, we showed that a number of key factors of type-I IFN pathway were more expressed in B57 cells than in A22 cells at the basal level, which likely contributes to the difference of resistance.

Collectively, our results pave the way for further studies to characterize the antiviral mechanisms mediating the protection and provide an array of potential key genes involved in the resistance to VHSV orchestrated by the major QTL previously reported.

Results

A major QTL controls the differences of resistance to VHSV in B57 and A22 fish

To understand the mechanisms underlying the differences of susceptibility to VHSV between B57 and A22 isogenic lines, we first looked for the presence of the major QTL we previously identified [13]. To do so, F2 segregating offspring were produced by backcrossing a B57-A22 F1 hybrid and a parental B57 (BC57-A22). BC57-A22 offspring were then waterborne challenged with VHSV 07–71, and individuals were genotyped for 8 markers (microsatellites or SNP) belonging to the major QTL area on chromosome Omy3 (RT31 linkage group). The presence of a QTL for resistance in the region was then tested using an interval mapping method implemented in the QTLMap software. As shown in Fig. 1a, a highly significant QTL was found in this area, confirming the key role of this genomic region in the difference of

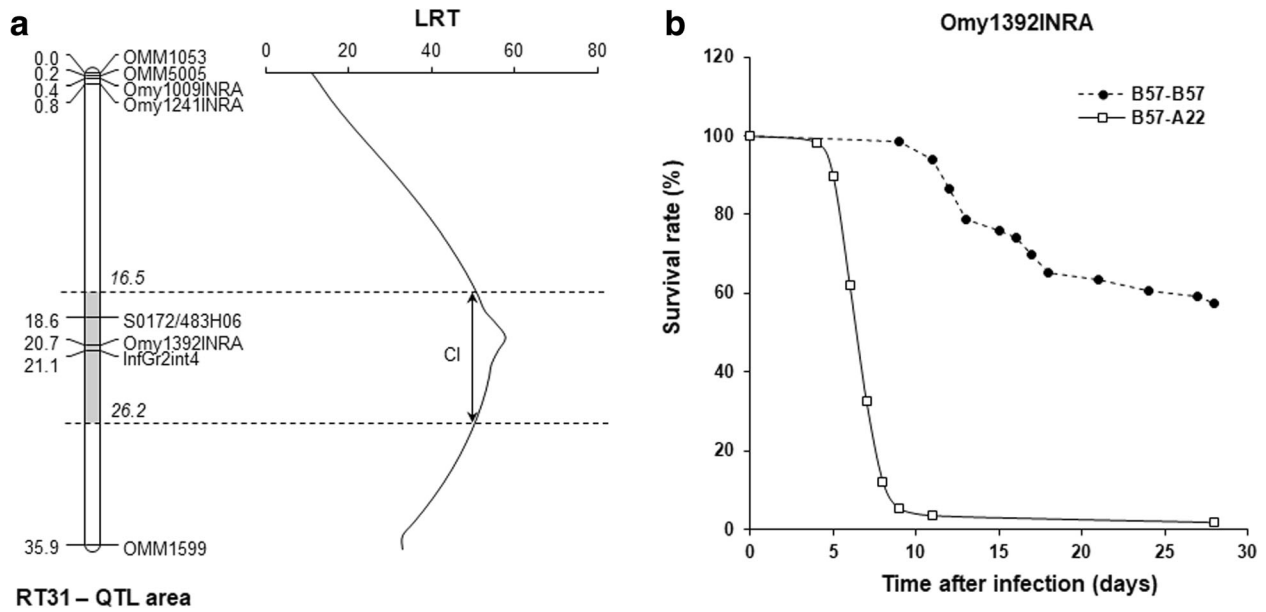

Fig. 1 Detection of the major QTL associated with resistance to VHSV on Omy3 (linkage group RT31) in a B57-A22 backcross. **a** Likelihood ratio profiles for survival associated QTL on Omy3 in a B57-A22 backcross. Two aquaria of 119 and 120 fish from a B57-A22 backcross were infected with VHSV 07–71 (waterborne challenge). A total of 8 markers localized in the previously identified QTL area on Omy3 were genotyped. Genetic distance (cM) between the markers is indicated on the left. Likelihood (LRT) values were obtained using the QTLMap software. The 95% confidence interval (CI) of the QTL was obtained using the Hendge Li method and is indicated in grey. **b** Conservation of the effect of the QTL on survival rate in BCB57-A22 backcross progeny after infection with VHSV 07–71 by injection. 125 fish from a B57-A22 backcross were injected with VHSV. Mortality was monitored daily and surviving fish were sacrificed at day 28 post infection. The allelic status at Omy1392INRA marker was determined for every fish, and cumulative death curves were built for the two alternative genotypes (B57-A22 and B57-B57)

resistance to VHSV among lines B57 (resistant) and A22 (susceptible). Moreover, our results allow to map the major QTL more precisely, most likely between S0172/483H06 and Omy1392INRA markers within a limited area as defined by the interval of confidence. Notably, 27% of the phenotypic variance of the time to death after infection was explained by the genotype of challenged fish at Omy1392INRA marker ($p < 0.001$). To go deeper into its characterization, we aimed to determine whether the QTL was observed whatever the route of infection. To answer this question, 125 BC57-A22 offspring were injected intraperitoneally with VHSV (strain 07–71), and individuals were genotyped for Omy1392INRA, one of the flanking markers of the most likely position of the QTL. Survival curves were then determined according to the allelic status at Omy1392INRA (124 genotypes out of 125 individuals were clearly determined). Among the 41 surviving fish at the end of the challenge, 39 were homozygous for B57 allele (resistant) at Omy1392INRA (B57-B57), when 56 out of 83 dead fish were heterozygous (B57-A22) at the marker ($\chi^2 = 43.3$; $p < 0.001$). Moreover, the kinetics of mortality was dramatically faster in the heterozygous progeny (Fig. 1b), suggesting a dominant susceptibility effect.

This result highlights the importance of this genomic region for the resistance to VHSV whatever the route of infection (waterborne or via intraperitoneal injection). Also, they indicate that A22 and B57 lines constitute a relevant pair of genetic backgrounds to understand the nature of genetic resistance to VHSV in rainbow trout.

Transcriptional response of A22 and B57 cells induced by inactivated VHSV

To understand the early transcriptomic differences in response to VHSV in resistant and susceptible isogenic lines, B57 and A22 derived cell lines were inoculated with inactivated VHSV (07–71 strain), which induces a significant type I IFN response even if it may not exactly recapitulate the infection with the live VHSV. Using inactivated virus limited the biases of stimulation when comparing A22 and B57 transcriptome responses. Indeed, infection with active VHSV would induce a substantial accumulation of viral RNA in A22 cells (but not B57 cells), which may saturate the viral sensing system [12]. In contrast, the inactivated virus led to a comparable exposure of A22 and B57 cells to viral stimulation, and avoided heavy contamination of the transcriptome by viral RNA. Gene expression was analyzed by RNAseq 24 h after virus inoculation: differentially expressed genes between cells incubated with the virus and controls were determined for each line, then compared across genetic backgrounds. This time point was selected based on our previous analysis of the type I IFN response in A22 and B57 cells, to warrant the detection of a

potential contrast between the responses in the two genetic backgrounds. We have previously observed that the type I IFN response to VHSV infection was much faster in B57 cells, with mRNA for the IFNϕ1 (aka IFN1) already expressed at 4 h post infection (hpi), while it was just detectable in A22 cells only at 8hpi. To observe a well-developed response we therefore characterized the transcriptome of both cell lines 24 h after incubation with the inactivated virus. Differentially expressed genes between cells incubated with the virus and controls were determined for each line, then compared across genetic backgrounds. Almost twice as many genes were modulated by the inactivated virus in the B57 cell line (3380 genes), compared to the A22 cell line (1747 genes) (Fig. 2a;

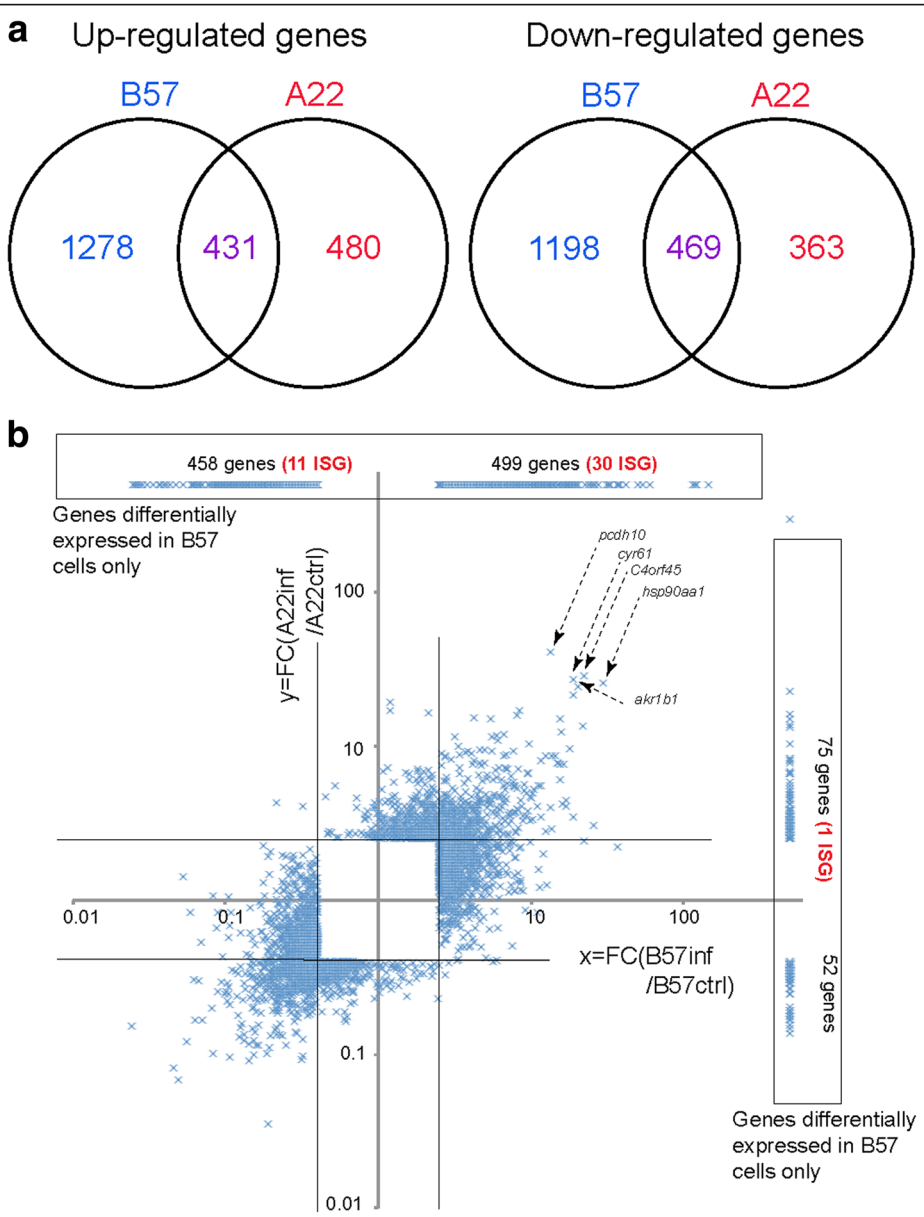

Fig. 2 Global analysis of RNAseq data. **a** Venn diagram showing the number of genes significantly induced (respectively repressed) in A22 or B57 cells ($p < 0.01$; Fold Change (FC > 2.5 or < 0.4) by inactivated VHSV: A22ind and B57ind (respectively A22rep and B57rep). Numbers of genes modulated in A22 only are in red, numbers of genes modulated only in B57 are in Blue, and numbers of genes modulated in both are in purple; numbers in categories empty by definition are in grey background. **b** LogFC/logFC representation. Average FC values are represented for genes significantly modulated ($p < 0.01$; Fold Change (FC > 2.5 or < 0.4) by inactivated VHSV. The FC of genes differentially expressed in only one cell line were represented on a line set up at an arbitrary level of 100 (induced genes) or 0.01 (repressed genes) on the axis of the other, for a clear representation of the data. The numbers of such genes are indicated in the figure. Genes with a homolog in the list considered by Schoggins et al. [29] were counted as ISG, as in Fig. 3

Additional file 1). About 50% of modulated genes were respectively up- and down regulated in each genetic background: 1711 up for 1669 down in B57, and 913 up for 834 down in A22. Importantly, only 431 and 469 genes were commonly up- (respectively down-) regulated in both cell lines, meaning that most of the transcriptional response was cell line specific. The stronger response in B57 cells was also demonstrated by higher fold changes of the genes modulated in B57 (and not in A22), compared to those modulated in A22 (and not in B57) (Fig. 2b, compare the line at the top of panel B with the column at the right side); additionally, 956 genes induced or repressed in B57 cells were not detected in A22 cells (28%), while only 126 differential genes in A22 were not expressed in B57 (7%). Overall, the dynamics of transcriptional changes across the basal gene expression level was not obviously different between A22 and B57 cells (Additional file 1). Taken together, these results suggest a much stronger response to virus inoculation in B57 cells compared to A22 cells.

Strong induction of innate immune-related pathways in B57 following VHSV inoculation

To analyze the nature of the transcriptomic response to VHSV in both genetic backgrounds, we performed a functional annotation analysis mapping zebrafish homologs of rainbow trout modulated genes to zebrafish pathways in the KEGG database. As shown in Additional file 2, VHSV induced the modulation of metabolic pathways, such as sugar and lipid pathways, as well as global cellular signaling pathways, such as mTOR and MAPK. Interestingly, genes belonging to sugar metabolism were induced in both A22 and B57, in line with a previous observation that glycolytic pathways were induced after VHSV infection in zebrafish [28] (Table 1). Cell cycle-related pathways were found downregulated also in both cell lines (Table 2), which may reflect their common ability to slow cellular growth in response to virus infection.

Interestingly, pathways related to innate immunity (Table 1) and GO terms (data not shown) linked to viral infection were significantly elicited only in B57 cells, comprising genes involved in the interaction between cytokines and their receptors, and genes involved in Jak-STAT signaling pathways. Importantly, the rainbow trout homolog of zebrafish *ifnphi1* gene was upregulated (FC = 3.9) in B57 and was not detected in A22, confirming an early activation of IFN response in B57 and not in A22, which likely contributes to the difference of susceptibility between the two cell lines [12].

Cells with VHSV resistant background express a much stronger type I IFN response than susceptible A22 cells

Type I IFN pathway was an obvious target for a detailed comparison of the response of the two cell lines. To get a comprehensive overview of the ability of B57 to rapidly express ISGs after virus inoculation, we compared the type I IFN response triggered by the inactivated virus in B57 and A22 cells. To this purpose, we first mapped on the type I IFN pathway the expression of all trout genes having an ortholog in the list of human ISG used by Shoggins et al. in their systematic functional screen [29] (Additional file 3), together with genes that have been characterized as ISG in fish (Fig. 3). We also mapped the expression of the paralogs of these trout genes, since multiple copies due to whole genome duplication events during fish evolution have often complementary, related functions. Strikingly, most of the 78 ISG and related genes that were induced by the virus in B57 cells were not up-regulated or not even detected in A22 (i.e., 64 genes, see map of the IFN pathway in Fig. 3), including canonical markers of the type I IFN response such as *viperin/rsad2, isg15, ifi44, dhx58, ifit5* and *irf1*. In addition to these ISG homologs, fish specific ISG like *gig* [30], were up-regulated in B57 but not in A22 cells. Fourteen genes were induced in both B57 and A22 (but

Table 1 DR pathways induced in trout cell lines after inoculation with VHSV

Induced pathways			
B57		A22	
1711 RT sequences / 1029 DR genes		*913 RT sequences / 580 DR genes*	
KEGG pathway	*p*value	KEGG pathway	*p*value
Glycerophospholipid metabolism	0.0001	Fructose and mannose metabolism	0.002
Cytokine-cytokine receptor interaction	**0.01**	Biosynthesis of unsaturated fatty acids	0.01
Jak-STAT signaling pathway	**0.05**	Progesterone-mediated oocyte maturation	0.01
Fructose and mannose metabolism	0.06	Sphingolipid metabolism	0.01
Endocytosis	0.06	Fatty acid elongation	0.03
MAPK signaling pathway	0.08	Glutathione metabolism	0.03
Metabolic pathways	0.098	Inositol phosphate metabolism	0.05

DR Danio rerio
RT rainbow trout
Bold: Pathways related to antiviral innate immune response

Table 2 DR pathways repressed in trout cell lines after inoculation with VHSV

Repressed pathways			
B57		A22	
1669 RT sequences / 1004 DR genes		*834 RT sequences / 532 DR genes*	
KEGG pathway	*p*value	KEGG pathway	*p*value
FoxO signaling pathway	0.001	p53 signaling pathway	0.0004
Notch signaling pathway	0.01	Cell cycle	0.0006
p53 signaling pathway	0.01	Herpes simplex infection	0.002
Peroxisome	0.02	Apoptosis	0.04
Cell cycle	0.02	Retinol metabolism	0.07
Propanoate metabolism	0.03	Glycosaminoglycan biosynthesis - CS / DS	0.096
Apoptosis	0.05		
Wnt signaling pathway	0.07		
TGF-beta signaling pathway	0.07		
Purine metabolism	0.08		

DR Danio rerio
RT rainbow trout

generally more induced in B57) and only 7 genes were induced in A22 only. Interestingly, the *crfb1* gene encoding the type I IFN receptor was up-regulated in B57 only (Fig. 3; Additional file 3). Regarding repressed genes, those with homologs in the Schoggins's dataset that were downregulated in B57 were not repressed in A22, underscoring the differences of the two responses (Fig. 3).

As an alternative approach to define potential ISG, we also identified, among the list of genes modulated either in B57 or in A22 by the inactivated VHSV, genes with a human homolog in the Interferome database (section type I IFN) [31] (Additional file 4). This analysis identified 128 genes induced more than five times in B57 cells, for only 37 in A22, confirming the trend seen for the Schoggins's ISG dataset.

Hence, a strong and typical type I IFN response was induced in B57 cells derived from fish resistant to VHSV infection, while cells from the susceptible genetic background A22 up-regulated only a few genes belonging to the IFN related pathway. However, A22 cells did show some transcriptional response implicating genes of the type I IFN pathway. Thus, a few typical markers of this pathway were responding after incubation with the inactivated virus in both A22 and B57, including *irf7*, one *cd9* and one *ddit4*, two *tnfsf10*, and several *map3k5* and *fintrim* genes. Finally, a few genes with IFN-inducible human homologs, were induced in A22 but not in B57, comprising *cyp1B1*, *angPTL1*, a *serpin1* and three *map3K5* genes.

These results raised the question of the respective inducibility of the relevant ISG markers in each genetic background. In particular, were ISG induced in B57 but not in A22 after 24 h incubation with the attenuated virus actually inducible in the latter genetic background? To address this issue, the expression level of a set of typical ISG comprising *ifi44*, *irf7* or *rsad2* was determined in the spleen of A22 fish three and 6 days after VHSV infection by immersion. As shown in Fig. 4, a strong induction of these genes was observed, indicating that their induction by a viral stimulation was not intrinsically impaired in the A22 background.

In summary, it is clear that the A22 response to viral infection is qualitatively and quantitatively different from the one seen in B57, either because genes are modulated (or not) by distinct mechanisms, and/or because the kinetics of the response is different in B57 and A22 cells. In fact, while the total numbers of up- or down- regulated genes are lower in A22 than in B57 cells, the A22-specific response represents more than 840 genes, mostly without obvious connection to antiviral immunity.

A22 and B57 responses to viral stimulation are not globally correlated to the difference in the steady state level of gene expression

We then performed an analysis of transcriptome of A22 and B57 cells at the steady state to better understand the context of their response to the virus. The genes with significantly different basal expression levels in the two genetic backgrounds were identified and are listed in Additional file 5. Out of about 15,000 genes accurately measured, we found 1692 genes more expressed in B57 [$0.4 < FC < 2.5$; adj $pval < 0.01$], while 1425 genes were preferentially expressed in A22. Overall, 25% of these 4117 genes differentially expressed between A22 and B57 at steady state were either up- or down- regulated after viral stimulation in at least one cell line (i.e., 1042 genes out of a total of 4238 genes up or down regulated by the viral stimulation either in A22 or in B57). No

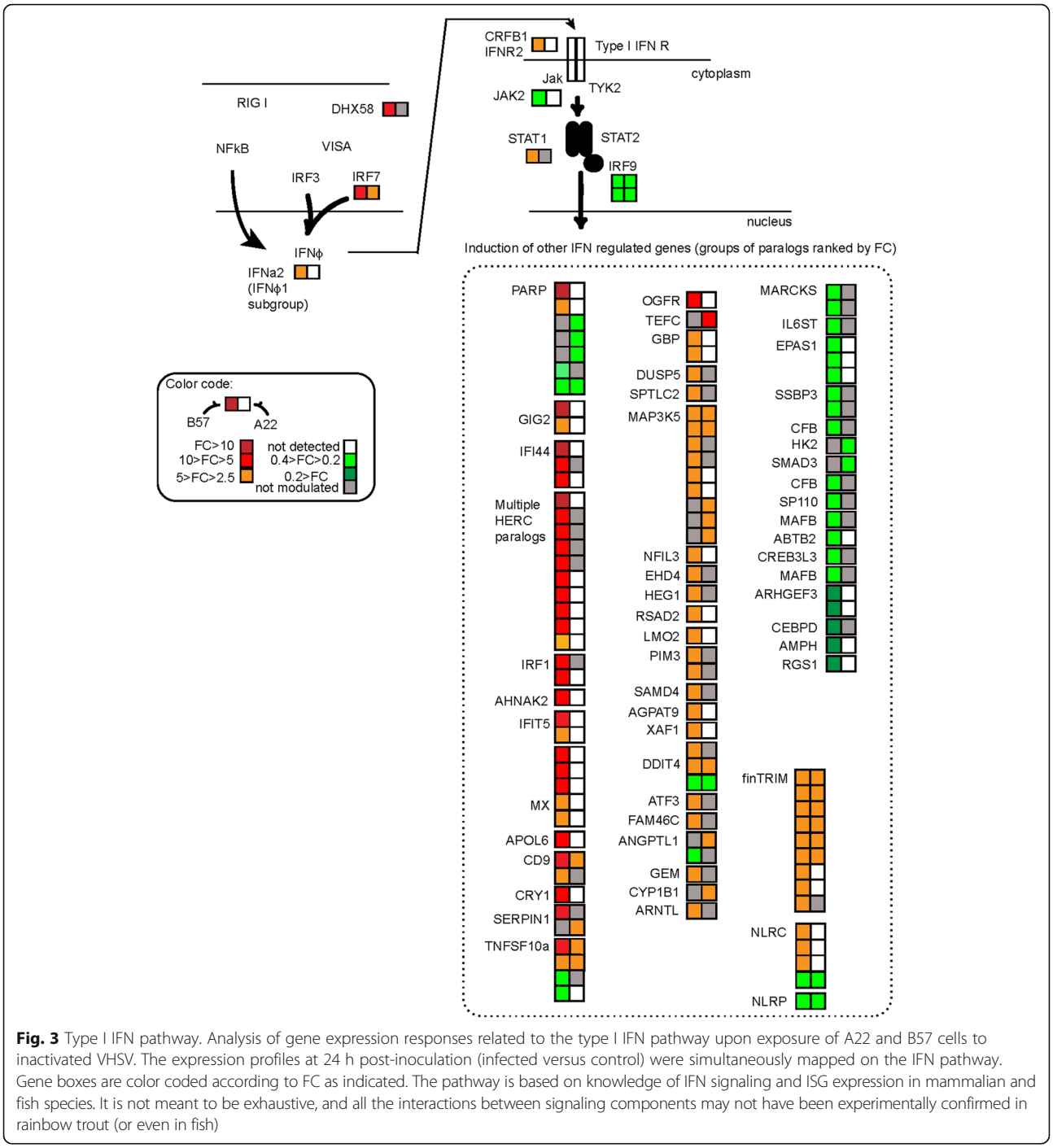

Fig. 3 Type I IFN pathway. Analysis of gene expression responses related to the type I IFN pathway upon exposure of A22 and B57 cells to inactivated VHSV. The expression profiles at 24 h post-inoculation (infected versus control) were simultaneously mapped on the IFN pathway. Gene boxes are color coded according to FC as indicated. The pathway is based on knowledge of IFN signaling and ISG expression in mammalian and fish species. It is not meant to be exhaustive, and all the interactions between signaling components may not have been experimentally confirmed in rainbow trout (or even in fish)

clear correlation was observed between FC in A22 or in B57 treated with VHVS and the ratio A22/B57 in naive controls; also, no pattern of distribution in the response to VHSV was detected between A22 and B57 up- or down- regulated genes either. The only general trend was that genes highly expressed in a given genetic background generally show slightly lower FC in the response to the viral stimulation.

Naive B57 cells exhibits higher expression of Jak/STAT-related genes than A22 cells

We then looked for specific functional modules that were differentially expressed in steady state B57 and A22 transcriptomes, and might be important for the resistance status. As shown in Table 3, a functional annotation of genes overexpressed in naive B57 cells compared to A22 cells pointed the Jak/STAT signaling pathway,

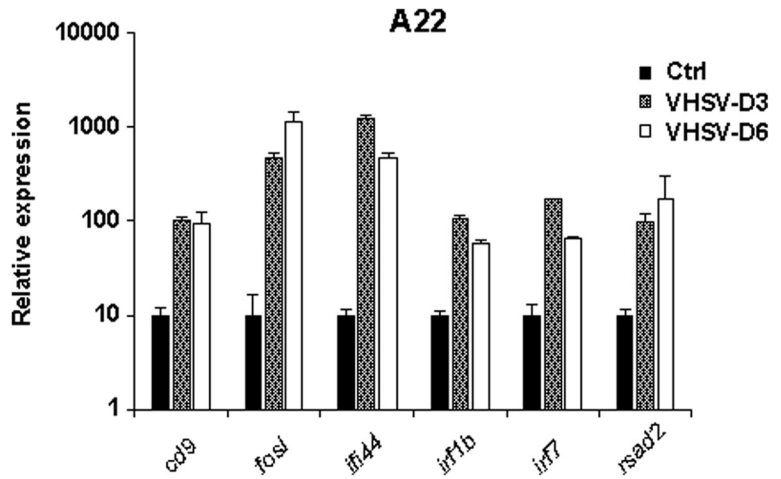

Fig. 4 ISG expression is not impaired in A22 fish. A22 fish were infected with VHSV 07–71. Fish were sacrificed at day 3 and 6 post virus inoculation, and RNA was extracted from spleen of infected animals. Gene expression was then assessed by qRT-PCR. Results are expressed as means ± SD relative gene expression compared to uninfected control tissue (Ctrl, set at 10) from three biological replicates (except VHSV D6 – two biological replicates) in technical duplicates

based on the homologs of *jak1*, *jak2b*, *stat1*, and *irf9* that are implicated in the Jak/STAT pathway activation. This may explain, at least partly, the ability of B57 cells to mount a faster and more efficient IFN response after virus infection compared to A22 cells.

On the other side, genes highly expressed in A22 cells included genes belonging to cell to cell adhesion, focal adhesion and tight junctions, including the homolog of the *fna1* gene. As fibronectin (*fn1a*) was described as the first VHSV receptor at the cell surface of rainbow trout cells [32], the higher rexpression of this receptor might actually contribute to the susceptibility to viral infection observed in A22. Notably, the MAPK pathway (which includes kinases involved in inflammation and cell proliferation) was also enriched among genes highly expressed in A22 cells, suggesting that this activation pathway may be pre-set in this background (Table 3) in a way that would not favor its contribution to IFN signaling.

Genes with top contrasted expression between A22 and B57 after viral stimulation point to several ISGs

We then combined the comparisons between A22 and B57 transcriptomes at steady state, and between control and stimulated cells for each background, to identify genes with the largest difference of absolute expression level. We considered the parameter r defined as follows, to translate at best the contrast of expression in B57 and A22, between stimulated cells and steady state:

Table 3 DR pathways modulated in B57 or A22 genetic background

Induced in B57		Induced in A22	
1692 RT sequences / 1082 DR genes		*2425 RT sequences / 1399 DR genes*	
KEGG pathway	*p*value	KEGG pathway	*p*value
Lysosome	0.01	Focal adhesion	0.00003
Ether lipid metabolism	0.01	Regulation of actin cytoskeleton	0.00004
Phosphatidylinositol signaling system	0.01	ECM-receptor interaction	0.0001
Inositol phosphate metabolism	0.01	p53 signaling pathway	0.0007
Porphyrin and chlorophyll metabolism	0.03	Tight junction	0.0027
Notch signaling pathway	0.04	MAPK signaling pathway	0.01
Glycerophospholipid metabolism	0.04	Steroid biosynthesis	0.02
Adherens junction	0.05	Vascular smooth muscle contraction	0.02
Jak-STAT signaling pathway	0.08	Wnt signaling pathway	0.02
TGF-beta signaling pathway	0.09	Folate biosynthesis	0.04

DR Danio rerio
RT rainbow trout
Bold: Pathways related to antiviral innate immune response

$$r = \frac{FC(viral\ stimulation)\ in\ B57}{FC(viral\ stimulation)\ in\ A22} \times \frac{expression\ in\ B57\ at\ steady\ state}{expression\ in\ A22\ at\ steady\ state}$$

r is defined only for FC with adjusted p values < 0.01.

Values of r are given in Additional file 3. Five ISG were among genes with the highest value of r: i.e. *dhx58, irf1, cd9, ogfr, and cyp1B1.* Several *fintrim* proteins were also highlighted by this analysis for high (a *btr/trim39* like GSONMG00054800001 and a *Trim35* like GSONMG00023727001) or low (a *MIDLINE1* homolog, GSONMG00073000001) r values. An homolog of *RPT3*, encoding a chemosensory receptor transporter protein, was expressed forty times more in B57 than in A22 at steady state, and was induced 16 times in B57 but only 4 times in A22, leading to a r value of 168. Strikingly, this gene is a paralog of the ISG *RTP4*, and was among the most strongly up-regulated genes by VHSV infection in the whole trout larvae at first feeding and 3 weeks later in our previous study [33]. In this case, fish were from the INRA genetically diverse trout strain "INRA-SY", indicating that the strong up-regulation of *rtp3* is not a particularity of the A22/B57 isogenic lines.

The QTL area contains several genes involved in antiviral innate immunity but no DEG

While genes with highly contrasted expression in A22 and B57 cells following the viral stimulation may act downstream of the genetic switch determining the resistance, they constitute potentially interesting candidates for studies of antiviral mechanisms as conspicuous outliers in the response to the infection.

To investigate whether such genes might be located in the genomic region containing the QTL of resistance to VHSV, DEG exhibiting high values of the B57/A22 ratio ($r > 19$) (Additional file 3) were mapped on the rainbow trout genome assembly (GCA_002163495.1; 2017) [34]. The top induced or repressed genes in B57 compared to A22 at the basal level were also mapped, (A22/B57 < 0.015 or > 110, respectively, (Additional file 5)), as well as ISGs specifically up-regulated in B57 after virus stimulation. As shown in Additional file 6, none of these genes are located in the telomeric region of chromosome 3 close to the QTL region. In keeping with this, while the *fn1* gene encoding the fibronectin 1 which is a VHSV receptor [32] was overexpressed in A22 compared to B57, it was found on chromosome 7 and cannot represent the primary explanation of the lack of resistance linked to A22 genetic background. To complete this exploratory survey, we also mapped 20 additional key factors of the type I IFN response. Interestingly, several cytokine receptors, such as *crfb4* and *ifnar1b* as well as *tlr7* and *LOC110520614/tlr8a1* (which were previously characterized as encoding the RNA sensors Toll-like receptors 7 and 8, respectively [35]) were found close to the expected QTL peak (less than 1 Mb from the markers closest to the QTL peak, ie S0172/483H06 andOmy1392INRA, see Additional file 7). A gene encoding a Complement C1q-like protein, orthologous to another typical ISG, was also detected in this region, but out of the QTL area (Additional file 7). These observations indicate that a number of important players of the type I IFN response are encoded by genes located in the neighborhood of the QTL, calling for further functional characterization of the gene content of this region.

Discussion

In this work, we combined two complementary approaches of quantitative genetics and transcriptome analysis to obtain new insights into the complex mechanisms involved in the resistance of rainbow trout to the rhabdovirus VHSV.

In our previous studies on rainbow trout resistance to VHSV, we identified a major QTL from crosses between resistant and susceptible trout families, which largely explained both fish survival after an immersion challenge with the virus and viral replication in fin explants [13]. We also derived fibroblast-like cell lines from resistant (B57) and susceptible (A22) double-haploid rainbow trout isogenic lines, and observed that their resistance was fully consistent with the one of the parental fish lines [12]. Altogether, these results indicated that intrinsic/innate mechanisms play a major role in resistance.

In order to further investigate the mechanisms involved, we focused here on the two cell lines (A22 and B57) with contrasted resistance. We first applied a QTL approach to these genetic backgrounds to confirm that the difference among the two lines was driven by the same QTL (i.e. most likely the same innate/intrinsic mechanism). Moreover, we extended the phenotyping of resistance using immersion vs injection route of infection, and demonstrated that the main resistance mechanisms are not limited to the virus entry into the host but do rely on.

We previously observed an early induction of *ifn1* (a fish type I IFN also known as *ifnφ1*) by VHSV infection in the resistant cell line B57, but not in the A22 susceptible cells [12]. This observation suggested a possible role of the type I IFN response in resistance, but in the context of a strong difference of viral replication between susceptible and resistant cells. To normalize the stimulation conditions, we used here a virus inactivated by β-propiolactone. Our transcriptome-wide RNAseq study confirmed a drastic difference of type IFN response 24 h post viral stimulation: more than 60 ISG were modulated in B57 only, while seven ISG were

modulated only in A22. This difference was not due to an intrinsic defect of the IFN or ISG in A22, which would suppress their induction: in infected A22 fish, where the virus replicates quickly, these genes get strongly up-regulated 3 days post infection. Hence, it rather appears that the sensing, signaling, or amplifying layers of the type I IFN response, potentially affecting its speed and/or its amplitude, are different between B57 and A22 cells, and leads to the contrasted response observed here. As the structure of the IFN pathway is complex, with many positive feedback loops at multiple levels, it is difficult at this stage to identify the defective factors. Further QTL approaches using advanced backcrosses and/or additional families (e.g. GWAS approaches) to precise the QTL region and to identify the key causing gene would help to address this issue. Interestingly, the global transcriptome response - not only the IFN response - was overall weaker in A22 cells, which might be linked to a lower capacity to respond - directly or indirectly - to the VHSV stimulation beyond the IFN pathway. However, the A22 response was still significant with more than 1700 genes up- or down- regulated by the virus stimulation. Importantly, genes induced in both A22 and B57 at comparable levels, should be less (or not) affected by the genetic differences discussed above. Among those genes are a few typical ISGs playing well-defined roles in the antiviral response, such as *irf7* or *cd9*. The functions of others remains undefined in the context of the resistance to VHSV. The case of *fintrim* [16, 36] is particularly interesting: discovered as VHSV- and IFN- induced genes in rainbow trout leukocytes [16], they display signatures of positive selection suggesting that they may be involved in the antiviral response [36]. However, a direct IFN-dependent antiviral activity has been shown for only one member of this large gene family in zebrafish [37], and it is not clear whether all *fintrim* are actually involved in the IFN response. Our observations also suggest that a number of *fintrim*, which are induced similarly in A22 and B57, may play a role in the antiviral defense independently of the IFN response, a possible strategy to counteract viral subversion strategies. Further investigations will be necessary to understand the diversity of the antiviral mechanisms mediated by these highly diversified factors [37].

A differential regulation of the type I IFN response in cells resistant and susceptible to VHSV might suggest a very general mechanism, potentially common to many viruses. This is not the case since the VHSV-resistant B57 line is in fact quite susceptible to a related novirhaboviruses, the Infectious Hematopoietic Necrosis Virus (IHNV) [38]. In fact, the subtle mechanisms of pathogen-sensing and IFN signaling differ markedly between viruses, with multiple systems of viral subversion. Hence, most resistance mechanisms are likely to be specific for a virus - or a small group of related viruses.

Regarding the genetic determinism of the resistance to VHSV, our study bridges a gap between our primary QTL description [13] and the characterization of the response in fibroblastic resistant and susceptible cell lines to viral stimulation. First, our data showed the presence of a major QTL for fish resistance to VHSV between B57 (resistant) and A22 (susceptible) genetic backgrounds, which matched exactly with the one we identified previously in other genetic backgrounds [13]. This observation validated the importance of this region for the resistance to VHSV in multiple haplotypes. Furthermore, our data clarified the type of mechanisms corresponding to the QTL for resistance to VHSV. The QTL had been initially defined for a waterborne VHSV infection, fish injected intraperitoneally showing very high level of mortality, whatever their QTL haplotype [9]. Hence, the resistance appeared somewhat linked to a possible blockage of virus entry into the host. We showed here that the QTL is also relevant for the severity of the disease after virus injection, indicating that underlying resistance mechanisms are actually active during VHSV propagation in the host, but may not be sufficient to block the infection after an intraperitoneal injection. This view is also well consistent with our previous data from cell lines [12], which suggested an innate/intrinsic mechanism potentially active in all cells and likely not restricted to entry sites in fins [32], or possibly in skin or mucosa. The presence of this major QTL needs to be further confirmed in different populations, particularly in the different isogenic lines exhibiting contrasted resistance to VHSV we previously described [9] to generalize its importance for the resistance to VHSV across all rainbow trout genotypes. At this stage, the presence of this QTL and the importance of its effect in outbred commercial populations of rainbow trout still have to be evaluated to determine whether this QTL could be used for marker assisted selection of naturally resistant animals in a breeding program.

Besides unifying observations made in vivo after VHSV infection via two routes and results from in vitro experiments, our data also define for the first time the limits of the QTL within a region bounded by Omy1241INRA and OMM1599 (Fig. 1). The QTL was first described in gynogenetic double-haploid F2 individuals obtained from a F1 female and localized in the telomeric region of Omy3 [13]. However, the low recombination rate in this region during female meiosis, did not allow to discriminate the position of the different markers of the area and to define the limits of the QTL confidence interval [39]. In this study, the presence of the QTL was confirmed by backcrossing a F1 male with a homozygote female. Thanks to the higher recombination in the

telomeric regions of the chromosomes during the male meiosis, it was possible to segregate the locations of the different markers on the chromosome, and thereby to refine the position of the QTL and identify the bounded markers.

The more accurate localization of the QTL area and the progress of the rainbow trout Omyk_1 genome assembly ([34], GCA_002163495.1) opened the door to the analysis of the gene content of the main region determining the resistance to VHSV. Whereas none of the DEG identified in these study were found in the predicted QTL, *tlr7* and *LOC110520614/tlr8a1*, which encode the Toll-like receptors 7 and 8 (TLR7 and TLR8) are located in the telomeric region of chromosome 3 [35] (Additional file 6), very close to Omy1392INRA marker (Additional file 7). While the expression of these positional candidate genes is not modulated after VHSV inoculation regardless the genetic background (Additional file 7), a functional mutation in the sequence of these key regulators of the IFN response may explain the observed differences in both susceptibility to VHSV and expression of innate immune genes in resistant and susceptible lines. Indeed, it has been suggested that impaired *tlr7* response might lead to a higher susceptibility to VHSV in Olive flounder (*Paralichthys olivaceus*) [40]. The implication of genes located in this region and their connection to the QTL remain to be demonstrated. Additionally, our analysis did not address modification of the microRNA repertoire, or the possible bias in splicing induced during the response to the virus, which may contribute to differences in susceptibility to VHSV.

Conclusions

In conclusion, our results improve our knowledge in interactions between rainbow trout and VHSV and open the door to the understanding of the natural resistance to viral infection in fish. By combining a transcriptomic and a genetic approach, we confirmed the relevance of innate immune factors in the resistance to VHSV. The understanding and quantification of the QTL effect would pave the way to the development of attractive selective breeding protocols - where marker assisted selection is advantageous – against VHSV, a major threat in rainbow trout commercial populations.

Methods

QTL analysis

Experimental family design

F0 breeders come from the previously described INRA rainbow trout isogenic lines [9]. B57 and A22 were selected as resistant and susceptible lines to VHSV 07–71 infection. A B57 female was crossed with a hormonally sex-reversed A22 male to produce the F1 hybrid progeny B57-A22. A hormonally sex-reversed B57-A22 male was then back-crossed with a B57 female to produce the segregating F2 progeny (BCB57-A22) used for QTL detection.

Waterborne infection, genotyping and QTL detection

Waterborne challenges using BCB57-A22 juveniles and the VHSV strain 07–71 (serotype 1) were previously described [10]. Two aquaria of 119 and 120 fish were infected. Dead fish were removed twice a day, surviving fish were sacrificed at the end of the challenge (day 39 post-infection), and DNA from every individual was extracted as described [13]. Fish were then genotyped for 8 markers (OMM1053, OMM5005, Omy1009INRA, S0172/483H06, Omy1392INRA, InfGr2int4, and OMM1599) localized in the area of the VHSV major QTL on Omy3 (RT31 linkage group) as described [13]. QTL detection was performed using QTLMap software with a Cox model-based method as described [13, 41, 42]. The 95% confidence interval of the QTL was obtained using the Hendge Li (HL) method [43]. The QTL effect (% of explained phenotypic variance) was estimated by testing the within family effect of the alternative alleles at Omy1392INRA marker (ANOVA with SAS software). QTL effect on survival was estimated using time to death after infection (TTD), assuming a Gaussian distribution and fixing the maximum TTD at day 39.

VHSV infection by injection

The infection by intraperitoneal injection was performed with 125 juveniles from the BC57-A22 progeny that were injected with the VHSV 07–71 strain (5000–10 000 PFU per fish) as previously described [9]. Dead fish were removed daily, surviving fish were sacrificed at the end of the challenge at day 28 after infection, and individuals DNAs were extracted as described [13]. Fish were then genotyped for Omy1392INRA, a microsatellite marker close to the most likely position of the VHSV major QTL on Omy3 linkage group.

Transcriptome deep sequencing analysis

Cell lines, virus, and RNA preparation

Fibroblastic cell lines derived from A22 and B57 ovaries were already described [12]. Briefly, cell lines were derived as described for the RTG-2 line: ovary were trypsinised under mild shaking for 2 h, and the cell suspension was cultured at 20 °C in modified Mac Pherson Stoker eagle's medium supplemented with 10% fetal calf serum, and 100 IU per ml penicillin and 100 μg per ml streptomycin. Several cell lines with typical fibroblast morphology were obtained for each parental fish clone, and displayed similar levels of susceptibility of VHSV for a given genetic background. Cells used in this study have passaged 20 times. VHSV 07–71 strain (genotype 1) was inactivated using β-propiolactone at 1:4000 for 1 h at room temperature. Inactivated virus was then kept at 4 °

C for 72 h to eliminate β-propiolactone-induced cytotoxic effects. Cells were inoculated with the inactivated virus (MOI 1) for 24 h. Total RNA was then extracted from three replicates per cell lines using RNeasy Mini Kit (Qiagen) following manufacturer's instructions.

Illumina library preparation and sequencing

The 12 mRNA-Seq libraries were prepared using TruSeq™ RNA Sample Preparation Kit (Illumina) according to the manufacturer's instructions. Briefly, Poly-A RNA were purified from 4 μg of total RNA using oligo(dT) magnetic beads, fragmented and retro-transcribed using random primers. Complementary-DNAs were end-repaired and 3-adenylated, indexed adapters were then ligated. Ten rounds of PCR amplification were performed and the PCR products were size selected on a 2% agarose E-Gel (Thermo Scientific). Libraries were checked for quality on Agilent High Sensitivity DNA Kit and quantified with the QPCR NGS Library Quantification kit (Agilent Technologies). cDNA libraries were tagged and grouped in nine pools in equal ratios and sequenced in pair-end 2x100bp on Illumina HiSeq2000 with TruSeq™ v3 Kit.

Mapping reads and gene expression counts

The read quality was checked with FastQC in the ng6 environment [44]. Reads were then spliced-aligned to the 46,535 genes from the trout reference genome [45] using TopHat v2.0.5 software [46] with the following parameters –r 10 –max-intron-length set to 25,000. The average number of read per sample (R1 + R2) was 90.5 million ±20.3, of which 65.9% ± 0.7 were mapped unambiguously. Secondary mapping (ie, mapping on two or more sites) represented 6.1% ± 0.6 of the total number of reads. All the resulting bam files were merged to produce a unique reference alignment on which the discovery of new genes and transcripts was performed using Cufflinks 2.0.0 [47] with the parameter -l set to 25,000. The resulting GTF file was used as a unique reference for the quantification step of the 12 available samples. The quantification was performed using a locally modified version of cufflinks (sig-cufflinks, available upon request on sigenae.org), which produces, per sample, an additional file containing the counts of aligned reads and read pairs. All the count files were merged to produce the final expression table.

Identification of differentially expressed genes

Differentially expressed genes between cells treated with the inactivated virus and controls were identified for each cell line. These DEG lists were then compared between A22 and B57. In parallel we also determined DEG between the control A22 and B57, to compare transcriptome differences at steady state, and the DEG between stimulated A22 and stimulated B57 to confirm that the result was similar the analysis of the stimulation within each cell line (data not shown). DEG were identified using DESeq2 1.16 (BioConductor) [48] and R: 3–4-2 [49]. Briefly, raw counts of genes were subjected to a minimal pre-filtering step by removing rows for which the count sum in 12 samples is less than 1. Raw counts were normalized for library size and normalized data were fitted thanks to a negative binomial general linear model. Estimates of Log Fold Changes (LFCs) are shrunken in a manner that removes the problem of exaggerated LFCs for low counts [47], and curbs the risk for erroneous interpretation when using the r parameter as defined above. The shrinkage of LFC estimates can be described as a bias-variance trade-off. Data were adjusted for multiple testing using the Benjamini-Hochberg procedure (adjusted *p*value). The design formula included two factors: the genotype (B57 and A22) and the condition (control versus virus-inoculated). An interaction term (genotype x condition) was added to the formula in order to test if the condition effect differs across genotype. Reference levels for genotype factor and condition factor were set respectively to B57 and to control using the "relevel" function. Genes with an adjusted *p*value less than 0.01 and an absolute Fold Change (FC) > 2.5 or FC < 0.4 were considered as DEGs. Venn diagram were plotted by using Venny 2.1.0 [50].

Functional annotation analysis

Rainbow trout protein models [45] were compared to reference zebrafish and human proteomes using blastp (BLAST®, [51]), and the best blast hit annotations were collected. For analysis of multigenic families comprising members induced by the virus, the annotation table was manually curated (for example in Fig. 2). To perform functional annotation analysis of DEG, we used DAVID 6.8 [52, 53] and the zebrafish pathway database in the Kyoto Encyclopedia of Genes and Genomes (KEGG) using DAVID basic parameters (count: minimum 2; *p*value < 0.1). Zebrafish homologs of rainbow trout DEG were used. We are aware that doing so, we lost potentially interested information regarding the expression levels of multiple trout paralogs. Modulated pathways are presented in Table 1 (induced & repressed genes after virus inoculation together), Table 2 (induced genes after virus inoculation only), and Table 3 (induced genes in B57 or in A22 at the basal level). A selection of Rainbow trout genes were mapped on the rainbow trout genome and are presented in Additional file 6.

Quantification of ISG expression in A22 fish

Waterborne challenges using juveniles and the VHSV strain 07–71 (serotype 1) were previously described [10]. Five VHSV-infected A22 fish and six non-infected control fish were used. Three fish were sacrificed at day 3 post infection, and the two remaining animals were sacrificed at day 6 post-infection. Total RNA was extracted

Table 4 List of primers used for qRT-CPR quantification of rainbow trout genes

cd9	Forward	CGCTCAGTATGTGGACAAAGG
	Reverse	CGCATTGGACTCAAAGAGGT
fosl	Forward	CTCAGGGCTTCCCACATTAG
	Reverse	ACGGTAAAGGATGTCACAGGA
ifi44	Forward	GCTGCACTGAGGAACTTTGA
	Reverse	ACCAGGGCATTATGTGTTGA
irfb1	Forward	GTCCAGAGAGCCAATGGAGT
	Reverse	GTCGGTGTAAGGGATGTCGT
irf7	Forward	ACCAAGCGTTTCATGATGGT
	Reverse	TCCTCTATGTGTGGGCTTCC
rsad2	Forward	GCAACTCCAAGCAGTGTCAA
	Reverse	AAACCTCTCTTTGCTTCCTCAA
actin	Forward	GGTGGTACGGCCAGAGGC
	Reverse	GGGAGAAGATGACCCAGATCATG

from the spleen using RNeasy Mini Kit (Qiagen). RNA were reverse transcribed into cDNA using SuperscriptII reverse transcriptase (Fischer Scientific) and gene expression was assessed by qPCR using a CFX96 thermocycler (BioRad) following manufacturer's instruction. Primers used for the detection of rainbow trout *cd9*, *fosl*, *ifi44*, *irf1b*, *irf7*, and *rsad2* are presented in Table 4. All gene expressions were normalized to *actin* expression. QPCR primers were designed using Primer3, and validated for target specificity and for an amplification efficiency > 80%.

Additional files

Additional file 1: Similar transcriptional response dynamics in B57 and A22 cells. The distribution of the fold change of all induced genes, or only ISG as defined for Fig. 2, was represented across the basal level of gene expression. (PDF 360 kb)

Additional file 2: DR pathways modulated in trout cell lines after inoculation with VHSV. (XLSX 10 kb)

Additional file 3: Description of genes significantly up- or down- regulated by incubation with attenuated VHSV in B57 or A22 cells (adj. $p < 0.01$, FC > 2,5 or < 0.4). (XLSX 1214 kb)

Additional file 4: List of rainbow trout genes significantly induced after incubation with inactivated VHSV (adj. $p < 0.01$, FC > 2,5 or < 0.4), having human putative homolog(s) registered in the Interferome database (Section type I IFN) [http://interferome.org/interferome/home.jspx]. (XLSX 208 kb)

Additional file 5: Description of genes significantly up- or down-regulated in B57 naïve cells compared to A22 naïve cells. (XLSX 878 kb)

Additional file 6: Mapping of DEG and innate immune-related genes on the rainbow trout reference genome. (XLSX 17 kb)

Additional file 7: Mapping of candidates genes and microsatellite/SNP markers on the two versions of the rainbow trout genome. (XLSX 11 kb)

Abbreviations

DEG: differentially expressed genes; FC: fold change; IFN: interferon; IHNV: Infectious Hematopoietic Necrosis Virus; IPNV: infectious pancreatic necrosis virus; ISG: Interferon Stimulated genes; KEGG: Kyoto Encyclopedia of Genes and Genomes; NV: non virion non-structural protein; QTL: major quantitative trait locus; RNAseq : RNA sequencing; VHSV: viral hemorrhagic septicemia virus

Acknowledgements

We thank our colleague C. Torhy (INRA) for excellent technical support, and Drs C. Langevin and A. Benmansour (INRA) for helpful discussions. Rainbow trout isogenic lines used as broodstock to produce the QTL family are maintained at INRA experimental facilities PEIMA (Pisciculture Expérimentale des Monts d'Arrée, Sizun, France). The VHSV in vivo challenges were performed at the INRA experimental platform Infectiologie Expérimentale des Rongeurs et des Poissons (IERP) - Domaine de Vilvert, Jouy-en-Josas, France.

Funding

This work was supported by the Animal Health and Animal Genetics divisions of INRA (ACTIV project) and by the INRA Action incitative "Bioressources" (grant AntiVIC-RS 2010). The research leading to these results has received funding from the European Community's Seventh Framework Programme (FP7, 2007–2013), Research Infrastructures action, under the grant agreement No. FP7–228394 (NADIR). E.R. VERRIER was a recipient of a PhD fellowship co-funded by Animal Genetics and Animal Health Divisions of INRA.

Availability of data and materials

The dataset generated during the current study is available in the NCBI Sequence Read Archive (SRA) under accession number SRP133208 (BioProject PRJNA434811, http://www.ncbi.nlm.nih.gov/bioproject/434811).

Authors' contributions

PB and EQ initiated the study and supervised research. ERV, CG, ND, EQ and PB designed the waterborne experimental infections. CC, CG, CH, FK, ERV and DE performed experiments and acquired the data. ERV, ND, CC, CH, FK and EQ analyzed the survival data and performed the QTL analyses. ERV, CG, DL, FJ, AR, DE, LJ, CK, EQ and PB processed and analyzed RNAseq data. ERV, LJ and PB performed the functional annotation and the mapping of candidate genes in the genome. ERV, PB, EQ were major contributors in writing the manuscript, and all the other authors were involved in drafting the manuscript and revised it. All authors read and approved the final manuscript.

Ethics approval

Animals were handled in strict accordance with good animal practice as defined by the European Union guidelines for the handling of laboratory animals (http://ec.europa.eu/environment/chemicals/lab_animals/home_en.htm), and the animal work was approved by the Direction of the Veterinary Services of Versailles (authorization numbers 78e28 and 58e37) and by the Ethics committee COMETHEA (protocol 12/053).

Consent for publication

Not applicable.

Competing interests

The authors declare that they have no competing interests.

Publisher's Note

Author details

[1]VIM, INRA, Université Paris-Saclay, 78350 Jouy-en-Josas, France. [2]GABI, INRA, AgroParisTech, Université Paris-Saclay, 78350 Jouy-en-Josas, France. [3]GenPhySE, INRA, Université de Toulouse INPT ENSAT, Université de Toulouse INPT ENVT, 52627 Castanet-Tolosan, France. [4]Plateforme Bioinformatique Toulouse, Midi-Pyrénées UBIA, INRA, 52627 Castanet-Tolosan, France. [5]Present address: Inserm, Institut de Recherche sur les Maladies Virales et Hépatiques UMRS1110, Université de Strasbourg, F-67000 Strasbourg, France. [6]Present address: GenPhySE, INRA, Université de Toulouse INPT ENSAT, Université de Toulouse INPT ENVT, 52627 Castanet-Tolosan, France. [7]Present address: BioEpAR, INRA, Oniris, 44307 Nantes, France.

Received: 21 February 2018 Accepted: 11 June 2018
Published online: 19 June 2018

References

1. Lafferty KD, Harvell CD, Conrad JM, Friedman CS, Kent ML, Kuris AM, Powell EN, Rondeau D, Saksida SM. Infectious diseases affect marine fisheries and aquaculture economics. Annu Rev Mar Sci. 2015;7:471–96.
2. Bain MB, Cornwell ER, Hope KM, Eckerlin GE, Casey RN, Groocock GH, Getchell RG, Bowser PR, Winton JR, Batts WN, et al. Distribution of an invasive aquatic pathogen (viral hemorrhagic septicemia virus) in the Great Lakes and its relationship to shipping. PLoS One. 2010;5(4):e10156.
3. Skall HF, Olesen NJ, Mellergaard S. Viral haemorrhagic septicaemia virus in marine fish and its implications for fish farming–a review. J Fish Dis. 2005; 28(9):509–29.
4. Crane M, Hyatt A. Viruses of fish: an overview of significant pathogens. Viruses. 2011;3(11):2025–46.
5. Meyers TR, Winton JR. Viral hemorrhagic septicemia virus in North America. Annu Rev Fish Dis. 1995;5:3–24.
6. Epizooties Old. Manual of Diagnostic Tests for Aquatic Animals. 5th ed. Paris: Office International des Epizooties; 2006.
7. Dorson M, Quillet E, Hollebecq MG, Torhy C, Chevassus B. Selection of rainbow trout resistant to viral haemorrhagic septicaemia virus and transmission of resistance by gynogenesis. Vet Res. 1995;26(5–6):361–8.
8. Henryon M, Berg P, Olesen N, Kjaer T, Slierendrecht W, Jokumsen A, Lund I. Selective breeding provides an approach to increase resistance of rainbow trout (Onchorhynchus mykiss) to the diseases, enteric redmouth disease, rainbow trout fry syndrome, and viral haemorrhagic septicaemia. Aquaculture. 2005;250:621–36.
9. Quillet E, Dorson M, Le Guillou S, Benmansour A, Boudinot P. Wide range of susceptibility to rhabdoviruses in homozygous clones of rainbow trout. Fish Shellfish Immunol. 2007;22(5):510–9.
10. Quillet E, Dorson M, Aubard G, Torhy C. In vitro viral haemorrhagic septicaemia virus replication in excised fins of rainbow trout: correlation with resistance to waterborne challenge and genetic variation. Dis Aquat Org. 2001;45(3):171–82.
11. Quillet E, Dorson M, Aubard G, Torhy C. In vitro assay to select rainbow trout with variable resistance/susceptibility to viral haemorrhagic septicaemia virus. Dis Aquat Org. 2007;76(1):7–16.
12. Verrier ER, Langevin C, Tohry C, Houel A, Ducrocq V, Benmansour A, Quillet E, Boudinot P. Genetic resistance to rhabdovirus infection in teleost fish is paralleled to the derived cell resistance status. PLoS One. 2012;7(4):e33935.
13. Verrier ER, Dorson M, Mauger S, Torhy C, Ciobotaru C, Hervet C, Dechamp N, Genet C, Boudinot P, Quillet E. Resistance to a rhabdovirus (VHSV) in rainbow trout: identification of a major QTL related to innate mechanisms. PLoS One. 2013;8(2):e55302.
14. Boudinot P, Massin P, Blanco M, Riffault S, Benmansour A. vig-1, a new fish gene induced by the rhabdovirus glycoprotein, has a virus-induced homologue in humans and shares conserved motifs with the MoaA family. J Virol. 1999;73(3):1846–52.
15. Trobridge GD, Chiou PP, Leong JA. Cloning of the rainbow trout (Oncorhynchus mykiss) Mx2 and Mx3 cDNAs and characterization of trout mx protein expression in salmon cells. J Virol. 1997;71(7):5304–11.
16. O'Farrell C, Vaghefi N, Cantonnet M, Buteau B, Boudinot P, Benmansour A. Survey of transcript expression in rainbow trout leukocytes reveals a major contribution of interferon-responsive genes in the early response to a rhabdovirus infection. J Virol. 2002;76(16):8040–9.
17. Langevin C, van der Aa LM, Houel A, Torhy C, Briolat V, Lunazzi A, Harmache A, Bremont M, Levraud JP, Boudinot P. Zebrafish ISG15 exerts a strong antiviral activity against RNA and DNA viruses and regulates the interferon response. J Virol. 2013;87(18):10025–36.
18. Zou J, Secombes CJ. Teleost fish interferons and their role in immunity. Dev Comp Immunol. 2011;35(12):1376–87.
19. Verrier ER, Langevin C, Benmansour A, Boudinot P. Early antiviral response and virus-induced genes in fish. Dev Comp Immunol. 2011;35(12):1204–14.
20. Langevin C, Aleksejeva E, Passoni G, Palha N, Levraud JP, Boudinot P. The antiviral innate immune response in fish: evolution and conservation of the IFN system. J Mol Biol. 2013;425(24):4904–20.
21. Poynter SJ, DeWitte-Orr SJ. Fish interferon-stimulated genes: the antiviral effectors. Dev Comp Immunol. 2016;65:218–25.
22. Cho SY, Kwon YK, Nam M, Vaidya B, Kim SR, Lee S, Kwon J, Kim D, Hwang GS. Integrated profiling of global metabolomic and transcriptomic responses to viral hemorrhagic septicemia virus infection in olive flounder. Fish Shellfish Immunol. 2017;71:220–9.
23. Pereiro P, Dios S, Boltana S, Coll J, Estepa A, Mackenzie S, Novoa B, Figueras A. Transcriptome profiles associated to VHSV infection or DNA vaccination in turbot (Scophthalmus maximus). PLoS One. 2014;9(8):e104509.
24. Shi M, Huang R, Du F, Pei Y, Liao L, Zhu Z, Wang Y. RNA-seq profiles from grass carp tissues after reovirus (GCRV) infection based on singular and modular enrichment analyses. Mol Immunol. 2014;61(1):44–53.
25. Valenzuela-Miranda D, Boltana S, Cabrejos ME, Yanez JM, Gallardo-Escarate C. High-throughput transcriptome analysis of ISAV-infected Atlantic salmon Salmo salar unravels divergent immune responses associated to head-kidney, liver and gills tissues. Fish Shellfish Immunol. 2015;45(2):367–77.
26. Xu BH, Zhong L, Liu QL, Xiao TY, Su JM, Chen KJ, Wang HQ, Dai YJ, Chen J. Characterization of grass carp spleen transcriptome during GCRV infection. Genet Mol Res : GMR. 2016;15(2) https://doi.org/10.4238/gmr.15026650.
27. Robledo D, Taggart JB, Ireland JH, McAndrew BJ, Starkey WG, Haley CS, Hamilton A, Guy DR, Mota-Velasco JC, Gheyas AA, et al. Gene expression comparison of resistant and susceptible Atlantic salmon fry challenged with infectious pancreatic necrosis virus reveals a marked contrast in immune response. BMC Genomics. 2016;17:279.
28. Encinas P, Rodriguez-Milla MA, Novoa B, Estepa A, Figueras A, Coll J. Zebrafish fin immune responses during high mortality infections with viral haemorrhagic septicemia rhabdovirus. A proteomic and transcriptomic approach. BMC Genomics. 2010;11:518.
29. Schoggins JW, Wilson SJ, Panis M, Murphy MY, Jones CT, Bieniasz P, Rice CM. A diverse range of gene products are effectors of the type I interferon antiviral response. Nat. 2011;472(7344):481–5.
30. Li S, Sun F, Zhang YB, Gui JF, Zhang QY. Identification of DreI as an antiviral factor regulated by RLR signaling pathway. PLoS One. 2012;7(3):e32427.
31. Rusinova I, Forster S, Yu S, Kannan A, Masse M, Cumming H, Chapman R, Hertzog PJ. Interferome v2.0: an updated database of annotated interferon-regulated genes. Nucleic Acids Res. 2013;41(Database issue):D1040–6.
32. Bearzotti M, Delmas B, Lamoureux A, Loustau AM, Chilmonczyk S, Bremont M. Fish rhabdovirus cell entry is mediated by fibronectin. J Virol. 1999;73(9): 7703–9.
33. Castro R, Jouneau L, Tacchi L, Macqueen DJ, Alzaid A, Secombes CJ, Martin SA, Boudinot P. Disparate developmental patterns of immune responses to bacterial and viral infections in fish. Sci Rep. 2015;5:15458.
34. Gao G, Nome T, Pearse D, Moen T, Naish K, Thorgaard GH, Lien S, Palti Y. A new single nucleotide polymorphism database for rainbow trout generated through whole genome resequencing. Front Genet. 2018; https://doi.org/10.3389/fgene.2018.00147.
35. Palti Y, Gahr SA, Purcell MK, Hadidi S, Rexroad CE, Wiens GD. Identification, characterization and genetic mapping of TLR7, TLR8a1 and TLR8a2 genes in rainbow trout (Oncorhynchus mykiss). Dev Comp Immunol. 2010;34: 219–33.
36. van der Aa LM, Levraud JP, Yahmi M, Lauret E, Briolat V, Herbomel P, Benmansour A, Boudinot P. A large new subset of TRIM genes highly diversified by duplication and positive selection in teleost fish. BMC Biol. 2009;7:7.
37. Langevin C, Aleksejeva E, Houel A, Briolat V, Torhy C, Lunazzi A, Levraud JP, Boudinot P. FTR83, a member of the large fish-specific finTRIM family, triggers IFN pathway and counters viral infection. Front Immunol. 2017; 8:617.
38. Verrier ER, Ehanno A, Biacchesi S, Le Guillou S, Dechamp N, Boudinot P, Bremont M, Quillet E. Lack of correlation between the resistances to two rhabdovirus infections in rainbow trout. Fish Shellfish Immunol. 2013;35(1): 9–17.
39. Sakamoto T, Danzmann RG, Gharbi K, Howard P, Ozaki A, Khoo SK, Woram RA, Okamoto N, Ferguson MM, Holm LE, et al. A microsatellite linkage map of rainbow trout (Oncorhynchus mykiss) characterized by large sex-specific differences in recombination rates. Genet. 2000;155(3):1331–45.
40. Avunje S, Oh MJ, Jung SJ. Impaired TLR2 and TLR7 response in olive flounder infected with viral haemorrhagic septicaemia virus at host susceptible 15 degrees C but high at non-susceptible 20 degrees C. Fish Shellfish Immunol. 2013;34(5):1236–43.
41. Moreno CR, Elsen JM, Le Roy P, Ducrocq V. Interval mapping methods for detecting QTL affecting survival and time-to-event phenotypes. Genet Res. 2005;85(2):139–49.
42. Filangi O, Moreno C, Gilbert H, Legarra A, Le Roy P, Elsen J-M. QTLMap, a software for QTL detection in outbred populations. In: Proceedings of the

9th World Congress on Genetics Applied to Livestock Production. Leipzig; 2010. (GER); 2010: n° 787; http://www.wcgalp.org/proceedings/2010.
43. Li H. A quick method to calculate QTL confidence interval. J Genet. 2011; 90(2):355–60.
44. Mariette J, Escudie F, Allias N, Salin G, Noirot C, Thomas S, Klopp C. NG6: integrated next generation sequencing storage and processing environment. BMC Genomics. 2012;13:462.
45. Berthelot C, Brunet F, Chalopin D, Juanchich A, Bernard M, Noel B, Bento P, Da Silva C, Labadie K, Alberti A, et al. The rainbow trout genome provides novel insights into evolution after whole-genome duplication in vertebrates. Nat Commun. 2014;5:3657.
46. Trapnell C, Pachter L, Salzberg SL. TopHat: discovering splice junctions with RNA-Seq. Bioinformatics. 2009;25(9):1105–11.
47. Trapnell C, Williams BA, Pertea G, Mortazavi A, Kwan G, van Baren MJ, Salzberg SL, Wold BJ, Pachter L. Transcript assembly and quantification by RNA-Seq reveals unannotated transcripts and isoform switching during cell differentiation. Nat Biotechnol. 2010;28(5):511–5.
48. Love MI, Huber W, Anders S. Moderated estimation of fold change and dispersion for RNA-seq data with DESeq2. Genome Biol. 2014;15(12):550.
49. R: A language and environment for statistical computing. [https://www.R-project.org/].
50. Venny. An interactive tool for comparing lists with Venn's diagrams. [http://bioinfogp.cnb.csic.es/tools/venny/].
51. Altschul SF, Gish W, Miller W, Myers EW, Lipman DJ. Basic local alignment search tool. J Mol Biol. 1990;215(3):403–10.
52. Huang d W, Sherman BT, Lempicki RA. Systematic and integrative analysis of large gene lists using DAVID bioinformatics resources. Nat Protoc. 2009; 4(1):44–57.
53. Huang d W, Sherman BT, Lempicki RA. Bioinformatics enrichment tools: paths toward the comprehensive functional analysis of large gene lists. Nucleic Acids Res. 2009;37(1):1–13.

9.3 Turon-Lagot V et al., Virologie 2019;23:149-159

Virologie 2019, 23 (3) : 149-59

Virus de l'hépatite D : cycle viral et nouvelles stratégies thérapeutiques

Vincent Turon-Lagot
Antonio Saviano
Catherine Schuster
Éloi R. Verrier

Université de Strasbourg, Inserm, Institut de recherche sur les maladies virales et hépatiques UMR_S1110, F-67000 Strasbourg, France

Résumé. De récentes estimations suggèrent qu'environ 70 millions de personnes sont infectées par le virus de l'hépatite D (ou delta, HDV). HDV est un petit virus satellite du virus de l'hépatite B (HBV) capable d'achever son cycle viral uniquement en présence de ce dernier. L'hépatite D est la forme la plus sévère d'hépatite virale chronique. Elle est responsable d'une aggravation et d'une accélération de la progression de la maladie hépatique, en comparaison des patients monoinfectés par le HBV. Les traitements actuels, basés sur l'interféron pégylé sont peu efficaces et ne permettent que rarement l'élimination définitive du virus. L'absence d'un modèle d'étude simple a longtemps enfreint la compréhension des interactions HDV-hépatocytes, et notamment l'identification de facteurs hépatiques impliqués dans le cycle viral. Ces facteurs sont des cibles d'intérêt pour le développement de nouvelles stratégies thérapeutiques dont certaines sont en cours d'essai clinique. Cette revue résume les connaissances actuelles de la virologie moléculaire du HDV et fait le point sur les nouvelles solutions thérapeutiques en cours de développement.

Mots clés : HDV, virus hépatiques, stratégies antivirales

Abstract. An estimated 70 million people are chronically infected with hepatitis D (delta) virus (HDV) worldwide. HDV is a small satellite virus of hepatitis B virus (HBV) requiring HBV for the completion of its cycle. Hepatitis D is the most severe form of chronic viral hepatitis. It is responsible for an acceleration and an aggravation of chronic liver disease compared to HBV monoinfected patients. Current treatments based on pegylated interferon rarely allow viral clearance in chronically infected patients. For long time, the absence of easy-to-use models has limited the knowledge on virus-host interactions. Notably, hepatocyte host factors involved in the viral life cycle remain largely unknown. These host factors are potential therapeutic targets for novel treatment strategies, including molecules currently evaluated in clinical trials. This review summarizes our knowledge on HDV molecular virology and innovative therapeutic strategies targeting hepatocyte host factors.

Key words: HDV, hepatotropic viruses, antiviral strategies

Introduction : épidémiologie

L'hépatite D ou delta est considérée comme la forme la plus sévère d'hépatite virale chronique. Identifié initialement chez des patients atteints d'hépatite B chronique (HBC) comme un nouvel antigène du virus de l'hépatite B (HBV pour *hepatitis B virus*) [1], l'agent pathogène responsable est un petit virus à ARN infectant exclusivement les hépatocytes et nécessitant la présence de HBV pour achever son cycle réplicatif [2, 3]. Identifié aujourd'hui comme le plus petit virus capable d'infecter les animaux, le virus de l'hépatite D (HDV pour *hepatitis D virus*) est responsable d'une accélération et d'une aggravation de la progression de la maladie hépatique chez les patients souffrant d'HBC [4], déjà première cause mondiale de carcinome hépatocellulaire [5]. Initialement, il était estimé que l'hépatite D touchait environ 5 % des patients chroniquement infectés par le HBV, soit entre 15 et 20 millions de patients dans le monde [4]. Une récente

Correspondance : E.R. Verrier
<e.verrier@unistra.fr>

doi:10.1684/vir.2019.0776

Pour citer cet article : Turon-Lagot V, Saviano A, Schuster C, Verrier ÉR. Virus de l'hépatite D : cycle viral et nouvelles stratégies thérapeutiques. *Virologie* 2019; 23(3) : 149-59 doi:10.1684/vir.2019.0776

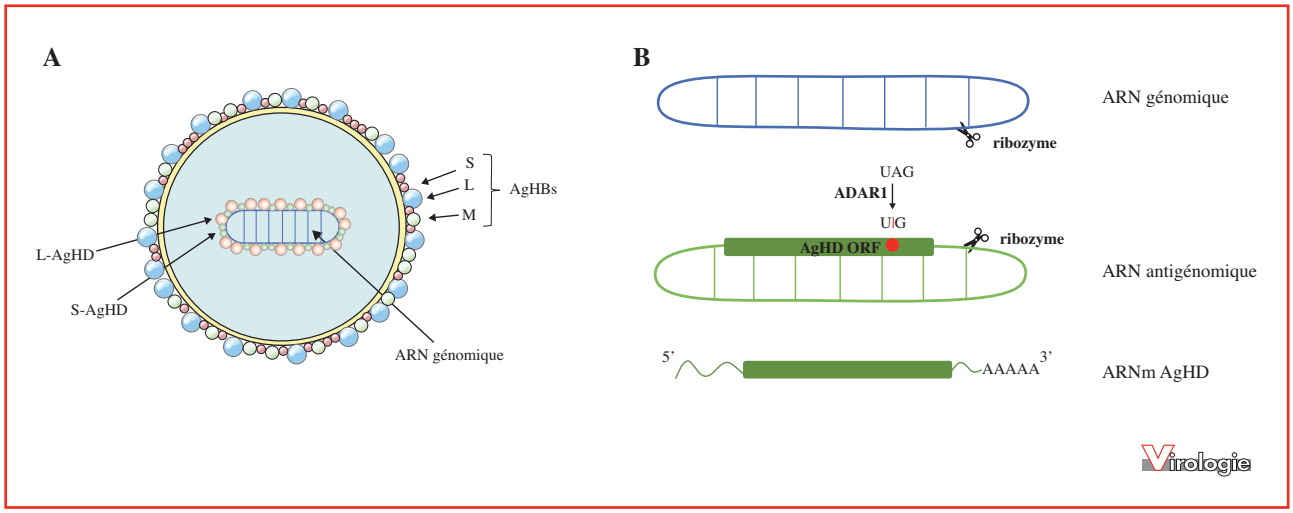

Figure 1. Structure du virus de l'hépatite D (HDV). (A) Représentation schématique de la particule virale du HDV. Le virion est composé d'une enveloppe lipidique dans laquelle sont enchâssées les trois formes des protéines d'enveloppe du virus de l'hépatite B (HBV) qui forment l'AgHBs (S, M et L). Le génome du HDV est composé d'un ARN simple brin circulaire à polarité négative entouré par les deux formes de l'antigène delta (L-AgHD et S-AgHD) formant le complexe ribonucléoprotéique. **(B)** Le génome du HDV est fortement apparié (> 70 % d'appariement) induisant une structure en bâtonnet. Il contient une séquence ribozyme qui catalyse la fragmentation des différentes unités de génome produites au cours de la réplication en cercles roulants. La transcription de l'ARN génomique permet la synthèse de deux ARNs différents : l'ARN antigénomique et l'ARNm AgHD. L'ARN antigénomique contient également une séquence ribozyme et permet la néosynthèse d'ARN génomique. Il contient également un site d'édition. L'enzyme ADAR1 catalyse la modification d'une adénosine (A) du codon stop de l'ORF S-AgHD en inosine (I). Cette édition de l'ARN induit la production de la seconde forme de AgHD, plus longue de 19 acides aminés.

méta-analyse présente une prévalence mondiale de 0,98 % inégalement répartie à travers le globe, correspondant à une prévalence de 10,58 % chez les patients HBV [6]. Même si les deux chiffres sont difficilement conciliables (de 62 millions à 27 millions de patients en fonction de l'approche), cette étude suggère un nombre de patients infectés par le HDV dans le monde bien plus important que les études précédentes. Certaines régions telles le bassin méditerranéen (27,8 % des patients atteints d'hépatite) [7], l'Afrique du Nord (20,7 % des patients atteints d'hépatite) [8] et l'Afrique centrale (38 % des patients atteints d'hépatite) [9] sont particulièrement touchées. En Europe et aux États-Unis, une majorité de patients infectés par le HDV sont des usagers de drogue injectable [6]. En dépit de la généralisation de la vaccination anti-HBV, la prévalence du HDV augmente dans les pays développés, ce rebond étant notamment dû à l'immigration depuis les régions endémiques mais également au manque de vigilance des populations à risque à l'égard des virus hépatiques [10].

À l'heure actuelle, aucun traitement ne permet efficacement d'éliminer le virus [4]. La recherche de nouvelles solutions thérapeutiques a longtemps été freinée par le manque de connaissances des interactions HDV-hépatocytes, en grande partie dû à l'absence de modèle d'étude simple. Des découvertes récentes sont à l'origine d'avancées significatives dans la compréhension du cycle viral, notamment dans l'identification de nouveaux facteurs hépatiques impliqués dans le cycle viral, donnant lieu à l'émergence de nouvelles stratégies de traitement, dont certaines sont actuellement testées en essai clinique.

Virologie moléculaire du HDV

Structure des virions

Le HDV est un petit virus enveloppé satellite du HBV d'environ 35 nm de diamètre (*figure 1*) [2]. Il est caractérisé par la présence d'une enveloppe comportant les antigènes de surface du HBV (AgHBs), indispensables à la formation des particules virales, qui contient le génome viral circulaire associé aux deux formes de l'antigène delta (AgHD) formant un complexe ribonucléoprotéique (RNP) [2, 11]. Cet ARN circulaire de polarité négative permet l'expression d'ARNm codant pour les formes, courte (S-AgHD) et longue (L-AgHD) de l'antigène delta, toutes deux impliquées dans le cycle réplicatif et la formation de la RNP virale [4]. Cette structure très particulière lui confère une place à part dans la classification des virus, seul représentant du genre non classé des Deltavirus. Le HDV est décliné en 8 génotypes hétérogènes inégalement répartis sur l'ensemble du globe [12]. Si le génotype 1 est retrouvé dans le monde entier, les génotypes 5 et 8 prédo-

minent en Afrique. Les génotypes 2 et 4, associés à une maladie hépatique moins agressive [13] sont retrouvés en Extrême-Orient. Enfin, le génotype 3, associé à un risque accru d'insuffisance hépatique est principalement présent en Amérique du Sud [12, 13].

Origine du HDV : évolution depuis un viroïde de plante ou d'un ARN cellulaire ?

L'origine du HDV n'est à ce jour pas connue mais deux hypothèses majeures coexistent depuis une vingtaine d'années et proposent que HDV dérive soit de viroïdes de plantes soit d'un ARNm cellulaire.

Parmi les caractéristiques du génome du HDV, sa structure circulaire et son fort taux d'appariement (*figure 1B*) le rapprochent fortement des génomes de viroïdes de plante, petits ARN circulaires simple brin à haut potentiel réplicatif, de taille cependant bien inférieure au génome du HDV, comprise entre 250 et 400 nucléotides [14-16]. Une autre différence notable est la présence sur l'antigénome du HDV d'un cadre ouvert de lecture codant pour l'antigène delta, alors que les génomes de viroïdes (à l'exception du scRYMV [17]) ne codent pour aucune protéine. En revanche, le mécanisme de réplication du génome, intégralement tributaire des ARN polymérases ADN dépendantes eucaryotes, est relativement similaire au mécanisme retrouvé chez certains viroïdes, comme les Avsunviroïdes [16]. Contrairement au HDV, les viroïdes de plantes ne s'assemblent pas en virions et se transmettent d'une plante à une autre par les graines ou des blessures, et aux cellules voisines au sein d'une plante infectée *via* les plasmodesmes [18]. Jusqu'à ce jour, aucune transmission active de cellule à cellule n'a été observée pour le HDV. Malgré tout, ces similitudes suggèrent que le HDV et les viroïdes pourraient descendre d'un même ancêtre commun, ou que l'un soit le précurseur de l'autre. L'hypothèse que le HDV provienne d'un viroïde ayant acquis une séquence codante lors de son évolution a été proposée en 1996 après la découverte dans le génome humain d'un gène codant pour une protéine interagissant avec l'antigène du virus (DIPA pour *delta-interacting protein A*) et présentant 60 % de similarité avec la séquence de la protéine virale [19]. De cette découverte, Brazas et Ganem ont émis l'hypothèse que le HDV dérive d'un ARN semblable à un viroïde ayant capturé la séquence codant pour la protéine DIPA à partir de l'ARNm cellulaire. D'autres travaux suggèrent que le HDV pourrait dériver d'un ARN cellulaire. Il y a une dizaine d'années, une étude démontra la présence d'une activité ribozyme dans la séquence de l'ARNm codant pour la *cytoplasmic polyadenylation element-binding protein 3* (CPEB3) [20]. Ce ribozyme se trouve dans un intron de l'ARNm de *CPEB3* et s'apparente au ribozyme du HDV par sa structure et son activité biochimique. Le fait que ce ribozyme ne soit présent que chez les mammifères a conduit les auteurs à émettre l'hypothèse que le génome du HDV pourrait dériver du transcriptome humain. L'un des arguments repose sur la mise en évidence des ARNs cellulaires circulaires (cARN) décrits dès le début des années 90 [21]. Ces cARN sont abondants et interviennent dans différents processus de régulation, comme la prolifération cellulaire et la progression cancéreuse, et interagissent notamment avec des microARN. Chaque cARN peut interagir avec plusieurs copies d'un même microARN et jouer ainsi un rôle d'« éponge » à microARN [22-24]. Toutefois, les cARN actuellement décrits ne comportent ni la séquence pouvant coder pour AgHD, ni l'activité ribozyme. De plus, la très récente description d'un virus partageant de nombreuses similarités avec le HDV chez les oiseaux, mais ne semblant pas dépendre d'un hépadnavirus pour l'achèvement de son cycle viral infirme l'hypothèse d'un HDV exclusivement humain [25].

Cycle viral du HDV

Les virions HDV et HBV partagent les mêmes protéines d'enveloppe ; aussi, le mécanisme d'entrée dans les hépatocytes est supposé identique pour les deux virus. Le cycle viral est initié par l'attachement de la particule virale à la surface des hépatocytes *via* son interaction avec les chaînes de sucres des protéoglycanes à héparane sulfate (HSPG) [26], dont GPC5 [27] (*figure 2*). Il se lie ensuite de manière spécifique à son récepteur hépatocytaire, le transporteur d'acides biliaires NTCP (*sodium-taurocholate co-transporting polypeptide)*, induisant l'entrée du virus dans la cellule [28]. Les 75 résidus myristoylés en N-terminal du domaine pré-S1 de la grande protéine d'enveloppe du HBV interagissent avec NTCP, potentiellement au niveau du site de liaison des acides biliaires [29, 30]. Un autre domaine du transporteur est impliqué dans l'entrée du virus mais sans interaction directe avec l'enveloppe virale, sa fonction dans l'entrée restant inconnue [28]. La liaison à NTCP induit l'endocytose de la particule virale selon un mécanisme encore inconnu. Le transport de la RNP du HDV du cytoplasme vers le noyau est également peu documenté, mais un signal NLS (signal de localisation nucléaire) a été identifié et caractérisé dans les deux formes d'AgHD [31].

Le génome du HDV ne codant pour aucune protéine non structurale, la réplication virale et la transcription de l'ARNm sont entièrement dépendantes des polymérases cellulaires. Le génome sert de matrice pour la transcription d'ARNm du HDV par l'ARN polymérase II. Une première forme d'ARNm est exportée dans le cytoplasme permettant la production de la forme courte S-AgHD. La protéine S-AgHD est importée dans le noyau et stimule la réplication virale [32], au cours de laquelle le génome

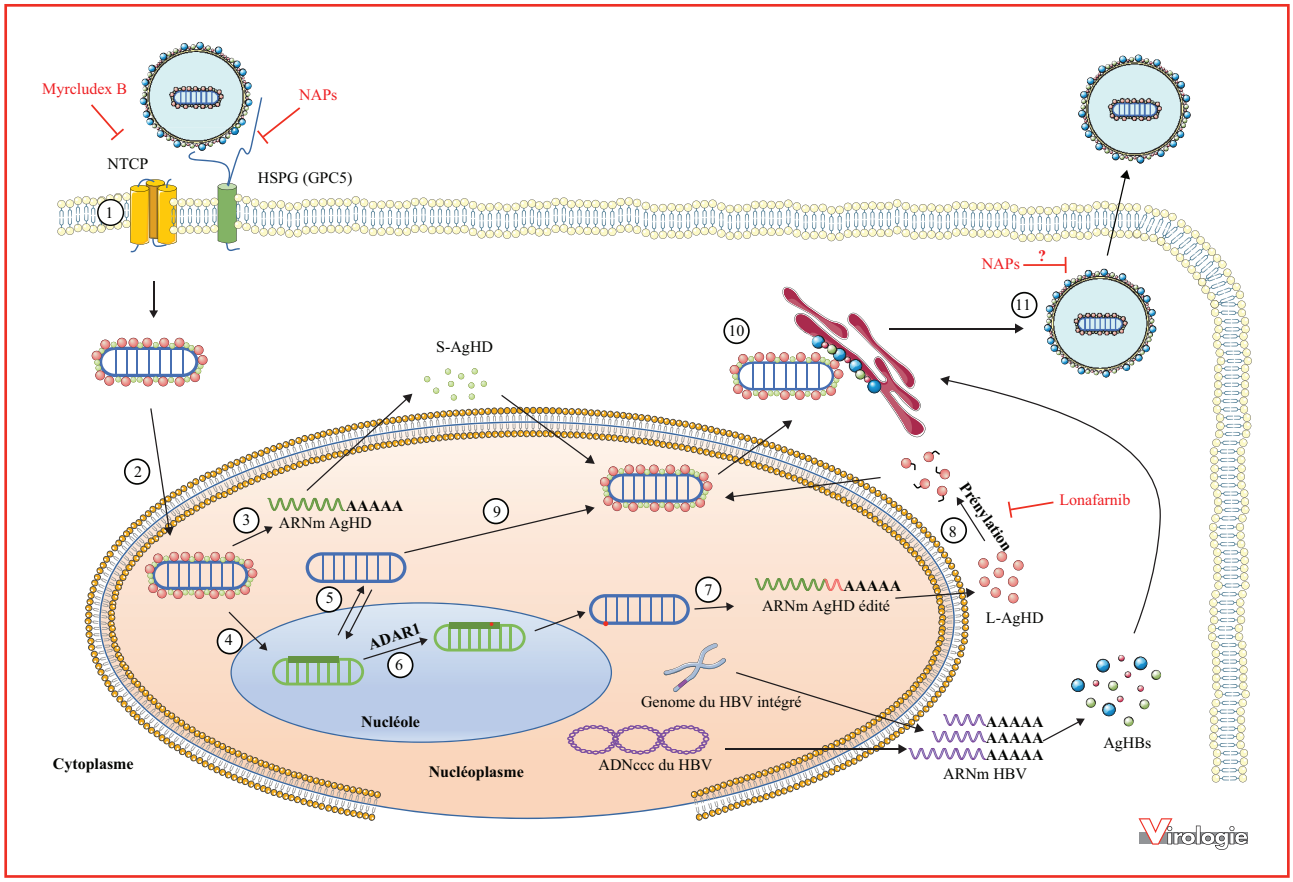

Figure 2. Cycle viral du HDV. (1) Le cycle viral débute par l'attachement aux protéoglycanes à sulfate d'héparane (HSPG), dont Glypican 5 (GPC5) à la surface des hépatocytes. La région pré-S1 de L-AgHBs se lie ensuite au récepteur spécifique du HBV et du HDV, le transporteur d'acides biliaires, NTCP. La particule virale est endocytée et la RNP virale est libérée dans le cytoplasme. **(2)** Elle est ensuite acheminée au noyau grâce au signal de localisation nucléaire présent sur les AgHD. **(3)** L'ARN polymerase II transcrit l'ARNm AgHD qui est ensuite exporté dans le cytoplasme où il est traduit pour produire la forme courte « *Small* » de AgHD (S-AgHD). **(4)** L'ARN polymerase II synthétise l'ARN antigénomique du HDV qui est ensuite transféré dans le nucléole. **(5)** Dans le nucléole, l'ARN antigénomique sert de matrice pour la néosynthèse d'ARN génomique par un mécanisme de cercle roulant. **(6)** L'ARN antigénomique est édité par l'action de l'enzyme ADAR1, supprimant le codon stop de l'ORF S-AgHD. **(7)** L'ARN antigénomique édité est transcrit en ARN génomique, induisant la synthèse de l'ARNm édité plus long. Ce dernier est exporté dans le cytoplasme où il est traduit en forme longue « *Large* » de AgHD (L-AgHD). **(8)** L-AgHD contient un site de prénylation qui est farnésylé par une farnésyltransférase cellulaire avant d'être transféré dans le noyau. **(9)** Les deux formes de AgHD interagissent avec les ARN génomiques néo-synthétisés afin de former de nouvelles ribonucléoprotéines virales qui sont exportées dans le cytoplasme. **(10)** Les ribonucléoprotéines virales interagissent, *via* une cystéine farnésylée de L-AgHD, avec la partie cytosolique de l'enveloppe du HBV au niveau du réticulum endoplasmique permettant leur enveloppement. **(11)** Les virions néoformés sont excrétés de la cellule infectée. Les différents antiviraux sont indiqués en rouge. L'hépatocyte représenté est également infecté par le HBV, indiqué par la présence l'ADNccc ou de son génome intégré (cycle complet non représenté).

du HDV recrute l'ARN polymérase II pour la synthèse de multimères d'ARN antigénomique par un mécanisme en cercle roulant [4]. L'activité ribozyme de l'antigénome catalyse l'auto-clivage des multimères en monomères, qui sont ensuite circularisés. L'ARN antigénomique du HDV sert ensuite de matrice à la synthèse de nouvelles copies de génome du HDV, également selon un mécanisme en cercle roulant *via* l'ARN polymérase II [4]. Bien que la réplication du HDV soit majoritairement portée par l'ARN polymérase II, plusieurs études suggèrent une implication des ARN polymérases I et III dans la synthèse de l'ARN antigénomique [33, 34]. Il est généralement admis que la transcription des ARN génomiques et antigénomiques a lieu dans deux compartiments nucléaires différents. La transcription de l'ARN génomique a lieu dans le nucléoplasme et celle de l'ARN antigénomique se déroule dans le nucléole [35]. Durant la phase tardive de réplication, l'ARN antigénomique du HDV est édité *via* l'enzyme ADAR1 (*adenosine deaminase acting on RNA 1*), une adénosine du codon stop de S-AgHD étant transformée en inosine [4] ce qui conduira après réplication au remplacement du codon stop en codon tryptophane (*figure 2*). La nouvelle version

des ARN génomiques produits sert alors de matrice pour la transcription d'ARNm codant pour une forme plus longue, L-AgHD. Cette allongement C-terminale de 19 acides aminés contient notamment un signal d'export nucléaire (NES) [36] et un site de prénylation sur la cystéine 211 qui est farnésylée *via* une farnésyltransférase cellulaire après traduction [37, 38]. L-AgHD farnésylé est transféré dans le noyau et inhibe la réplication virale, ce qui a pour conséquence d'orienter le cycle viral vers l'assemblage de nouveaux virions [39]. L'ARN génomique néoformé s'associe avec S-AgHD et L-AgHD afin de former de nouvelles RNP qui sont ensuite exportées du noyau, grâce au NES de L-AgHD, par la voie TAP/Aly [40]. La cystéine farnésylée de L-AgHD permet l'interaction des RNP virales avec la partie cytosolique de AgHBs à la membrane du réticulum endoplasmique. L'interaction entre la RNP virale et AgHBs induit l'enveloppement des nouveaux virions ainsi que leur sécrétion, selon des voies encore inconnues [41]. HDV est donc tributaire de l'expression d'AgHBs pour achever son cycle viral. Au sein d'un hépatocyte préalablement infecté par le HBV, AgHBs peut être exprimé à partir de l'ADNccc du HBV mais aussi d'une version intégrée du génome viral dans le génome de la cellule hôte (*figure 2*). La réplication active du HBV ne semble en effet pas indispensable à la production de virions HDV [42].

Si les grandes étapes du cycle sont à présent bien décrites, de nombreuses zones d'ombre persistent quant aux interactions moléculaires entre HDV et facteurs hépatiques dont le virus dépend fortement pour l'achèvement de son cycle réplicatif.

Interactions virus-hôte

Comme le démontre la réplication de son génome, entièrement réalisée *via* les ARN polymérases, le HDV est extrêmement dépendant des facteurs des cellules hôtes pour l'accomplissement de son cycle réplicatif. Même si ces interactions sont encore largement méconnues, un certain nombre d'acteurs cellulaires ont été décrits. Récemment, un criblage génomique a montré la forte dépendance du HDV à la biosynthèse des pyrimidines. En effet, l'inhibition de l'enzyme CAD (pour *Carbamyl-phosphate synthase II / Aspartate carbamoyltransférase / Dihydroorotase*), qui catalyse les trois premières étapes de la synthèse de l'uridine, inhibe fortement la réplication du HDV *in vitro*, sans impacter la réplication du HBV dans le laps de temps de l'étude [43]. De plus, l'inhibition du récepteur alpha des œstrogènes (ESR1), qui régule l'expression de CAD, inhibe également la réplication virale. En plus de la synthèse des pyrimidines, les résultats du criblage suggèrent l'importance d'autres facteurs cellulaires dans l'infection HDV, notamment des gènes impliqués dans la résistance à l'insuline ou la voie de signalisation HIF-1 (*hypoxia-inducible factor*). À ce jour, il est décrit que l'AgHD interagit avec plus d'une centaine de protéines, dont beaucoup sont impliquées dans le métabolisme de l'ARN, mais également des hélicases à ARN, l'histone H1, ou encore des sous-unités de l'ARN polymerase II [44]. Les ARNs du HDV se lient également avec des protéines cellulaires, notamment la protéine kinase R ou ADAR1, qui catalyse l'édition de l'ARN antigénomique [45-47]. Au niveau des senseurs de l'immunité innée, le génome du HDV est détecté par l'hélicase MDA5 (*melanoma differenciation associated gene 5*), induisant la production d'IFN de type I et III [48]. La production d'ISG (*interferon stimulated gene*) n'a cependant que peu d'effet sur la réplication du HDV, qui inhibe activement les voies de signalisation de la réponse immunitaire innée en inhibant la phosphorylation de STAT1 (*signal transducer and activator of transcription* 1) et STAT2, et par conséquent l'expression des ISG [49]. En revanche, L-AgHD induit l'activation de NF-kB (*nuclear factor kappa B*) et de STAT3 *via* le stress oxydatif [50]. L'activation de ces facteurs de transcription participe à l'état inflammatoire hépatique et pourrait expliquer l'aggravation et l'accélération de la maladie hépatique chez le patient.

Par ailleurs, l'infection par le HDV induit chez les patients une réponse immunitaire adaptative soutenue. En effet, une étude menée sur des patients atteints d'hépatite virale HBV, HBV/HDV ou virus de l'hépatite C (HCV pour *hepatitis C virus*) a montré que les patients HDV présentent les taux les plus élevés de lymphocytes T CD4$^+$ perforine-positifs [51]. Ces lymphocytes éliminent les cellules infectées et jouent probablement un rôle dans la progression plus rapide de la maladie hépatique chez les patients HDV. L'infection induit également une réponse immunitaire *via* les lymphocytes T CD8$^+$ [52], mais un échappement viral par mutations est observé chez les patients, limitant le contrôle de l'infection. Ces lymphocytes T CD8$^+$ reconnaissant des épitopes du HDV sont retrouvés à la fois chez les patients chroniques et chez les patients ayant résolu l'infection, suggérant que ces mutations pourraient expliquer au moins en partie la mise en place d'une infection chronique, les mutants HDV échappant au contrôle des cellules T CD8$^+$ [52].

Importance clinique

Histoire naturelle

Chez le patient, il existe deux types d'infection par le HDV : 1) la co-infection initiale simultanée d'un patient sain par le HBV et le HDV, qui évolue chez la majorité des adultes vers l'élimination spontanée des virus (> 95 % des cas), comme lors d'une mono-infection HBV [53], avec cependant un risque accru d'hépatite fulminante [54, 55] ; 2) la surinfection HDV chez un patient HBC, qui évolue majoritairement vers une infection persistante et une

hépatite D chronique (environ 80 % des cas), caractérisée par une inflammation et une fibrose hépatiques progressant avec un risque trois fois plus élevé vers la cirrhose que chez les patients HBC [53, 56]. De plus, le risque de survenue d'un carcinome hépatocellulaire est trois fois plus élevé que pour des patients HBC [57]. En comparaison des autres hépatites chroniques, l'hépatite D est marquée par une progression rapide vers la cirrhose, et un risque de mortalité plus élevé [4].

Diagnostic

Actuellement, il existe trois méthodes de détection du HDV mais ces méthodes restent inégalement disponibles et de fiabilité variable. Lors de l'infection aiguë, le HDV exprime et sécrète fortement AgHD qui peut être détecté par ELISA. Cependant, ce test n'est réalisable que lors des deux premières semaines d'infection, l'AgHD n'étant ensuite exprimé que de manière transitoire [58, 59].

La seconde méthode consiste à détecter les anticorps anti-HDV [60]. Les IgM sont les premières produites, concomitamment aux IgM anti-HBc (anti-*HBV core protein*) dans le cas d'une co-infection. Les IgG anti-HDV produites ensuite persistent dans le sérum des patients, que l'infection aiguë ait été résolue ou qu'elle soit devenue chronique. Chez les patients positifs pour AgHBs, la détection des IgG et IgM (Ig totaux) anti-HDV est généralement la première phase de diagnostic d'une infection HDV, même si le risque de faux-négatifs existe [10]. De plus, la détection d'IgG anti-HDV ne permet actuellement pas de conclure à une réplication active du virus, les IgG persistant en cas d'infection résolue spontanément. Une nouvelle méthode récemment développée, Q-MAC (*quantitative microarray antibody capture)*, en plus d'être largement plus sensible et spécifique que les précédentes, permettrait, en fonction de l'intensité du signal, de discriminer les patients présentant ou non une activité réplicative du HDV, même si ce test nécessite encore des études sur des cohortes plus larges [61, 62].

La troisième méthode consiste à détecter l'ARN viral du HDV dans le sérum des patients par qRT-PCR, seul marqueur d'une réplication active du HDV dans les hépatocytes. La détection de l'ARN viral, après détection des Ig totaux anti-HDV, dans le sérum permet de distinguer une infection aiguë résolue, d'une infection chronique. Cependant, les différents tests disponibles en fonction des pays n'ont pas la même sensibilité ni la même précision dans la détermination de la charge virale. De plus, le HDV ayant une forte variabilité génétique, les tests ne détectent pas efficacement les 8 génotypes viraux [63, 64]. L'Organisation mondiale de la santé (OMS) a récemment mis en place un ARN standard international afin de permettre aux laboratoires d'exprimer leurs résultats en unité internationale (UI). Depuis, plusieurs kits de détection de la charge virale ont été développés permettant une meilleure détection de tous les génotypes ainsi qu'une meilleure reproductibilité. L'un de ces kits, l'Eurobioplex HDV kit, a montré sur des échantillons de patients une forte sensibilité, précision et reproductibilité, dans la détection de tous les génotypes du HDV [65]. Une mesure précise de la charge virale du HDV chez les patients est nécessaire car elle est le seul moyen de mesurer et d'analyser la réplication virale afin de suivre l'efficacité des traitements antiviraux.

Traitements actuels

Les méthodes de détection du HDV et le suivi des patients évoluent mais les traitements actuels reposent toujours sur l'utilisation de l'interféron-alpha pégylé (PEG-IFNα), peu spécifique et responsable d'effets secondaires marqués tels qu'état grippal, anémie, dépression, conduisant parfois à un arrêt anticipé du traitement. Les réponses au traitement, de l'ordre de 30 %, sont partielles et conduisent rarement à l'élimination persistante de la charge virale [66-68]. Il est à noter que les analogues de nucléo(s)tides (NUC) utilisés dans le traitement contre le HBV sont inefficaces contre le HDV [12]. Plusieurs éléments peuvent expliquer la difficulté de traitement du HDV. Premièrement, le HDV ne code pour aucune enzyme dans son génome dont la fonction pourrait être ciblée par un traitement antiviral direct. Si le ribozyme du génome présente bien une activité enzymatique, les tentatives d'utilisation d'inhibiteurs de ribozyme se sont heurtées à une très forte toxicité *in vitro*, limitant leur caractérisation antivirale [69]. Par ailleurs, en plus d'une forte diminution de la réplication du HDV, il est nécessaire d'inhiber l'expression d'AgHBs, responsable du rebond de charge virale HDV après arrêt du traitement PEG-IFNα, même si le sujet a développé une réponse virologique soutenue [70]. Cette inhibition n'est cependant observée que chez une minorité de patients à l'aide des traitements PEG-IFNα actuels (10 % environ) [70].

Par conséquent, de nouvelles stratégies de traitement du HDV sont attendues. Dans ce contexte, les molécules ciblant les facteurs hépatiques peuvent être de nouvelles armes antivirales, dont l'efficacité a été démontrée pour d'autres virus hépatiques [71-73]. Ce type de stratégie nécessite toutefois une connaissance approfondie des cycles viraux et des interactions moléculaires entre virus et facteurs cellulaires.

Perspectives thérapeutiques : molécules ciblant l'hôte

Actuellement, plusieurs traitements sont en phase avancée d'essai clinique (*tableau 1*). Ils ciblent différentes étapes

Tableau 1 Molécules antivirales en essai clinique.

	Cible cellulaire / étape du cycle viral	Stade essai clinique	Administration	Avantages	Inconvénients	Références
Myrcludex B	NTCP / inhibiteur d'entrée	Phase II	Injection sous-cutanée 2, 5 ou 10 mg + 245 mg Ténofovir par jour (24 semaines)	1,6-2,7 log réduction ARN HDV	Rechute chez 60-83 % des patients	Wedemeyer *et al.*, 2018
Lonafarnib (LNF) + Ritonavir (RTV)	Farnésylation / inhibiteur d'assemblage	Phase II	Orale 50-100 mg LNF + 100 mg RTV par jour (24 semaines)	1,6 log réduction ARN HDV ; ARN HDV indétectable chez 1 patient	Forte augmentation des ALT après arrêt du traitement chez 30 % des patients ; pas de données sur rechutes	Wedemeyer *et al.*, 2017
REP2139	? / Sécrétion d'AgHBs	Phase II	Injection intraveineuse 500 mg par semaine (15 semaines), 250 mg + 180 µg Peg-IFN (15 semaines), 180 µg Peg-IFN (33 semaines)	ARN HDV indétectable chez 7 patients sur 11	Forte augmentation des ALT, pas de données sur rechutes	Bazinet *et al.*, 2017 ; Vaillant, 2018

du cycle viral à savoir : l'entrée virale, l'assemblage des particules virales et la sécrétion d'AgHBs.

Inhibiteur de l'entrée virale : l'exemple du Myrcludex B

Le HBV et le HDV utilisent la même enveloppe virale et, de ce fait, le même récepteur, NTCP [74]. Ce récepteur spécifique du foie, a rapidement été considéré comme une cible thérapeutique d'intérêt après la découverte de son rôle dans l'entrée des deux virus (pour des revues, voir [74, 75]). Si de nombreux inhibiteurs de NTCP décrits ont montré une activité antivirale prometteuse, c'est un lipopeptide dérivé de la partie pré-S1 de l'enveloppe du HBV qui concentre l'essentiel des attentions. Même avant la découverte du récepteur, ce peptide était connu pour son activité préventive *in vivo*, inhibant l'infection par le HBV et le HDV dans un modèle murin [76]**.** Le peptide pré-S1, site de liaison de l'enveloppe virale au récepteur, se fixe spécifiquement sur NTCP [77-79]. La forme commerciale du peptide, le Myrcludex B, peptide myristoylé dérivant des 47 acides aminés en N-terminal du domaine pré-S1 d'AgHBs, a été testé pour son activité antivirale dans de nombreux modèles *in vitro* et *in vivo* et en essai clinique [80]. Dans cet essai, 24 patients HDV co-infectés HBV ont été divisés en trois groupes afin de recevoir, pendant 24 semaines, des injections sous-cutanées quotidiennes de 2 mg de Myrcludex B, couplé ou non au Peg-IFNα, comparé à un traitement Peg-IFNα seul. Le critère principal de l'étude reposait sur la mesure du taux d'AgHBs. Aucune baisse significative d'AgHBs n'a été observée chez les patients après traitement. Toutefois, dans le groupe de patients traités uniquement avec Myrcludex B, 6 patients (75 %) ont montré une stabilisation des ALT (alanine aminotransférase) et 4 patients (50 %) ont montré une baisse de l'ARN HDV sérique de plus d'un log. De plus, l'élimination du virus a été atteinte chez 2 patients (25 %). Le groupe traité avec Myrcludex B en combinaison au Peg-IFNα a montré de meilleurs résultats avec l'ARN HDV devenu indétectable chez 5 patients (62,5 %), en revanche l'ARN HDV est réapparu chez tous les patients après arrêt du traitement, quel que soit le traitement administré [81]. Plus récemment, les résultats d'un essai multicentrique ouvert de phase II ont été rendus publics [82]. Cet essai, réalisé sur une cohorte de 120 patients co-infectés HBV/HDV, avait pour but de déterminer la tolérance et l'efficacité d'un traitement composé de différentes doses de Myrcludex B en combinaison avec du ténofovir, un inhibiteur de la transcriptase inverse du HBV [83]. Les patients, divisés en quatre groupes, ont reçu quotidiennement 2, 5 ou 10 mg de Myrcludex B par injection sous-cutanée en combinaison avec du ténofovir (245 mg/jour), comparé à un traitement au ténofovir seul pendant 24 semaines. Après cette phase, tous les patients ont ensuite suivi un traitement au ténofovir pen-

dant 24 semaines. Le critère principal était une diminution de l'ARN HDV de 2 log ou une absence d'ARN viral détectable. À la fin du traitement, l'ARN HDV avait diminué en moyenne entre 1,6 et 2,7 log, la plus forte dose de Myrcludex B étant reliée à la baisse d'ARN HDV la plus forte. Un suivi à 12 semaines sur une partie des patients a révélé la rechute de l'infection chez 60 % à 83 % des patients en fonction des groupes. Plus récemment, les résultats provisoires de l'étude de phase II MYR203 indiquent des niveaux indétectables de HDV chez 9 des 15 patients traités 48 semaines avec une dose quotidienne de Myrcludex B (2 mg) en combinaison avec le PEG-IFNα [84]. Probablement insuffisant en monothérapie, l'utilisation du Myrcludex B semble donc bénéfique chez les patients HDV en combinaison avec du ténofovir ou du PEG-IFNα. Cependant, quelques effets secondaires ont été enregistrés (démangeaisons, augmentation des acides sériques, etc.) et les questions en suspens restent la sécurité et la tolérance à long terme, notamment chez les patients cirrhotiques.

Inhibiteur de l'assemblage : lonafarnib

Durant le cycle viral du HDV, la protéine L-AgHD est farnésylée et cette étape précède l'interaction avec AgHBs. L'inhibition de la farnésylation de L-AgHD inhibe l'assemblage des nouvelles particules virales dans des modèles cellulaires et murins [85, 86]. Le lonafarnib est un inhibiteur de farnésylation qui a d'abord été testé comme anti-cancéreux et ayant des effets bénéfiques chez les patients atteints du syndrome de Hutchinson-Gilford (progéria) [87]. Bien que son efficacité n'ait pas été démontrée dans ce contexte, les premières études ont fourni des données de tolérance chez le patient. Un premier essai chez des patients HDV a été réalisé durant lequel deux doses de lonafarnib (100 mg et 200 mg) ont été administrées deux fois par jour par voie orale pendant 28 jours. Comparés à un placebo, les deux groupes de patients ont montré une baisse significative de l'ARN HDV (0,73 log pour le groupe 100 mg ; 1,54 log pour le groupe 200 mg). En revanche, le traitement n'a induit aucune baisse ni des ALT, ni des AgHBs, et le taux d'ARN HDV est revenu à la normale chez la totalité des patients à la fin de la période de suivi. De plus, tous les patients ayant reçu la plus forte dose de lonafarnib ont subi de forts effets secondaires tels que des diarrhées, des nausées et une perte de poids [88]. Afin d'améliorer l'absorption dans le sang de lonafarnib et diminuer les effets secondaires, quatre études de phases II appelées LOWR-HDV ont été réalisées avec un traitement lonafarnib en combinaison avec le ritonavir, un inhibiteur du cytochrome P450-3A4 qui est le principal acteur du métabolisme du lonafarnib et améliore sa stabilité sans effet antiviral direct [89]. De manière générale, ces études ont montré que la combinaison des deux traitements permet de diminuer la dose de lonafarnib administrée quotidiennement et d'améliorer la tolérance chez le patient [90, 91]. Cette combinaison de traitement a une meilleure efficacité sur la diminution de l'ARN HDV mais cette forte baisse est en général observée pour la moitié des patients seulement, et aucune information sur le suivi de ces patients après arrêt du traitement n'est encore disponible.

Les polymères d'acides nucléiques

Les polymères d'acides nucléiques (NAP) sont des oligonucléotides phosphorothioés leur conférant une résistance à la dégradation et à la dénaturation *in vivo*. Ils possèdent une activité inhibitrice à large spectre contre plusieurs virus comme le HCV [92] ou le virus herpes simplex [93]. Bien que leur mécanisme d'action précis ne soit pas connu avec précision, différents NAPs inhibent l'entrée des particules HDV *in vitro* [94]. De plus, les NAPs semblent inhiber la sécrétion d'AgHBs, affectant potentiellement le cycle du HDV *via* divers mécanismes [95]. Leur activité est indépendante de leur séquence mais dépendante de leur taille et de leur hydrophobicité [95]. La première étude *in vivo* a été conduite chez des canards infectés par le HBV du canard (DHBV) et traités pendant 28 jours avec le NAP REP2055. L'étude a montré une baisse d'AgHBs dans le sérum et de l'ADN DHBV, jusqu'à 16 semaines post-traitement, ainsi qu'une augmentation des anticorps anti-DHBV [96]. La tolérance et l'efficacité de REP2055 ainsi que de REP2139, un dérivé de REP2055, ont été étudiées dans une étude portant sur des patients HBV positifs à AgHBe. Pour chacun des composés, le traitement en monothérapie a montré une baisse de AgHBs dans le sérum de 2 à 7 log et de l'ADN HBV de 3 à 9 log. De plus, les traitements ont été accompagnés d'une production d'anticorps anti-HBs [97]. Le NAP REP2139 ayant montré une meilleure tolérance chez les patients ainsi qu'une forte efficacité, il a ensuite été utilisé dans une nouvelle étude afin d'évaluer sa tolérance et son efficacité en co-traitement avec Peg-IFNα sur des patients co-infectés avec HBV et HDV. Les patients ont été injectés une fois par semaine par voie intraveineuse avec 500 mg de REP2139-Ca seul pendant 15 semaines. Le traitement a été suivi par 15 semaines de traitement avec 250 mg de REP2139-Ca combiné à 180 µg de Peg-IFNα puis 33 semaines de traitement avec 180 µg de Peg-IFNα seul [98]. Après traitement, les patients ont été suivis pendant deux ans et l'ARN HDV est resté indétectable chez 7 patients (64 %), avec les AgHBs et l'ADN HBV en-dessous du seuil de détection chez 4 (36 %) et 6 (54 %) patients, respectivement [99]. Les résultats obtenus lors de ces études sont pour l'instant les plus convaincants, cependant les cohortes étudiées restent de petite taille et les effets restent à confirmer sur de plus grandes populations. De plus, le mode d'administration n'est pas adapté à un traitement

de longue durée. De nouvelles études seront menées afin de tester la tolérance du traitement en administration sous-cutanée. Enfin, le traitement au Peg-IFNα a induit chez 5 patients une forte augmentation des ALT [99]. Les patients de l'étude étant non-cirrhotiques, cette augmentation est restée asymptomatique et s'est résolue après arrêt du traitement. Le traitement pourrait cependant être plus délétère chez des patients cirrhotiques.

Conclusion

L'hépatite D reste aujourd'hui incurable et représente une menace de santé publique majeure pour des millions de patients à travers le monde. Les données épidémiologiques actuelles sont des estimations approximatives car la présence du HDV chez les patients HBV est encore trop peu souvent recherchée dans certains pays. En plus d'une meilleure détection, les traitements nécessitent également d'être améliorés. Les avancées récentes sur le cycle viral ont permis l'émergence de nouvelles solutions thérapeutiques qui démontrent l'intérêt des molécules ciblant l'hôte dans le traitement contre ce virus. La caractérisation exhaustive des facteurs hépatocytaires impliqués dans le cycle viral permettra à terme le développement de nouvelles solutions thérapeutiques pour l'éradication de ce virus hépatique majeur.

Remerciements. Les travaux de l'unité résumés dans cette revue ont notamment été financés par l'Agence nationale de la recherche sur le sida et les hépatites virales (ANRS). Cette revue est écrite dans le cadre du LabEx HepSYS (ANR-10-LAB-28). Vincent Turon-Lagot bénéficie d'un contrat doctoral (MRES) du ministère de l'Enseignement supérieur et de la Recherche.

Figures : certains éléments de figure ont été reproduits ou modifiés avec l'autorisation de Servier Medical Art (licence : https://creativecommons.org/licenses/by/3.0/fr/).

Liens d'intérêt : les auteurs déclarent n'avoir aucun lien d'intérêt en rapport avec l'article.

Références

1. Rizzetto M, Canese MG, Aricò S, Crivelli O, Trepo C, Bonino F, Verme G. Immunofluorescence detection of new antigen-antibody system (delta/anti-delta) associated to hepatitis B virus in liver and in serum of HBsAg carriers. *Gut* 1977 ; 18 : 997-1003.

2. Rizzetto M, Hoyer B, Canese MG, Shih JW, Purcell RH, Gerin JL. Delta Agent : association of delta antigen with hepatitis B surface antigen and RNA in serum of delta-infected chimpanzees. *Proc Natl Acad Sci U S A* 1980 ; 77 : 6124-8.

3. Sureau C, Guerra B, Lanford RE. Role of the large hepatitis B virus envelope protein in infectivity of the hepatitis delta virion. *J Virol* 1993 ; 67 : 366-72.

4. Sureau C, Negro F. The hepatitis delta virus: Replication and pathogenesis. *J Hepatol* 2016 ; 64 : S102-16.

5. Trépo C, Chan HLY, Lok A. Hepatitis B virus infection. *Lancet* 2014 ; 384 : 2053-63.

6. Chen HY, Shen DT, Ji DZ, Han PC, Zhang WM, *et al*. Prevalence and burden of hepatitis D virus infection in the global population: a systematic review and meta-analysis. *Gut* 2018 ; sous presse. doi:10.1136/gutjnl-2018-316601.

7. Amini N, Alavian SM, Kabir A, Aalaei-Andabili SH, Saiedi Hosseini SY, Rizzetto M. Prevalence of hepatitis d in the eastern mediterranean region: systematic review and meta analysis. *Hepat Mon* 2013 ; 13 : e8210.

8. Daw MA, Daw AM, Sifennasr NEM, Draha AM, Daw AM, Daw AM, *et al*. The Epidemiology of Hepatitis D Virus in North Africa: A Systematic Review and Meta-Analysis. *Scientific World Journal* 2018 : 9312650.

9. Stockdale AJ, Chaponda M, Beloukas A, Phillips RO, Matthews PC, Papadimitropoulos A, *et al*. Prevalence of hepatitis D virus infection in sub-Saharan Africa : a systematic review and meta-analysis. *Lancet Glob Health* 2017 ; 5 : e992-1003.

10. Noureddin M, Gish R. Hepatitis delta : epidemiology, diagnosis and management 36 years after discovery. *Curr Gastroenterol Rep* 2014 ; 16 : 365.

11. Bonino F, Heermann KH, Rizzetto M, Gerlich WH. Hepatitis delta virus : protein composition of delta antigen and its hepatitis B virus-derived envelope. *J Virol* 1986 ; 58 : 945-50.

12. Koh C, Heller T, Glenn JS. Pathogenesis of and New Therapies for Hepatitis D. *Gastroenterology* 2019 ; 156 : 461-76.

13. Farci P, Niro GA. Clinical features of hepatitis D. *Semin Liver Dis* 2012 ; 32 : 228-36.

14. Tsagris EM, Martínez de Alba AE, Gozmanova M, Kalantidis K. Viroids. *Cell Microbiol* 2008 ; 10 : 2168-79.

15. Tabler M, Tsagris M. Viroids : petite RNA pathogens with distinguished talents. *Trends Plant Sci* 2004 ; 9 : 339-48.

16. Flores R, Gas ME, Molina-Serrano D, Nohales MÁ D, Carbonell A, Gago S, *et al*. Viroid replication : rolling-circles, enzymes and ribozymes. *Viruses* 2009 ; 1 : 317-34.

17. AbouHaidar MG, Venkataraman S, Golshani A, Liu B, Ahmad T. Novel coding, translation, and gene expression of a replicating covalently closed circular RNA of 220 nt. *PNAS* 2014 ; 111 : 14542-7.

18. Takeda R, Ding B. Viroid intercellular trafficking: RNA motifs, cellular factors and broad impacts. *Viruses* 2009 ; 1 : 210-21.

19. Brazas R, Ganem D. A cellular homolog of hepatitis delta antigen: implications for viral replication and evolution. *Science* 1996 ; 274 : 90-4.

20. Salehi-Ashtiani K, Lupták A, Litovchick A, Szostak JW. A genome-wide search for ribozymes reveals an HDV-like sequence in the human CPEB3 gene. *Science* 2006 ; 313 : 1788-92.

21. Nigro JM, Cho KR, Fearon ER, Kern SE, Ruppert JM, Oliner JD, *et al*. Scrambled exons. *Cell* 1991 ; 64 : 607-13.

22. Zhang J, Liu H, Hou L, Wang G, Zhang R, Huang Y, *et al*. Circular RNA_LARP4 inhibits cell proliferation and invasion of gastric cancer by sponging miR-424-5p and regulating LATS1 expression. *Mol Cancer* 2017 ; 16 : 151.

23. Fu L, Chen Q, Yao T, Li T, Ying S, Hu Y, Guo J. Hsa_circ_0005986 inhibits carcinogenesis by acting as a miR-129-5p sponge and is used as a novel biomarker for hepatocellular carcinoma. *Oncotarget* 2017 ; 8 : 43878-88.

24. Han D, Li J, Wang H, Su X, Hou J, Gu Y, *et al*. Circular RNA circMTO1 acts as the sponge of microRNA-9 to suppress hepatocellular carcinoma progression. *Hepatology* 2017 ; 66 : 1151-64.

25. Wille M, Netter HJ, Littlejohn M, Yuen L, Shi M, Eden JS, *et al*. A Divergent Hepatitis D-Like Agent in Birds. *Viruses* 2018 ; 10 : E720.

26. Schulze A, Gripon P, Urban S. Hepatitis B virus infection initiates with a large surface protein-dependent binding to heparan sulfate proteoglycans. *Hepatology* 2007 ; 46 : 1759-68.

27. Verrier ER, Colpitts CC, Bach C, Heydmann L, Weiss A, Renaud M, *et al*. A targeted functional RNA interference screen uncovers glypican 5 as an entry factor for hepatitis B and D viruses. *Hepatology* 2016 ; 63 : 35-48.

28. Li W, Urban S. Entry of hepatitis B and hepatitis D virus into hepatocytes : Basic insights and clinical implications. *J Hepatol* 2016 ; 64 : S32-40.

29. Yan H, Zhong G, Xu G, He W, Jing Z, Gao Z, *et al*. Sodium taurocholate cotransporting polypeptide is a functional receptor for human hepatitis B and D virus. *Elife* 2012 ; 1 : e00049.

30. Ni Y, Lempp FA, Mehrle S, Nkongolo S, Kaufman C, Fälth M, *et al*. Hepatitis B and D viruses exploit sodium taurocholate co-transporting polypeptide for species-specific entry into hepatocytes. *Gastroenterology* 2014 ; 146 : 1070-83.

31. Alves C, Freitas N, Cunha C. Characterization of the nuclear localization signal of the hepatitis delta virus antigen. *Virology* 2008 ; 370 : 12-21.

32. Chou HC, Hsieh TY, Sheu GT, Lai MM. Hepatitis delta antigen mediates the nuclear import of hepatitis delta virus RNA. *J Virol* 1998 ; 72 : 3684-90.

33. Modahl LE, Lai MM. Transcription of hepatitis delta antigen mRNA continues throughout hepatitis delta virus (HDV) replication: a new model of HDV RNA transcription and replication. *J Virol* 1998 ; 72 : 5449-56.

34. Macnaughton TB, Shi ST, Modahl LE, Lai MMC. Rolling circle replication of hepatitis delta virus RNA is carried out by two different cellular RNA polymerases. *J Virol* 2002 ; 76 : 3920-7.

35. Huang WH, Chen YS, Chen PJ. Nucleolar targeting of hepatitis delta antigen abolishes its ability to initiate viral antigenomic RNA replication. *J Virol* 2008 ; 82 : 692-9.

36. Lee CH, Chang SC, Wu CH, Chang MF. A novel chromosome region maintenance 1-independent nuclear export signal of the large form of hepatitis delta antigen that is required for the viral assembly. *J Biol Chem* 2001 ; 276 : 8142-8.

37. Glenn JS, Watson JA, Havel CM, White JM. Identification of a prenylation site in delta virus large antigen. *Science* 1992 ; 256 : 1331-3.

38. Otto JC, Casey PJ. The hepatitis delta virus large antigen is farnesylated both in vitro and in animal cells. *J Biol Chem* 1996 ; 271 : 4569-72.

39. Hwang SB, Lai MM. Isoprenylation masks a conformational epitope and enhances trans-dominant inhibitory function of the large hepatitis delta antigen. *J Virol* 1994 ; 68 : 2958-64.

40. Huang HC, Lee CP, Liu HK, Chang MF, Lai YH, Lee YC, Huang C. Cellular Nuclear Export Factors TAP and Aly Are Required for HDAg-L-mediated Assembly of Hepatitis Delta Virus. *J Biol Chem* 2016 ; 291 : 26226-38.

41. Hwang SB, Lai MM. Isoprenylation mediates direct protein-protein interactions between hepatitis large delta antigen and hepatitis B virus surface antigen. *J Virol* 1993 ; 67 : 7659-62.

42. Freitas N, Cunha C, Menne S, Gudima SO. Envelope proteins derived from naturally integrated hepatitis B virus DNA support assembly and release of infectious hepatitis delta virus particles. *J Virol* 2014 ; 88 : 5742-54.

43. Verrier ER, Weiss A, Bach C, Heydmann L, Turon-Lagot V, Kopp A, *et al*. Combined small molecule and loss-of-function screen uncovers estrogen receptor alpha and CAD as host factors for HDV infection and antiviral targets. *Gut* 2019 ; sous presse. doi:10.1136/gutjnl-2018-317065.

44. Cao D, Haussecker D, Huang Y, Kay MA. Combined proteomic-RNAi screen for host factors involved in human hepatitis delta virus replication. *RNA* 2009 ; 15 : 1971-9.

45. Mota S, Mendes M, Penque D, Coelho AV, Cunha C. Changes in the proteome of Huh7 cells induced by transient expression of hepatitis D virus RNA and antigens. *J Proteomics* 2008 ; 71 : 71-9.

46. Mota S, Mendes M, Freitas N, Penque D, Coelho AV, Cunha C. Proteome analysis of a human liver carcinoma cell line stably expressing hepatitis delta virus ribonucleoproteins. *J Proteomics* 2009 ; 72 : 616-27.

47. Sikora D, Greco-Stewart VS, Miron P, Pelchat M. The hepatitis delta virus RNA genome interacts with eEF1A1, p54(nrb), hnRNP-L, GAPDH and ASF/SF2. *Virology* 2009 ; 390 : 71-8.

48. Zhang Z, Filzmayer C, Ni Y, Sültmann H, Mutz P, Hiet MS, *et al*. Hepatitis D virus replication is sensed by MDA5 and induces IFN-β/λ responses in hepatocytes. *J Hepatol* 2018 ; 69 : 25-35.

49. Pugnale P, Pazienza V, Guilloux K, Negro F. Hepatitis delta virus inhibits alpha interferon signaling. *Hepatology* 2009 ; 49 : 398-406.

50. Williams V, Brichler S, Khan E, Chami M, Dény P, Kremsdorf D, Gordien E. Large hepatitis delta antigen activates STAT-3 and NF-κB via oxidative stress. *J Viral Hepat* 2012 ; 19 : 744-53.

51. Aslan N, Yurdaydin C, Wiegand J, Greten T, Ciner A, Meyer MF, *et al*. Cytotoxic CD4+ T cells in viral hepatitis. *J Viral Hepat* 2006 ; 13 : 505-14.

52. Karimzadeh H, Kiraithe MM, Oberhardt V, Alizei ES, Bockmann J, Zur Wiesch JS, *et al*. Mutations in Hepatitis D Virus Allow it to Escape Detection by CD8+ T Cells and Evolve at the Population Level. *Gastroenterology* 2019. Sous presse. doi:10.1053/j.gastro.2019.02.003.

53. Negro F. Hepatitis D virus coinfection and superinfection. *Cold Spring Harb Perspect Med* 2014 ; 4 : a021550.

54. Smedile A, Verme G, Cargnel A, Dentico P, Opolon P, Vergani D, *et al*. Influence of Delta Infection on Severity of Hepatitis B. *The Lancet* 1982 ; 320 : 945-7.

55. Govindarajan S, Chin KP, Redeker AG, Peters RL. Fulminant B viral hepatitis: role of delta agent. *Gastroenterology* 1984 ; 86 : 1417-20.

56. Fattovich G, Boscaro S, Noventa F, Pornaro E, Stenico D, Alberti A, *et al*. Influence of hepatitis delta virus infection on progression to cirrhosis in chronic hepatitis type B. *J Infect Dis* 1987 ; 155 : 931-5.

57. Fattovich G, Giustina G, Christensen E, Pantalena M, Zagni I, Realdi G, Schalm SW. Influence of hepatitis delta virus infection on morbidity and mortality in compensated cirrhosis type B. The European Concerted Action on Viral Hepatitis (Eurohep). *Gut* 2000 ; 46 : 420-6.

58. Shattock AG, Morgan BM. Sensitive enzyme immunoassay for the detection of delta antigen and anti-delta, using serum as the delta antigen source. *J Med Virol* 1984 ; 13 : 73-82.

59. Shattock AG, Morris MC. Evaluation of commercial enzyme immunoassays for detection of hepatitis delta antigen and anti-hepatitis delta virus (HDV) and immunoglobulin M anti-HDV antibodies. *J Clin Microbiol* 1991 ; 29 : 1873-6.

60. Aragona M, Macagno S, Caredda F, Crivelli O, Lavarini C, Maran E, *et al*. Serological response to the hepatitis delta virus in hepatitis D. *Lancet* 1987 ; 1 : 478-80.

61. Chen X, Oidovsambuu O, Liu P, Grosely R, Elazar M, Winn VD, *et al*. A novel quantitative microarray antibody capture assay identifies an extremely high hepatitis delta virus prevalence among hepatitis B virus-infected mongolians. *Hepatology* 2017 ; 66 : 1739-49.

62. Mahale P, Aka PV, Chen X, Liu P, Fram BJ, Wang AS, *et al*. Hepatitis D Viremia Among Injection Drug Users in San Francisco. *J Infect Dis* 2018 ; 217 : 1902-6.

63. Brichler S, Le Gal F, Butt A, Chevret S, Gordien E. Commercial real-time reverse transcriptase PCR assays can underestimate or fail to quantify hepatitis delta virus viremia. *Clin Gastroenterol Hepatol* 2013 ; 11 : 734-40.

64. Brichler S, Le Gal F, Neri-Pinto F, Mansour W, Roulot D, Laperche S, Gordien E. Serological and molecular diagnosis of hepatitis delta virus infection: results of a French national quality control study. *J Clin Microbiol* 2014 ; 52 : 1694-7.

65. Le Gal F, Dziri S, Gerber A, Alloui C, Ben Abdesselam Z, Roulot D, *et al*. Performance Characteristics of a New Consensus Commercial Kit for Hepatitis D Virus RNA Viral Load Quantification. *J Clin Microbiol* 2017 ; 55 : 431-41.

66. Lempp FA, Ni Y, Urban S. Hepatitis delta virus : insights into a peculiar pathogen and novel treatment options. *Nat Rev Gastroenterol Hepatol* 2016 ; 13 : 580-9.

67. Wedemeyer H, Yurdaydìn C, Dalekos GN, Erhardt A, Çakaloğlu Y, Değertekin H, *et al*. Peginterferon plus Adefovir versus Either Drug Alone for Hepatitis Delta. *N Engl J Med* 2011 ; 364 : 322-31.

68. Yurdaydin C. New treatment option for delta virus: is a cure in sight ? *J Viral Hepat* 2019 ; sous presse. doi:10.1111/jvh.13081.

69. Buchmann B, Döhner K, Schirdewahn T, Sodeik B, Manns MP, Wedemeyer H, *et al*. A screening assay for the identification of host cell requirements and antiviral targets for hepatitis D virus infection. *Antiviral Res* 2017 ; 141 : 116-23.

70. Heidrich B, Yurdaydın C, Kabaçam G, Ratsch BA, Zachou K, Bremer B, *et al*. Late HDV RNA relapse after peginterferon alpha-based therapy of chronic hepatitis delta. *Hepatology* 2014 ; 60 : 87-97.

71. Baumert TF, Verrier ER, Nassal M, Chung RT, Zeisel MB. Host-targeting agents for treatment of hepatitis B virus infection. *Curr Opin Virol* 2015 ; 14 : 41-6.

72. Colpitts CC, Verrier ER, Baumert TF. Targeting Viral Entry for Treatment of Hepatitis B and C Virus Infections. *ACS Infect Dis* 2015 ; 1 : 420-7.

73. Crouchet E, Wrensch F, Schuster C, Zeisel MB, Baumert TF. Host-targeting therapies for hepatitis C virus infection: current developments and future applications. *Therap Adv Gastroenterol* 2018 ; 11 : 1-15.

74. Verrier ER, Heydmann L, Baumert TF, Schuster C. Le transporteur d'acides biliaires NTCP, un acteur majeur dans l'infection par les virus humains des hépatites offrant de nouvelles perspectives thérapeutiques. *Virologie* 2018 ; 22 : 55-66.

75. Verrier ER, Colpitts CC, Sureau C, Baumert TF. Hepatitis B virus receptors and molecular drug targets. *Hepatol Int* 2016 ; 10 : 567-73.

76. Petersen J, Dandri M, Mier W, Lütgehetmann M, Volz T, Weizsäcker F, von F, *et al*. Prevention of hepatitis B virus infection *in vivo* by entry inhibitors derived from the large envelope protein. *Nature Biotechnol* 2008 ; 26 : 335-41.

77. Barrera A, Guerra B, Notvall L, Lanford RE. Mapping of the hepatitis B virus pre-S1 domain involved in receptor recognition. *J Virol* 2005 ; 79 : 9786-98.

78. Gripon P, Cannie I, Urban S. Efficient Inhibition of Hepatitis B Virus Infection by Acylated Peptides Derived from the Large Viral Surface Protein. *J Virol* 2005 ; 79 : 1613-22.

79. Lütgehetmann M, Mancke LV, Volz T, Helbig M, Allweiss L, Bornscheuer T, *et al*. Humanized chimeric uPA mouse model for the study of hepatitis B and D virus interactions and preclinical drug evaluation. *Hepatology* 2012 ; 55 : 685-94.

80. Bogomolov P, Alexandrov A, Voronkova N, Macievich M, Kokina K, Petrachenkova M, *et al*. Treatment of chronic hepatitis D with the entry inhibitor myrcludex B: First results of a phase Ib/IIa study. *J Hepatol* 2016 ; 65 : 490-8.

81. Farci P, Niro GA. Current and Future Management of Chronic Hepatitis D. *Gastroenterol Hepatol (N Y)* 2018 ; 14 : 342-51.

82. Wedemeyer H, Bogomolov P, Blank A, Allweiss L, Dandri-Petersen M, Bremer B, *et al*. Final results of a multicenter, open-label phase 2b clinical trial to assess safety and efficacy of Myrcludex B in combination with Ténofovir in patients with chronic HBV/HDV co-infection. *J Hepatol* 2018 ; 68 : S3.

83. Lou L. Advances in Nucleotide Antiviral Development from Scientific Discovery to Clinical Applications: Ténofovir Disoproxil Fumarate for Hepatitis B. *J Clin Transl Hepatol* 2013 ; 1 : 33-8.

84. Wedemeyer H, Schöneweis K, Bogomolov P, Voronkova N, Chulanov V, Stepanova T, *et al*. Interim Results of a Multicentre. Open-Label Phase 2 Clinical Trial (MYR203) to Assess Safety and Efficacy of Myrcludex B in Combination with Peg-Interferon Alpha 2a in Patients with Chronic HBV/Hdv Co-Infection. *Hepatology* 2018 ; 68 : S11A.

85. Bordier BB, Marion PL, Ohashi K, Kay MA, Greenberg HB, Casey JL, Glenn JS. A prenylation inhibitor prevents production of infectious hepatitis delta virus particles. *J Virol* 2002 ; 76 : 10465-72.

86. Bordier BB, Ohkanda J, Liu P, Lee SY, Salazar FH, Marion PL, *et al*. In vivo antiviral efficacy of prenylation inhibitors against hepatitis delta virus. *J Clin Invest* 2003 ; 112 : 407-14.

87. Berndt N, Hamilton AD, Sebti SM. Targeting protein prenylation for cancer therapy. *Nat Rev Cancer* 2011 ; 11 : 775-91.

88. Koh C, Canini L, Dahari H, Zhao X, Uprichard SL, Haynes-Williams V, *et al*. Oral prenylation inhibition with lonafarnib in chronic hepatitis D infection: a proof-of-concept randomised, double-blind, placebo-controlled phase 2A trial. *Lancet Infect Dis* 2015 ; 15 : 1167-74.

89. Yurdaydin C, Keskin O, Kalkan Ç, Karakaya F, Çalişkan A, Karatayli E, *et al*. Optimizing lonafarnib treatment for the management of chronic delta hepatitis: The LOWR HDV-1 study. *Hepatology* 2018 ; 67 : 1224-36.

90. Wedemeyer H, Port K, Deterding K, Wranke A, Kirschner J, Bruno B, *et al*. A phase 2 dose-escalation study of lonafarnib plus ritonavir in patients with chronic hepatitis D : final results from the lonafarnib with ritonavir in HDV-4 (LOWR HDV-4) study. *J Hepatol* 2017 ; 66 : S24.

91. Koh C, Surana P, Han T, Fryzek N, Kapuria D, Etzion O, *et al*. A phase 2 study exploring once daily dosing of ritonavir boosted lonafarnib for the treatment of chronic delta hepatitis – end of study results from the LOWR HDV-3 study. *J Hepatol* 2017 ; 66 : S101-2.

92. Matsumura T, Hu Z, Kato T, Dreux M, Zhang YY, Imamura M, *et al*. Amphipathic DNA polymers inhibit hepatitis C virus infection by blocking viral entry. *Gastroenterology* 2009 ; 137 : 673-81.

93. Bernstein DI, Goyette N, Cardin R, Kern ER, Boivin G, Ireland J, *et al*. Amphipathic DNA polymers exhibit antiherpetic activity in vitro and in vivo. *Antimicrob Agents Chemother* 2008 ; 52 : 2727-33.

94. Beilstein F, Blanchet M, Vaillant A, Sureau C. Nucleic Acid Polymers Are Active against Hepatitis Delta Virus Infection In Vitro. *J Virol* 2018 ; 92 : e01416-1417.

95. Vaillant A. Nucleic acid polymers : Broad spectrum antiviral activity, antiviral mechanisms and optimization for the treatment of hepatitis B and hepatitis D infection. *Antiviral Res* 2016 ; 133 : 32-40.

96. Noordeen F, Scougall CA, Grosse A, Qiao Q, Ajilian BB, Reaiche-Miller G, *et al*. Therapeutic Antiviral Effect of the Nucleic Acid Polymer REP 2055 against Persistent Duck Hepatitis B Virus Infection. *PLoS ONE* 2015 ; 10 : e0140909.

97. Al-Mahtab M, Bazinet M, Vaillant A. Safety and Efficacy of Nucleic Acid Polymers in Monotherapy and Combined with Immunotherapy in Treatment-Naive Bangladeshi Patients with HBeAg+ Chronic Hepatitis B Infection. *PLoS ONE* 2016 ; 11 : e0156667.

98. Bazinet M, Pântea V, Cebotarescu V, Cojuhari L, Jimbei P, Albrecht J, *et al*. Safety and efficacy of REP 2139 and pegylated interferon alfa-2a for treatment-naive patients with chronic hepatitis B virus and hepatitis D virus co-infection (REP 301 and REP 301-LTF): a non-randomised, open-label, phase 2 trial. *Lancet Gastroenterol Hepatol* 2017 ; 2 : 877-89.

99. Vaillant A. REP 2139: Antiviral Mechanisms and Applications in Achieving Functional Control of HBV and HDV Infection. *ACS Infect Dis* 2018. Sous presse. doi:10.1021/acsinfecdis.8b00156.

9.4 Verrier ER et al., Cell Rep 2016;17:1357–1368

Article

Cell Reports

Solute Carrier NTCP Regulates Innate Antiviral Immune Responses Targeting Hepatitis C Virus Infection of Hepatocytes

Graphical Abstract

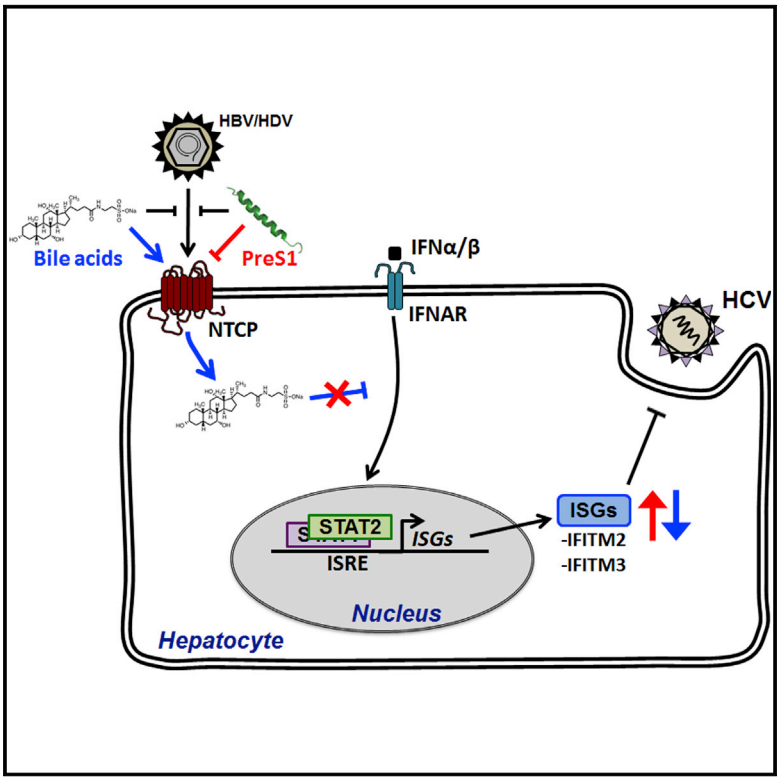

Authors

Eloi R. Verrier, Che C. Colpitts, Charlotte Bach, ..., Catherine Schuster, Mirjam B. Zeisel, Thomas F. Baumert

Correspondence

mirjam.zeisel@unistra.fr (M.B.Z.), thomas.baumert@unistra.fr (T.F.B.)

In Brief

Verrier et al. identify the sodium taurocholate co-transporter NTCP as a host factor regulating HCV infection. NTCP-mediated bile acid transport regulates innate responses targeting HCV infection. NTCP is a mediator of innate immunity and plays a role in the infection of multiple hepatotropic viruses.

Highlights

- NTCP is involved in hepatocyte infection by multiple viruses via distinct mechanisms
- NTCP facilitates HCV infection by modulating innate antiviral responses
- Solute carrier NTCP is a regulator of antiviral immune responses in the liver
- This function is relevant for infection and therapies for hepatotropic viruses

Accession Numbers

GSE85092

Verrier et al., 2016, Cell Reports *17*, 1357–1368
October 25, 2016
http://dx.doi.org/10.1016/j.celrep.2016.09.084

Cell Reports
Article

Solute Carrier NTCP Regulates Innate Antiviral Immune Responses Targeting Hepatitis C Virus Infection of Hepatocytes

Eloi R. Verrier,[1,2,14] Che C. Colpitts,[1,2,14] Charlotte Bach,[1,2] Laura Heydmann,[1,2] Laetitia Zona,[1,2] Fei Xiao,[1,2] Christine Thumann,[1,2] Emilie Crouchet,[1,2] Raphaël Gaudin,[1,2] Camille Sureau,[3] François-Loïc Cosset,[4,5,6,7,8] Jane A. McKeating,[9,10] Patrick Pessaux,[1,2,11] Yujin Hoshida,[12,13] Catherine Schuster,[1,2] Mirjam B. Zeisel,[1,2,*] and Thomas F. Baumert[1,2,11,15,*]

[1]INSERM, U1110, Institut de Recherche sur les Maladies Virales et Hépatiques, 67000 Strasbourg, France
[2]Université de Strasbourg, 67000 Strasbourg, France
[3]INTS, Laboratoire de Virologie Moléculaire, 75015 Paris, France
[4]CIRI-International Center for Infectiology Research, 69364 Lyon Cedex 07, France
[5]INSERM, U1111, 69007 Lyon, France
[6]Ecole Normale Supérieure, 69007 Lyon, France
[7]Centre National de la Recherche Scientifique (CNRS) UMR 5308, 69007 Lyon, France
[8]LabEx Ecofect, University of Lyon, 69007 Lyon, France
[9]Centre for Human Virology, University of Birmingham, Birmingham, UK
[10]NIHR Liver Biomedical Research Unit, University of Birmingham, Birmingham, UK
[11]Institut Hospitalo-universitaire, Pôle Hépato-digestif, Nouvel Hôpital Civil, 67000 Strasbourg, France
[12]Division of Liver Diseases, Department of Medicine, Icahn School of Medicine at Mount Sinai, New York, NY 10029, USA
[13]Liver Cancer Program, Tisch Cancer Institute, Icahn School of Medicine at Mount Sinai, New York, NY 10029, USA
[14]Co-first author
[15]Lead Contact
*Correspondence: mirjam.zeisel@unistra.fr (M.B.Z.), thomas.baumert@unistra.fr (T.F.B.)
http://dx.doi.org/10.1016/j.celrep.2016.09.084

SUMMARY

Chronic hepatitis B, C, and D virus (HBV, HCV, and HDV) infections are the leading causes of liver disease and cancer worldwide. Recently, the solute carrier and sodium taurocholate co-transporter NTCP has been identified as a receptor for HBV and HDV. Here, we uncover NTCP as a host factor regulating HCV infection. Using gain- and loss-of-function studies, we show that NTCP mediates HCV infection of hepatocytes and is relevant for cell-to-cell transmission. NTCP regulates HCV infection by augmenting the bile-acid-mediated repression of interferon-stimulated genes (ISGs), including *IFITM3*. In conclusion, our results uncover NTCP as a mediator of innate antiviral immune responses in the liver, and they establish a role for NTCP in the infection process of multiple viruses via distinct mechanisms. Collectively, our findings suggest a role for solute carriers in the regulation of innate antiviral responses, and they have potential implications for virus-host interactions and antiviral therapies.

INTRODUCTION

Hepatitis B and C viruses (HBV and HCV) are the leading causes of chronic liver disease worldwide (El-Serag, 2012). With ~400 million individuals chronically infected with HBV or HCV and at risk for severe liver disease, these viruses are a major global health burden (El-Serag, 2012; Wedemeyer et al., 2015). Although HBV and HCV differ in their genomic organization and life cycles, these viruses exclusively infect human hepatocytes (Baumert et al., 2014), suggesting that liver-specific factors are important for the life cycle of both viruses.

Viral entry pathways contribute to HBV and HCV liver tropism. HCV requires a number of host proteins, including cluster of differentiation 81 (CD81), scavenger receptor BI (SR-BI), claudin-1 (CLDN1), occludin (OCLN), and accessory factors, such as epidermal growth factor receptor (EGFR), to enter hepatocytes (Baumert et al., 2014; Lupberger et al., 2011; Martin and Uprichard, 2013; Zeisel et al., 2013b; Zona et al., 2013). Some of these host factors interact directly with HCV glycoproteins, whereas others contribute to HCV internalization by promoting co-receptor associations and inducing intracellular signaling pathways (Kim et al., 2013; Lupberger et al., 2011). While key host factors mediating HCV entry are well characterized (Zeisel et al., 2013a), it is only partially understood how cell entry is regulated. Furthermore, the role of innate immune responses targeting HCV entry is poorly understood.

The sodium taurocholate co-transporting polypeptide (NTCP), a bile acid transporter expressed at the hepatocyte basolateral membrane (Claro da Silva et al., 2013), was identified previously as a receptor for HBV and hepatitis D virus (HDV) (Ni et al., 2014; Yan et al., 2012). HDV can use HBV envelope proteins to assemble infectious particles and is widely used as a surrogate model to study HBV entry (Sureau, 2010). Exogenous NTCP

expression in NTCP-lacking human hepatoma cell lines (such as Huh7 and HepG2) renders these cells susceptible to HBV/HDV entry (Ni et al., 2014; Yan et al., 2012). The natural ligands of NTCP (i.e., conjugated and hydrophilic bile acids) compete with HBV/HDV for NTCP binding and inhibit viral infection (Yan et al., 2014). In contrast, bile acids have been shown to enhance HCV replication (Chang and George, 2007; Chhatwal et al., 2012), although the mechanisms are not yet defined. Furthermore, whether bile acid transporters such as NTCP play a role in infection of alternative hepatotropic viruses, such as HCV, is unclear. In this study, we tested the role of NTCP in HCV infection, and we identified the mechanisms by which a solute carrier affects infectivity of three major hepatotropic viruses.

RESULTS

NTCP Overexpression Enhances HCV Infection

To investigate the effect of NTCP expression on HCV infection, we transduced the Huh7.5.1 cell line (Zhong et al., 2005) to express human NTCP. Huh7.5.1-NTCP cells expressed significantly higher NTCP mRNA and protein levels (Figure 1A) and surface levels of NTCP (Figure S1A) than parental Huh7.5.1 cells. To confirm that NTCP is functional as a viral host factor in these cells, Huh7.5.1-NTCP cells were infected with recombinant HDV. Huh7.5.1-NTCP cells supported HDV infection, as demonstrated by the presence of HDV RNA and delta antigen (HDAg) 7 days post-inoculation (Figure 1B). Moreover, HDV infection was inhibited by the HBV preS1-derived peptide (Figure 1B), which binds to NTCP and prevents HBV/HDV entry (Schieck et al., 2013).

To assess if NTCP expression affects HCV infection, we used cell culture-derived HCV (HCVcc) and lentiviral particles pseudotyped with HCV E1E2 glycoproteins (HCVpp) of different genotypes. Expression of NTCP significantly enhanced HCVcc (Jc1 and JcR2A) infection and HCVpp (genotypes 1b, 2a, 3a, and 4) entry compared to the parental cells (normalized as 100%) (Figures 1C and 1D). Interestingly, entry of vesicular stomatitis virus pseudoparticles (VSVpp) and murine leukemia virus pseudoparticles (MLVpp) was not significantly affected by NTCP expression under these conditions (Figure 1D). The growth of Huh7.5.1 and Huh7.5.1-NTCP cells after seeding was similar, indicating that our observations were unrelated to effects on cell proliferation (Figure S1B). Furthermore, the effect of NTCP on HCV entry/infection was independent of the infectivity levels of different HCVpp and HCVcc strains (Figures S1C and S1D).

Since HCV can infect cells by direct cell-to-cell transmission (Meredith et al., 2013; Timpe et al., 2008), we evaluated the role of NTCP in this mode of viral dissemination. HCV-replicating Huh7.5.1 cells were co-cultured with GFP-expressing Huh7.5 cells (Lupberger et al., 2011; Xiao et al., 2014) transduced or not to express NTCP (Figure 1E). In this assay, the presence of an anti-envelope E2 antibody inhibits cell-free infection, allowing the specific assessment of cell-to-cell transmission. NTCP expression significantly increased the percentage of GFP-positive HCV-infected cells, suggesting that NTCP also plays a role in cell-to-cell spread (Figures 1F and 1G).

Silencing NTCP Expression Inhibits HCV Infection

We confirmed the role of NTCP in HCV infection by silencing NTCP expression in Huh7.5.1-NTCP cells using a small interfering RNA (siRNA) targeting NTCP, prior to infection with HCVcc. Following NTCP silencing in Huh7.5.1-NTCP cells, total protein expression was decreased by ~80%, which was reflected by decreased surface expression (Figure 2A). This corresponded to a significant decrease in HCVcc infection (Figure 2B). To rule out potential off-target effects, we tested multiple NTCP-targeting small hairpin RNA (shRNA) sequences in Huh7.5.1-NTCP cells. We confirmed that a decrease in NTCP expression (by shNTCP2 and shNTCP3) (Figure 2C) correlated with a decrease in HCVcc infection (Figure 2D). Furthermore, silencing NTCP expression with shNTCP2 decreased protein expression by >80% (Figure 2E), which significantly decreased entry of HCVpp into Huh7.5.1-NTCP cells (Figure 2F), confirming the relevance of NTCP for HCV entry.

NTCP Modulates HBV/HDV and HCV Infection via Distinct Mechanisms

To assess whether NTCP interacts directly with HCV glycoproteins, we measured binding of recombinant soluble HCV E2 (sE2) to cells. We observed no significant difference in sE2 binding to NTCP-expressing or parental cells (Figure 3A). However, sE2 treatment of Huh7.5.1 cells inhibited HCVcc infection (Figure 3B), confirming the functionality of the sE2 protein. These findings indicate that NTCP is not involved in E2 binding. Furthermore, NTCP expression did not affect the expression of canonical HCV entry factors in Huh7.5.1-NTCP cells compared to the parental cells (Figure 3C).

We next tested the effect of the HBV preS1-derived peptide, which is known to bind to NTCP and inhibit HBV/HDV entry (Ni et al., 2014). Although preS1 inhibited HDV infection of Huh7.5.1-NTCP cells after 1 hr pre-treatment, it had no effect on HCVpp entry under these conditions (Figure 3D), indicating that the HBV preS1-binding domain of NTCP is not required to promote HCV entry. We next evaluated whether the bile acid transporter function of NTCP is important for HCV entry. Huh7.5.1-NTCP cells were treated with the HBV preS1-derived peptide (König et al., 2014; Slijepcevic et al., 2015), which inhibits bile acid uptake in vitro (IC_{50}, 4 nM) (Ni et al., 2014), for 24, 48, and 72 hr prior to the addition of HDV, HCVpp, or VSVpp (Figures 3E–3G). PreS1 treatment (200 nM) significantly inhibited HCVpp entry in a time-dependent manner, with a maximal inhibition of ~70% after 72 hr (Figure 3E). Under these conditions, VSVpp entry also was reduced by preS1, although to a lesser extent (Figure 3F), suggesting a general effect on viral infection. In contrast, HDV infection was impaired by preS1 regardless of the treatment duration (Figure 3G). HCVcc infection also was decreased by 72-hr preS1 treatment (Figure 3H), confirming that our observations are relevant for the infectious virus and the full HCV life cycle. Taken together, our data suggest that long-term preS1 inhibition of NTCP-mediated bile acid transport perturbs cellular physiology to modulate HCV entry.

PreS1-Mediated Inhibition of NTCP Induces Interferon-Stimulated Gene Expression

Since preS1 only affected HCV entry after long-term treatment (Figure 3), we hypothesized that the bile acid transport activity

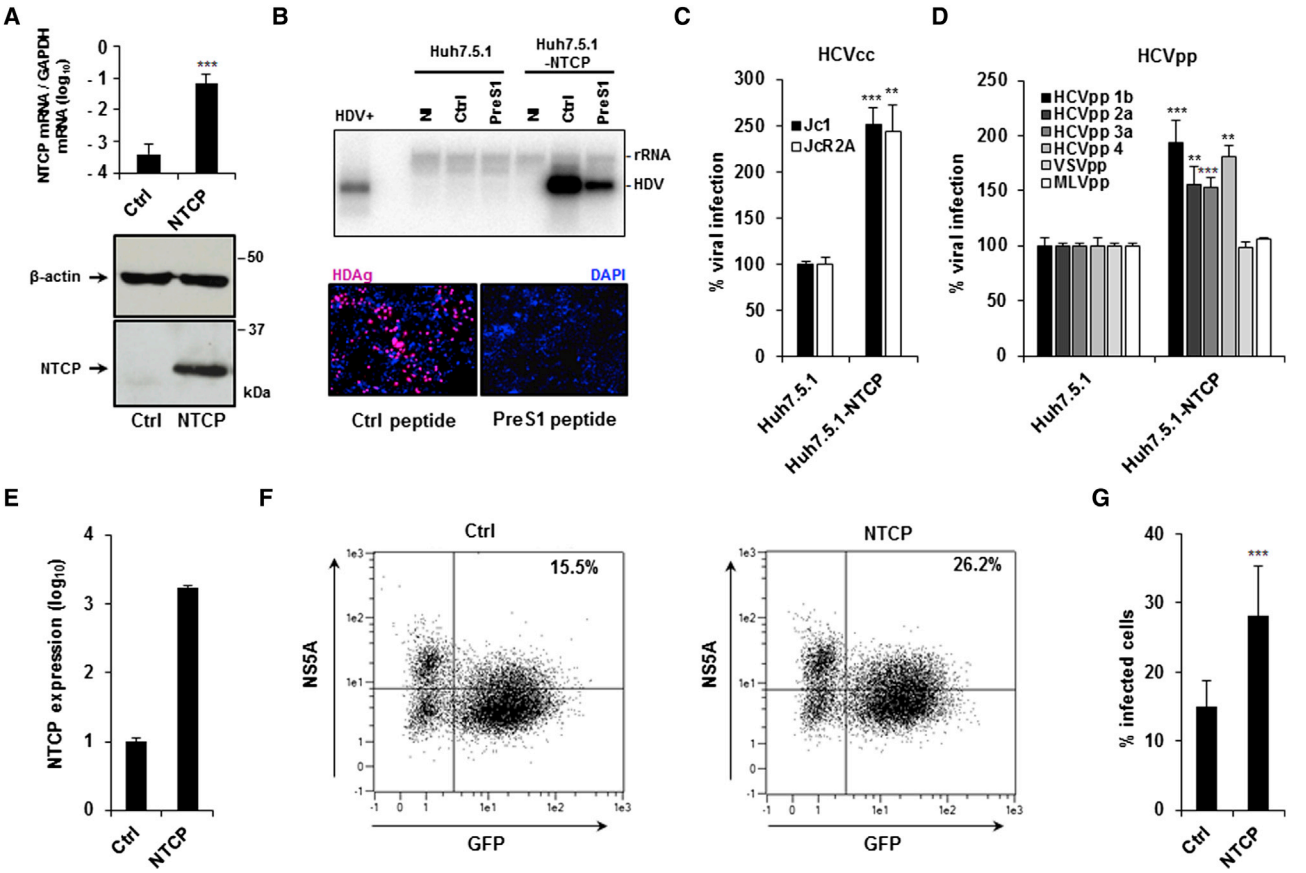

Figure 1. NTCP Expression Modulates HCV Infection

(A) NTCP expression in Huh7.5.1-NTCP cells compared to parental Huh7.5.1 cells evaluated by qRT-PCR and western blot. qRT-PCR results are expressed as means ± SD. NTCP expression was normalized by GAPDH expression (log) from three independent experiments performed in triplicate (n = 9).

(B) Functional evaluation of HDV infection in Huh7.5.1-NTCP cells using northern blot and immunofluorescence (IF). Huh7.5.1 and Huh7.5.1-NTCP cells were treated with an HBV-derived preS1 peptide (PreS1) or with a control peptide (Ctrl) (200 nM) and infected with recombinant HDV for 7 days. HDV RNA was detected by northern blot. HDV+ corresponds to ~2×10^7 HDV RNA genome equivalents extracted from HDV particles produced in Huh7 cells. NI, non-infected cells. One experiment is shown. For IF analysis, cells were fixed 7 days after infection and stained with HDAg-specific antibodies purified from HBV/HDV co-infected patients. HDV-positive cells are visualized in red. Cell nuclei were stained with DAPI (blue). One experiment is shown.

(C and D) HCVcc and HCVpp infection of NTCP-overexpressing cells. Huh7.5.1 and Huh7.5.1-NTCP cells were infected with HCVcc (C, Luc-Jc1 and Luc-JcR2A; D, HCVpp (genotypes 1b, 2a, 3a, and 4), VSVpp, and MLVpp). Infection was assessed after 72 hr by measuring luciferase activity. Results are expressed as means ± SEM percentage virus infection relative to parental Huh7.5.1 cells from three independent experiments (one performed in triplicate, one in quintuplicate, and one in hextuplicate; n = 14) (C) or three independent experiments performed in triplicate (n = 9, except MLVpp: two independent experiments performed in triplicate, n = 6).

(E–G) NTCP overexpression increases HCV cell-to-cell transmission. HCV-electroporated Huh7.5.1 were transduced or not (Ctrl) with lentiviruses expressing NTCP. (E) NTCP expression was assessed by qRT-PCR. Results are expressed as means ± SD relative NTCP expression (log) compared to NTCP expression in non-transduced cells (set at 1) from one experiment performed in triplicate (n = 3). Cells were then co-cultured with GFP-expressing Huh7.5.1 cells in the presence of neutralizing antibody AP33. (F and G) After NS5A staining, HCV cell-to-cell transmission was assessed by flow cytometry as the percentage of GFP- and NS5A-positive cells. One experiment is shown (F) and results are expressed as means ± SD percentage infected cells from two independent experiments (one performed in hextuplicate and one in nonuplicate; n = 15) (G).

of NTCP induces metabolic or transcriptional changes that regulate virus infection. To test this hypothesis, we evaluated the effect of preS1-NTCP binding on gene expression in hepatoma cells. We performed genome-wide microarray analyses of Huh7.5.1-NTCP cells that were treated with preS1 or a scrambled peptide (200 nM) for 48 hr. Gene set enrichment analysis (GSEA) indicated that preS1 treatment induces the expression of genes involved in bile acid and fatty acid metabolism, as previously described (Oehler et al., 2014). Unexpectedly, preS1 treatment also induced the expression of genes involved in innate immunity, such as IFNα responses and the Jak/Stat-signaling pathway (Table 1; Figure 4A). Interestingly, *IFITM2* and *IFITM3*, which encode two restriction factors targeting HCV entry (Narayana et al., 2015), were among the preS1-induced genes (Figure 4B).

To confirm that IFITMs function as restriction factors in Huh7.5.1-NTCP cells, we exogenously overexpressed IFITM2 and IFITM3 (Figure 4C). Indeed, IFITM2 and IFITM3 overexpression in Huh7.5.1-NTCP cells inhibited HCVcc infection (Figure 4D). However, as endogenous *IFITM2* expression in Huh7.5.1 and

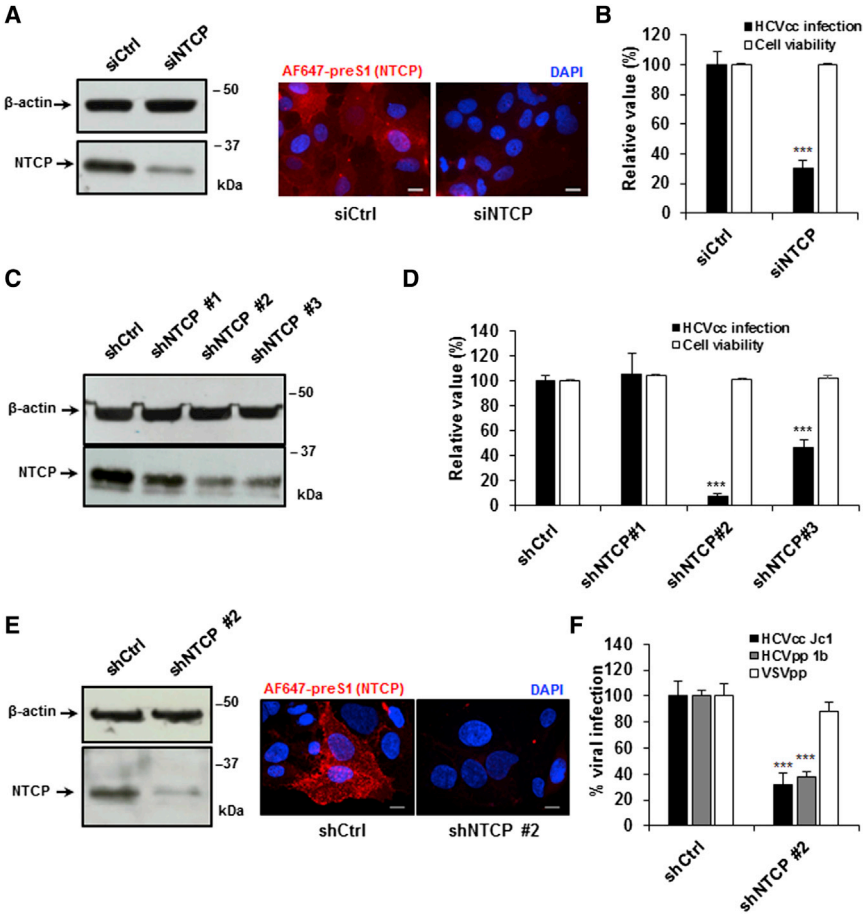

Figure 2. Silencing NTCP Expression Inhibits HCV Infection in Human Hepatocytes

(A and B) NTCP silencing in hepatoma cell lines. Huh7.5.1-NTCP cells were transfected with siRNA control (siCtrl) or siRNA targeting NTCP (siNTCP). siRNA efficacy was assessed 72 hr after transfection by western blot and IF (scale bar, 10 μm) (A), and cell viability was assessed using PrestoBlue reagent (B). 3 days after NTCP silencing, Huh7.5.1-NTCP cells were infected with HCVcc (Luc-Jc1). Infection was assessed after 72 hr by measuring luciferase activity. Results are expressed as means ± SEM percentage cell viability compared to cells treated with siCtrl from three independent experiments (one performed in sextuplicate and two performed in octuplicate; n = 22) and means ± SEM percentage HCVcc infection from four independent experiments performed in quadruplicate (n = 16) (B).

(C–F) Effect of shNTCP silencing in hepatoma cells. Huh7.5.1-NTCP cells were transduced with lentiviruses expressing shRNAs targeting NTCP (shNTCP1, shNTCP2, or shNTCP3) or control shRNA (shCtrl). shRNA efficacy was assessed 72 hr after transduction by western blot (C) or by western blot and IF (scale bar, 10 μm) (E). Cell viability was assessed using PrestoBlue reagent (D). Results are expressed as means ± SEM percentage cell viability from three independent experiments performed in octuplicate (n = 24). 3 days after NTCP silencing, Huh7.5.1-NTCP cells were infected with HCVcc (Luc-Jc1) (D and F), HCVpp (genotype 1b) (F), or VSVpp (F). Infection was assessed after 72 hr by measuring luciferase activity. Results are expressed as means ± SEM percentage HCVcc infection from three independent experiments (two performed in quadruplicate and one in sextuplicate; n = 14) (D), or they are expressed as means ± SEM percentage pseudoparticle entry from three independent experiments performed in triplicate (n = 9) (F) and as means ± SEM percentage HCVcc infection from three independent experiments performed in quadruplicate (n = 12) (F).

Huh7.5.1-NTCP cells was low and at the limit of detection, we focused on *IFITM3* in further functional studies. Notably, IFITM3 expression was decreased at the protein level by ~60% in Huh7.5.1-NTCP cells compared to parental cells (Figure 4E), suggesting that NTCP modulates *IFITM3* expression. To confirm that the changes in gene expression were directly related to NTCP and not to off-target effects of preS1, we selected *IFITM3* and two other genes involved in IFNα responses (*PARP9* and *CXCL10*) which were induced by preS1 treatment (Figure 4B), and we compared their expression levels in Huh7.5.1 and Huh7.5.1-NTCP cells. As expected, Huh7.5.1-NTCP cells had decreased mRNA expression of *IFITM3*, *PARP9*, and *CXCL10* compared to parental cells (Figure 4F), confirming the specific role of NTCP in the suppression of these genes. These data support previous findings that preS1 binds with high specificity to NTCP without off-target effects (Bogomolov et al., 2016).

Bile Acid Transport through NTCP Modulates the Expression of Interferon-Stimulated Genes to Affect HCV Infection

The gene expression analyses implied that NTCP facilitates HCV entry by altering the expression of interferon-stimulated genes (ISGs). Given that the physiological function of NTCP is to transport bile acids, and bile acids are known to affect ISG expression in hepatocytes (Graf et al., 2010; Podevin et al., 1999), we hypothesized that bile acid transport by NTCP regulates the expression of ISGs and viral infection. Since IFITM3 functions as an HCV restriction factor in our model system (Figure 4D), we selected *IFITM3* as a representative ISG for functional studies to probe the link between NTCP and the IFN response. To ensure that IFN responses are indeed functional in Huh7.5.1-NTCP cells, we treated cells with Poly(I:C) and IFNα2, and we evaluated ISG induction by the expression of *IFITM3*. Poly(I:C) stimulation of Huh7.5.1-NTCP cells significantly increased *IFITM3* expression (Figure S2A). Moreover, STAT1 phosphorylation (Figure S2B) and *IFITM3* mRNA expression (Figure S2C) were markedly induced after IFNα2 treatment. This induction was repressed by a specific antibody targeting the type I IFN receptor (IFNAR) (Figures S2B and S2C).

We then evaluated the effect of NTCP on IFN responses in these cells. The mere presence of NTCP decreased mRNA expression of *IFITM3* by ~50% compared to parental cells (Figure 5A). The addition of bile acid (100 μM sodium taurocholate) to Huh7.5.1-NTCP cells decreased *IFITM3* mRNA expression even

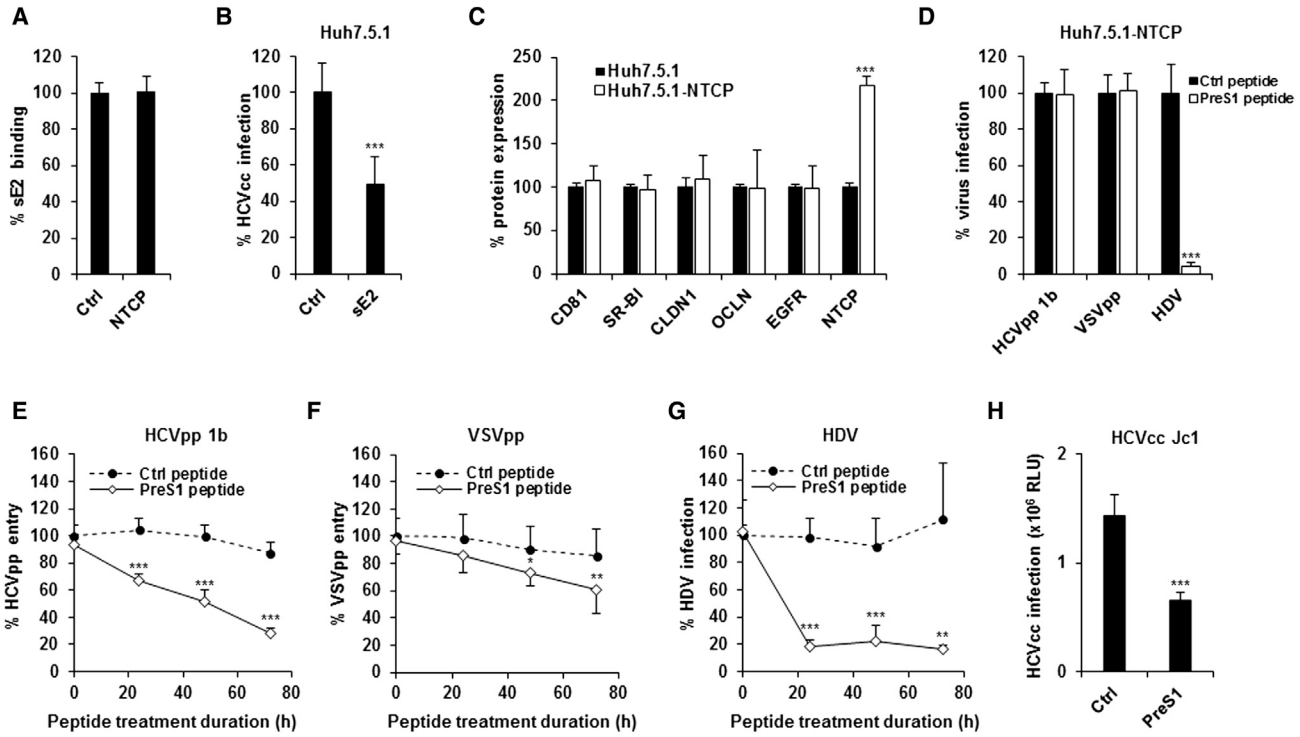

Figure 3. Distinct Roles of NTCP in HDV/HBV and HCV Infections

(A) Flow cytometry analysis of HCV glycoprotein sE2 binding to Huh7.5.1 (Ctrl) and Huh7.5.1-NTCP (NTCP). Results are expressed as means ± SD percentage sE2 binding compared to control cells from three independent experiments (two performed in triplicate and one in quadruplicate; n = 10).

(B) sE2 binding inhibits HCVcc infection. Huh7.5.1 cells were treated with soluble sE2 and then infected with HCVcc (Luc-Jc1). Infection was assessed after 72 hr by measuring luciferase activity. Results are expressed as means ± SD percentage HCVcc infection from three independent experiments performed in triplicate (n = 9).

(C) Flow cytometry analysis of HCV entry factor expression in Huh7.5.1-NTCP cells. Results are expressed as percentage protein expression compared to parental Huh7.5.1 cells (set at 100%) from four independent experiments performed in duplicate (n = 8).

(D) Effect of HBV preS1-derived peptide on HDV, HCVpp (genotype 1b), and VSVpp entry into Huh7.5.1-NTCP cells. Huh7.5.1-NTCP cells were treated for 1 hr with preS1 or Ctrl peptide (200 nM). For HDV, cells were then infected with recombinant HDV for 7 days. Total RNA was purified and HDV RNA was detected by qRT-PCR. Results are expressed as percentage HDV RNA level compared to non-treated Huh7.5.1-NTCP cells from three independent experiments performed in triplicate (n = 9). For HCVpp (genotype 1b) and VSVpp, cells were infected with pseudoparticles and infection was assessed after 72 hr by luciferase activity. Results are expressed as means ± SD percentage viral entry from three independent experiments performed in quintuplicate (n = 15).

(E–G) Time-dependent inhibition of viral entry by preS1 treatment. Cells were treated with preS1 or Ctrl peptide for 24, 48, and 72 hr prior to infection with HCVpp (genotype 1b), VSVpp, or HDV. Infection was assessed as described above. (E) Results are expressed as means ± SD percentage HCVpp entry from five independent experiments performed in triplicate (n = 15). (F) Results are expressed as means ± SD percentage VSVpp entry from four independent experiments performed in triplicate (n = 12). (G) Results are expressed as means ± SD percentage HDV infection from three independent experiments performed in duplicate (n = 6).

(H) Treatment with preS1 inhibits HCVcc infection. Cells were treated with preS1 or Ctrl peptide for 72 hr prior to infection with HCVcc (Luc-Jc1). Infection was assessed after 72 hr by measuring luciferase activity. Results are expressed as means ± SD HCVcc infection (relative light unit, RLU) from three independent experiments performed in triplicate (n = 9).

further, whereas blocking bile acid transport with the preS1 peptide restored *IFITM3* mRNA expression to the levels observed in Huh7.5.1 cells (Figure 5A). These findings suggest that the effect of NTCP on ISG expression and HCV infection is dependent on bile acid. Indeed, the addition of supplementary bile acid in the cell culture medium dose-dependently increased HCVcc infection in Huh7.5.1-NTCP cells, but not in parental cells (Figure 5B).

We next evaluated the effect of preS1 treatment on IFITM3 protein expression and HCV infection in the presence of bile acids. Reflecting our observations of the mRNA level (Figure 5A), IFITM3 protein expression was decreased in Huh7.5.1-NTCP cells compared to Huh7.5.1 cells in the presence of bile acid (Figure 5C). However, treatment of Huh7.5.1-NTCP cells with preS1 (to block bile acid uptake) under these conditions induced a 2-fold increase in IFITM3 protein expression, effectively restoring it to the level observed in Huh7.5.1 cells (Figure 5C). Furthermore, treatment of Huh7.5.1-NTCP cells with the preS1 peptide in the presence of bile acid inhibited HCVcc infection (Figure 5D). We did not observe these effects in Huh7.5.1 cells (Figures 5C and 5D), confirming that the bile acid-mediated effect is dependent on NTCP.

Interestingly, when we silenced *IFITM3* expression (Figure 5E) in the presence of bile acid, we observed an increase in HCV infection (Figure 5F). However, this effect was no longer

Table 1. Hallmark Gene Sets Significantly Induced, Positive NES[a], or Repressed, Negative NES, after preS1 Treatment in Huh7.5.1-NTCP Cells Shown in Figure 4

Gene Set	NES[a]	p value	FDR[b]
Bile acid metabolism	2.32	<0.001	<0.001
Coagulation	2.25	<0.001	<0.001
Xenobiotic metabolism	2.20	<0.001	<0.001
Fatty acid metabolism	2.20	<0.001	<0.001
Heme metabolism	2.04	<0.001	<0.001
Adipogenesis	1.91	<0.001	<0.001
Peroxisome	1.90	<0.001	<0.001
Interferon alpha response	1.90	<0.001	<0.001
Oxidative phosphorylation	1.90	<0.001	<0.001
Estrogen response late	1.89	<0.001	<0.001
Angiogenesis	1.72	0.002	0.003
Cholesterol homeostasis	1.68	0.004	0.005
Hypoxia	1.61	<0.001	0.010
Interferon gamma response	1.60	<0.001	0.009
Reactive oxygen species pathway	1.59	0.013	0.010
Estrogen response early	1.58	<0.001	0.011
Myogenesis	1.57	0.002	0.012
IL2 STAT5 signaling	1.54	<0.001	0.013
IL6 JAK STAT3 signaling	1.54	0.008	0.014
Complement	1.49	0.003	0.021
MTORC1 signaling	−1.50	0.005	0.012
Unfolded protein response	−1.82	<0.001	<0.001
G2M checkpoint	−2.01	<0.001	<0.001
E2F targets	−2.02	<0.001	<0.001
MYC targets V2	−2.54	<0.001	<0.001
MYC targets V1	−2.64	<0.001	<0.001

[a]Normalized enrichment score.
[b]False discovery rate.

observed in the presence of preS1 to block bile acid uptake into the cells or in the absence of bile acid (Figure 5F). These results suggest that bile acid-mediated suppression of other ISGs (which may otherwise compensate the absence of an individual ISG) is necessary to observe a functional effect of *IFITM3* silencing on HCV infection. Differences in bile acid levels in cell culture medium also may explain why IFITM3 was not identified as an HCV restriction factor in previous screens (Brass et al., 2009).

NTCP-Mediated Bile Acid Transport Affects ISG Expression and HCV Entry into Primary Human Hepatocytes

For validation in a more physiological context, we investigated the role of NTCP during HCV entry into primary human hepatocytes (PHHs). First, we silenced NTCP expression in PHHs using an NTCP-targeting siRNA. Following transfection of siNTCP, the expression of NTCP protein was reduced by ~50% (Figure 6A). The decrease in NTCP expression correlated with a significant decrease in the entry of HCVpp genotype 1b (Figure 6B).

We next evaluated whether NTCP-mediated bile acid transport affects ISG expression in PHHs. We treated PHHs with bile acid in the presence or absence of preS1 and performed genome-wide microarray analyses. GSEA showed that bile acid treatment of PHHs suppressed the expression of genes involved in the IFNα response (normalized enrichment score [NES] −2.11; p value < 0.001; false discovery rate [FDR] < 0.001) (Figure 6C) as well as other immune-related pathways. However, treatment of PHHs with preS1 under these conditions induced the expression of genes involved in the IFNα response (NES 1.5; p value = 0.014; FDR = 0.035) to restore their expression levels to normal conditions (i.e., PHHs in the absence of bile acid) (Figure 6D). These findings are consistent with our microarray analyses in Huh7.5.1-NTCP cells (Figure 4), where expression of genes involved in IFNα responses was regulated by treatment with preS1. Interestingly, *IFITM1*, *IFITM2*, and *IFITM3* were among the genes suppressed by bile acid treatment of PHHs (Figure 6C), and their expression could be rescued by the addition of preS1 (Figure 6D). Moreover, the effects we observed in PHHs were dependent on the presence of bile acid, as treatment with preS1 in the absence of bile acid did not have a major impact on the expression of these genes (data not shown).

We next evaluated the functional effect of these changes in ISG expression on HCVpp entry into PHHs. Treatment of PHHs with bile acid increased HCVpp genotype 1b entry, and the addition of preS1 under these conditions restored the level of infection to that observed in the absence of bile acid (Figure 6E). Interestingly, the concentration of bile acid required to see a robust effect for HCVpp entry into PHHs was higher than for HCVcc infection of Huh7.5.1-NTCP cells (Figure 5B), which may reflect different bile acid uptake efficiency in PHHs or that the effect is more potent when the full HCV life cycle is measured and ISGs targeting different steps of the viral infection cycle are involved. Finally, to confirm that the activity of preS1 is linked to IFN responses, we tested the effect of preS1 in the presence of an antibody blocking the type I IFN receptor. In the presence of this antibody, preS1 no longer inhibited HCVpp entry into PHHs (Figure 6F), suggesting that the inhibitory effect of preS1 against HCV entry is indeed mediated by the IFN signal transduction cascade and resulting IFN responses in PHHs.

DISCUSSION

NTCP was recently described as a major receptor for HBV and HDV entry. Here we show that NTCP also plays a role in HCV infection. Exogenous expression of NTCP in Huh7.5.1 hepatoma cells increased HCV infection, whereas silencing of NTCP expression reduced HCV entry (Figures 1 and 2). Using microarray analyses in cell lines (Figure 4) and PHHs (Figure 6), we discovered that NTCP-mediated bile acid transport regulates innate antiviral responses, thereby inhibiting HCV infection and uncovering a role for NTCP as a regulator of antiviral immunity.

Innate antiviral responses mediated by ISGs have been shown to target multiple steps during viral infection, including entry (Liu et al., 2011; Smith et al., 2014). IFITM1, IFITM2, and IFITM3, which belong to a group of five IFN-induced transmembrane

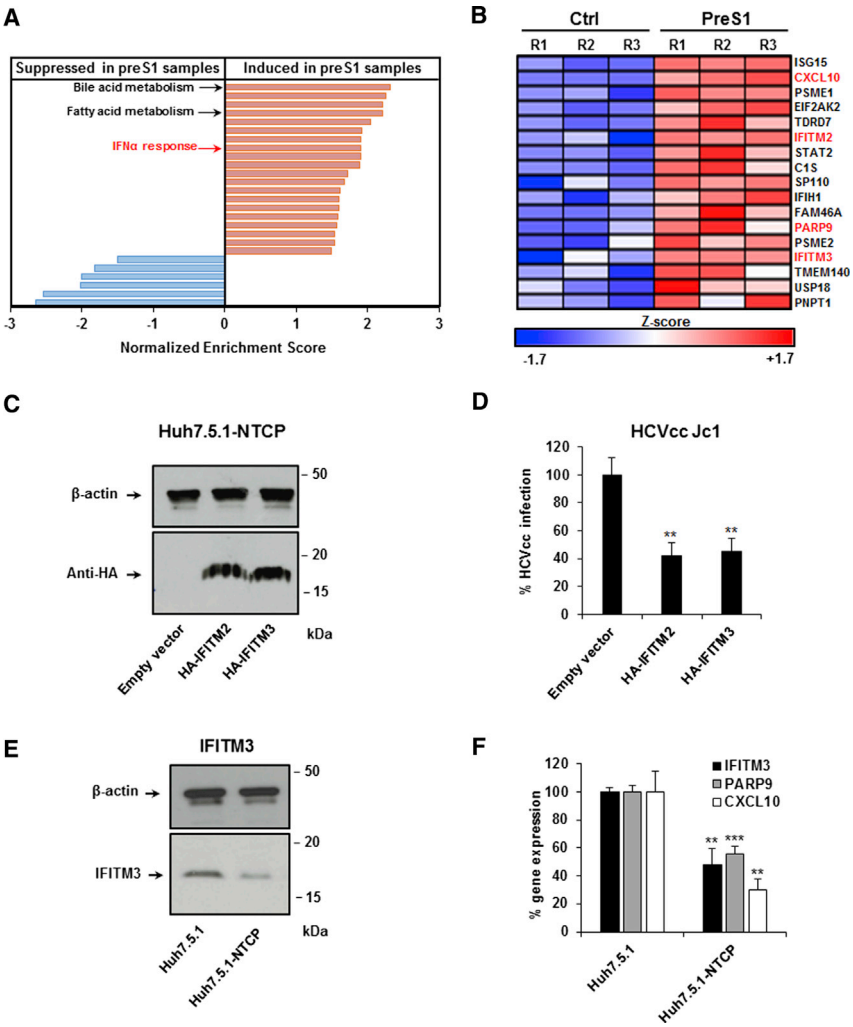

Figure 4. Binding of HBV-Derived preS1 Peptide to NTCP Increases ISG Expression

Huh7.5.1-NTCP cells were treated with preS1 or control peptide for 48 hr. Cells were then lysed and total RNA was extracted and purified. Total gene expression was analyzed by genome-wide microarray. Three independent biological replicates per condition from one experiment were analyzed.

(A) Schematic representation of Hallmark gene sets that are significantly induced (red, including bile acid metabolism and IFNα response) or repressed (blue) following preS1 treatment, based on Table 1. $p < 0.05$ and FDR < 0.05 were considered statistically significant.

(B) List of individual IFNα response genes that are significantly ($p < 0.05$) overexpressed following preS1 treatment. Individual *Z* scores for each sample are presented. Negative *Z* score (blue) and positive *Z* score (red) correspond to repression and induction of the indicated genes, respectively.

(C and D) IFITM2 and IFITM3 overexpression inhibits HCV infection. Huh7.5.1-NTCP cells were transfected with an empty vector, pCMV-HA-hIFITM2, or pCMV-HA-hIFITM3 for 3 days. (C) Expression of transduced proteins as assessed by anti-HA western blot is shown. (D) Transduced cells were then infected for 3 days with HCVcc (Luc-Jc1). Infection was assessed after 72 hr by measuring luciferase activity. Results are expressed as means ± SD percentage HCVcc infection compared to control cells (set at 100%) from three independent experiments performed in triplicate (n = 9).

(E) IFITM3 protein expression in hepatoma cells. IFITM3 protein expression was assessed by western blot in Huh7.5.1 and Huh7.5.1-NTCP cells. One experiment is shown.

(F) *IFITM3*, *PARP9*, and *CXCL10* expression in hepatoma cells. Basal expression of *IFITM3*, *PARP9*, and *CXCL10* mRNA was quantified by qRT-PCR in Huh7.5.1 and Huh7.5.1-NTCP cells. Results are expressed as means ± SD percentage gene expression compared to expression levels in Huh7.5.1 cells (set at 100%) from three independent experiments performed in triplicate (n = 9).

proteins (Smith et al., 2014), have been shown to exert broad antiviral activity against a range of viruses, including VSV, HIV, dengue virus, influenza virus, and Zika virus (Savidis et al., 2016; Smith et al., 2014). Interestingly, IFITM2 and IFITM3 were recently reported to restrict HCV infection at a late entry step by targeting HCV for lysosomal degradation following endocytosis (Narayana et al., 2015). IFITM1 was shown to interact with HCV co-receptors at tight junctions to disrupt the HCV entry process by alternative mechanisms (Wilkins et al., 2013).

Given that bile acids have been shown to modulate cellular antiviral responses (Graf et al., 2010; Podevin et al., 1999), we hypothesized that NTCP affects the induction of ISG expression via its bile acid transport activity. Indeed, the expression of ISGs (including *IFITM1*, *IFITM2*, and *IFITM3*) in PHHs was suppressed by the addition of bile acid (Figure 6C). However, expression of these ISGs in PHHs was restored by addition of the preS1 peptide, which blocks NTCP-mediated bile acid uptake (Figure 6D). Furthermore, modulation of the expression of IFITM3 by bile acid or preS1 treatment had a clear functional effect on HCV infection (Figures 5 and 6). Our findings are consistent with a previous report showing that bile acids affect HCV replication (Chhatwal et al., 2012), probably by similar mechanisms as those we describe here. In this study, we selected *IFITM3* as a representative ISG for functional characterization, but the expression of other ISGs is also affected by bile acids (Figure 6), likely contributing further to the overall effect on HCV infection. Since ISGs broadly restrict viral infection, this is consistent with the time-dependent effect of preS1 on VSVpp entry that we observed (Figure 3).

Our data suggest that NTCP facilitates HCV infection by modulating bile acid transport and ISG expression. ISGs also restrict HCV cell-to-cell transmission (Meredith et al., 2014), consistent with our finding that NTCP contributes to HCV cell-to-cell spread (Figures 1E–1G). It should be noted that NTCP expression did not appear to affect HCV entry in a recent Huh7 cell line model (Meredith et al., 2016). Huh7.5.1 cells are derived from Huh7.5 cells, which differ from Huh7 cells by a single point mutation in the retinoic acid-inducible gene-I (Bartenschlager

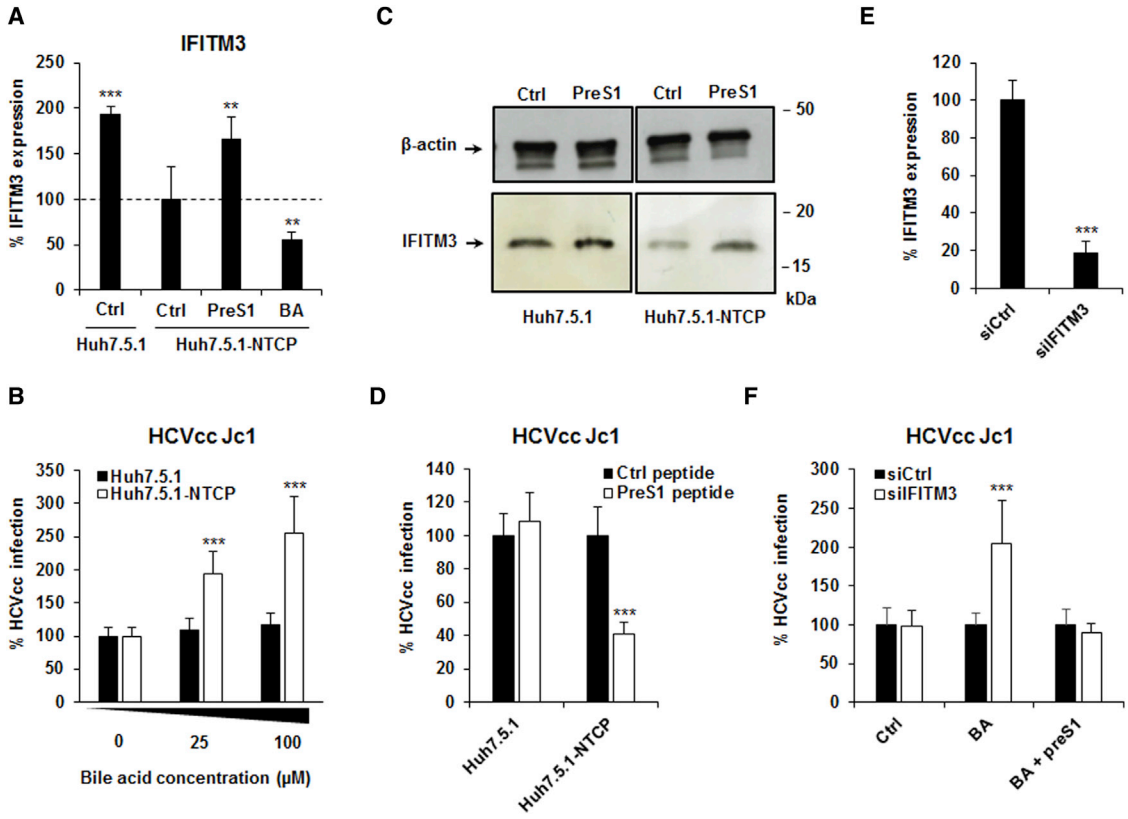

Figure 5. Bile Acid Uptake Enhances HCV Infection by Decreasing ISG Expression

(A) The impact of bile acid and preS1 treatment on *IFITM3* expression. Huh7.5.1-NTCP cells were treated with the bile acid (BA) sodium taurocholate (100 μM) or with 200 nM preS1 for 72 hr. IFITM3 expression was then quantified by qRT-PCR. Results are expressed as means ± SD percentage IFITM3 expression compared to untreated (Ctrl) Huh7.5.1-NTCP cells (set at 100%) from three independent experiments performed in duplicate (n = 6).

(B) The impact of bile acid on HCVcc infection. Huh7.5.1 and Huh7.5.1-NTCP cells were treated 0, 25, or 100 μM sodium taurocholate for 72 hr and then infected with HCVcc (Luc-Jc1). Results are expressed as means ± SD percentage HCVcc infection compared to untreated (Ctrl) Huh7.5.1 and Huh7.5.1-NTCP cells (both set at 100%) from three independent experiments performed in triplicate (n = 9).

(C and D) Effect of preS1-mediated inhibition of bile acid uptake on IFITM3 protein expression and HCVcc infection. Huh7.5.1 and Huh7.5.1-NTCP cells were treated with sodium taurocholate (100 μM) in the presence or absence of preS1 peptide for 72 hr. (C) IFITM3 protein expression was assessed by western blot. One experiment is shown. (D) Cells were then infected by HCVcc (Jc1) for 3 days. Results are expressed as means ± SD percentage HCVcc infection compared to Huh7.5.1 and Huh7.5.1-NTCP cells treated with control peptide (both set at 100%) from three independent experiments performed in triplicate (n = 9).

(E and F) Silencing of *IFITM3* expression increases HCV infection in a bile acid-dependent manner. Huh7.5.1-NTCP cells were transfected with siRNA control (siCtrl) or siRNA targeting IFITM3 (siIFITM3) and then treated for 72 hr in the absence or presence of BA (100 μM) in the presence of either preS1 or Ctrl peptide (200 nM). (E) Then 3 days after transfection, silencing efficacy was assessed by measuring expression of *IFITM3* mRNA by qRT-PCR. Results are expressed as means ± SD percentage *IFITM* expression from four independent experiments performed in triplicate (n = 12). (F) Cells were then infected with HCVcc Luc-Jc1. Infection was assessed after 72 hr by measuring luciferase activity. Results are expressed as means ± SD percentage HCVcc infection compared to cells treated with siCtrl (set at 100% for each condition) from four independent experiments performed in triplicate (n = 12).

and Pietschmann, 2005; Zhong et al., 2005). This may explain the differences observed between the two cell lines. Moreover, differences in bile acid concentrations in cell culture medium may be responsible for differences in the effect of NTCP on cell entry of HCV (Figure 5C). However, our loss-of-function studies and microarray analyses in PHHs (Figure 6) clearly demonstrate the impact of NTCP on HCV infection in primary cells with physiological innate immune responses.

For HBV/HDV infection, viral entry requires direct interaction with NTCP (Ni et al., 2014; Yan et al., 2012). Furthermore, HBV binding to NTCP may interfere with the physiological function of NTCP (i.e., bile acid uptake), and NTCP ligands can abrogate HBV/HDV infection (Oehler et al., 2014; Yan et al., 2014). In contrast, NTCP modulates HCV entry independently of direct binding mechanisms. We confirmed the inhibitory effect of the HBV preS1-derived peptide on HDV infection following 1-hr treatment (Figure 3D), but we did not see a corresponding effect on HCV infection under these conditions. Furthermore, the effect of NTCP on HCV infection does not appear to involve HCV E2 or binding factors CD81 and SR-BI (Pileri et al., 1998; Scarselli et al., 2002) (Figures 3A and 3B). NTCP expression did not modulate the expression of canonical entry factors CLDN1 and OCLN or EGFR either (Figure 3C).

Other mechanisms may contribute to the effects of NTCP on viral entry and infection that we observed. Indeed, modulation of NTCP bile acid transport activity by preS1 affected IFN

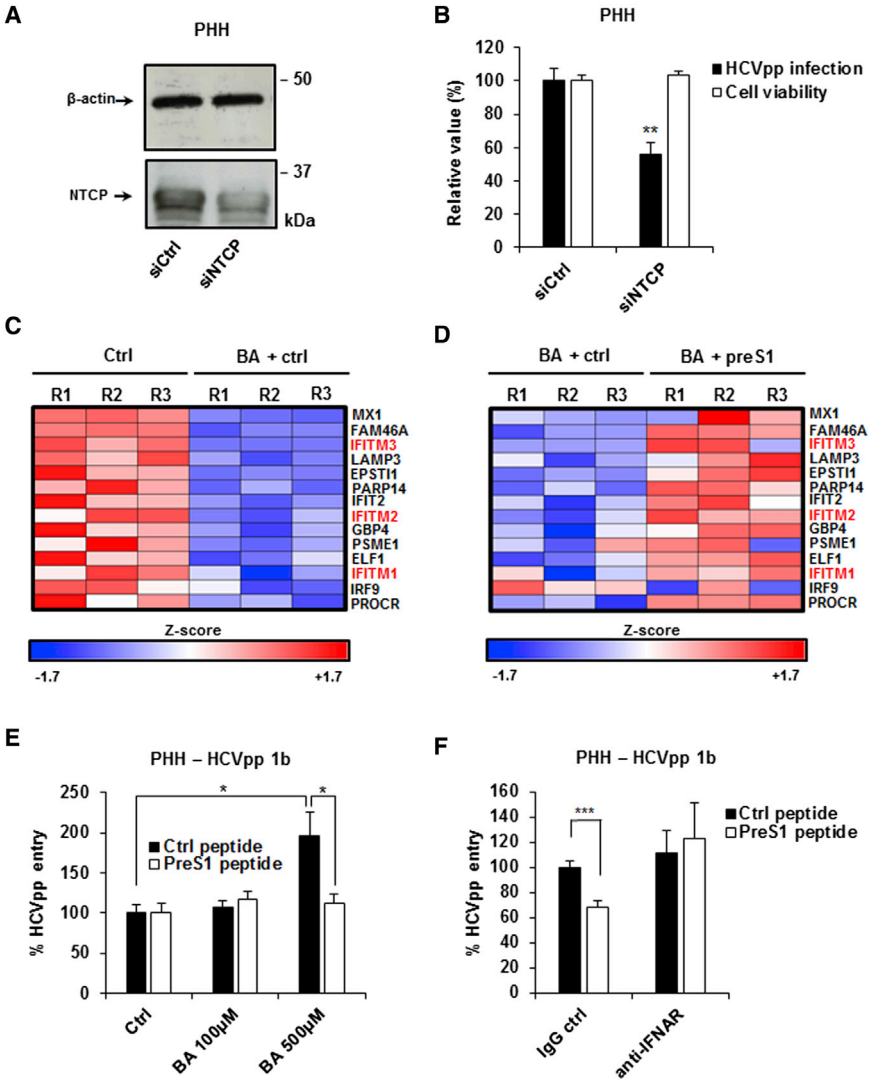

Figure 6. NTCP-Mediated Bile Acid Uptake Modulates ISG Expression and HCV Entry in PHHs

(A and B) Silencing NTCP expression in PHHs. PHHs were transfected with siRNA control (siCtrl) or siRNA targeting NTCP (siNTCP). 3 days after transfection, siRNA efficacy was assessed by western blot (A), and cell viability was assessed using PrestoBlue reagent (B). Results are expressed as means ± SEM percentage cell viability compared to cells treated with siCtrl from two independent experiments performed in quintuplicate (n = 10) (B). 3 days after NTCP silencing, PHHs were incubated with HCVpp (genotype 1b). Infection was assessed after 72 hr by measuring luciferase activity. Results are expressed as means ± SEM percentage HCVpp entry from three independent experiments performed in triplicate (n = 9) (B).

(C and D) Bile acids modulate the expression of ISGs in PHHs. PHHs from a single donor were treated with the bile acid (BA) sodium taurocholate (500 μM) in the presence or absence of the preS1 peptide (400 nM) for 48 hr. Cells were then lysed and total RNA was extracted and purified. Total gene expression was analyzed by genome-wide microarray. Three independent biological replicates per condition were analyzed. (C) Individual IFNα response genes that are significantly ($p < 0.05$) repressed following BA treatment are shown. Individual *Z* scores for each sample are presented. Negative *Z* score (blue) and positive *Z* score (red) correspond to repression and induction of the indicated genes, respectively. (D) Effect of preS1 treatment on the expression of IFNα response genes presented in (C). Individual *Z* scores for each sample are presented.

(E) Effect of bile acid and preS1 treatment on HCVpp infection in PHHs. PHHs were treated with increasing concentrations (0, 100, and 500 μM) of BA in the presence of either preS1 or Ctrl peptide (400 nM) for 72 hr and then infected with HCVpp (genotype 1b). Infection was assessed after 72 hr by measuring luciferase activity. Results are expressed as means ± SEM percentage HCVpp entry compared to untreated PHHs in the presence of the control peptide (set at 100%) from four independent experiments performed in triplicate (n = 12).

(F) PreS1 inhibition of HCVpp entry is dependent on the IFN-signaling pathway in PHHs. PHHs were treated with 500 μM BA in the presence of preS1 or a scrambled control peptide (400 nM), with or without treatment with an antibody targeting the type I IFN receptor (IFNAR) for 72 hr. Cells were then infected with HCVpp (genotype 1b) and infection was assessed after 72 hr by measuring luciferase activity. Results are expressed as means ± SEM percentage HCVpp entry compared to PHHs treated with the control peptide and an IgG control (set at 100%) from three independent experiments (one performed in triplicate and two in quintuplicate; n = 13).

responses, but also bile acid metabolism and cholesterol homeostasis in Huh7.5.1-NTCP cells as well as other pathways (Table 1). In particular, modulation of bile acid metabolism and cholesterol homeostasis by preS1 would alter cellular cholesterol pools, which has been shown to affect the activation of type I IFN responses (York et al., 2015) and may potentially contribute to the effect on HCV infection that we observed. Furthermore, modulation of signaling and transcription factor targets (Table 1) may have additional effects on viral replication and translation.

Our results demonstrate that NTCP, acting by distinct mechanisms, is relevant for the three major viruses causing chronic hepatitis and liver disease. This finding could contribute to the development of antiviral strategies targeting NTCP. Targeting viral cell entry with receptor antagonists, antibodies, peptides, and receptor kinase inhibitors has provided perspectives to prevent and treat chronic hepatitis B and C infections (Colpitts et al., 2015). Myrcludex B, a preS1-derived peptide targeting NTCP (Ni et al., 2014; Volz et al., 2013), has been shown to protect against HBV infection (Petersen et al., 2008), to modulate viral spread in animal models (Volz et al., 2013), and to decrease HDV viral load in patients in a phase II clinical trial (Bogomolov et al., 2016). Here we show that preS1-NTCP binding enhances the expression of ISGs. These data suggest that myrcludex B may inhibit HBV

infection by a dual mode of action, by interfering with viral binding and potentially increasing ISG expression. NTCP-targeting agents in clinical development also may inhibit HCV infection, which is of interest particularly for patients with HBV/HDV/HCV co-infections.

NTCP is a member of the solute carrier (SLC) family of proteins, a group of membrane proteins having crucial roles in many physiological functions (César-Razquin et al., 2015). However, these proteins are relatively uncharacterized. Here we uncover NTCP as a mediator of innate antiviral responses in hepatocytes and establish a role for NTCP in the entry process of multiple viruses. Our data uncover an important role of SLCs in virus-host interactions by linking their function to the regulation of innate immune responses. Moreover, bile acid transport through SLCs profoundly affects liver gene expression (Table 1).

Overall, we have identified NTCP as a regulator of innate immune responses in the human liver. These findings improve the understanding of virus-host interactions in the human liver, and they may open perspectives for the development of broad antiviral therapies targeting hepatotropic viruses that cause chronic liver disease and cancer.

EXPERIMENTAL PROCEDURES

Cell Lines

The sources for 293T and Huh7.5.1 cells have been described (Lupberger et al., 2011). Huh7.5.1 cells were seeded in six-well plates at 50% confluency 1 day prior to transduction with human NTCP-expressing VSVpp (GeneCopoeia). Cells were incubated in DMEM (Gibco) containing 10% fetal bovine serum (Dutscher). After 3 days, the cells were expanded and selected for NTCP expression with 1.8 μg/mL puromycin.

PHHs

Liver tissue from patients undergoing surgical resection was obtained with informed consent from all patients. The respective protocols were approved by the Ethics Committee of the University of Strasbourg Hospitals (CPP 10-17). PHHs were isolated from liver resection tissue and cultured in William's E medium (Sigma) (Krieger et al., 2010; Lupberger et al., 2011).

Viral Infection

Lentiviral pseudoparticles expressing HCV envelope glycoproteins (HCVpp strains HCV-J [1b], JFH1 [2a], NIH S52 [3a], and UKN4.21.16 [4]), VSVpp, MLVpp, as well as cell culture-derived HCVcc (Luc-Jc1 and Luc-JcR2A) were generated as described (Fofana et al., 2010; Lupberger et al., 2011). Huh7.5.1 cells and PHHs were infected as described (Krieger et al., 2010; Lupberger et al., 2011). Pseudoparticle entry and HCVcc infection were assessed by measuring luciferase activity 72 hr post-infection (Krieger et al., 2010; Lupberger et al., 2011). HDV production and infection have been described (Verrier et al., 2016) (see the Supplemental Experimental Procedures).

Gene Expression Analyses in Huh7.5.1-NTCP Cells and PHHs Treated with Bile Acids and preS1 Peptide

Huh7.5.1-NTCP cells were treated with preS1 or a control peptide (200 nM) for 48 hr. Alternatively, PHHs were treated with bile acids (500 μM) in presence of preS1 or a control peptide (400 nM) for 48 hr. Total RNA from three biological replicates per condition from one experiment was then extracted using the ReliaPrep Kit (Promega), and 200 ng was subjected to genome-wide transcriptome profiling using HumanHT-12 beadarray (Illumina), following the manufacturer's protocol. Raw scanned data were normalized by cubic spline algorithm using Illumina normalizer module of GenePattern genomic analysis toolkit (http://software.broadinstitute.org/cancer/software/genepattern), as previously described (Hoshida et al., 2008). Modulated molecular pathways were determined using GSEA (Subramanian et al., 2005).

Statistical Analysis

Each experiment was performed at least two times in an independent manner. The number of independent experiments as well as the total number of biological replicates (n) are indicated in the figure legends. Statistical analyses were performed using Mann-Whitney U test by comparing values from every biological replicate per study (indicated by "n" in the figure legends); $p < 0.05$ (*), $p < 0.01$ (**), and $p < 0.001$ (***) were considered statistically significant. Significant p values are indicated by asterisks in the individual figures. For microarray analyses, two-tailed unpaired Student's t test was performed by comparing the values from three biological replicates ($p < 0.05$ was considered statistically significant).

ACCESSION NUMBERS

The accession number for the datasets reported in this paper is GEO: GSE85092.

SUPPLEMENTAL INFORMATION

Supplemental Information includes Supplemental Experimental Procedures and two figures and can be found with this article online at http://dx.doi.org/10.1016/j.celrep.2016.09.084.

AUTHOR CONTRIBUTIONS

M.B.Z. and T.F.B. designed and supervised research. T.F.B. initiated the study. E.R.V., C.C.C., C.B., L.H., L.Z., F.X., C.T., E.C., R.G., and C.S. performed experiments. E.R.V., C.C.C., C.B., L.H., L.Z., F.X., C.T., E.C., R.G., C.S., Y.H., M.B.Z., and T.F.B. analyzed data. P.P. and F.-L.C. contributed key reagents. E.R.V., C.C.C., J.A.M., M.B.Z., and T.F.B. wrote the paper. E.R.V. and C.C.C. contributed equally to this work as first authors. M.B.Z. and T.F.B. contributed equally to this work as senior authors.

ACKNOWLEDGMENTS

We thank R. Bartenschlager (University of Heidelberg), C. Rice (Rockefeller University), T. Wakita (University of Tokyo), and J. Ball (University of Nottingham) for plasmids for HCVcc and HCVpp production; J. Taylor (Fox Chase Cancer Center) for HDV plasmid; F.V. Chisari (The Scripps Research Institute) for Huh7.5.1 cells; A. Patel (MRC Virology Unit) for Huh7.5-GFP cells and AP33; H. Hang and J. Yount (Rockefeller University) for IFITM plasmids; and D. Trono (Ecole Polytechnique Fédérale de Lausanne) and T. Pietschmann (Twincore) for lentiviral expression constructs. We also thank our colleagues J. Lupberger, H. El Saghire, N. van Renne, R. Tawar, and S. Durand. This work was supported by INSERM, the University of Strasbourg, the European Union (Infect-ERA hepBccc, ERC-2014-AdG-671231-HEPCIR, INTERREG-IV-Rhin Supérieur-FEDER-Hepato-Regio-Net, FP7 HepaMab, and EU H2020 Hep-CAR), Agence Nationale de Recherches sur le Sida et les hépatites virales (ANRS; 2012/239, 2012/318, 2013/108), and the French Cancer Agency (ARC IHU201301187). Research in the J.A.M. laboratory was funded by the Medical Research Council, the National Institute for Health Research (NIHR) Birmingham Liver Biomedical Research Unit, EU FP7 PathCO, and EU H2020 Hep-CAR. This work has been published under the framework of the LABEX ANR-10-LAB-28 and benefits from a funding from the state managed by the French National Research Agency as part of the Investments for the future program. C.C.C. acknowledges fellowships from the Canadian Institutes of Health Research (201411MFE- 338606-245517) and the Canadian Network on Hepatitis C.

Received: April 18, 2016
Revised: August 10, 2016
Accepted: September 26, 2016
Published: October 25, 2016

REFERENCES

Bartenschlager, R., and Pietschmann, T. (2005). Efficient hepatitis C virus cell culture system: what a difference the host cell makes. Proc. Natl. Acad. Sci. USA *102*, 9739–9740.

Baumert, T.F., Meredith, L., Ni, Y., Felmlee, D.J., McKeating, J.A., and Urban, S. (2014). Entry of hepatitis B and C viruses - recent progress and future impact. Curr. Opin. Virol. *4*, 58–65.

Bogomolov, P., Alexandrov, A., Voronkova, N., Macievich, M., Kokina, K., Petrachenkova, M., Lehr, T., Lempp, F.A., Wedemeyer, H., Haag, M., et al. (2016). Treatment of chronic hepatitis D with the entry inhibitor myrcludex B: First results of a phase Ib/IIa study. J. Hepatol. *65*, 490–498.

Brass, A.L., Huang, I.C., Benita, Y., John, S.P., Krishnan, M.N., Feeley, E.M., Ryan, B.J., Weyer, J.L., van der Weyden, L., Fikrig, E., et al. (2009). The IFITM proteins mediate cellular resistance to influenza A H1N1 virus, West Nile virus, and dengue virus. Cell *139*, 1243–1254.

César-Razquin, A., Snijder, B., Frappier-Brinton, T., Isserlin, R., Gyimesi, G., Bai, X., Reithmeier, R.A., Hepworth, D., Hediger, M.A., Edwards, A.M., and Superti-Furga, G. (2015). A call for systematic research on solute carriers. Cell *162*, 478–487.

Chang, K.O., and George, D.W. (2007). Bile acids promote the expression of hepatitis C virus in replicon-harboring cells. J. Virol. *81*, 9633–9640.

Chhatwal, P., Bankwitz, D., Gentzsch, J., Frentzen, A., Schult, P., Lohmann, V., and Pietschmann, T. (2012). Bile acids specifically increase hepatitis C virus RNA-replication. PLoS ONE *7*, e36029.

Claro da Silva, T., Polli, J.E., and Swaan, P.W. (2013). The solute carrier family 10 (SLC10): beyond bile acid transport. Mol. Aspects Med. *34*, 252–269.

Colpitts, C.C., Verrier, E.R., and Baumert, T.F. (2015). Targeting viral entry for treatment of hepatitis B and C virus infections. ACS Infect. Dis. *1*, 420–427.

El-Serag, H.B. (2012). Epidemiology of viral hepatitis and hepatocellular carcinoma. Gastroenterology *142*, 1264–1273.

Fofana, I., Krieger, S.E., Grunert, F., Glauben, S., Xiao, F., Fafi-Kremer, S., Soulier, E., Royer, C., Thumann, C., Mee, C.J., et al. (2010). Monoclonal anti-claudin 1 antibodies prevent hepatitis C virus infection of primary human hepatocytes. Gastroenterology *139*, 953–964.

Graf, D., Haselow, K., Münks, I., Bode, J.G., and Häussinger, D. (2010). Inhibition of interferon-α-induced signaling by hyperosmolarity and hydrophobic bile acids. Biol. Chem. *391*, 1175–1187.

Hoshida, Y., Villanueva, A., Kobayashi, M., Peix, J., Chiang, D.Y., Camargo, A., Gupta, S., Moore, J., Wrobel, M.J., Lerner, J., et al. (2008). Gene expression in fixed tissues and outcome in hepatocellular carcinoma. N. Engl. J. Med. *359*, 1995–2004.

Kim, S., Ishida, H., Yamane, D., Yi, M., Swinney, D.C., Foung, S., and Lemon, S.M. (2013). Contrasting roles of mitogen-activated protein kinases in cellular entry and replication of hepatitis C virus: MKNK1 facilitates cell entry. J. Virol. *87*, 4214–4224.

König, A., Döring, B., Mohr, C., Geipel, A., Geyer, J., and Glebe, D. (2014). Kinetics of the bile acid transporter and hepatitis B virus receptor Na+/taurocholate cotransporting polypeptide (NTCP) in hepatocytes. J. Hepatol. *61*, 867–875.

Krieger, S.E., Zeisel, M.B., Davis, C., Thumann, C., Harris, H.J., Schnober, E.K., Mee, C., Soulier, E., Royer, C., Lambotin, M., et al. (2010). Inhibition of hepatitis C virus infection by anti-claudin-1 antibodies is mediated by neutralization of E2-CD81-claudin-1 associations. Hepatology *51*, 1144–1157.

Liu, S.Y., Sanchez, D.J., and Cheng, G. (2011). New developments in the induction and antiviral effectors of type I interferon. Curr. Opin. Immunol. *23*, 57–64.

Lupberger, J., Zeisel, M.B., Xiao, F., Thumann, C., Fofana, I., Zona, L., Davis, C., Mee, C.J., Turek, M., Gorke, S., et al. (2011). EGFR and EphA2 are host factors for hepatitis C virus entry and possible targets for antiviral therapy. Nat. Med. *17*, 589–595.

Martin, D.N., and Uprichard, S.L. (2013). Identification of transferrin receptor 1 as a hepatitis C virus entry factor. Proc. Natl. Acad. Sci. USA *110*, 10777–10782.

Meredith, L.W., Harris, H.J., Wilson, G.K., Fletcher, N.F., Balfe, P., and McKeating, J.A. (2013). Early infection events highlight the limited transmissibility of hepatitis C virus in vitro. J. Hepatol. *58*, 1074–1080.

Meredith, L.W., Farquhar, M.J., Tarr, A.W., and McKeating, J.A. (2014). Type I interferon rapidly restricts infectious hepatitis C virus particle genesis. Hepatology *60*, 1891–1901.

Meredith, L.W., Hu, K., Cheng, X., Howard, C.R., Baumert, T.F., Balfe, P., van de Graaf, K.F., Protzer, U., and McKeating, J.A. (2016). Lentiviral hepatitis B pseudotype entry requires sodium taurocholate co-transporting polypeptide and additional hepatocyte-specific factors. J. Gen. Virol. *97*, 121–127.

Narayana, S.K., Helbig, K.J., McCartney, E.M., Eyre, N.S., Bull, R.A., Eltahla, A., Lloyd, A.R., and Beard, M.R. (2015). The interferon-induced transmembrane proteins, IFITM1, IFITM2, and IFITM3 inhibit hepatitis C virus entry. J. Biol. Chem. *290*, 25946–25959.

Ni, Y., Lempp, F.A., Mehrle, S., Nkongolo, S., Kaufman, C., Fälth, M., Stindt, J., Königer, C., Nassal, M., Kubitz, R., et al. (2014). Hepatitis B and D viruses exploit sodium taurocholate co-transporting polypeptide for species-specific entry into hepatocytes. Gastroenterology *146*, 1070–1083.

Oehler, N., Volz, T., Bhadra, O.D., Kah, J., Allweiss, L., Giersch, K., Bierwolf, J., Riecken, K., Pollok, J.M., Lohse, A.W., et al. (2014). Binding of hepatitis B virus to its cellular receptor alters the expression profile of genes of bile acid metabolism. Hepatology *60*, 1483–1493.

Petersen, J., Dandri, M., Mier, W., Lütgehetmann, M., Volz, T., von Weizsäcker, F., Haberkorn, U., Fischer, L., Pollok, J.M., Erbes, B., et al. (2008). Prevention of hepatitis B virus infection in vivo by entry inhibitors derived from the large envelope protein. Nat. Biotechnol. *26*, 335–341.

Pileri, P., Uematsu, Y., Campagnoli, S., Galli, G., Falugi, F., Petracca, R., Weiner, A.J., Houghton, M., Rosa, D., Grandi, G., and Abrignani, S. (1998). Binding of hepatitis C virus to CD81. Science *282*, 938–941.

Podevin, P., Rosmorduc, O., Conti, F., Calmus, Y., Meier, P.J., and Poupon, R. (1999). Bile acids modulate the interferon signalling pathway. Hepatology *29*, 1840–1847.

Savidis, G., Perreira, J.M., Portmann, J.M., Meraner, P., Guo, Z., Green, S., and Brass, A.L. (2016). The IFITMs inhibit Zika virus replication. Cell Rep. *15*, 2323–2330.

Scarselli, E., Ansuini, H., Cerino, R., Roccasecca, R.M., Acali, S., Filocamo, G., Traboni, C., Nicosia, A., Cortese, R., and Vitelli, A. (2002). The human scavenger receptor class B type I is a novel candidate receptor for the hepatitis C virus. EMBO J. *21*, 5017–5025.

Schieck, A., Schulze, A., Gähler, C., Müller, T., Haberkorn, U., Alexandrov, A., Urban, S., and Mier, W. (2013). Hepatitis B virus hepatotropism is mediated by specific receptor recognition in the liver and not restricted to susceptible hosts. Hepatology *58*, 43–53.

Slijepcevic, D., Kaufman, C., Wichers, C.G., Gilglioni, E.H., Lempp, F.A., Duijst, S., de Waart, D.R., Elferink, R.P., Mier, W., Stieger, B., et al. (2015). Impaired uptake of conjugated bile acids and hepatitis b virus pres1-binding in na(+) -taurocholate cotransporting polypeptide knockout mice. Hepatology *62*, 207–219.

Smith, S., Weston, S., Kellam, P., and Marsh, M. (2014). IFITM proteins-cellular inhibitors of viral entry. Curr. Opin. Virol. *4*, 71–77.

Subramanian, A., Tamayo, P., Mootha, V.K., Mukherjee, S., Ebert, B.L., Gillette, M.A., Paulovich, A., Pomeroy, S.L., Golub, T.R., Lander, E.S., and Mesirov, J.P. (2005). Gene set enrichment analysis: a knowledge-based approach for interpreting genome-wide expression profiles. Proc. Natl. Acad. Sci. USA *102*, 15545–15550.

Sureau, C. (2010). The use of hepatocytes to investigate HDV infection: the HDV/HepaRG model. Methods Mol. Biol. *640*, 463–473.

Timpe, J.M., Stamataki, Z., Jennings, A., Hu, K., Farquhar, M.J., Harris, H.J., Schwarz, A., Desombere, I., Roels, G.L., Balfe, P., and McKeating, J.A.

(2008). Hepatitis C virus cell-cell transmission in hepatoma cells in the presence of neutralizing antibodies. Hepatology *47*, 17–24.

Verrier, E.R., Colpitts, C.C., Bach, C., Heydmann, L., Weiss, A., Renaud, M., Durand, S.C., Habersetzer, F., Durantel, D., Abou-Jaoudé, G., et al. (2016). A targeted functional RNA interference screen uncovers glypican 5 as an entry factor for hepatitis B and D viruses. Hepatology *63*, 35–48.

Volz, T., Allweiss, L., Ben MBarek, M., Warlich, M., Lohse, A.W., Pollok, J.M., Alexandrov, A., Urban, S., Petersen, J., Lütgehetmann, M., and Dandri, M. (2013). The entry inhibitor Myrcludex-B efficiently blocks intrahepatic virus spreading in humanized mice previously infected with hepatitis B virus. J. Hepatol. *58*, 861–867.

Wedemeyer, H., Dore, G.J., and Ward, J.W. (2015). Estimates on HCV disease burden worldwide - filling the gaps. J. Viral Hepat. *22* (*Suppl 1*), 1–5.

Wilkins, C., Woodward, J., Lau, D.T., Barnes, A., Joyce, M., McFarlane, N., McKeating, J.A., Tyrrell, D.L., and Gale, M., Jr. (2013). IFITM1 is a tight junction protein that inhibits hepatitis C virus entry. Hepatology *57*, 461–469.

Xiao, F., Fofana, I., Heydmann, L., Barth, H., Soulier, E., Habersetzer, F., Doffoël, M., Bukh, J., Patel, A.H., Zeisel, M.B., and Baumert, T.F. (2014). Hepatitis C virus cell-cell transmission and resistance to direct-acting antiviral agents. PLoS Pathog. *10*, e1004128.

Yan, H., Zhong, G., Xu, G., He, W., Jing, Z., Gao, Z., Huang, Y., Qi, Y., Peng, B., Wang, H., et al. (2012). Sodium taurocholate cotransporting polypeptide is a functional receptor for human hepatitis B and D virus. eLife *1*, e00049.

Yan, H., Peng, B., Liu, Y., Xu, G., He, W., Ren, B., Jing, Z., Sui, J., and Li, W. (2014). Viral entry of hepatitis B and D viruses and bile salts transportation share common molecular determinants on sodium taurocholate cotransporting polypeptide. J. Virol. *88*, 3273–3284.

York, A.G., Williams, K.J., Argus, J.P., Zhou, Q.D., Brar, G., Vergnes, L., Gray, E.E., Zhen, A., Wu, N.C., Yamada, D.H., et al. (2015). Limiting cholesterol biosynthetic flux spontaneously engages type I IFN signaling. Cell *163*, 1716–1729.

Zeisel, M.B., Felmlee, D.J., and Baumert, T.F. (2013a). Hepatitis C virus entry. Curr. Top. Microbiol. Immunol. *369*, 87–112.

Zeisel, M.B., Lupberger, J., Fofana, I., and Baumert, T.F. (2013b). Host-targeting agents for prevention and treatment of chronic hepatitis C - perspectives and challenges. J. Hepatol. *58*, 375–384.

Zhong, J., Gastaminza, P., Cheng, G., Kapadia, S., Kato, T., Burton, D.R., Wieland, S.F., Uprichard, S.L., Wakita, T., and Chisari, F.V. (2005). Robust hepatitis C virus infection in vitro. Proc. Natl. Acad. Sci. USA *102*, 9294–9299.

Zona, L., Lupberger, J., Sidahmed-Adrar, N., Thumann, C., Harris, H.J., Barnes, A., Florentin, J., Tawar, R.G., Xiao, F., Turek, M., et al. (2013). HRas signal transduction promotes hepatitis C virus cell entry by triggering assembly of the host tetraspanin receptor complex. Cell Host Microbe *13*, 302–313.

9.5 Verrier ER et al., Hepatology 2016;63:35-48

HEPATOLOGY
Official Journal of the American Association for the Study of Liver Diseases

A Targeted Functional RNA Interference Screen Uncovers Glypican 5 as an Entry Factor for Hepatitis B and D Viruses

Eloi R. Verrier,[1,2] Che C. Colpitts,[1,2] Charlotte Bach,[1,2] Laura Heydmann,[1,2] Amélie Weiss,[3] Mickaël Renaud,[3] Sarah C. Durand,[1,2] François Habersetzer,[4] David Durantel,[5] Georges Abou-Jaoudé,[6] Maria M. López Ledesma,[7] Daniel J. Felmlee,[1,2] Magali Soumillon,[8] Tom Croonenborghs,[9,10] Nathalie Pochet,[9] Michael Nassal,[11] Catherine Schuster,[1,2] Laurent Brino,[3] Camille Sureau,[6] Mirjam B. Zeisel,[1,2] and Thomas F. Baumert[1,2,4]

Chronic hepatitis B and D infections are major causes of liver disease and hepatocellular carcinoma worldwide. Efficient therapeutic approaches for cure are absent. Sharing the same envelope proteins, hepatitis B virus and hepatitis delta virus use the sodium/taurocholate cotransporting polypeptide (a bile acid transporter) as a receptor to enter hepatocytes. However, the detailed mechanisms of the viral entry process are still poorly understood. Here, we established a high-throughput infectious cell culture model enabling functional genomics of hepatitis delta virus entry and infection. Using a targeted RNA interference entry screen, we identified glypican 5 as a common host cell entry factor for hepatitis B and delta viruses. *Conclusion*: These findings advance our understanding of virus cell entry and open new avenues for curative therapies. As glypicans have been shown to play a role in the control of cell division and growth regulation, virus–glypican 5 interactions may also play a role in the pathogenesis of virus-induced liver disease and cancer. (HEPATOLOGY 2016;36:35-48)

See Editorial on Page 11

Hepatitis B virus (HBV) is a small, enveloped DNA virus[1] and a leading cause of liver cirrhosis and hepatocellular carcinoma (HCC) worldwide. More than 350 million individuals are chronically infected with HBV.[2] Among these, 5%-10% are likely coinfected with hepatitis delta virus (HDV) and exhibit an increased HCC risk.[3] HDV is a small RNA satellite virus of HBV that uses the HBV envelope proteins to assemble into infectious particles and enter its target cell.[4] Nucleos(t)ide analogues and interferon-based treatment can control HBV infection, but virus eradication and cure remain largely unattainable.[5] While HDV can partially respond to interferon-based treatment,[6] long-term response is marginal.[6,7]

Abbreviations: CsA, cyclosporin A; DMSO, dimethylsulfoxide; dpi, day postinoculation; ELISA, enzyme-linked immunosorbent assay; GAPDH, glyceraldehyde 3-phosphate dehydrogenase; GPC, glypican; HBeAg, hepatitis B e antigen; HBsAg, HBV surface antigen; HBV, hepatitis B virus; HCC, hepatocellular carcinoma; HCV, hepatitis C virus; HDAg, hepatitis delta antigen; HDV, hepatitis delta virus; HSPG, heparan sulfate proteoglycan; IF, immunofluorescence; IgG, immunoglobulin G; mRNA, messenger RNA; NTCP, sodium/taurocholate cotransporting polypeptide; PBS, phosphate-buffered saline; PEG, polyethylene glycol; PFA, paraformaldehyde; pgRNA, pregenomic RNA; PHH, primary human hepatocyte; pp, pseudoparticle; qRT-PCR, quantitative real-time polymerase chain reaction; RNAi, RNA interference; SDC, syndecan; siRNA, small interfering RNA.

From the [1]Inserm, U1110, Institut de Recherche sur les Maladies Virales et Hépatiques, Strasbourg, France; [2]Université de Strasbourg, Strasbourg, France; [3]IGBMC, Plateforme de Criblage Haut-débit, Illkirch, France; [4]Institut Hospitalo-Universitaire, Pôle Hépato-digestif, Nouvel Hôpital Civil, Strasbourg, France; [5]Inserm, U1052, CNRS UMR 5286, Cancer Research Center of Lyon, Université de Lyon, Lyon, France; [6]INTS, Laboratoire de Virologie Moléculaire, Paris, France; [7]Cátedra de Virología, Facultad de Farmacia y Bioquímica, Universidad de Buenos Aires, Buenos Aires, Argentina; [8]Broad Institute of Massachusetts Institute of Technology and Harvard, Cambridge, MA; [9]Program in Translational NeuroPsychiatric Genomics, Brigham and Women's Hospital, Harvard Medical School, Broad Institute of Massachusetts Institute of Technology and Harvard, Cambridge, MA; [10]KU Leuven Technology Campus Geel, AdvISe, Geel, Belgium; [11]Department of Internal Medicine II/Molecular Biology, University Hospital Freiburg, Freiburg, Germany.

Received March 25, 2015; accepted July 23, 2015.

Additional Supporting Information may be found at onlinelibrary.wiley.com/doi/10.1002/hep.28013/suppinfo.

Although many aspects of the HBV and HDV life cycles have been characterized in great detail, others, including viral entry, are still unexplored due to the lack of robust infectious tissue culture systems. Recently, the human sodium/taurocholate cotransporting polypeptide (hNTCP), a bile acid transporter expressed at the basolateral membrane of human hepatocytes, has been identified as a functional receptor of HBV and HDV.[8,9] Exogenous expression of hNTCP in permissive, nonsusceptible human hepatoma cells, such as HepG2 or Huh7, confers susceptibility to HBV and/or HDV infection, thereby constituting cell culture models for HBV/HDV entry.[8-10] However, their limited robustness and the requirement of dimethylsulfoxide (DMSO) and polyethylene glycol (PEG) preclude their use in a high-throughput format and for functional genomics.

Heparan sulfate proteoglycans (HSPGs), composed of a protein core carrying heparan sulfate glycosaminoglycan chains, are widely expressed at the cell surface of mammalian cells in a cell-specific and tissue-specific manner.[11] Many viruses use HSPGs for cell surface attachment and entry.[11,12] HSPGs contribute to HBV/HDV entry, as treatment of target cells or virions with heparinase or soluble heparin (a homologue of a highly sulfated prototype member of the glycosaminoglycan family), respectively, inhibits viral infection.[13,14] HBV is believed to first attach to HSPGs at the hepatocyte surface, through the antigenic loop of the HBV envelope protein[15] and possibly a contribution of the preS1 domain of the large HBV envelope protein.[13] Subsequently, HBV binding to NTCP is engaged by the preS1 domain, which interacts with a discrete domain of NTCP.[8,9] However, the detailed HBV/HDV entry mechanisms are still poorly understood.[10,16,17] Particularly, the HSPG core protein responsible for HBV/HDV attachment remains to be identified.

Viral entry is an important antiviral target complementing direct-acting antivirals targeting the viral polymerase. Indeed, a myristoylated HBV preS1-derived peptide (Myrcludex B) and cyclosporin A (CsA)[18,19] potently inhibit HBV and HDV entry,[17] and Myrcludex B has shown antiviral efficacy in humans.[20] Unraveling the HBV/HDV entry process may thus uncover further antiviral targets.

In this study, we established a robust HDV infection assay based on a novel NTCP-expressing Huh7 cell line that does not require the use of infection-enhancing treatments with DMSO and PEG. Using an RNA interference (RNAi)–based loss-of-function screen, we showed that this model system is amenable to functional genomics and identified glypican 5 (GPC5) as a previously undiscovered HBV and HDV entry factor and antiviral target.

Materials and Methods

Patient Samples. Human material including serum from patients with chronic HBV/HDV infection followed at the Strasbourg University Hospitals, Strasbourg, France, was obtained with informed consent. Primary human hepatocytes (PHHs) were obtained from liver tissue from patients undergoing liver resection for liver metastasis at the Strasbourg University Hospitals with informed consent. Protocols were approved by the local ethics committee of the Strasbourg University Hospitals (CPP 10-17).

Cell Lines and Human Hepatocytes. Huh7[21] and HepG2[22] cells have been described. PHHs were isolated and cultured as described.[22] The HepAD38 cell line is an inducible human hepatoblastoma cell line harboring an integrated tetracycline-responsive 1.2-fold HBV genome (serotype ayw, genotype D) and has been described.[23]

Reagents. DMSO and PEG 8000 were from Sigma-Aldrich; CsA was from Sandimmun (Novartis, Switzerland). HBV preS1-derived peptide, HBV preS1-derived peptide labeled with Alexa Fluor 647 fluorophore, and scrambled peptide control were synthesized by Bachem (Switzerland). The enhanced chemiluminescence reagent and Hyperfilms were from GE Healthcare.

Supported by Inserm, University of Strasbourg, the European Union (EU-INTERREG-IV-Rhin Supérieur-FEDER Hepato-Regio-Net 2012; ERC-2008-AdG-233130-HEPCENT; FP7 305600 HepaMab; EU Infect-Era hepBccc), ANRS (2012/318, 2013/108), and the French Cancer Agency (ARC IHU201301187). This work has been published under the framework of the LABEX ANR-10-LAB-28 and benefits from funding from the state managed by the French National Research Agency as part of the Investments for the future program. Also supported by a fellowship from the Canadian Institutes of Health Research (201411MFE-338606-245517, to C.C.C.).

Address reprint requests to: Thomas F. Baumert, M.D., Inserm U1110, Institut de Recherche sur les Maladies Virales et Hépatiques, 3 Rue Koeberlé, 67000 Strasbourg, France. E-mail: thomas.baumert@unistra.fr; tel: +33 3 68 85 37 03; fax: +33 3 68 85 37 24. Or: Camille Sureau, Ph.D., Laboratoire de Virologie Moléculaire, Institut National de la Transfusion Sanguine, 6 rue Alexandre-Cabanel, 75739 Paris, France. E-mail: csureau@ints.fr; fax: +33 1 44 49 30 56.

View this article online at wileyonlinelibrary.com.

DOI 10.1002/hep.28013

Potential conflict of interest: Nothing to report.

Small Interfering RNAs Used for Functional Studies. ON-TARGETplus small interfering RNA (siRNA) pools (Dharmacon) targeting the transcripts of SLC10A1 (NTCP), syndecan (SDC) family genes, GPC family genes, HSPG2 (perlecan), and agrin were reverse-transfected into cells with Lipofectamine RNAiMAX (Invitrogen) as described.[22] Subsequently, an individual siRNA of the pool (Dharmacon) targeting GPC5 was used: GPC5 no. 3, targeted sequence CUUCAAAC GUCCAGCUCUA.

Establishment of Stable NTCP-Overexpressing Hepatoma Cell Lines. The NTCP expression vector was generated containing the full open reading frame of human NTCP complementary DNA (SLC10A1; GenBank L21893.1) inserted between the *Hind*III and *Xba*I restriction sites of the pRc-CMV plasmid (Invitrogen). Huh7 cells were cultured in William's medium E supplemented with 10% fetal bovine serum (Fetaclone-II; Thermo Scientific) and gentamicin. After transfection of Huh7 cells with pRc-CMV-NTCP plasmid DNA, transfected cells were selected for neomycin (G418) resistance, and isolated clones were tested for susceptibility to HDV infection as described.[24] One clone (referred to here as Huh-106) was selected based on the high level of intracellular HDV RNA that accumulated 9 days postinoculation (dpi) with HDV virions. Huh-106 cells were maintained at a concentration of 250 μg/mL G418. HepG2 cells were seeded in six-well plates at 50% confluence 1 day prior to transduction with human NTCP-expressing vesicular stomatitis virus pseudoparticles (pp) (GeneCopoeia). After 3 days, cells were expanded and selected for NTCP expression with 0.9 μg/mL puromycin. HepG2-NTCP cells were maintained at a concentration of 0.9 μg/mL puromycin.

Analysis of Messenger RNA Expression by Quantitative Real-Time Polymerase Chain Reaction. Total RNA was extracted from cells using the RNeasy Mini Kit (Qiagen). Gene expression in the total RNA extracts was assessed using quantitative real-time polymerase chain reaction (qRT-PCR). Reverse-transcription of total RNA extracts was performed using MAXIMA reverse-transcriptase (Thermo Scientific). Quantitative PCR was performed using a Corbett rotor gene 6000 (Qiagen) following the manufacturer's instructions. Primers and TaqMan probes for NTCP, GPC5, SDC4, and glyceraldehyde 3-phosphate dehydrogenase (GAPDH) messenger RNA (mRNA) detection were from Applied Biosystems. All values were normalized to GAPDH expression.

Protein Expression Analysis. Immunoblots of cell lysates using protein–specific antibodies (rabbit polyclonal anti-NTCP antibody [Sigma; HPA042727], rabbit anti-GPC5 monoclonal antibody [Abcam; EPR6756(B)], and mouse anti-β-actin monoclonal antibody [Sigma; A5441]) were performed following GE Healthcare protocols using Hybond-P membranes and visualized using enhanced chemiluminescence western blotting detection reagents following the manufacturer's instructions. For western blot detection of NTCP, cell lysates were pretreated with peptide-N-glycosidase (New England Biolabs, Evry, France) following the manufacturer's instructions. For fluorescent detection of NTCP protein in cells, an HBV preS1-derived peptide labeled with Alexa Fluor 647 fluorophore (Bachem, Switzerland) was used as described.[8,9] Cells were treated with the peptide for 1 hour at 37°C and then fixed with 4% paraformaldehyde (PFA). Fluorescent imaging was performed using an Axio Observer Z1 microscope (Carl Zeiss, Germany). NTCP expression at the cell surface was quantified by flow cytometry as described.[8,22]

HDV Production and Infection. The HDV recombinant plasmid pSVLD3 and the HBV expression vector pT7HB2.7 were used for production of HDV ribonucleoprotein and of L, M, and S HBV surface antigen (HBsAg) proteins.[25] Huh7.5.1 cells were transfected with the two plasmids using FuGENE HD Transfection Reagent. HDV-containing supernatants were harvested 9 days after transfection and subsequently used for infection experiments. For HDV infection, Huh-106 cells were plated in 96-well or 384-well plates and maintained in culture for 1 day without DMSO. HBV preS1-derived peptide or scrambled peptide control (control), CsA, rabbit anti-GPC5 antibody, rabbit anti-SDC4 antibody (Life Technologies; 36-3100), and rabbit control immunoglobulin G (IgG; Invitrogen) were added to the cell medium 1 hour before infection with recombinant HDV with or without PEG at the indicated concentrations. Cells were cultured in primary hepatocyte maintenance medium[8] containing 2% DMSO following infection to slow cell growth. HDV infection was assessed 7 dpi by immunofluorescence (IF) or qRT-PCR.

Detection of Hepatitis Delta Antigen and HDV RNA in Infected Cells. Cells were washed with phosphate-buffered saline (PBS) and fixed with 4% PFA. Nonspecific binding sites were saturated using 0.5% bovine serum albumin, and cells were permeabilized using 0.05% saponin. Cells were stained with an antibody targeting the hepatitis delta antigen (HDAg) purified from serum of an HBV/HDV coinfected patient[26] and Alexa Fluor 647-labeled secondary antibody targeting human IgGs (Jackson Research). Cell nuclei were stained with 4′,6-diamidino-2-phenylindole. Fluorescent imaging was performed using an Axio Observer Z1 microscope (Carl Zeiss, Germany). Total RNA extraction and reverse-

transcription were performed as described above. Quantitative PCR was performed using the SensiFAST Probe No-ROX Kit (Bioline) and Corbett rotor gene 6000 (Qiagen) following the manufacturer's instructions. The following specific primers for HDV RNA quantification were used: forward primer 5′-GCATGGTCCCAGCCT CC-3′, reverse primer 5′-CTTCGGGTCGGCATGG-3′; TaqMan probe 5′-[fluorescein amidite]-ATGCCCAGGT CGGAC-[Black Hole Quencher-1]-3′. All values were normalized to GAPDH (Applied Biosystems) expression.

HBV Production and Infection. HBV infectious particles from sera of HBV carriers (genotype D) were concentrated with a 30% sucrose cushion and purified using a 10%-45% iodixanol density gradient. Recombinant HBV (strain ayw, genotype D) was obtained by 100-fold concentration of supernatant of HepAD38 cells using 8% PEG.[23] HepG2-NTCP cells were plated in 96-well plates and maintained in culture for 1 day without DMSO prior to HBV infection in the presence of 4% PEG. Cells were cultured in 2% DMSO primary hepatocyte maintenance medium following infection to slow cell growth. HBV infection was assessed 10 dpi by immunodetection of HBsAg using an HBsAg-specific monoclonal antibody (NCL-HBsAg-2, clone 1044/341; Leica Biosystems) and by qRT-PCR quantification of HBV pregenomic RNA (pgRNA) using the following primers and probe[27]: forward primer 5′-GGTCCCCT AGAAGAAGAACTCCCT-3′, reverse primer 5′-CATT GAGATTCCCGAGAT TGAGAT-3′; TaqMan probe 5′-[6-fluorescein amidite]-TCTCAATCGCCGCGTC GCAGA-[carboxytetramethylrhodamine]-3′. All values were normalized to GAPDH (Applied Biosystems) expression.

Analysis of HBV and HDV Binding to Liver Cells. Huh-106 and HepG2-NTCP cells were incubated for 1 hour at 37°C with a GPC5-specific or control antibody at various time points before and after virus inoculation. Recombinant HBV was pretreated with PBS, heparin (30 μg/mL), rGPC5 (5 μg/mL and 30 μg/mL; R&D Systems), or rSDC4 (30 μg/mL; R&D Systems) for 30 minutes at 37°C. Cells were washed twice with cold PBS and then incubated with pretreated HBV or HDV in the presence of 4% PEG for 24 hours at 16°C. Unbound virions were removed by three washes with PBS, and cells and bound virions were lysed. A 24-hour incubation period was chosen based on previous observations showing the requirement of a >16-hour virus/cell exposure[28,29] and given that transcription from incoming viral DNA and *de novo* production of virus are not detectable prior to 2 and 3 dpi, respectively.[29] Therefore, the HBV DNA that is associated with cells at 24 hours postinoculation represents HBV particles that have attached to the cells during this time period and potentially virions that have been internalized following attachment, but does not include progeny virions. DNA was extracted from HepG2-NTCP cells according to the QiaAMP DNA MiniKit protocol (Qiagen). HBV total DNA was detected by qPCR using the following primers and probe[27]: forward primer 5′-CA CCTCGCCTAATCATC-3′, reverse primer 5′-GGAAA GAAGTCAGAAGGCA-3′; TaqMan probe 5′-[fluorescein amidite]-TGGAGGCTTCAACAGTAGGACATGAA C-[carboxytetramethylrhodamine]-3′. A standard curve generated from known HBV genome copies was used for quantification. Values were normalized to initial DNA concentration. Total RNA was extracted from Huh-106 cells and HDV RNA was quantified as described above.

Analysis of HBV Replication in Huh-106 Cells With Silenced GPC5 Expression. Huh-106 cells were reverse-cotransfected with the replication-competent HBV expression plasmid adwR9[30] and GPC5-targeting or control siRNAs using Lipofectamine RNAiMAX (Invitrogen). Three days after transfection, HBV DNA was purified and quantified from lysates by qPCR as described above. Hepatitis B e antigen (HBeAg) and HBsAg in cell culture supernatants were quantified using enzyme-linked immunosorbent assays (ELISAs) N0140 and N0019 (Diasorin). Cytoplasmic HBV core antigen was quantified using a sandwich ELISA as described.[31]

Statistical Analysis. All experiments were performed at least three times in an independent manner. Statistical analyses were performed using a Student *t* test or Mann-Whitney test; $P < 0.01$ was considered statistically significant. Significant *P* values are indicated by asterisks in the individual figures.

Results

A Novel hNTCP-Overexpressing Huh7 Cell Line Readily Susceptible for HDV Infection. Aiming to develop a high-throughput system for functional genomics, we established a Huh7-NTCP cell line in which constitutive hNTCP expression is under the control of a cytomegalovirus promoter. Out of 120 single-cell clones, one, termed Huh-106, was found reproducibly susceptible to HDV infection irrespective of the culture conditions. Huh-106 cells express significantly higher levels of NTCP (mRNA and protein) than the parental Huh7 cells (Fig. 1A,B). Moreover, an AF647-labeled peptide derived from the HBV preS1 domain known to bind NTCP,[8,9] specifically bound to Huh-106 cells, demonstrating high levels of cell surface NTCP expression (Fig. 1C,D). To confirm NTCP function, Huh-106 cells were inoculated with recombinant HDV. Indeed, Huh-106 cells were susceptible to HDV entry,

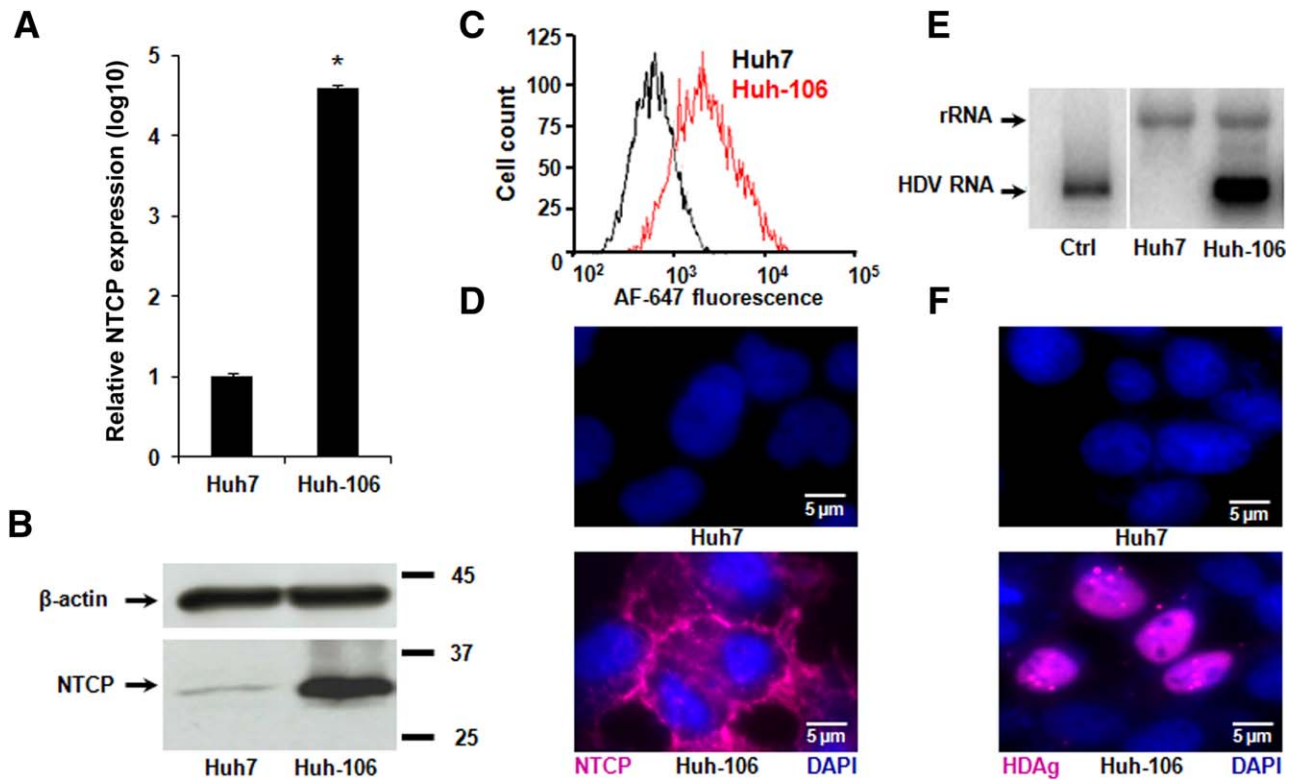

Fig. 1. Production of HDV permissive cell lines overexpressing human NTCP. (A) Relative NTCP expression in Huh-106 cells compared to parental Huh7 cells using qRT-PCR. Results are expressed as means ± standard deviation showing NTCP mRNA expression normalized to GAPDH mRNA expression from three experiments performed in duplicate. (B) Detection of NTCP protein by western blot. Cell lysates were treated with peptide-N-glycosidase and subsequently subjected to immunoblotting using a mouse monoclonal anti-NTCP antibody (Sigma). One representative experiment is shown. (C) Quantification of NTCP at the cell surface by flow cytometry using a labeled HBV preS1-derived peptide. Cells were treated for 1 hour with Alexa Fluor 674–labeled HBV preS1-derived peptide (200 nM) and fixed with 4% PFA. NTCP expression was assessed by flow-cytometric quantification of bound preS1 peptide. One representative experiment is shown. (D) Fluorescence microscopic analysis of NTCP expression in Huh7 and Huh-106 cells. Cells were treated with Alexa Fluor 674–labeled HBV preS1-derived peptide (200 nM) and fixed with 4% PFA before visualization using fluorescence microscopy. HBV preS1-derived peptide binding is shown in red. One representative experiment is shown. (E,F) Functional evaluation of NTCP cell lines using HDV infection. Huh-106 and Huh7 cells were infected with recombinant HDV for 7 days. (E) Total RNA was purified and HDV RNA was detected by northern blot. Control corresponds to approximately 2×10^7 HDV RNA genome equivalents extracted from HDV particles produced in Huh7 cells. One representative experiment is shown. (F) HDV-positive cells were visualized in red after HDAg immunodetection with an anti-HDAg antibody. Cell nuclei were stained with 4′,6-diamidino-2-phenylindole (blue). One representative experiment is shown. Abbreviations: DAPI, 4′,6-diamidino-2-phenylindole; rRNA, ribosomal RNA.

as demonstrated by detectable intracellular HDAg and HDV RNA (Fig. 1E,F) at 7 dpi.

Most current *in vitro* HBV/HDV infection systems require the addition of PEG to the inoculum to increase infection.[8,9,29] PEG may modulate viral entry by bypassing virus–host factor interactions. To assess whether PEG increases viral entry in our model, we inoculated Huh-106 cells with HDV in the presence of increasing concentrations of PEG. Approximately 15%-25% of Huh-106 cells were infected in the absence of PEG treatment compared to 30% of HDAg-positive cells after 6% PEG treatment (Fig. 2A,B). Notably, a two-fold increase of HDV-positive cells is observed in the presence of 8% PEG but with significant toxicity (Fig. 2B). Silencing of NTCP expression with siRNA prior to inoculation (Fig. 2C) led to a significant decrease (from 22% to 7%) of HDV-positive cells when cells were inoculated in the absence of PEG. In contrast, in the presence of 6% PEG, only a slight but insignificant decrease of infection was observed (Fig. 2D), suggesting that HDV infection in the absence of PEG is more susceptible to RNAi-based perturbation studies. These data indicate that our model efficiently supports HDV infection in the absence of PEG.

Treatment of cell cultures with DMSO prior to inoculation has also been shown to improve HBV and HDV infection, possibly by modifying NTCP trafficking.[8,9,32] When Huh-106 cells were treated for 2 days with 2% DMSO prior to inoculation (Fig. 2E), no change in NTCP localization at the cell surface or in HDV infection was observed. Taken together, our data show that the Huh-106 cells are readily susceptible to HDV infection in the absence of PEG and DMSO and, hence, in conditions amenable to functional genomics and RNAi-based loss of function studies.

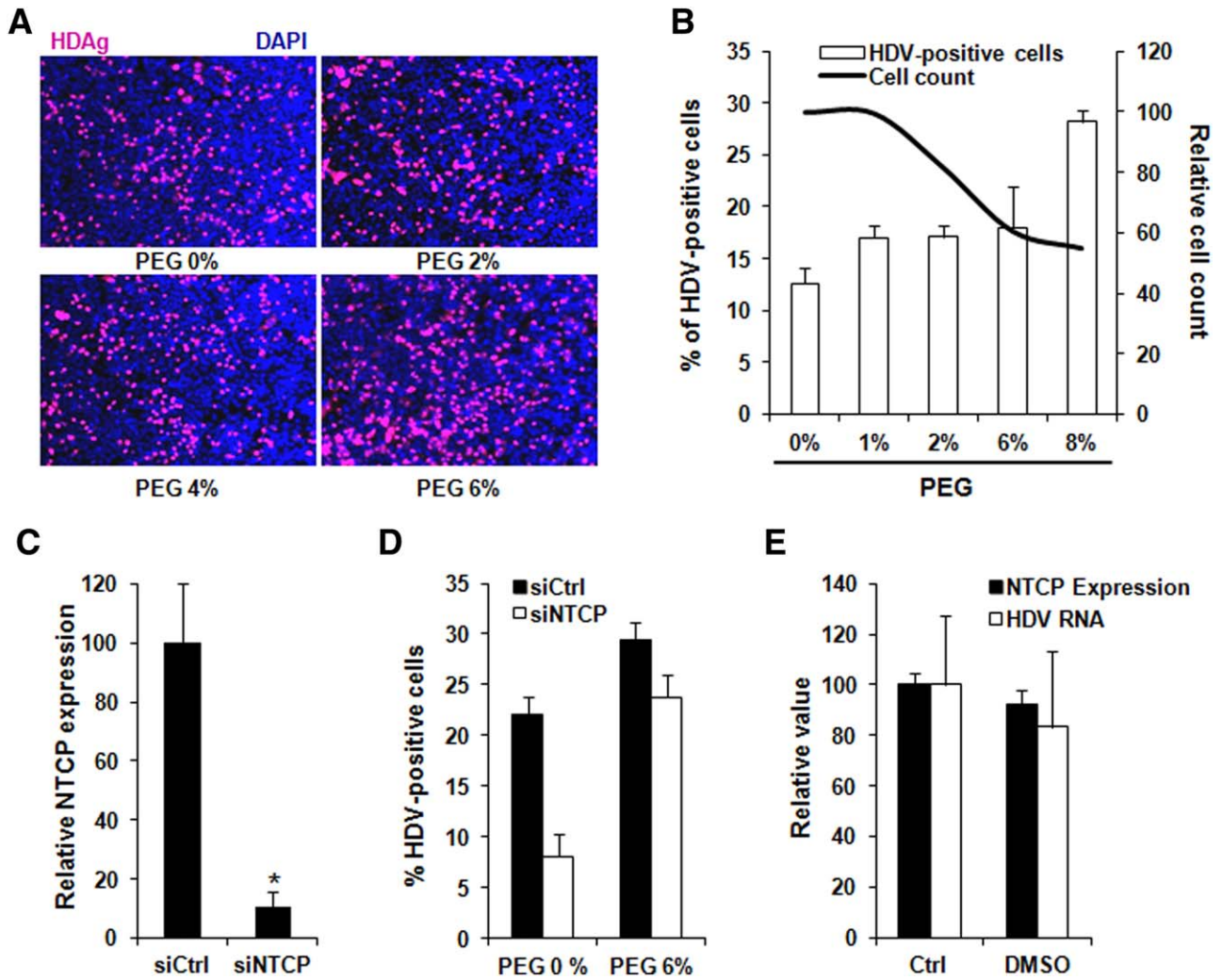

Fig. 2. HDV infection in Huh-106 cells is PEG-independent and DMSO-independent. (A) The effect of PEG on HDV infection. Huh-106 cells were infected with HDV in the presence of increasing concentrations of PEG (0%, 2%, 4%, 6%). Infection was assessed 7 dpi by IF. (B) Effect of PEG on cell viability. Huh-106 cells were infected with HDV in the presence of increasing concentrations of PEG. Infection was measured 7 dpi by quantification of HDV-positive cells. Results are expressed as mean ± standard deviation percentage of HDV-infected cells from one representative experiment performed in triplicate. The number of cells 7 dpi was evaluated by quantification of viable 4′,6-diamidino-2-phenylindole–stained nuclei. Results are expressed as means ± standard deviation percentage of cells relative to cells infected in the absence of PEG from one representative experiment performed in triplicate. (C,D) Effect of PEG treatment on silencing of NTCP expression. NTCP expression was silenced in Huh-106 cells. Two days posttransfection silencing efficacy was assessed by qRT-PCR (C), and cells were infected with HDV in the presence or absence of 6% PEG. Infection was measured 7 dpi by quantification of HDV-positive cells (D). Results are expressed as means ± standard deviation percentage of infected cells from three independent experiments performed in triplicate. (E) Effect of DMSO treatment on NTCP expression and HDV infection. Huh-106 cells were treated for 2 days with 2% DMSO. NTCP expression at the cell surface was assessed by flow cytometry as described in Fig. 1. Cells were then infected with HDV, and infection was assessed 7 dpi by quantification of HDV RNA. Results are expressed as means ± standard deviation percentage NTCP expression at the cell surface or percentage HDV infection relative to control from three independent experiments performed in triplicate. Abbreviation: DAPI, 4′,6-diamidino-2-phenylindole.

Development of a High-Throughput System for Functional Perturbations of the HDV Life Cycle. To establish a high-throughput model enabling perturbation studies of the HDV life cycle, we applied an automated imaging system for detection of viral infection using a 96-well or a 384-well plate format and immunodetection of intracellular HDAg. As HDAg localizes in Huh7 cells predominantly to the nucleus (Fig. 1F), a simple 4′,6-diamidino-2-phenylindole–HDAg costaining allows for discrimination of infected versus noninfected cells. To determine the best conditions for infection assay, HDAg detection was performed at 5, 7, and 9 dpi. While about 5% of cells were HDAg-positive at 5 dpi, 20% were positive at 7 dpi (Fig. 3A-D), and no further increase was observed at 9 dpi (Fig. 3A). Furthermore, the level of intracellular HDV RNA was measured at 5, 7, and 9 dpi. A significant increase was observed between 5 and 7 dpi, and no further increase was observed at 9 dpi (Fig. 3C).

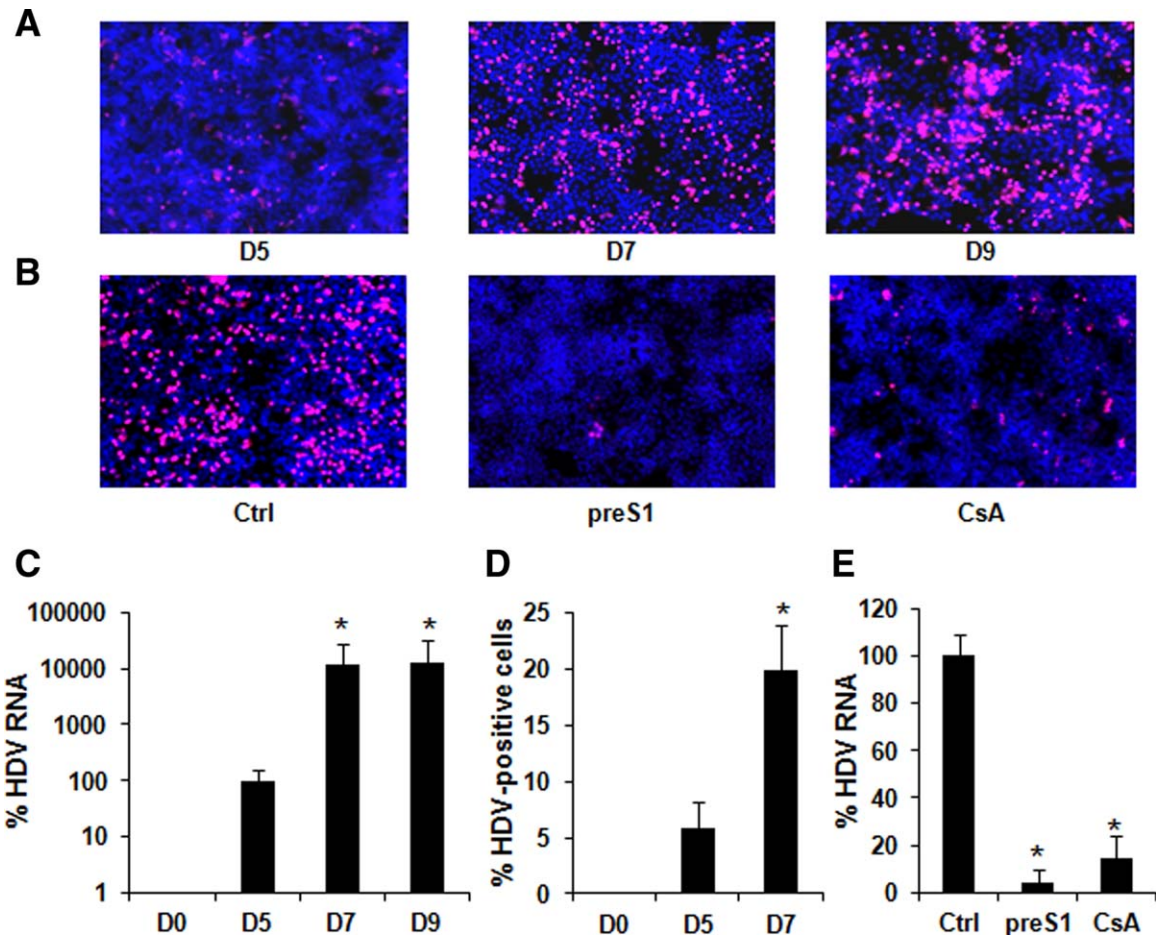

Fig. 3. A high-throughput assay for drug screening and functional genomics of HDV infection using Huh-106 cells. (A,C,D) HDV time-course of infection. Huh-106 cells were infected in 96-well (A,C) and 384-well (D) plates with HDV for 5, 7, and 9 days. (A,D) Infection was assessed by quantification of HDAg-positive cells after HDAg immunodetection. One representative experiment (A) and means ± standard deviation percentage HDV-positive cells from three independent experiments performed in triplicate (D) are shown. (C) Total RNA was extracted after 5, 7, and 9 dpi; and HDV infection was assessed by qRT-PCR quantification of HDV RNA normalized to GAPDH mRNA. Results are expressed as means ± standard deviation relative to the HDV RNA level at 5 dpi, set at 100% from three experiments performed in triplicate. (B,E) Inhibition of HDV infection using NTCP inhibitors. Cells were treated for 1 hour with HBV-derived preS1 peptide (200 nM) or with CsA (8 μM) and subsequently infected with HDV for 7 days. Infection was assessed by HDAg immunodetection (B) or qRT-PCR quantification of HDV RNA (E). Results are expressed as means ± standard deviation percentage HDV infection from three independent experiments performed in triplicate.

According to these data, we developed a functional high-throughput HDV infection protocol by infecting Huh-106 cells in 96-well or 384-well plates with HDV (without PEG and DMSO preincubation) for 7 days before quantification of HDAg-positive cells using IF. To ascertain the robustness of this model to monitor inhibition of HDV infection, we silenced NTCP expression using siRNA and incubated Huh-106 cells with NTCP inhibitors. As shown by a marked decrease in the number of HDAg-positive cells (Fig. 3B) and HDV RNA levels (Fig. 3E), HDV infection was impaired by preincubation with an HBV preS1-derived peptide or CsA, which are known to block NTCP function,[8,9,18,33] and following silencing of NTCP expression (Fig. 2D). Collectively, these data demonstrate that our model is suitable for high-throughput perturbation screens.

A Targeted RNAi Entry Screen Identifies GPC5 as a Host Cell Entry Factor. We next applied this cell-based model for a targeted RNAi HDV entry screen (Fig. 4A). Given the importance of HSPGs for HDV/HBV attachment and entry, we investigated their role in HDV infection by silencing the expression of all genes belonging to the HSPG families (Fig. 4B). Huh-106 cells were transfected with pools of four siRNAs 2 days before exposure to HDV for 24 hours (Fig. 4A). Only silencing of GPC5 expression inhibited HDV infection, leading to a 45% decrease in the number of HDAg-positive cells at 7 dpi (Fig. 4B). Nonspecific toxic effects were excluded by two independent cell viability assays (Supporting Fig. S1). To validate the role of GPC5 in HDV entry, we performed additional silencing studies using individual GPC5-specific siRNAs. A 50%

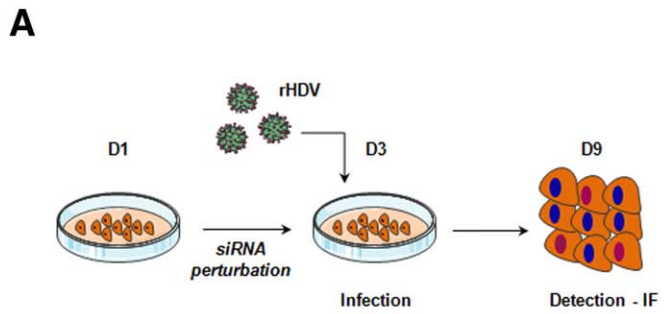

B

Gene symbol	Gene - family	HDV-positive cells (% relative to Ctrl)	Cell count (% relative to Ctrl)
Ctrl		100.0 ± 1.1	100.0 ± 1.4
SDC1	Syndecan	91.3 ± 3.3	105.6 ± 1.9
SDC2		75.4 ± 0.9	118.0 ± 3.9
SDC3		81.2 ± 2.1	93.0 ± 11.0
SDC4		87.0 ± 0.4	118.2 ± 4.1
GPC1	Glypican	83.3 ± 1.5	111.0 ± 1.4
GPC2		80.2 ± 1.4	115.4 ± 5.4
GPC3		88.6 ± 1.6	99.7 ± 0.4
GPC4		83.4 ± 1.5	115.6 ± 8.4
GPC5		**55.7 ± 3.3**	**98.7 ± 5.9**
GPC6		89.0 ± 1.6	110.9± 4.0
HSPG2	Perlecan	117.5 ± 2.1	81.7 ± 6.9
AGRN	Agrin	95.6 ± 1.5	108.8 ± 9.5

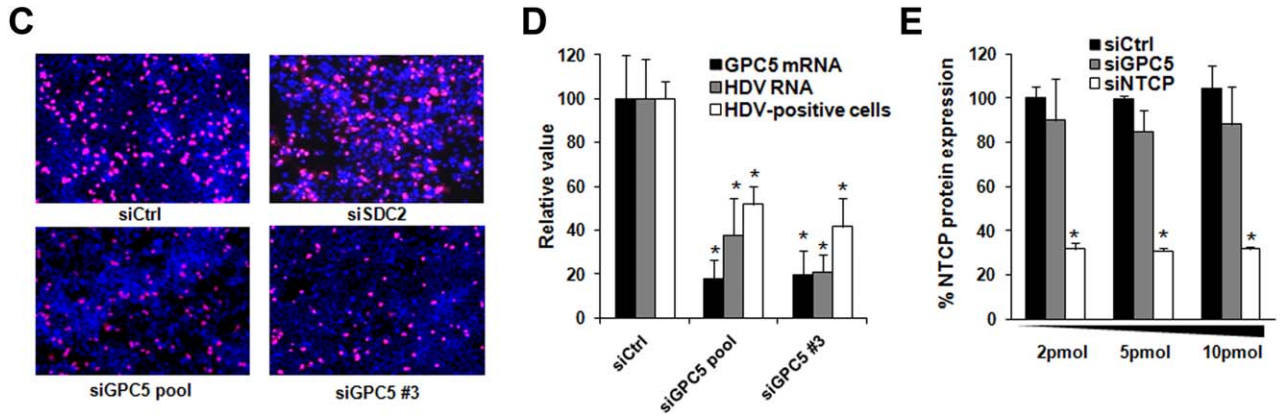

Fig. 4. A targeted functional RNAi HDV entry screen uncovers GPC5 as an HDV entry factor. (A) Flowchart of the siRNA screen. Huh-106 cells were reverse-transfected with siRNAs 48 hours prior to infection with HDV for 24 hours. HDV infection was measured 7 dpi by IF and quantification of HDV-positive cells. (B) Effect of HSPG gene silencing on HDV infection. Cells were transfected with siRNAs targeting the transcripts of genes belonging to members of different HSPG families and then infected as described in Fig. 3. Results are expressed as means ± standard deviation percentage HDV-positive cells or percentage cell count relative to control siRNA transfected cells from one experiment performed in triplicate. (C,D) Confirmation of GPC5 involvement in HDV infection using an individual siRNA. Huh-106 cells were silenced using an SDC2-specific siRNA pool, a GPC5-specific siRNA pool, or the individual GPC5-specific siRNA #3 for 48 hours and then infected with HDV. Infection was revealed 7 dpi by IF (C), quantification of HDV-positive cells, and qRT-PCR quantification of HDV RNA (D). Silencing efficacy was assessed by qRT-PCR (D). Results are expressed as means ± standard deviation percentage mRNA expression, HDV-positive cells, or HDV RNA from three independent experiments performed in triplicate. (E) Effect of GPC5 silencing on NTCP expression at the cell surface. Huh-106 cells were silenced for NTCP of GPC5 expression for 2 days using increasing quantities of siRNA. NTCP expression at the cell surface was assessed by flow cytometry. Results are expressed as means ± standard deviation percentage NTCP expression from three independent experiments performed in triplicate.

decrease in the number of HDAg-positive cells and a strong reduction of HDV RNA were observed after transfection of Huh-106 cells with GPC5 siRNA #3, similar to the siRNA pool (Fig. 4C,D). In contrast, only a minimal effect on HDV infection was observed after silencing of SDC2, an HSPG that was not identified in the RNAi screen. To verify that GPC5 silencing did not simply affect NTCP expression, we evaluated NTCP expression in GPC5-silenced Huh-106 cells. NTCP expression at the cell surface was not affected by GPC5 silencing (Fig. 4E). These data identify GPC5 as an HDV entry factor candidate.

GPC5 Mediates HDV Entry Into Human Hepatocytes. To validate the role of GPC5 as an HDV entry factor, we performed mechanistic studies using an antibody targeting GPC5. The GPC5-specific antibody inhibited HDV infection of Huh-106 cells in a dose-dependent manner, contrary to an antibody targeting SDC4, another HSPG expressed in the liver and involved in hepatitis C virus (HCV) attachment[34] but not identified in our RNAi screen (Fig. 5B). Finally, we validated the functional role of GPC5 as an HDV entry factor in PHHs, the natural target cells of HDV, which express high levels of GPC5 protein (Fig. 5A). PHH cultures were silenced for GPC5 expression using siRNAs (Fig. 5C), inoculated with HDV before assessing viral infection using IF. In contrast to cell lines, HDAg was detected predominantly in the cytoplasm of PHHs. Silencing of NTCP and GPC5 similarly resulted in a marked decrease of HDAg-positive cells (Fig. 5D),

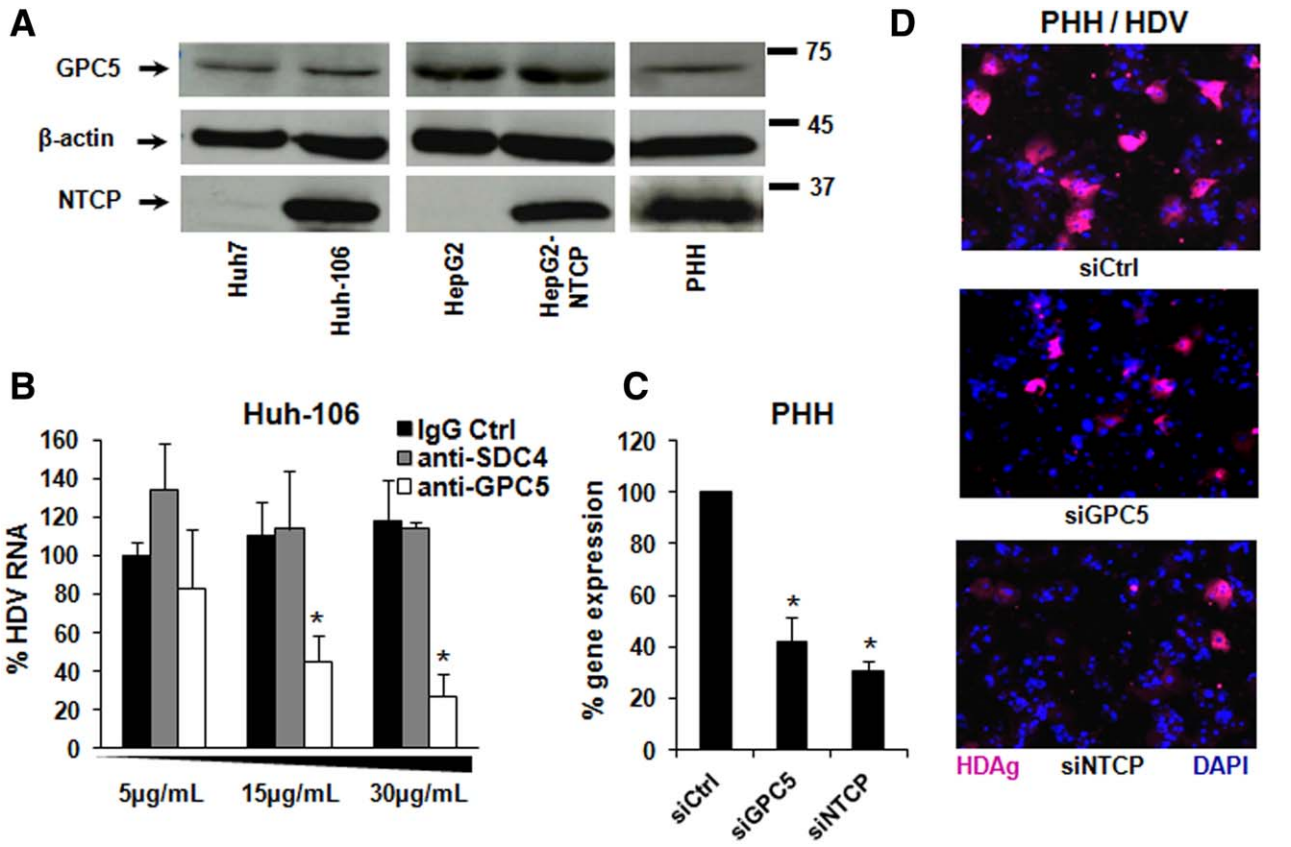

Fig. 5. GPC5 is a specific HDV entry factor in hepatoma cells and human hepatocytes. (A) GPC5 and NTCP protein expression in different cell culture models assessed by western blot. (B) Inhibition of HDV infection using anti-GPC5 antibody. Huh-106 cells were treated for 1 hour with an antibody targeting GPC5, an antibody targeting SDC4, or a control IgG at different concentrations. Cells were then infected with HDV in the presence of the antibody. Infection was assessed 7 dpi by qRT-PCR quantification of HDV RNA. Results are expressed as means ± standard deviation percentage HDV infection from three independent experiments performed in triplicate. (C,D) GPC5 silencing inhibits HDV infection in PHHs. PHHs were transfected with siRNAs targeting GPC5 or NTCP 2 days prior to infection with HDV for 7 days. Silencing efficacy was assessed by qRT-PCR of GPC5 and NTCP mRNA (C), and HDV infection was assessed by IF as described in Fig. 1 (D). One representative experiment is shown. Abbreviation: DAPI, 4′,6-diamidino-2-phenylindole.

in agreement with a functional role of GPC5 as an entry factor for HDV infection of human hepatocytes.

GPC5 Mediates HBV, but not HCV, Entry. Because HBV and HDV are believed to use the same receptors and early steps of viral entry, we next evaluated whether GPC5 is also an entry factor for HBV. Because HepG2 cells were shown to be better adapted to HBV infection assays than Huh7 cells,[8,9] we established an HepG2-NTCP cell line for productive HBV infection, as confirmed by immunodetection of HBsAg and HBV-specific pgRNA postinoculation (Supporting Fig. S2). The specificity of RT-PCR for pgRNA, but not viral DNA, was confirmed by the lack of signal upon prior DNAse treatment (Supporting Fig. S2). Inhibition of HBV infection using a preS1-derived peptide (Supporting Fig. S2) and time-course experiments demonstrating *de novo* synthesis of HBeAg (assessed by ELISA), HBsAg (assessed by IF), covalently closed circular DNA (assessed by qPCR), and HBV RNA (assessed by qRT-PCR of HBV pgRNA or total HBV RNA using RNA-seq) confirmed that the signals were from *de novo* synthesis and not from incoming virions (Supporting Fig. S3).

To determine whether GPC5 is also required for HBV infection, GPC5 expression was silenced in HepG2-NTCP cells. Silencing of GPC5 expression decreased HBV infection, as measured by the number of HBsAg-positive cells and the level of intracellular HBV pgRNA at 10 dpi, similar to observations following NTCP silencing (Fig. 6A-D). To assess whether GPC5 is a specific entry factor for HBV and HDV or may also contribute to HCV entry, we studied its functional role for HCV entry using HCVpp. The silencing of GPC5 expression does not affect HCVpp entry (Fig. 6E,F), indicating that GPC5 specifically mediates HBV and HDV entry into hepatocytes.

GPC5 Mediates Attachment of the Virion to the Target Cell Surface. To investigate the steps of the HBV entry process involving GPC5, we tested its role in

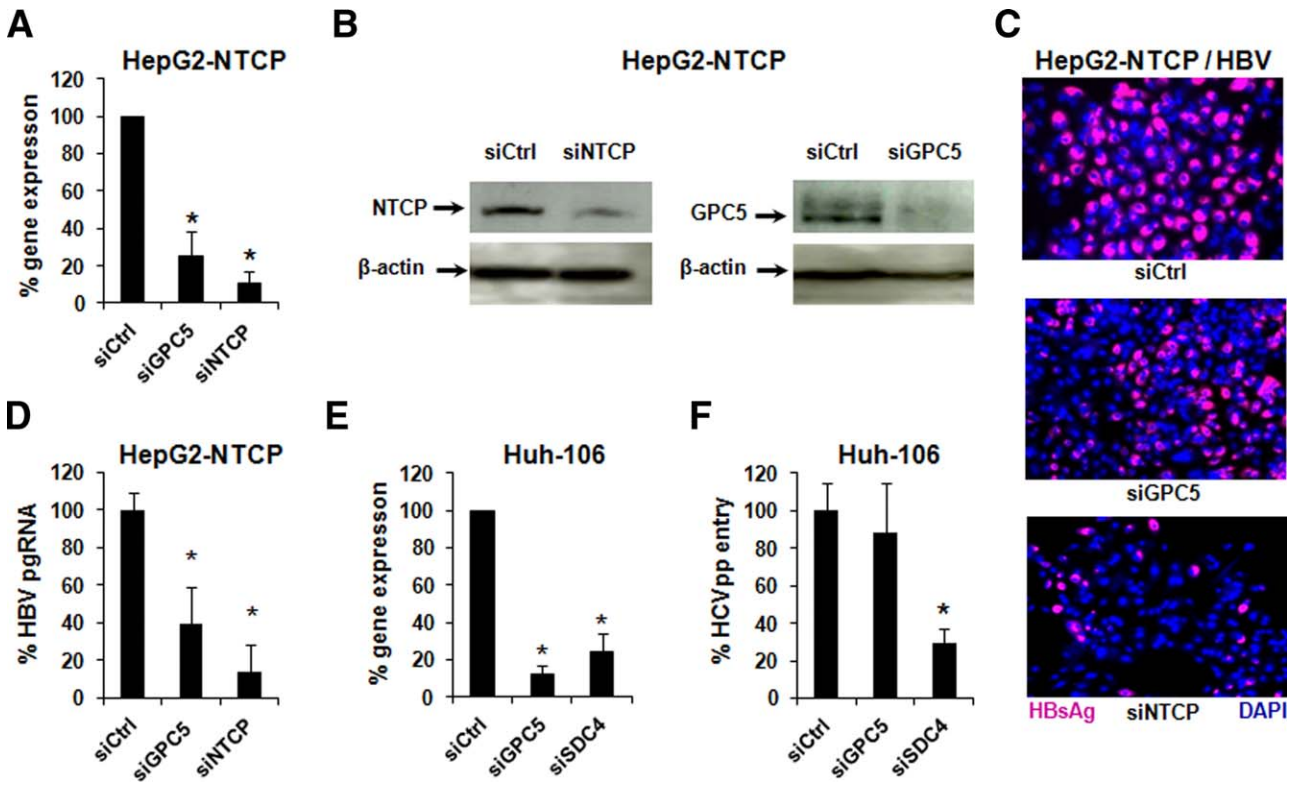

Fig. 6. GPC5 is an HBV host entry factor. (A-D) GPC5 silencing inhibits HBV infection in HepG2-NTCP cells. HepG2-NTCP cells were transfected with siRNAs targeting GPC5 and NTCP. Silencing efficacy was assessed after 2 days by qRT-PCR (A, means ± standard deviation percentage mRNA expression normalized to GAPDH mRNA expression from three independent experiments performed in duplicate) and western blot (B, one representative experiment is shown). Cells were then infected by HBV for 10 days, and infection was detected by IF (C, one representative experiment is shown) and qRT-PCR quantification of HBV pgRNA (D). Results are expressed as means ± standard deviation percentage HBV pgRNA levels from three independent experiments performed in triplicate. (E,F) GPC5 silencing does not affect HCVpp entry. Huh-106 cells were transfected with siRNAs targeting GPC5 and SDC4 48 hours prior to infection with HCVpp genotype 1b for 3 days. Silencing efficacy was assessed by qRT-PCR (E). HCVpp entry was measured by quantification of luciferase activity (F). Results are expressed as means ± standard deviation percentage HCVpp entry relative to control siRNA transfected cells from three independent experiments performed in triplicate. Abbreviation: DAPI, 4′,6-diamidino-2-phenylindole.

HBV binding to HepG2-NTCP cells. Similar to pretreatment of virions with heparin, which is known to inhibit HBV-HSPG binding, silencing of GPC5 expression significantly decreased HBV binding (Fig. 7A), strongly suggesting that GPC5 is a major player in HBV/HDV attachment at the cell surface of hepatocytes. To ascertain the ability of GPC5 to interact with the HBV envelope, we performed a competition experiment in which HBV was pretreated with soluble recombinant GPC5 protein (rGPC5). Recombinant GPC5 neutralized HBV at concentrations similar to heparin, unlike soluble recombinant SDC4 (rSDC4) (Fig. 7B). Moreover, pretreatment of Huh-106 and HepG2-NTCP cells with an anti-GPC5 antibody inhibited HDV and HBV binding, respectively (Fig. 7C). However, HBV binding was no longer inhibited when the anti-GPC5 antibody or recombinant protein was added 12 hours after virus inoculation (Fig. 7D; Supporting Fig. S4), confirming that GPC5 plays a role in the early steps of virus entry. Furthermore, to rule out that GPC5 inhibits HBV infection by interfering with other steps of the HBV life cycle, we studied the effect of GPC5 silencing on HBV replication in stably HBV-replicating HepAD38 cells.[23] Neither HBsAg nor HBV pgRNA was affected by silencing of GPC5 expression, suggesting that GPC5 has no functional role in HBV replication (Fig. 8A,B). To confirm that GPC5 has no effect on HBV replication when HBV DNA and GPC5 siRNA are present in the same cells, Huh-106 cells were cotransfected with siRNA and a plasmid encoding the HBV genome prior to measurement of soluble HBsAg and HBeAg in cell culture supernatants and quantification of viral capsids (by HBV core antigen ELISA) and viral DNA (by qPCR) in cytoplasmic lysates. Using this approach, HBV DNA and protein levels were not affected by GPC5 silencing (Fig. 8C,D,E). Collectively, these data demonstrate that GPC5 contributes to viral entry by mediating the initial attachment of HBV to its target cell.

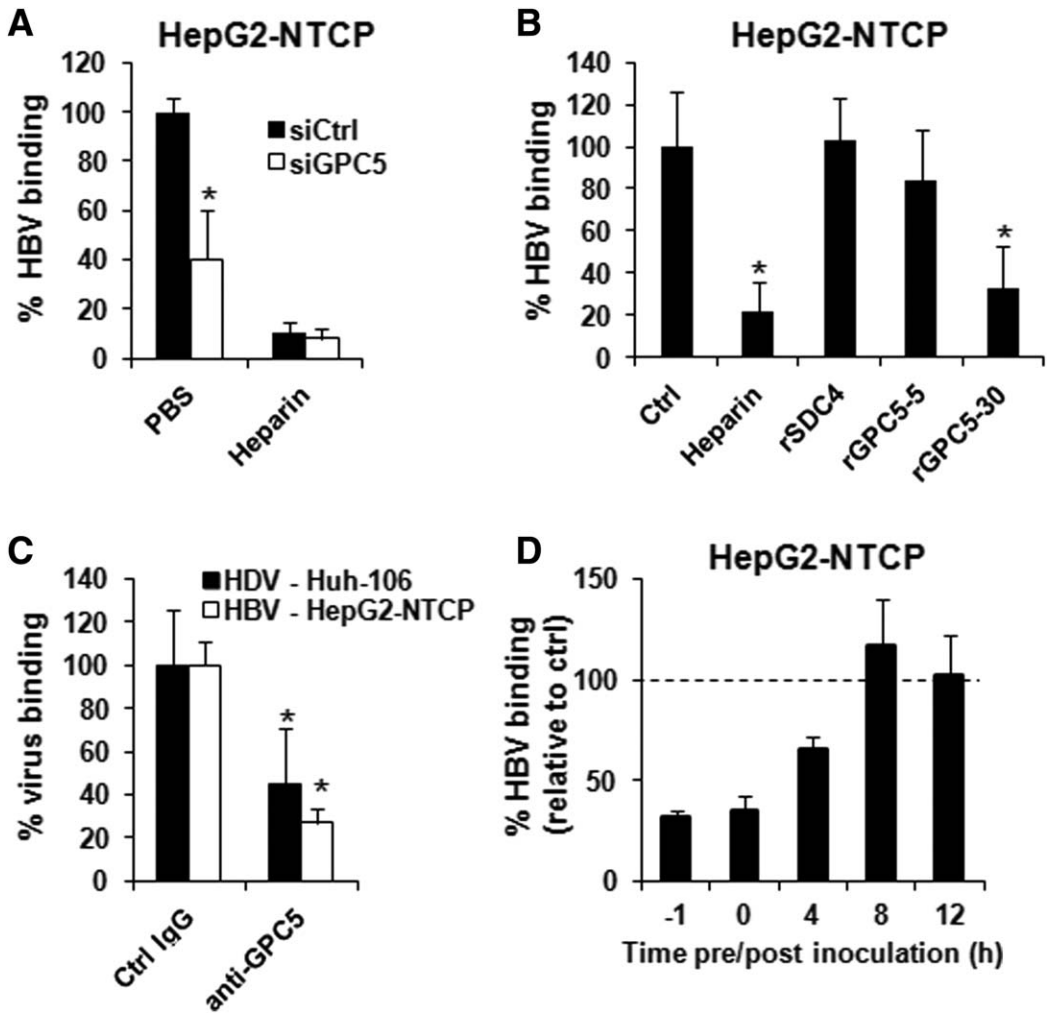

Fig. 7. GPC5 mediates binding of HBV and HDV virions to the liver cell surface. (A) GPC5 silencing inhibits HBV binding. HepG2-NTCP cells silenced for GPC5 expression were treated for 24 hours at 16°C with HBV particles pretreated or not (PBS) with heparin (30 μg/mL). HBV binding was measured by qPCR quantification of total HBV DNA bound to cells after 24 hours. Results are expressed as means ± standard deviation percentage HBV binding relative to control siRNA transfected cells treated with PBS from three independent experiments performed in duplicate. (B) Neutralization of HBV infectious particles using soluble recombinant GPC5 protein (rGPC5). HBV particles were pretreated for 30 minutes at 37°C with heparin (30 μg/mL), with soluble recombinant SDC4 (rSDC4, 30 μg/mL), or with rGPC5 at the indicated concentrations. HBV binding was measured by qPCR quantification of total HBV DNA bound to cells after 24 hours. Results are expressed as means ± standard deviation percentage HBV binding relative to control cells from three independent experiments performed at least in duplicate. (C) A specific anti-GPC5 antibody inhibits HDV and HBV binding at the cell surface. Huh-106 and HepG2-NTCP cells were incubated for 1 hour at 37°C with an anti-GPC5 antibody or a rabbit control IgG and then incubated for 24 hours at 16°C with HDV and HBV infectious particles, respectively. HBV and HDV binding was measured by qPCR quantification of total HBV DNA and HDV RNA bound to cells after 24 hours. Results are expressed as means ± standard deviation percentage HBV or HDV binding relative to control cells treated with a control IgG from three independent experiments performed at least in duplicate. (D) Time course of antibody-mediated inhibition of HBV binding. HepG2-NTCP cells were incubated with an anti-GPC5 antibody at various time points before and after incubation with HBV particles as indicated. HBV binding was measured by qPCR quantification of total HBV DNA bound to cells after 24 hours. Results are expressed as means ± standard deviation percentage HBV binding relative to cells incubated with control antibody from two independent experiments performed in triplicate.

Discussion

Here, we report a novel cell-based infection model system that allows the screening of host factors involved in HDV infection in functional assays (Fig. 4). Using this model and a loss-of-function approach, we identified GPC5 as an HDV/HBV entry factor. The functional role of GPC5 as an entry factor for these two viruses was confirmed by several lines of evidence and complementary approaches: (1) silencing of GPC5 expression decreased HDV and HBV infection in NTCP-expressing hepatoma cells and PHHs (Figs. 4–6), (2) an anti-GPC5 antibody impaired viral infection (Fig. 5), and (3) HBV binding to the cell surface decreased after silencing GPC5 expression or pretreatment of HBV with rGPC5 (Fig. 7), confirming a direct interaction between the virus and GPC5. Notably, the HBV–GPC5

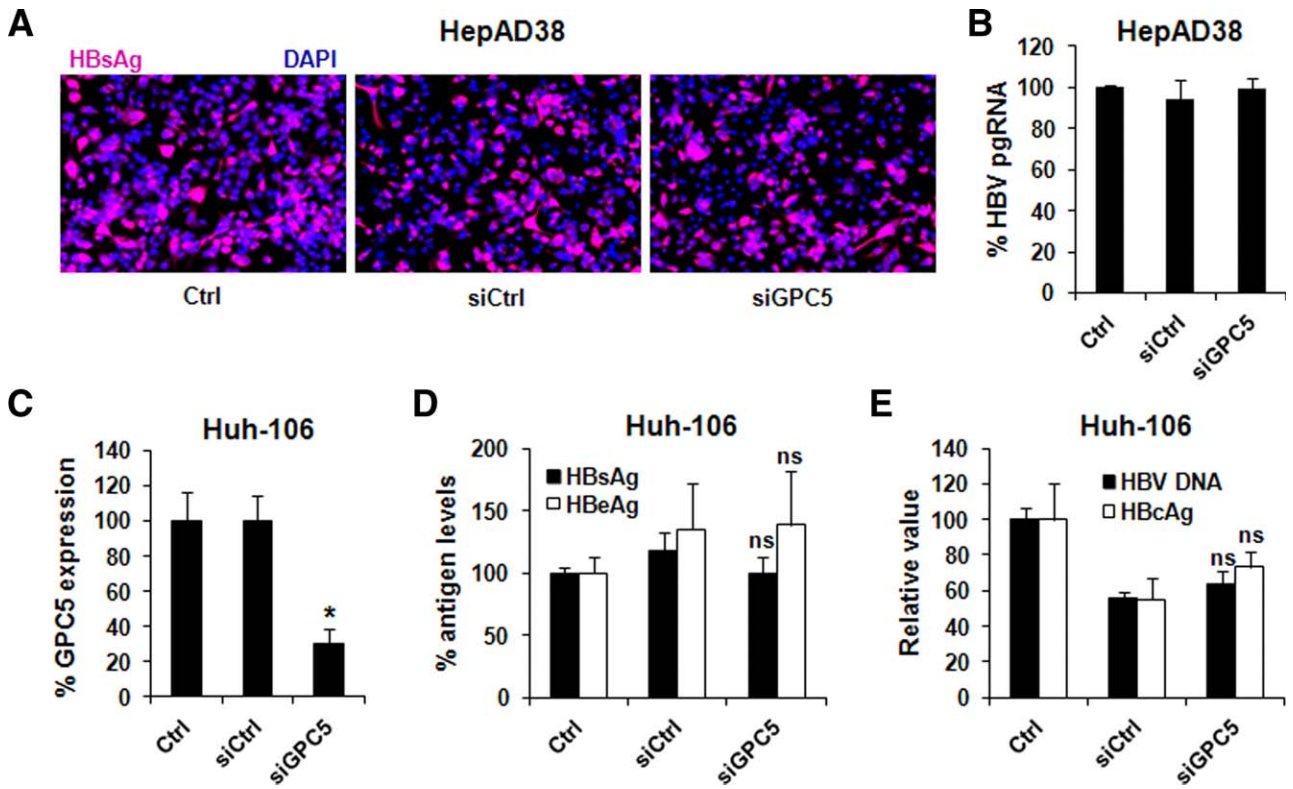

Fig. 8. GPC5 is not involved in HBV replication and production. (A,B) Absent effect of GPC5 silencing on HBV production in HepAD38 cells. HepAD38 cells stably replicating HBV were transfected with siRNAs targeting GPC5. Three days after transfection, the HBsAg level was evaluated by IF (A, one representative experiment is shown) and HBV pgRNA level was assessed by qRT-PCR quantification (B). Results are expressed as means ± standard deviation percentage HBV pgRNA levels relative to control nontransfected cells from three independent experiments performed in triplicate. (C-E) Absent effect of GPC5 silencing on HBV replication in Huh-106 cells. Huh-106 cells were reverse-cotransfected with a plasmid encoding the HBV genome (adwR9) or control plasmid and siGPC5 or control siRNA. Silencing efficacy was assessed by qRT-PCR 3 days after transfection (C). Three days after transfection, HBV replication was assessed by quantification of HBeAg and HBsAg in the supernatants (D) and total HBV DNA and HBV core antigen in cell lysates (E). Results are expressed as means ± standard deviation percentage GPC5 expression, HBV antigen, and DNA levels normalized to the HBV plasmid-only control (control) set as 100% from three independent experiments performed in triplicate. Abbreviation: DAPI, 4′,6-diamidino-2-phenylindole; ns, nonsignificant difference between nontargeting control siRNA and siGPC5.

interaction was independent of NTCP expression (Figs. 4 and 5).

PEG has been shown to favor HBV infection in PHH cultures,[35] and it is used, as well as DMSO, in most of the *in vitro* HBV and HDV infection systems based on NTCP-expressing hepatoma cells.[8,9,18] In our study, we observed that the use of PEG and DMSO was not necessary for conducting high-throughput *in vitro* HDV infection assays that are adapted to functional siRNA and small molecule screening. We thus made the choice of using these PEG/DMSO-free conditions for practical reasons in conducting the assays but also for clarity in the interpretation of the data. Although DMSO is known to induce polarization and differentiation of hepatocytes in culture, it may also affect transcriptomic patterns of cells[36] and modulate the expression of factors involved in viral entry independently of differentiation.

Using this model system and an RNAi approach to uncover which HSPG(s) mediate(s) HBV/HDV entry, we identified GPC5 as a host factor involved in the initiation of HDV and HBV infection. GPC5 is a member of the glypican family, a group of six HSPGs (GPC1-6) that are attached to the cell membrane by a glycosylphosphatidylinositol anchor.[37] Glypicans are coreceptors for numerous heparin-binding factors, and they regulate the signaling activity of many growth factors, including Wnts and hedgehogs.[37] GPC5 is highly expressed during development in a tissue-specific manner, suggesting a major role in morphogenesis.[38] In adult tissues, GPC5 is mainly expressed in the brain, kidney, and liver.[39] Modulation of GPC5 expression is observed in various cancers and other disorders, including nephrotic syndrome,[39] alveolar and embryonal rhabdomyosarcoma,[40] and lung cancer in nonsmoker patients.[41] However, a comprehensive understanding of the GPC5 functions has yet to be established. Here, we report that GPC5 acts as an entry factor for both HBV and HDV through its interactions with the HBV envelope proteins during viral attachment. Given its tissue distribution and high expression level in

the liver, GPC5 may contribute to the hepatotropism of HBV and HDV. Unlike other glypican members, GPC5 carries chondroitin sulfate chains in addition to heparan sulfate chains.[37] Chondroitin sulfate chains can function as receptors for porcine circovirus 2 and herpes simplex virus,[42,43] suggesting a role for these polysaccharides in microbial adherence. The presence of chondroitin sulfate, in addition to heparan sulfate, could explain the specificity of GPC5 as an HBV/HDV attachment factor compared to other glypican members. In line with a recent study,[44] we observed that silencing of GPC5 expression had no effect on HCV entry. Similar to HBV, HCV attachment to hepatocytes is mediated by HSPGs[45]; and two recent studies identified SDC1 and SDC4 as mediators of HCV attachment.[34,44] Our data demonstrate that neither of these two HSPGs is involved in HBV entry, highlighting high specificity of virus–HSPG interactions at the surface of hepatocytes. Our binding data indicate that GPC5 is involved in the initial attachment of the virus at the hepatocyte surface, likely at a step prior to HBV preS1 binding to NTCP, which would subsequently trigger viral entry. The interaction between the HBV envelope and GPC5 may involve both glycosaminoglycans and the GPC5 core protein.

Because glypicans have been shown to play a role in the control of cell division and growth regulation, virus–GPC5 interactions may also play a role for pathogenesis of virus-induced liver disease and cancer. Indeed, HBV[46] and HCV[47] can transmit signals during hepatocyte binding and cell entry. In turn, glypicans are involved in the modulation of several signal transduction pathways. In particular, GPC3, a closely related member in the glypican family, may serve as a biomarker and target of HCC therapy.[48] GPC3 modulates fibroblast growth factor 2 and hedgehog signaling pathways in HCC (reviewed in Ho and Kim[48]). Similarly, GPC5 modulates fibroblast growth factor 2 signaling and stimulates hedgehog signaling in rhabdomyosarcoma cells.[49,50] However, its potential role in liver disease has not yet been studied. Collectively, the interaction between GPC5 and HBV envelope proteins may modify glypican-specific signaling pathways with potential implications for liver disease progression and hepatocarcinogenesis.

Furthermore, GPC5 may represent a previously undiscovered target for urgently needed antiviral therapies. Targeting viral entry using NTCP inhibitors is a promising approach for HBV treatment.[16] Myrcludex B, an HBV preS1 NTCP-targeting peptide, strongly inhibits HBV infection *in vivo*[19] and is currently being evaluated in a phase 2 clinical trial.[17] Thus, inhibiting HBV–GPC5 interactions using small molecules or antibodies (Fig. 5) opens new perspectives for control or cure of HBV and HDV infections.

Acknowledgment: We thank Dr. A. Regev (The Broad Institute of MIT and Harvard, Cambridge, MA) for coordinating RNA-seq analyses and helpful discussions, Dr. J. Taylor (Fox Chase Cancer Center, Philadelphia, PA) for providing HDV expression plasmids, Prof. P. Pessaux (Inserm U1110 and Institut Hospitalo-Universitaire, Pôle Hépato-digestif, Nouvel Hôpital Civil, Strasbourg, France) for providing liver resections for isolation of human hepatocytes, and Prof. S. Urban (University of Heidelberg, Heidelberg, Germany) for helpful discussions. We acknowledge P. Fritsch (IGBMC, Illkirch, France) for excellent technical assistance.

References

1. Glebe D, Bremer CM. The molecular virology of hepatitis B virus. Semin Liver Dis 2013;33:103-112.
2. Trepo C, Chan HL, Lok A. Hepatitis B virus infection. Lancet 2014; 384:2053-2063.
3. Fattovich G, Giustina G, Christensen E, Pantalena M, Zagni I, Realdi G, et al. Influence of hepatitis delta virus infection on morbidity and mortality in compensated cirrhosis type B. The European Concerted Action on Viral Hepatitis (Eurohep). Gut 2000;46:420-426.
4. Taylor JM. Virology of hepatitis D virus. Semin Liver Dis 2012;32: 195-200.
5. Gish R, Jia JD, Locarnini S, Zoulim F. Selection of chronic hepatitis B therapy with high barrier to resistance. Lancet Infect Dis 2012;12:341-353.
6. **Wedemeyer H**, **Yurdaydin C**, Dalekos GN, Erhardt A, Cakaloglu Y, Degertekin H, et al. Peginterferon plus adefovir versus either drug alone for hepatitis delta. N Engl J Med 2011;364:322-331.
7. Ciancio A, Rizzetto M. Chronic hepatitis D at a standstill: where do we go from here? Nat Rev Gastroenterol Hepatol 2014;11:68-71.
8. **Yan H**, **Zhong G**, Xu G, He W, Jing Z, Gao Z, et al. Sodium taurocholate cotransporting polypeptide is a functional receptor for human hepatitis B and D virus. Elife 2012;1:e00049.
9. Ni Y, Lempp FA, Mehrle S, Nkongolo S, Kaufman C, Falth M, et al. Hepatitis B and D viruses exploit sodium taurocholate co-transporting polypeptide for species-specific entry into hepatocytes. Gastroenterology 2014;146:1070-1083.
10. Watashi K, Urban S, Li W, Wakita T. NTCP and beyond: opening the door to unveil hepatitis B virus entry. Int J Mol Sci 2014;15:2892-2905.
11. Bishop JR, Schuksz M, Esko JD. Heparan sulphate proteoglycans fine-tune mammalian physiology. Nature 2007;446:1030-1037.
12. Chen Y, Gotte M, Liu J, Park PW. Microbial subversion of heparan sulfate proteoglycans. Mol Cells 2008;26:415-426.
13. Schulze A, Gripon P, Urban S. Hepatitis B virus infection initiates with a large surface protein-dependent binding to heparan sulfate proteoglycans. Hepatology 2007;46:1759-1768.
14. Lamas Longarela O, Schmidt TT, Schoneweis K, Romeo R, Wedemeyer H, Urban S, et al. Proteoglycans act as cellular hepatitis delta virus attachment receptors. PLoS One 2013;8:e58340.
15. Sureau C, Salisse J. A conformational heparan sulfate binding site essential to infectivity overlaps with the conserved hepatitis B virus a-determinant. Hepatology 2013;57:985-994.
16. Baumert TF, Meredith L, Ni Y, Felmlee DJ, McKeating JA, Urban S. Entry of hepatitis B and C viruses—recent progress and future impact. Curr Opin Virol 2014;4C:58-65.

17. Urban S, Bartenschlager R, Kubitz R, Zoulim F. Strategies to inhibit entry of HBV and HDV into hepatocytes. Gastroenterology 2014;147: 48-64.
18. Watashi K, Sluder A, Daito T, Matsunaga S, Ryo A, Nagamori S, et al. Cyclosporin A and its analogs inhibit hepatitis B virus entry into cultured hepatocytes through targeting a membrane transporter, sodium taurocholate cotransporting polypeptide (NTCP). Hepatology 2014; 59:1726-1737.
19. **Volz T**, **Allweiss L**, Barek MB, Warlich M, Lohse AW, Pollok JM, et al. The entry inhibitor Myrcludex-B efficiently blocks intrahepatic virus spreading in humanized mice previously infected with hepatitis B virus. J Hepatol 2013;58:861-867.
20. Bogomolov P, Voronkova N, Allweiss L, Dandri M, Schwab M, Lempp FA, et al. A proof-of-concept phase 2a clinical trial with HBV/HDV entry inhibitor Myrcludex B. Hepatology 2014;60:1279a-1280a.
21. Blanchet M, Sureau C, Labonte P. Use of FDA approved therapeutics with hNTCP metabolic inhibitory properties to impair the HDV lifecycle. Antiviral Res 2014;106:111-115.
22. **Lupberger J**, **Zeisel MB**, Xiao F, Thumann C, Fofana I, Zona L, et al. EGFR and EphA2 are host factors for hepatitis C virus entry and possible targets for antiviral therapy. Nat Med 2011;17:589-595.
23. Ladner SK, Otto MJ, Barker CS, Zaifert K, Wang GH, Guo JT, et al. Inducible expression of human hepatitis B virus (HBV) in stably transfected hepatoblastoma cells: a novel system for screening potential inhibitors of HBV replication. Antimicrob Agents Chemother 1997;41: 1715-1720.
24. Sureau C. The use of hepatocytes to investigate HDV infection: the HDV/HepaRG model. Methods Mol Biol 2010;640:463-473.
25. Blanchet M, Sureau C. Infectivity determinants of the hepatitis B virus pre-S domain are confined to the N-terminal 75 amino acid residues. J Virol 2007;81:5841-5849.
26. Habersetzer F, Moenne-Loccoz R, Meyer N, Schvoerer E, Simo-Noumbissie P, Dritsas S, et al. Loss of hepatitis B surface antigen in a real-life clinical cohort of patients with chronic hepatitis B virus infection. Liver Int 2015;35:130-139.
27. Laras A, Koskinas J, Dimou E, Kostamena A, Hadziyannis SJ. Intrahepatic levels and replicative activity of covalently closed circular hepatitis B virus DNA in chronically infected patients. Hepatology 2006;44:694-702.
28. Barrera A, Guerra B, Notvall L, Lanford RE. Mapping of the hepatitis B virus pre-S1 domain involved in receptor recognition. J Virol 2005; 79:9786-9798.
29. Gripon P, Rumin S, Urban S, Le Seyec J, Glaise D, Cannie I, et al. Infection of a human hepatoma cell line by hepatitis B virus. Proc Natl Acad Sci USA 2002;99:15655-15660.
30. Baumert TF, Yang C, Schurmann P, Kock J, Ziegler C, Grullich C, et al. Hepatitis B virus mutations associated with fulminant hepatitis induce apoptosis in primary Tupaia hepatocytes. Hepatology 2005;41: 247-256.
31. Ren S, Nassal M. Hepatitis B virus (HBV) virion and covalently closed circular DNA formation in primary tupaia hepatocytes and human hepatoma cell lines upon HBV genome transduction with replication-defective adenovirus vectors. J Virol 2001;75:1104-1116.
32. Iwamoto M, Watashi K, Tsukuda S, Aly HH, Fukasawa M, Fujimoto A, et al. Evaluation and identification of hepatitis B virus entry inhibitors using HepG2 cells overexpressing a membrane transporter NTCP. Biochem Biophys Res Commun 2014;443:808-813.
33. **Nkongolo S**, **Ni Y**, Lempp FA, Kaufman C, Lindner T, Esser-Nobis K, et al. Cyclosporin A inhibits hepatitis B and hepatitis D virus entry by cyclophilin-independent interference with the NTCP receptor. J Hepatol 2014;60:723-731.
34. Lefevre M, Felmlee DJ, Parnot M, Baumert TF, Schuster C. Syndecan 4 is involved in mediating HCV entry through interaction with lipoviral particle-associated apolipoprotein E. PLoS One 2014;9:e95550.
35. Gripon P, Diot C, Guguen-Guillouzo C. Reproducible high level infection of cultured adult human hepatocytes by hepatitis B virus: effect of polyethylene glycol on adsorption and penetration. Virology 1993;192: 534-540.
36. Pal R, Mamidi MK, Das AK, Bhonde R. Diverse effects of dimethyl sulfoxide (DMSO) on the differentiation potential of human embryonic stem cells. Arch Toxicol 2012;86:651-661.
37. Filmus J, Capurro M, Rast J. Glypicans. Genome Biol 2008;9:224.
38. Song HH, Filmus J. The role of glypicans in mammalian development. Biochim Biophys Acta 2002;1573:241-246.
39. Okamoto K, Tokunaga K, Doi K, Fujita T, Suzuki H, Katoh T, et al. Common variation in GPC5 is associated with acquired nephrotic syndrome. Nat Genet 2011;43:459-463.
40. Gordon AT, Brinkschmidt C, Anderson J, Coleman N, Dockhorn-Dworniczak B, Pritchard-Jones K, et al. A novel and consistent amplicon at 13q31 associated with alveolar rhabdomyosarcoma. Genes Chromosomes Cancer 2000;28:220-226.
41. **Li Y**, **Sheu CC**, **Ye Y**, **de Andrade M**, **Wang L**, **Chang SC**, et al. Genetic variants and risk of lung cancer in never smokers: a genome-wide association study. Lancet Oncol 2010;11:321-330.
42. Bergefall K, Trybala E, Johansson M, Uyama T, Naito S, Yamada S, et al. Chondroitin sulfate characterized by the E-disaccharide unit is a potent inhibitor of herpes simplex virus infectivity and provides the virus binding sites on gro2C cells. J Biol Chem 2005;280:32193-32199.
43. Misinzo G, Delputte PL, Meerts P, Lefebvre DJ, Nauwynck HJ. Porcine circovirus 2 uses heparan sulfate and chondroitin sulfate B glycosaminoglycans as receptors for its attachment to host cells. J Virol 2006;80:3487-3494.
44. Shi Q, Jiang J, Luo G. Syndecan-1 serves as the major receptor for attachment of hepatitis C virus to the surfaces of hepatocytes. J Virol 2013;87:6866-6875.
45. Barth H, Schafer C, Adah MI, Zhang F, Linhardt RJ, Toyoda H, et al. Cellular binding of hepatitis C virus envelope glycoprotein E2 requires cell surface heparan sulfate. J Biol Chem 2003;278:41003-41012.
46. **Oehler N**, **Volz T**, Bhadra OD, Kah J, Allweiss L, Giersch K, et al. Binding of hepatitis B virus to its cellular receptor alters the expression profile of genes of bile acid metabolism. Hepatology 2014;60:1483-1493.
47. Mailly L, Xiao F, Lupberger J, Wilson GK, Aubert P, Duong FHT, et al. Clearance of persistent hepatitis C virus infection using a monoclonal antibody specific for thight junction protein claudin-1. Nat Biotechnol 2015;33:549-554.
48. Ho M, Kim H. Glypican-3: a new target for cancer immunotherapy. Eur J Cancer 2011;47:333-338.
49. Li F, Shi W, Capurro M, Filmus J. Glypican-5 stimulates rhabdomyosarcoma cell proliferation by activating Hedgehog signaling. J Cell Biol 2011;192:691-704.
50. Williamson D, Selfe J, Gordon T, Lu YJ, Pritchard-Jones K, Murai K, et al. Role for amplification and expression of glypican-5 in rhabdomyosarcoma. Cancer Res 2007;67:57-65.

Author names in bold designate shared co-first authorship.

Supporting Information

Additional Supporting Information may be found at onlinelibrary.wiley.com/doi/10.1002/hep.28013/suppinfo.